NUMERICAL AND EXPERIMENTAL STUDIES OF A DOUBLE-PIPE HELICAL HEAT EXCHANGER

Timothy J. Rennie

Department of Bioresource Engineering
McGill University, Montreal

Submitted August 2004

A thesis submitted to McGill University in partial fulfillment of the requirements of the degree of Doctor of Philosophy

Your file Votre référence
ISBN: 0-494-12936-0
Our file Notre référence
ISBN: 0-494-12936-0

ABSTRACT

A double-pipe helical heat exchanger was studied numerically and experimentally for both heat transfer and hydrodynamic characteristics. Numerical studies were performed with the aid of a commercial computational fluid dynamics package. Two sizes of the heat exchanger were investigated; the difference between the two was the diameter of the inner tube. Simulations were performed using various flow rates (laminar regime) in the inner tube and in the annulus, as well as for parallel flow and counterflow. The results of the Nusselt number in the inner tube were compared to similar experiments reported in the literature. A second study used the same numerical model; however several Prandtl numbers were used by varying the thermal conductivity of the fluid. Furthermore, the effects of thermally dependent thermal conductivities on the heat transfer characteristics were investigated. A third numerical study was performed using thermally dependent viscosities and non-Newtonian fluids. The objective was to determine the effects of these fluid properties on the heat transfer and pressure drop in the heat exchanger. The final numerical study involved the determination of the uniformity of the residence time and temperature distributions, as well as the heating/cooling uniformity. A method was developed based on the concept of thermal kill to estimate the heating/cooling uniformity.

Two physical models of the heat exchanger were designed, built, and instrumented for temperature measurements. Inlet and outlet temperatures were measured for a range of laminar flow velocities. Both parallel flow and counterflow configurations were tested. Overall heat transfer coefficients and Nusselt numbers were calculated and compared to the numerical results and to literature data.

Results from the numerical trials show that the inner Nusselt numbers in the heat exchanger were similar to literature data, despite the different boundary conditions. Nusselt numbers in the annulus were correlated to a modified Dean number. It was shown that the thermal resistance in the annulus to be the greatest limiting factor for the heat transfer, and heat transfer rates could be increased by increasing the inner tube diameter.

The Prandtl number was shown to affect the inner Nusselt number; however the effects were much greater at low Dean numbers. These differences were attributed to the difference in the developing thermal and hydrodynamic boundary layers. The studies with the thermally dependent thermal conductivities showed that the Nusselt number correlated well with a modified Graetz number.

Thermally dependent viscosity had little effect on the heat transfer; however it affected the pressure drop. Furthermore, it was shown that by keeping the flow rate in the inner tube or the annulus constant, the pressure drop in that section can be affected by changes in the flow rate in the opposite section, due to the change in the heat transfer rate and hence the average temperature and viscosity of the fluid. Non-Newtonian fluids showed little effect on the heat transfer rates, though they significantly affected the pressure drop relations.

The uniformity of the residence time and the temperature distribution were both increased in the inner tube with increasing flow rates. It was shown that a smaller gap size in the annulus resulted in more uniform residence times. Temperature distributions in the inner tube and the annulus were affected by changes in the flow velocity in the opposite section, with lower flow rates resulting in more uniform temperature distributions. Implications of using parallel flow versus counterflow, heating versus cooling, and flow rate are discussed.

Overall heat transfer coefficients and Nusselt numbers were calculated for the experimental data. The inner and annulus heat transfer coefficients were determined using Wilson plots. The results were compared to the numerical data and literature values and showed reasonable agreement.

RÉSUMÉ

Un échangeur de chaleur hélicoïdal à double tubes a été étudié de façons numérique et expérimentale tant pour ses caractéristiques hydrodynamiques que de transfert de chaleur. Les études numériques ont été conduites à l'aide d'un logiciel commercial numérique de dynamique des fluides. Deux échangeurs de chaleur ont été étudiés, la différence entre les deux étant le diamètre du tube intérieur. Des simulations ont été pratiquées utilisant divers débits (régime laminaire) dans le tube interne et dans le tube annulaire, ainsi que pour un courant parallèle ou opposé. Les résultats du nombre de Nusselt dans le tube interne ont été comparés à des expériences similaires présentées dans la littérature. Une deuxième étude a été conduite utilisant le même modèle numérique; toutefois, plusieurs nombres de Prandtl ont été utilisés, en variant la conductivité thermique du fluide. De plus, les effets des conductivités thermiques, dépendantes de la température, sur les caractéristiques de transfert de la chaleur ont été étudiées. Une troisième étude numérique a été conduite utilisant des viscosités dépendantes de la température et des fluides non Newtoniens. L'objectif était de déterminer les effets des propriétés de ces fluides sur le transfert de chaleur et sur la chute de pression dans l'échangeur de chaleur. L'étude numérique finale impliquait la détermination de l'uniformité du temps de résidence et la distribution de la température, ainsi que l'uniformité du réchauffement/refroidissement. Une méthode a été développée basée sur le concept de destruction thermique pour estimer l'uniformité du réchauffement.

Deux modèles physiques d'échangeur de chaleur ont été construits et instrumentés pour mesurer la température. Les températures à l'entrée et à la sortie ont été mesurées pour un intervalle de vitesse de débits laminaires. Les configurations de courant parallèle et opposé ont toutes deux été testées. Les coefficients de transfert de chaleur et les nombres de Nusselt ont été calculés et comparés aux résultats numériques et aux données de la littérature.

Les résultats des essais numériques démontrent que le nombre Nusselt interne dans l'échangeur de chaleur était similaire aux données de la littérature, malgré les différentes conditions aux limites. Les nombres de Nusselt dans le tube annulaire étaient corrélés à un nombre de Dean modifié. Il a été démontré que la résistance thermique dans

le tube annulaire était le plus grand facteur limitant pour le transfert de chaleur et que les taux de transfert de chaleur pouvaient être accrus en augmentant le diamètre du tube interne.

Il a aussi été démontré que le nombre de Prandtl affectait le nombre de Nusselt dans le tube intérieur; toutefois, les effets étaient plus bien importants lorsque le nombre de Dean était petit. Ces différences ont été attribuées à la différence dans le développement thermal et aux conditions aux limites hydrodynamiques. Les études avec les conductivités thermiques dépendantes de la température démontraient que le nombre de Nusselt avait une bonne corrélation avec un nombre de Graetz modifié.

La viscosité dépendante de la température avait peu d'effet sur le transfert de chaleur; toutefois, elle affectait la chute de pression. De plus, il a été démontré qu'en gardant un débit constant dans le tube interne ou dans le tube annulaire, la chute de pression dans cette section est affectée par des changements dans le débit de la section opposée; cela est dû au changement du taux de transfert de chaleur, et conséquemment au changement sur la température moyenne et la viscosité du fluide. Les fluides non Newtoniens avaient peu d'effet sur les taux de transfert de chaleur, bien qu'ils aient affecté significativement les relations des chutes de pression.

L'uniformité du temps de résidence et la distribution de température ont été toutes deux augmentées dans le tube interne avec des débits croissants. Il a été démontré qu'un plus petit espace dans le tube annulaire résultait en des temps de résidence plus uniformes. Les distributions de température dans le tube interne et dans le tube annulaire étaient affectées par les changements dans la vitesse du courant dans la section opposée, avec des débits plus faibles résultant dans des distributions de température plus uniformes. Les implications de l'utilisation des courants parallèles versus des flots contre-courants, du réchauffement versus le refroidissement ainsi que des débits différents sont discutées.

Les coefficients de transfert de chaleur et les nombres de Nusselt ont été calculés pour les données expérimentales. Les coefficients de transfert de chaleur dans le tube interne et dans le tube annulaire ont été déterminés à l'aide de la courbe Wilson. Les résultats ont été comparés aux données numériques et aux valeurs de la littérature et étaient raisonnablement en accord avec ces derniers.

ACKNOWLEDGEMENTS

Foremost, I would like to thank Dr. G. S. V. Raghavan for all his leadership and assistance during these past few years. It has been a great pleasure working for you, and I appreciate all that you have done for me.

My full gratitude to Dr. Valérie Orsat for so much support and guidance. Thanks for always being there with a smile and words of encouragement.

Yvan Gariépy: I thank you for all the time and advice that you gave towards the experimental aspect of this project.

To Dr. Venkatesh Sosle, Jianming Dai and Xiangjun Liao: What a road trip! It was an experience I will never forget.

During the first few years of this degree I had the opportunity to have many enthusiastic and profound discussions with Peter Alvo. I will always remember those times and you will be sadly missed.

Barry van Bergen, Claudia Beaudry, Predrag Sunjka, Joumana Abou Nohra, Cathy Proot, Trevor Helwig, Charles Walker, Opal Williams, and Baldur Bujatzeck; I thank you for your friendship throughout my studies.

I am grateful for the financial support provided from FCAR (Fonds pour la Formation de Chercheurs et l'Aide à la Recherche), McGill Majors Fellowship, Neil Croll Memorial Award, and the Walter M. Stewart Postgraduate Scholarship in Agriculture.

A special thanks to Veera Harnal for her continuous support throughout this degree. I could not have done it without your companionship.

My parents, Gordon and Linda, and my brother, Tony: You have always been there for me and have encouraged me to follow my dreams. This thesis is as much yours as it is mine.

There are so many other people to thank: Dr. Kok, Dr. Norris, the many undergraduate students whom I had the pleasure of teaching, fellow graduate students, and the list goes on. Thank you all for your kindness.

TABLE OF CONTENTS

LIST OF TABLES

LIST OF FIGURES

FORMAT OF THESIS

This thesis is submitted in the form of original papers suitable for journal publications. The thesis format has been approved by the **Graduate and Postdoctoral Studies Office, McGill University**, and follows the conditions outlined in the **"Thesis Preparation and Submission Guidelines, I. Thesis Preparation, C. Manuscript-based thesis"** which are as follows:

"As an alternative to the traditional thesis format, the dissertation can consist of a collection of papers of which the student is an author or co-author. These papers must have a cohesive, unitary character making them a report of a single program of research. The structure for the manuscript-based thesis must conform to the following:

1. Candidates have the option of including, as part of the thesis, the text of one or more papers submitted, or to be submitted, for publication, or the clearly-duplicated text (not the reprints) of one or more published papers. These texts must conform to the "Guidelines for Thesis Preparation" with respect to font size, line spacing and margin sizes and must be bound together as an integral part of the thesis. (Reprints of published papers can be included in the appendices at the end of the thesis.)

2. The thesis must be more than a collection of manuscripts. All components must be integrated into a cohesive unit with a logical progression from one chapter to the next. In order to ensure that the thesis has continuity, connecting texts that provide logical bridges preceeding [sic] and following each manuscript are mandatory.

3. The thesis must conform to all other requirements of the "Guidelines for Thesis Preparation" in addition to the manuscripts.

   The thesis must include the following:

   1. a table of contents;
   2. a brief abstract in both English and French;
   3. an introduction which clearly states the rational and objectives of the research;
   4. a comprehensive review of the literature (in addition to that covered in the introduction to each paper);
   5. a final conclusion and summary;
   6. a thorough bibliography;
   7. Appendix containing an ethics certificate in the case of research involving human or animal subjects, microorganisms, living cells, other biohazards and/or radioactive material.

4. As manuscripts for publication are frequently very concise documents, where appropriate, additional material must be provided (e.g., in appendices) in sufficient detail to allow a clear and precise judgement to be made of the importance and originality of the research reported in the thesis.

5. In general, when co-authored papers are included in a thesis the candidate must have made a substantial contribution to all papers included in the thesis. In addition, the candidate is required to make an explicit statement in the thesis as to who contributed to such work and to what extent. This statement should appear in a single section entitled "Contributions of Authors" as a preface to the thesis. The supervisor must attest to the accuracy of this statement at the doctoral oral defence. Since the task of the examiners is made more difficult in these cases, it is in the candidate's interest to clearly specify the responsibilities of all the authors of the co-authored papers."

In This thesis, Chapter IV is a development and testing of a numerical model in which Chapters VI, VII, and VII are based on. The numerical modeling involves the use of the commercial computational fluid dynamics package PHOENICS 3.3. A basic description of the software, along with some details to its use in this work is presented in Appendix A for the interested reader. These details have been left out of the manuscripts as the manuscripts are required to be concise and suitable for publishing in a scientific journal.

CONTRIBUTION OF AUTHORS

The work reported here was performed by the candidate and supervised by Dr. G. S. V. Raghavan of the Department of Bioresource Engineering, Macdonald Campus of McGill University. All work, numerical and experimental was done by the candidate, as well as all the data analysis and writing of the articles. The authorship of all articles (Chapters IV to VIII) is T. J. Rennie and G. S. V. Raghavan.

NOMENCLATURE

a	Constant
A	Area (m^2)
A	Constant
b	Constant
B	Constant
c	Constant
C	Capacity rate ($J \cdot s^{-1} \cdot K^{-1}$)
c_p	Specific heat ($J \cdot kg^{-1} \cdot K^{-1}$)
CFD	Computational fluid dynamics
CV	Coefficient of variation
d	Diameter of inner tube (m)
D	Diameter of annulus (m)
D_h	Hydraulic diameter (m)
De	Dean number = $\mathrm{Re}(d/2R)^{1/2}$
De^*	Modified Dean number
DRT	Decimal reduction time (s)
$E(t)$	Residence time distribution function (s^{-1})
f	Friction factor
Gz	Graetz number
Gz^*	Modified Graetz number
h	Heat transfer coefficient ($W \cdot m^{-2} \cdot K^{-1}$)
k	Thermal conductivity ($W \cdot m^{-1} \cdot K^{-1}$)
K	Dean number (original)
K	Consistency index ($kg \cdot s^{n-2} \cdot m^{-1}$)
L	Length of heat exchanger (m)
$LMTD$	Log mean temperature difference (K)
$\dot{m}$	Mass flow rate ($kg \cdot s^{-1}$)
n	Flow behaviour index
n	Power-law exponent

N	Population
NTU	Number of transfer units
Nu	Nusselt number, $Nu = hd/k$
Pr	Prandtl number, $\Pr = c_p \mu/k$
PTK	Proportion of thermal kill
q	Heat transfer rate ($J{\cdot}s^{-1}$)
Q	Parameter defined by Akiyama and Cheng (1972, 1974)
Q	Volumetric flow rate ($m^3{\cdot}s^{-1}$)
r	Radius of inner tube (m)
R	Radius of curvature (m)
Re	Reynolds number, $\mathrm{Re}= \rho v D_h/\mu$
Re*	Universal Reynolds number, $\mathrm{Re}^*= \rho v^{2-n} D_h^{\,n}/K[a+bn/n]^n 8^{n-1}$
t	Time (s)
T	Temperature (K)
ΔT_1	Temperature difference at inlet (K)
ΔT_2	Temperature difference at outlet (K)
u'	Strain rate (s^{-1})
U	Overall heat transfer coefficient ($W{\cdot}m^{-2}{\cdot}K^{-1}$)
UHF	Uniform heat flux boundary condition
UWT	Uniform wall temperature boundary condition
v	Average axial velocity ($m{\cdot}s^{-1}$)
V	Average velocity ($m{\cdot}s^{-1}$)
Vol	Volume (m^3)
x	Axial distance along tube (m)
z	Thermal resistance constant (°C)
ε	Effectiveness
ζ	Boundary layer thickness ratio
ρ	Density ($kg{\cdot}m^{-3}$)
μ	Dynamic viscosity ($kg{\cdot}m^{-1}{\cdot}s^{-1}$)
τ	Shear stress ($kg{\cdot}m^{-1}{\cdot}s^{-2}$)
τ	Residence time (s)

λ	Proportion of surviving microorganisms
σ^2	Second moment about the mean

Subscripts

abs	Absolute
asy	Asymptotic value
c	Cold/Curved
coldin	Cold fluid in
crit	Critical
cur	Curved tube
h	Hot
hotin	Hot fluid in
i	Inside/Inner
loc	Local
m	Mean
max	Maximum
min	Minimum
o	Initial/Outside/Outer
ref	Reference
s	Straight
x	Cross-section

I. GENERAL INTRODUCTION

1.1 Background

Helically coiled tubes can be found in many applications including food processing, nuclear reactors, compact heat exchangers, heat recovery systems, chemical processing, low value heat exchange, and medical equipment (Berger et al., 1983; Abdalla, 1994; Rao, 1994; Rabin and Korin, 1996; Bai et al., 1999; Sandeep and Palazoglu, 1999; Genssle and Stephan, 2000). Curved tubes are of interest to the medical community as blood flow occurs in many arteries that are curved (Zabielski, and Mestel, 1998a; Zabielski, and Mestel, 1998b). Helical coils are very alluring for various processes such as heat exchangers (Figure 1.1) and reactors because they can accommodate a large heat transfer area in a small space, with high heat transfer coefficients and narrow residence time distributions. Due to the extensive use of helical coils in these applications, knowledge about the pressure drop, flow patterns, and heat transfer characteristics are very important. Pressure drop characteristics are required for evaluating pump power required to over come pressure drops to provide the necessary flow rates. These pressure drops are also functions of the curvature of the tube. The curvature induces secondary flow patterns perpendicular to the main axial flow direction. Typically, fluid in the core of the tube moves towards the outer wall, then returns to the inner portion of tube by flowing back along the wall, as shown in Figure 1.2. This secondary flow can be expected to enhance heat transfer between the tube wall and the flowing fluid. Another advantage to using helical coils over straight tubes is that the residence time spread is reduced, allowing helical coils to be used to reduce axial dispersion in tubular reactors (Ruthven, 1971). Thus, for design of heat exchangers that contain curved tubes, or helically coiled heat exchangers, the heat transfer and hydrodynamic characteristics need to be known for different configurations

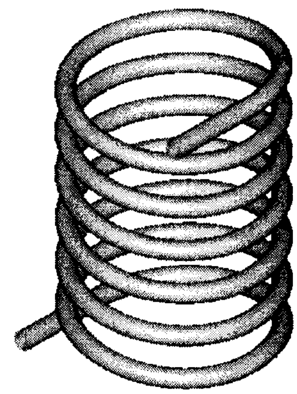

Figure 1.1: Diagram of helical coil

of the coil, including the ratio of tube radius to coil radius, pitch, and Reynolds and Prandtl numbers.

The fluid motion in curved pipes was first observed by Eustice in 1911. Since then numerous studies have been reported on the flow fields that arise in curved pipes (Dean, 1927, 1928; White, 1929; Hawthorne, 1951; Horlock, 1956; Barua, 1962; Austin and Seader, 1973) including helical coils, which is a subset of curved pipes. The flow fields have been observed experimentally and numerically. These studies have shown that the secondary flow pattern can change substantially in form (Figure 1.2) as some of the parameters are changed (in this case the Dean number).

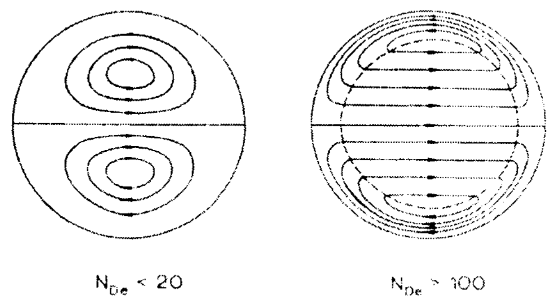

Figure 1.2: Secondary flow for low and high Dean numbers (Dravid et al., 1971)

The next logical step in observing the flow patterns was to study the patterns in heat transfer applications. This resulted in many papers giving results of the effect of Prandtl and Reynolds numbers on the flow patterns and on Nusselt numbers. The majority of the papers on heat transfer are for inside Nusselt numbers for either constant wall temperature or constant heat flux. There is little information on the outside heat transfer coefficients on helical coils, except for a few papers on the natural convection from helical coils (Ali, 1994, 1998; Xin and Ebadian, 1996, Rennie and Raghavan, 2000). Even in these cases, the wall temperature of the helical coil is considered to have a constant temperature or a constant heat flux. These two types of boundary conditions are often encountered in heat exchanger applications. The condition of constant wall temperature can be achieved, or closely approximated, by using steam as one of the media for heat transfer. The steam will condense on the coil at a given temperature (depending on the operating pressure) throughout the system. The amount of steam condensing at any one area will be based on the heat flux at that point. The build up of condensate on the pipes may lead to a slight deviation from a constant wall temperature in practice. Constant heat flux exchangers can be built by incorporating heating coils in or around the tube walls. By sending a current through the heating element the amount of heat produced at any point will be constant as the heat generated would be based on the current flowing in the heating element. However, deviations may occur if the heat generation of the heating element is temperature dependant, as the temperature will not be uniform over the length of the heating coil. For tubes made out of an electrical conducting material, it is also possible to simply apply an electric potential difference between the two ends of the tube and the current generated will heat the tube. Apart from these two boundary conditions, a third can be generated, which is neither constant wall temperature nor constant heat flux. Such is the case of fluid-to-fluid heat exchangers, where the walls of the heat exchanger separate the two fluids. In these situations the properties of both fluids need to be taken into consideration. Overall heat transfer coefficient can be calculated based on the log-mean temperature difference (LMTD), the amount of heat transferred, and the heat exchange surface area. However, this uses the assumption that the convection heat-transfer coefficients are constant throughout the heat exchanger. This assumption is often not valid when dealing with temperature dependent fluid properties, and becomes very complex as the heat transfer coefficients on one side of the tube could be affected by changes of flow rate or inlet temperatures on the other side of the heat exchanger. Little information is available for the overall heat transfer coefficient for helically coiled heat exchangers. This is primarily because the bulk of the research has been performed on constant wall temperature and constant heat flux conditions, and hence the fluid-to-fluid conditions have been overlooked in the study of helically coiled heat exchangers. Some information is available on designing fluid-to-fluid heat exchangers (Patil et al., 1982; Haraburda, 1995); however these are shell-and-tube heat exchangers, only one type of configuration that can be made with helical coils. Cleaning of helical coils can prove to be more difficult than its shell and tube counterpart; however the helical coil unit would require cleaning less often (Haraburda, 1995). A diagram for a shell-and tube heat exchanger is shown in Figure 1.3. The calculation of the heat transfer is based on a couple of assumptions (as discussed below) since no data are present in the literature for this type of configuration. There are two difficulties that arise for estimating the inside heat transfer coefficient. What is the type of boundary conditions present for the heat transfer? It is not a constant wall temperature, unless the fluid in the shell side is steam. On the other hand, the assumption of constant heat flux is not valid. The problem that is faced in this situation is that there is no information on how to accurately predict the heat transfer coefficient. Rough estimates can be made using either constant heat flux or constant wall temperature from the literature. The study of fluid-to-fluid heat transfer for this arrangement needs further investigation. The second difficulty is in estimating the area of the coil surface available to heat transfer. As can be seen in Figure 1.3, a solid baffle is placed at the core of the heat exchanger. In this configuration the baffle is needed so that the fluid will not flow straight through the shell with minimal interaction with the coil. This baffle changes the flow velocity around the coil and it is expected that there would be possible dead-zones in the area between the coils where the fluid would not be flowing. The heat would then have to conduct through the fluid in these zones, reducing the heat transfer effectiveness on the outside of the coil. Additionally, the recommendations for the calculation of the outside heat transfer coefficient is based on the flow over a bank of non-staggered circular tubes (Haraburda, 1995), which is another approximation to account for the complex geometry. Thus, the major drawbacks to this type of heat exchanger are the difficulty in predicting the heat transfer coefficients and the surface area available for heat transfer. These problems are brought on because of the lack of information in fluid-to-fluid helical heat exchangers (Prabhanjan, 2000) and the poor predictability of the flow around the outside of the coil.

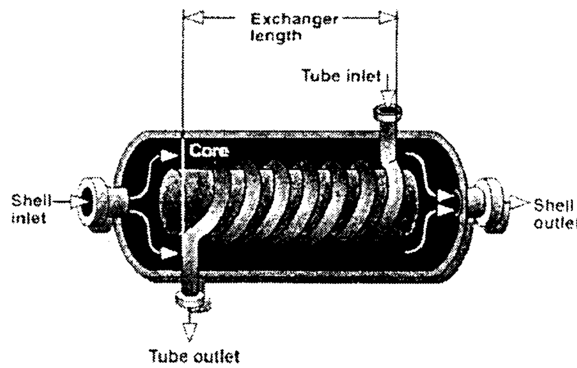

Figure 1.3: Shell-and-tube heat exchanger for three-phase flow (Haraburda, 1995)

1.2 Hypothesis

In order to overcome some of the problems with a shell-and–tube heat exchanger, a new design is required to limit the possible dead-zones, and to change the geometry to something that is easier to characterize. Thus, it is proposed to evaluate a double-pipe helical heat exchanger for fluid-to-fluid flow as shown in Figure 1.4 and Figure 1.5. This configuration is similar to a straight double-pipe heat exchanger, except that the tubes are both curved to take advantage of the space saving characteristics and the enhanced heat transfer coefficients of the helical geometry. There are some distinct advantages from this type of design. Firstly, the whole surface area of the coil will be exposed to moving fluid, eliminating the dead-zones that could be found in the shell-and-tube type of heat exchanger. Secondly, the flow in the outside tube will also experience secondary flows (Petrakis and Karahalios, 1997), though there has been little research reported in literature on this aspect of the flow. The form of the secondary flow would depend on the ratio of the tubes, amongst other factors (Petrakis and Karahalios, 1997). A representative secondary flow pattern is shown in Figure 1.6. Thirdly, this configuration should lead to a more standard approach for characterizing the heat transfer in the exchanger. The ratio of the two tube diameters may be one of the ways to characterize the heat transfer. However, some disadvantages may exist with such a configuration as well. Cleaning the heat exchanger may become more difficult as it is easier to design a shell that comes apart for cleaning than a coiled tube. The design of

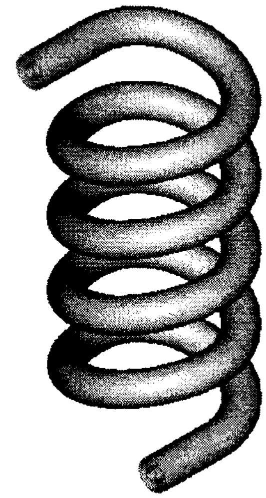

Figure 1.4: Double-pipe helical coil

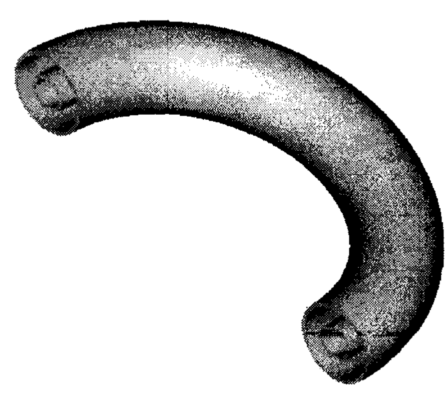

Figure 1.5: Close-up of double-pipe heat exchanger

a double-pipe helical heat exchanger requires information that is not available in the literature. One aspect is the fluid-to-fluid heat transfer coefficients. This needs further investigation. The optimal ratio of the tube sizes is also needed. It is unknown what would characterize the best ratios, whether it is a function of flow rates, secondary flows, and so forth. It would be expected that the outside heat transfer coefficient is dependant on the amount of secondary flow occurring in that tube. A full analysis of the heat transfer and hydrodynamic effects of a double-pipe helical heat exchanger would be beneficial for the heat transfer industry, including the food processing industry. There are advantages of using helical coils in the thermal processing of highly viscous and/or sensitive food products. These products could be processed at low velocities (laminar region), where they would undergo small shear stresses and the pumping requirements would be lower than with turbulent flow. However, the secondary flows would enhance the heat transfer, so that the high heat transfer coefficients could still be achieved. Overall, there is evidence that the residence time distributions would be narrower than in the straight tube, which leads to more uniform heating of the food, and possibly of better quality.

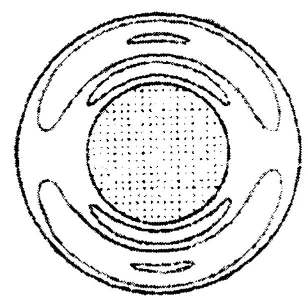

Figure 1.6: Secondary flows in annulus of a double-pipe helical coil (Petrakis and Karahalios, 1997)

II. GENERAL OBJECTIVES

The main objective of this research is to determine the heat transfer characteristics of a double-pipe helical heat exchanger, both numerically and experimentally, and to determine the effects of heat exchanger geometry and fluid properties on the heat transfer characteristics. To accomplish this goal, the following specific objectives were undertaken:

1. Development of a numerical model of the heat exchanger using PHOENICS 3.3 (Parabolic, Hyperbolic, or Elliptical Numerical Integration Codes Series).
2. Using the numerical model, the effects of coil size and flow rates on the Nusselt numbers in both the inner tube and the annulus and on the overall heat transfer coefficient were investigated.
3. Design and construction of a physical model of the heat exchanger.
4. Testing of the physical model under different flow rates and flow configurations (parallel flow and counterflow).
5. Comparison of the results from both numerical and experimental work.
6. Using the numerical model, the effects of the fluid thermal properties (Prandtl numbers and thermally dependent thermal conductivity) on the heat transfer characteristics of the heat exchanger were studied.
7. Using the numerical model, the effects of the thermally dependent viscosity and non-Newtonian fluids on the heat transfer characteristics and the pressure drop of the heat exchanger were established.
8. Using the numerical model, the key parameters viz., residence time, temperature, and heating/cooling uniformity of the product in the heat exchanger were examined.

III. LITERATURE REVIEW

3.1 Introduction

Extensive work has been completed on the flow and heat transfer characteristics in helical coils. The purpose of this literature review is to go through the main topics of interest. It should be kept in mind that the majority of the work that has been performed is based on either constant wall temperature or constant heat flux from the wall, neither of these conditions will be present in the proposed research, except as part of the validation of the numerical model. Likewise, many references claiming to describe helical coil flow and heat transfer is based on experiments or mathematic models that are designed with a toridinal coil or a toridinal coordinate system and does not take the pitch into account. There are a number of published papers and handbooks on this subject, for both hydrodynamic and heat transfer aspects. Kays and Perkins (1973), Berger et al., (1983) and Shah and Joshi (1987) are some of the more complete reviews.

3.2 Flow Pattern

The first observations of the curvature effect on flow in coiled tubes were noted at the turn of the 20th century. Grindley and Gibson (1908) noticed the curvature effect on flow in a coiled pipe while performing experiments on air viscosity. It was noted by Williams et al. (1902) that the location of the maximum axial velocity is shifted towards the outer wall of a curved tube. Eustice (1910) noted an increase in resistance to flow for the curved tube compared to the straight tube and this increase in resistance could be correlated to the curvature ratio. However, in coiling the tubes, considerable deformation occurred in the cross section of the tubes for some of the trials, causing an elliptical cross sectional shape. Eustice (1911) also noted that the curvature, even slight, tended to modify the critical velocity that is a common indicator of the transition from laminar to turbulent flow. By using ink injections into water flowing through coiled tubes, U-tubes and elbows, Eustice (1911) observed the pattern of the secondary flow. This secondary flow appears whenever a fluid flows in a curved pipe or channel. Eustice (1911) also noted the same general motion in turbulent flow when sand was introduced into a curved pipe.

The first attempt to mathematically describe the flow in a coiled tube was made by Dean (1927, 1928). The first paper (Dean, 1927) described a first approximation of the steady motion of incompressible fluid flowing through a coiled pipe with a circular cross-section. Although this approximation did give qualitative agreement with experimental observations, it failed to show the relation between the pressure gradient, the flow rate and the curvature for a curved pipe. In his successive work, Dean (1928) observed that the reduction in the rate of flow due to curvature depends on a single variable, K, which is equal to $2(\mathrm{Re})^2 r/R$ when the motion is slow, where Re is the Reynolds number, r is the radius of the pipe, and R is the radius of curvature. However, this work was done with the assumption that the ratio of r/R is small. This assumption greatly simplifies the four fundamental equations (continuity equation and the three momentum equations) without affecting the most important terms that decide the effect of curvature on the motion. Dean (1928) also noted that his analytical calculations only applied to stream-line motion. Dean's (1928) explanation for the requirement of a higher pressure gradient to maintain a given flow rate in a curved pipe was that some of the fluid is in continual oscillation between the central part of the pipe, where the velocity is high, and the outer portion of the pipe, where the velocity is low. This movement is due to the centrifugal forces caused by the pipe curvature and results in a loss of energy. This movement has no counterpart in streamline flow in straight pipes. Dean (1928) also presented the ratio of the flux in a curved pipe to that in a straight pipe for the same pressure gradient as being a function only of K for small r/R ratios. The relationship developed was only applicable up to $K = 650$.

C. M. White (1929) furthered the study of Dean for the laminar flow of water and mineral oil of different viscosities through curved pipes with curvature ratios of 1/15, 1/50, and 1/2050. White (1929) showed that the onset of turbulence did not depend on the value of the Reynolds number alone, nor the Dean criteria [$De = \mathrm{Re}(r/R)^{1/2}$]. For a curvature of 1/15, a Reynolds number of 9000 was needed to sustain turbulence, whereas for a curvature ratio of 1/2050 no marked difference for the critical velocity was needed to achieve turbulence compared to a straight tube. White (1929) concluded flow in curved pipes is more stable than flow in straight pipes. White (1929) also studied the resistance to flow as a function of the Dean criteria and the Reynolds number. For values of *De* less than 11.6, there was no difference in flow resistance compared to a straight pipe.

Topakoglu (1967) used an approximate solution using stream-functions to determine the flow pattern for steady laminar flows of an incompressible viscous fluid in curved pipes. Results showed that the flow rate depended on two independent variables, the Reynolds number and the curvature of the pipe. McConalogue and Srivastava (1968) performed numerical studies to determine the characteristics of the secondary flow for fully developed laminar flow. Their results showed that as the axial velocity was increased, the maximum value of the axial velocity moved towards the outer wall and the secondary vortices also migrated closer to the outer wall.

Numerical studies of laminar flow were performed by Truesdell and Adler (1970) using a square mesh. They found that the numerical procedure could be used to Dean numbers up to 200, further increase in the Dean number caused divergence of values resulting from their solution method. Helical coils with both circular and elliptical cross sections were used. The numerical procedure was based on toroidal geometry. Results were compared with experimental results from the literature. Smith (1976) analytically studied laminar flow in curved tubes for large Dean numbers. Results were presented for tubes with circular cross-sections as well as for tubes with triangular and rectangular cross-sections.

Dennis and Ng (1982) numerically studied laminar flow through a curved tube using a finite difference method with emphasis on two versus four vortex flow conditions. They ran simulations in the Dean range of 96 to 5000. The four vortex solutions would only appear for a Dean number greater than 956. Masliyah (1980) studied the secondary flow of a laminar flow in a curved semicircular duct using both numerical and experimental methods. The numerical results showed that for Dean numbers above 105, the secondary flow could have two solutions, either a two- or four-vortex secondary flow pattern, depending on the initial guess of the flow field. In the flow visualization studies both types of flows were observed. Nandakumar and Masliyah (1982) further studied this phenomena and reported that using a bipolar-toroidal coordinate system worked better for predicting the four-vortex solution, and that it was easier to produce four-vortex solutions for curved semicircular pipes than for curved circular pipes. However, using the results of a semicircular pipe as the initial conditions for pipes with increasing circularity made it possible to predict four-vortex solutions where a direct solution would fail in its endeavor (Nandakumar and Masliyah, 1982). Dennis and Riley (1991) developed an analytical solution for the fully developed laminar flow for high Dean numbers. Though they could not find a complete solution to the problem, they stated that there is strong evidence that at high Dean numbers the flow develops into an inviscid core with a viscous boundary layer at the pipe wall.

The flow of a magnetic fluid through a helical coil was studied analytically by Verma and Ram (1993) for low Reynolds number flows. They found that the torsion does not affect the flow rate, for the order that they considered. However, they also stated that the flow could not be expressed based only on the Dean number.

Park et al. (1999) used a laser photochromic velocimetry method to measure the velocity of the flow in a curved tube with Reynolds number of 250 and a curvature ratio of 1:6. Wall shear stress, the vorticity, and the pressure field were then determined from the measured velocities. The measured results were compared to numerical results and showed good agreement (Park et al., 1999).

Unsteady viscous flow in curved pipes varies somewhat compared to steady flow. Lyne (1970) predicted unsteady flow resulting from a sinusoidal pressure gradient. Results showed that the secondary flow could be in the opposite direction compared to steady pressure gradients; these predictions were validated with experimental work (Lyne, 1970). Zalosh and Nelson (1973) furthered the study of unsteady flows by studying pulsating flows in curved tubes for fully developed laminar flows with pressure gradients that oscillated sinusoidally in time. Three different solutions to the problem were given. The reversal of the secondary flow as noted by Lyne (1970) was also confirmed.

Studies on helically coiled tubes with rectangular cross sections have also been performed. Numerical studies by Joseph et al. (1975) were carried out for this geometry for laminar flow with Dean numbers ranging from 0.8 to 307.8. Their results for Dean numbers less than 100 showed two secondary flow vortices similar to that found with circular cross sections. However, when the Dean number was increased above 100, four vortices were present; they confirmed these vortices with experimental flow visualization experiments (Joseph et al., 1975). These studies were furthered to including oscillation of the coils (Joseph and Adler, 1975). Joseph and Adler (1975) found that if the oscillations are strong enough the secondary flow would reverse the direction.

Two-phase flow of an air-water mixture was studied by Whalley (1980) to determine the local liquid film thickness and the liquid film flowrate around the tube periphery. Results showed that for most cases the maximum liquid flowrate was on the inside of the bend. Film thickness varied substantially around the tube periphery.

The effect of bend curvature on fully developed turbulent pipe flow was studied by Anwer et al. (1989). Using a Reynolds number of 50 000 and a pipe-to-bend radius of 0.077, the authors measured the effects of a U-bend on the downstream flow after the bend. They showed that the flow was still affected by the bend at a distance of 18 pipe diameters downstream. The energy of the secondary flow is only dissipated by viscous dissipation, explaining why it takes so long for the flow to return to the expected straight tube profile (Anwer et al., 1989).

Flow patterns for turbulent flow in a curved tube were studied using large eddy simulations by Boersma and Nieuwstadt (1996) for fully developed flow. They compared their numerical results with experimental results from the literature and showed that their results from the large eddy simulations were acceptable and that this approach for determining secondary flow patterns is feasible. Huttl and Friedrich (2001) used direct numerical simulation for turbulent flow in straight, curved and helically coiled pipes in order to determine the effects of curvature and torsion on the flow patterns. They showed that turbulent fluctuations are reduced in curved pipes compared to the straight pipes. They also demonstrated that the effect of torsion on the axial velocity is much lower than the curvature effect (Huttl and Friedrich, 2001).

Three-phase flow involving an oil-air-water mixture was studied by Chen and Guo (1999) with the hope to use helical coils in a separation technique for the petroleum industry. More than four flow patterns were observed in their work. Correlations to predict the pressure drop were presented. Two-phase air-water mixture flows were studied in helically coiled tubes by Watanabe et al. (1993). The thickness of the water film on the wall of the tubes was measured at different points around the circumference of the tube. The wave height and its characteristics were discussed.

Anwer and So (1993) experimentally studied the effects of swirling flow on the flow patterns in a curved pipe. Their experimental setup consisted of a rotating drum which resulted in a swirling turbulent flow prior to entering a curved pipe. Their objectives were to study the combined effect of the swirl and the bend curvature on the secondary flows by measuring the shear stress, static pressure, and turbulent flow properties. For their case they found that the superimposed solid-body rotation (swirl) completely dominated the secondary flow, though they used a strong swirl and this many not be the case for weaker swirls. They also found that the wall static pressure was lower on the outer bend than the inner bend, which is opposite to normal secondary flow caused by curvature.

There are several papers published which deal with the flow in curved ducts with non-circular geometry and for curved channels, as well as for varying curvature. These works are not pertinent to this research project, though the interested reader can refer to the following selected papers for more information: Eason et al. (1994), Bolinder and Sunden (1996), Silva et al. (1999), Gammack and Hydon (2001), Thomson et al. (2001), Chandratilleke and Nursubyakto (2003), Eagles (2003).

3.3 Pressure Drop and Friction Factors

Ito (1959) performed experiments on smooth curved pipes with curvature ratios from 1/16.4 to 1/648 to determine the friction factors for turbulent flow. Ito (1959) presented resistance formulas based on the $1/7^{th}$ power law, and from the logarithmic velocity-distribution law. For $\mathrm{Re}(r/R)^2$ in the range of 0.034 to 300, the resistance law is as follows:

$$f_c\left(\frac{R}{r}\right)^{1/2} = 0.029 + 0.304\left[\mathrm{Re}\left(\frac{r}{R}\right)^2\right]^{-1/4} \tag{2.1}$$

For values of $\mathrm{Re}(r/R)^2$ below 0.034, the friction factor was equivalent to that of a straight pipe. For large values of $\mathrm{Re}(r/R)^2$ the following empirical equation was presented and may be used for $\mathrm{Re}(r/R)^2$ values over 6:

$$f_c\left(\frac{R}{r}\right)^{1/2} = \frac{0.316}{\left[\mathrm{Re}\left(\frac{r}{R}\right)^2\right]^{1/5}} \tag{2.2}$$

Barua (1962) analyzed the motion of flow in a stationary curved pipe for large Dean numbers. The analyses assumed a non turbulent core where fluid moved towards the outer periphery and a thin boundary layer where fluid moved back to the inner periphery of the tube. A relationship between the friction factor of a curved tube and a straight tube was made based on a power series in *De*. This was compared to the experimental observations of other authors and was found to be in fair agreement. The agreement was better for higher values of *De* than at low values. Nunge and Lin (1973) reported on the comparison of friction factors between straight tubes and curved tubes for varying curvature ratios, concentrating on highly curved tubes. Their work showed that at high Dean numbers, the ratio of the friction factors decreased for increasing curvature. These results contradicted the results of Austin and Seader (1973). Sarin (1997) showed that the highest shear stress was on the outside wall and the lowest shear stress was on the inside wall for an elliptical cross section. Tarbell and Samuels (1973) developed the following friction factor correlation that is based on the Reynolds number and the curvature ratio, rather than just the Dean number. It was recommended for situations with Dean number ranging from 20 to 500.

$$\frac{f_c}{f_s} = 1.0 + \left[8.279\times10^{-4} + \frac{7.964\times10^{-3}}{R/r}\right]\mathrm{Re} - 2.096\times10^{-7}\,\mathrm{Re}^2 \tag{2.3}$$

Akagawa et al. (1971) measured the pressure drop and developed a correlation for the flow of a two-phase (gas-liquid) flow for helically coiled tubes using different curvature ratios. They found that the friction factors in their work ranged from 1.1 to 1.5 times as much as that in a straight pipe.

Two phase flow of a gas-liquid mixture through helical coils was studied by Kasturi and Stepanek (1972) and they determined correlations for the pressure drop and the void fraction. A helical coil with an inner diameter of 12.5 mm and a radius of curvature of 332.5 mm was used for the following combinations: air-water, air-corn-sugar-water, air-glycerol-water, and air-butanol-water (Kasturi and Stepanek, 1972). The pressure drop was correlated with the Lockhart-Martinelli and Dukler's correlations and the void fraction was correlated with the Hughmark's correlation. In both cases, Kasturi and Stepanek (1972) suggested that the Lockhart-Martinelli parameter could be modified to obtain better correlations. New correlating parameters were developed to predict the pressure drop; these correlating parameters take the Lockhart-Martinelli parameters and Reynolds numbers into consideration (Stepanek and Kasturi, 1972).

Experimental studies of the pressure drop were performed by Rangacharyulu and Davies (1984) for two-phase flow of air-liquid. They developed a new correlation for the two-phase flow based on a modified Lockhart-Martinelli parameter.

Grundmann (1985) published a technical note on a friction diagram for hydraulic smooth pipes and helical coils. The friction factors for the helical pipes were based on previously published friction factor correlations. Hart et al. (1988) also produced a friction factor chart for helically coiled tubes. It covered a Reynolds range from 0 to 200 000, and a curvature ratio from 0 to 0.2. Hart et al. (1988) also reported on the experiments performed to determine pressure gradients for gas-liquid flows which included a small liquid holdup.

Jayanti and Hewitt (1991) discussed some of the discrepancies in the calculations of friction factors for helical coils. They suggested that the calculations of Van Dyke (1978) should be extended to higher order terms to evaluate the friction factor better.

Experiments of two-phase flow were performed by Czop et al. (1994) to determine the pressure drop, shear stress, and void fraction distribution in a helical coil. They tested several mass flow rates, gas mass fractions, and density ratios. They found that the results were different than those calculated using the Lockhart-Martinelli correlation, though they faired well with the Chisholm correlation.

Guo et al. (2001a) studied the effect of inclination of the helical coil on the friction factor for single-phase and two-phase flow. They found that there was little difference for the single-phase flow though there were significant effects for two-phase flow, with increases of the friction factor up to 70% depending on the inclination angle (Guo et al., 2001a). These same authors studied two-phase flow of steam-water to characterize pressure drop oscillations in a closed loop steam generator system (Guo et al., 2001b). Pressure drop characteristics for two-phase flow were also studied by Downing and Kojasoy (2002) for miniature helical channels. Their findings suggest that pressure drop in two-phase flow can be predicted using a two-phase flow multiplier that is applied to the pressure drop calculations of single-phase flow. However, the calculation of the single-phase pressure drop needs to be performed using a less severe curvature factor (Downing and Kojasoy, 2002). This is required because two-phase flow pressure drops are less affected by curvature than single-phase flows (Downing and Kojasoy, 2002). Xin et al. (1996) experimentally measured the pressure drop and the void fractions for an air-water mixture for vertically orientated coils. They presented correlations of the pressure drop based on the superficial Reynolds number for the water flow and the Lockhart-Martinelli parameter. Similar results were found by Awwad et al. (1995) in the study of two-phase flow of an air-water mixture. They found that the pressure drop was not only dependent on the Lockhart-Martinelli parameter, but also on the flow rates of both air and water.

Ali (2001) developed a correlation between pressure drop and flow rate for helical coils by using the Euler number, the Reynolds number and a new geometrical number which is a function of the equivalent diameter of the coil (taking pitch into account), the inside diameter of the tube, and length of the coiled tube. Ali (2001) suggested that there are four regions of flow, a laminar, a turbulent, and two ranges of transitional flow. Correlations for all the regions were developed based on the three characteristic numbers.

Velocity gradients at the wall of a torus and a helical tube were measured with an electrochemical method by Galier et al. (2003) for both laminar and turbulent flow regimes. Measurements of the wall velocity gradient were made at different locations around the tube circumference. For the torus, the highest measurements were made at the outer wall and the lowest at the inner wall, as expected. In the helical tube, these measurements were slightly offset from those of the torus.

3.4 Critical Reynolds Number and Transitional Flow

Taking data from his own experiments as well as that from previous investigations, Ito (1959) developed the following empirical relation to determine the critical Reynolds number for the range of curvature ratios of 1/15 to 1/860:

$$\mathrm{Re}_{crit} = 20000\left(\frac{r}{R}\right)^{0.32} \tag{2.4}$$

For curvature ratios less than 1/860, the critical Reynolds number was found to coincide with that of a straight pipe.

Soeberg (1988) showed, for $De > 100$, the Coriolis force to influence the stability of the laminar flow, in effect, delaying the transition from laminar to transitional flow to a higher Reynolds number. Soeberg (1988) also noted that this was weakly dependent on the curvature ratio.

Velocity measurements were made by Webster and Humphrey (1993) for transitional flow though helical coils using a laser-Doppler velocimeter for a coil with a curvature ratio of 1/18.2. Their findings indicate that the coil curvature suppresses turbulent fluctuations that would normally be present in the steep velocity gradients at the walls. This ability to suppress the turbulence diminished with increasing Reynolds number (Webster and Humphrey, 1993). Their results also showed unsteady flow even when the flow was not in the turbulent range. Others have observed these flow instabilities (Taylor, 1929; Sreenivasan and Strykowski, 1983). Webster and Humphrey (1997) performed flow visualization and showed traveling wave instability in the transitional region. Numerical calculations showed the presence of these traveling waves as well (Webster and Humphrey, 1997). When studying the downstream flow of a helical coil (in a straight section), Hon et al. (1999) showed that a traveling wave originated in the helical coil and affected the flow in the straight tube.

Yamamoto et al. (1995) studied the transition from laminar to turbulent flow for helical coils with large curvature and large torsion. They concluded that while the curvature has a stabilizing effect on the flow, the torsion had a destabilizing effect. Yamamoto et al. (1998) further investigated the effect of torsion on the stability of flow by first defining a torsion parameter and then proceeded to find the critical Dean number at different torsion parameter values. They showed that as the torsion parameter increased, the critical Dean number decreased at first, reaching a minimum, then began increasing again. The lowest critical Dean number in their work was at roughly 600 (Yamamoto et al., 1998).

3.5 Influence of Pitch

Germano (1982) introduced an orthogonal coordinate system to study the effect of torsion and curvature on the flow in a helical pipe. In the results of the perturbation method indicated that the torsion had a second order effect and curvature had a first order effect on the flow (Germano, 1982), contrary to the results of Wang (1981) where torsion had a first order effect. The difference between the two studies is attributed to the coordinate system; Germano (1982) had an orthogonal system, whereas Wang (1981) used a non-orthogonal system. Further studies by Tuttle (1990) indicated that the frame of reference (coordinate system) determines if the torsion effect is first or second order; however, Tuttle (1990) agreed with Wang's conclusion that the effects are first order as the method of Wang (1981) was the best method to determine the torsion effect. Further studies by Germano (1989) confirmed that the torsion has no first order effect on the flow.

Kao (1987) studied the torsion effect on fully developed flow in a helical pipe using a series expansion method to solve the governing differential equations. It was shown in the expansion that the secondary flow patterns were affected by torsion effects leading to distortions in the patterns from the classical symmetrical shape (Kao, 1987). Further, it was also shown that the volume flux for a given pressure gradient to be affected by torsion as well; although this does not appear in the first two orders of the series expansion, but it is in the third term in the series expansion of volume-flux ratios. The first two terms were identical to those presented by Dean (1928). However, in plotting the results of the secondary flow and the axial velocities, some deviations were found between the series and the numerical solutions, mainly due to anomaly of the series solution (Kao, 1987). For the same curvature and same Dean number, the effect of torsion is seen to reduce the resistance in the pipe (Kao, 1987).

The effect of pitch on heat transfer and pressure drop was studied by Austin and Soliman (1988) for the case of uniform wall heat flux. The results showed significant pitch effects on both the friction factor and the Nusselt number at low Reynolds numbers, though these effects weakened as the Reynolds number increased. Austin and Soliman

(1988) suggested that these pitch effects are due to free convection, and thus decrease as the forced convection becomes more dominant at higher Reynolds numbers.

Xie (1990) used a perturbation method to study the fully developed laminar flow in a helical pipe using a helical coordinate system. The results suggested that curvature has no effect on the flow rate within the order of the perturbation parameter (pipe radius multiplied by curvature) squared, and that torsion exerted a second-order effect on the secondary vortices. The torsion effect could be great enough to rotate the line separating the two vortices from vertical to horizontal, for very small Reynolds numbers.

Liu and Masliyah (1993) investigated the effect of pitch and torsion on the secondary flow fields for fully developed laminar flow. They determined that the critical value for the transition of two vortices to a single vortex was based on the Dean number, the normalized curvature ratio, and the normalized torsion. The pressure drop and friction factors were also studied for fully developed laminar flow. Their findings for the pressure drop and the friction factor were further validated by experimental results of Liu et al. (1994). Liu and Masliyah (1994) numerically studied laminar Newtonian flow and heat transfer development using fully parabolic equations in the axial direction. Their studies also took into consideration the pitch of the helix. The simulations were performed with a Dean range of 20 to 5000 and a Prandtl range of 0.1 to 500. Even for small Dean and Prandtl numbers, oscillation in the Nusselt number was observed (Liu and Masliyah, 1994). The magnitude of these oscillations damped out with increased axial distance. Torsion also played a role in the developing flow field. For high torsion, the secondary flow reduced to one vortex instead of the classical two. They also showed that for high Prandtl numbers, the temperature distribution split into two profiles for low Prandtl flow (similar to two vortices) and had only one profile for high Prandtl numbers. The temperature profiles were also a function of the Dean number.

The effect of the pitch on the Nusselt number in the laminar flow of helicoidal pipes was determined by Yang et al. (1995). Numerical results for fully developed flow with a finite pitch showed that the temperature gradient on one side of the pipe will increase with increasing torsion; however, the temperature gradient on the opposite will decrease. Overall, the Nusselt number slightly decreases with increasing torsion for low Prandtl numbers, but significantly decreases with larger Prandtl numbers (Yang et al., 1995). Yang and Ebadian (1996) extend this research to turbulent flow using a κ-ε model. As in the laminar case, the torsion rotated and distorted the temperature profiles. The effects of torsion could be enhanced by increasing the axial flow velocity.

Wang and Andrews (1995) numerically studied the laminar flow of an incompressible fluid in a duct with rectangular cross section. Their work was to establish the effects of pitch ratio, pressure gradient, and curvature ratio on the fluid velocity distribution and the fluid resistance for fully developed flow using a finite difference method. They concluded that the pitch ratio affects the pattern of the secondary flow and the friction factor. As the pitch ratio is increased, the two-vortex flow developed into a single vortex flow. Friction factor is mainly affected by the curvature ratio for rectangular helical duct flow (Wang and Andrews, 1995).

Hüttl and Friedrich (2000) studied direct numerical simulation of turbulent flow in helical coils to determine the effects of curvature and torsion. It was shown that the torsion increased the secondary flow effect and tended to change its pattern, while having negligible effects on the axial velocity. Curvature tended to decrease the turbulent kinetic energy compared to a straight pipe flow (Hüttl and Friedrich, 2000).

3.6 Axial Dispersion

Koutsky and Adler (1964) studied the axial dispersion in helical coils. Their work was in the aim of limiting the magnitude of axial dispersion with an attempt to approximate plug flow. Their research showed that helical tubes are superior to straight tubes or packed beds in minimizing axial dispersion and approaching plug flow due to the secondary flow for both laminar and turbulent flow regimes (Koutsky and Adler, 1964). These results are important in many continuous flow systems, such as in continuous chemical reactors (Koutsky and Adler, 1964). Similar results by van Andel et al. (1964) found that laminar gas flow in a helical coil approached ideal plug flow; however, this was not as dramatic with liquid flow, though there was still a great reduction in the spread of the residence time distribution compared to the flow in a straight pipe.

The residence time distribution for laminar flow was studied analytically by Ruthven (1971). The effect of the secondary flow was to reduce the range of residence times in comparison with a straight tube (Ruthven, 1971; Son and Singh, 2002). For small curvatures and Reynolds numbers, the residence time distribution function will be independent of the tube length, curvature, or the Reynolds number (Ruthven, 1971). For large curvature and Reynolds numbers, the assumptions made in the derivation of the residence time distribution are not valid. Trivedi and Vasudeva (1974) furthered this work by studying the residence time distribution for a diffusion-free laminar flow and presented empirical relationships to take into account the effect of the curvature ratio on the residence time distribution. Trivedi and Vasudeva (1975) found that helical coils could reduce axial dispersion by a factor up to 500 times for laminar flow, compared to the straight pipe flow. Nunge et al. (1972) analytically determined the dispersion coefficient for laminar flow in curved tubes and found the dispersion coefficient to increase substantially compared to a straight tube with the same pressure gradient, especially at low Reynolds numbers. Nauman (1977) found an error in the work of Ruthven (1971) and Trivedi and Vasudeva (1975) where the authors did not take into account the condition that the mean of the dimensionless residence time must be unity. Nauman (1977) showed that due to this error, there was roughly a 6% error in Ruthven's (1977) work. Nauman (1977) presented correct results of the work. Through experimental work, Saxena and Nigam (1979) showed that for very low Dean numbers (0.007), the residence time distribution in helical coils was identical to those of a straight tube.

Numerical calculations of the axial dispersion in helical tubes were studied by Janssen (1976) for the case with high molecular diffusion. Results showed that the axial dispersion in these cases could be characterized by De^2Sc (where Sc is the Schmidt number) when the $De < 16$ and $R/r > 20$ (Janssen, 1976). For $De^2Sc < 100$, there were no differences in the axial dispersion compared to a straight tube, whereas between 100 and 5000, the axial dispersion coefficient was found to decrease more than threefold (Janssen, 1976). Shetty and Vasudeva (1977) correlated experimental data with the same characteristic term (De^2Sc, though they expressed it as $DeSc^{1/2}$) used by Janssen (1976). They found that the experimental results were in decent agreement with the numerical predictions of Janssen (1976) and they presented an empirical equation relating dispersion coefficients with $DeSc^{1/2}$ (Shetty and Vasudeva, 1977).

Experiments performed by Saxena and Nigam (1984) studied the residence time distribution in helical coils with flow inversion. They constructed helical coils which, after a few turns, have a change in direction of the coil axis by 90 degrees. Their hypothesis is that by bending the helical coil, the secondary flows would have to shift and this would result in increased mixing, and hence a further reduction in the residence time distribution. They showed that this narrowed the distribution significantly, even at very low Dean numbers (in the order of $De \approx 3$).

Taylor dispersion in a curved tube was studied using both Monte Carlo and numerical techniques by Johnson and Kamm (1986). They examined the effects of secondary flow on axial dispersion for Dean numbers between 0 and 13, for curvature ratios less than 1:50, and for Schmidt numbers between 1 and 1000. They found reasonable fit with experimental data.

Lee et al. (1987) demonstrated mixing of fluids in a curved tube using an Eulerian perspective. They showed the material distribution at different tube-cross sections downstream of the inlet and quantified the amount of mixing.

The residence time distribution of particles flowing through a curved tube was studied by Salengke and Sastry (1994) for food processing applications. They used two different sizes of particles and three flow rates. Their results showed that the flow profile for the particles became closer to plug flow at higher flow rates and particle sizes. They also found that the normalized residence time was affected by the ratio of the particle diameter to the tube diameter and by the particle Froude number (Salengke and Sastry, 1994). These authors also varied the particle concentration and the radius of curvature of the tube in a separate study (Salengke and Sastry, 1996). They determined that the residence time and the residence time distribution were weakly affected by the radius of curvature but was strongly affected by the particle concentration. Increasing the particle concentration tended to increase the normalized residence time, however it did not have much of an influence on the residence time distribution. Further work for heat processing applications was performed by Sandeep et al. (1997). They measured the mean and minimum residence times, along with the standard deviation (for residence time distribution) for particles flowing in a non-Newtonian fluid in a helical coil. They studied the effects of viscosity, fluid flow rate, and the size and concentration of particles on the residence time. The ratio of the mean residence time to the minimal residence time in a helical coil was found to always fall between 1.05 and 1.11, for the conditions in their study (Sandeep et al., 1997).

Castelain et al. (1997) studied residence time distributions in helically coiled systems and in chaotic systems for Reynolds numbers in the range of 800 to 13 500. Their findings showed that for Reynolds numbers greater than 2 500, the chaotic systems had more than 20% less axial dispersion compared to helical coils with the same number of bends. In general, the mass Péclet number increased with increasing Reynolds number for helically coiled tubes (Castelain et al., 1997). The effect of chaotic systems on the rate of chemical reactions was studied by Sawyers et al. (1996) for simple chemical reactions. They compared the rates of reaction in chaotic systems to those in helical and straight tube reactors. The rate of reaction tended to be higher in the chaotic system (Sawyers et al., 1996). Further work on chaotic heat exchangers was performed by Mokrani et al. (1997). They compared the heat transfer rates between a chaotic system and a helical coil. The chaotic coil was built by assembling 90° bends and each bend was turned by 90° from the previous bend. Both heat exchangers had the same length and surface area. They found that the heat exchange in the chaotic coil was 13 to 27% higher than that of the helical coil. The Reynolds number of the flow ranged from 60 to 200.

Residence times for particles flowing in bends were studied by Grabowski and Ramaswamy (1998) experimentally for the flow of different food particles in both Newtonian and non-Newtonian fluids. They found that particles experienced a greater residence time in a curved tube than in a straight tube of the same length. The particle velocity was affected by the viscosity, and the shape and size of the particle.

Gao et al. (2002) studied liquid-solid separation of two-phase turbulent flow in curved pipes using a sand-water mixture. They performed two-dimensional numerical calculations for flow separation and performed experiments to test the model. Based on the results of these experiments they suggested some design ideas to enhance the separation efficiency.

The residence time distribution was determined for the flow of particles in helical tubes and in tubes that were bent in a figure-8 pattern by Palazoglu and Sandeep (2002). They found that the beneficial effect of the secondary flow in figure-8 coils was partially negated due to the crossing over, where the secondary flow would be forced to change directions. Curvature ratio and flow rate were found to be the most important parameters that affected the flow of the particles.

In an area related to axial dispersion, Kubie and Gardner (1977a) measured the size distribution and the maximum size of drops in a liquid-liquid system and studied the dispersion of drop over the tube cross section. These were done for both straight tubes and helically coiled tubes. There was good agreement between prediction and measurement for the experiments with helical coils, despite the fact that the secondary flow was not taken into account in the calculations. Kubie and Gardner (1977b) continued these studies by using a two-phase flow of *n*-butyl acetate and water, and iso-amyl alcohol and water mixtures in a helical coil. They determined that either completely stratified flows or flows with completely separated drops would occur until the velocities reached a high enough value when the drops would become small enough to be dispersed in the other fluid.

3.7 Heat Transfer

Seban and McLaughlin (1963) studied heat transfer in coiled tubes for both laminar and turbulent flows. They instrumented the coils with pressure taps and thermocouples. Thermocouples were placed on the inside and outside periphery of the coils at each turn. Plots of Nusselt versus Graetz numbers were presented for coils with curvature ratios of 1/17 and 1/104 with Reynolds numbers ranging from 12 to 5 600 for the laminar flow region. Prandtl numbers ranged from 100 to 657. The results showed that the outer periphery had higher Nusselt numbers than the inner (ratio of roughly four for the curvature ratio of 1/17), with both being substantially higher than theoretical Nusselt numbers for a straight pipe under the same conditions. The results also indicated an effect on the Nusselt numbers due to a thermal entry length. Seban and McLaughlin (1963) also correlated their Nusselt numbers based on the Reynolds number and the friction factor as:

$$\mathrm{Nu} = 0.644\,\mathrm{Pr}^{1/3}\left[\frac{f}{8}(\mathrm{Re})^2\frac{2r}{x}\right]^{1/3} \qquad (2.5)$$

However, Seban and McLaughlin (1963) fit their equation to the data using the above correlation in the following alternative form:

$$\mathrm{Nu} = \mathrm{A}\,\mathrm{Pr}^{1/3}\left[\frac{f}{8}(\mathrm{Re})^2\right]^{1/3} \tag{2.6}$$

The value of A was 0.13 for the coil and a curvature ratio of 1/17. The fit was not as good when the above equation was used for a curvature ratio of 1/104, though changing the value of A produced better fit. Seban and McLaughlin (1963) used the same experimental setup and methods to determine the friction factor and the Nusselt number relationships for turbulent flow of water in the same coils as mentioned above. The Reynolds and Prandtl numbers for the turbulent flow tests ranged from 6 000 to 65 600 and from 2.9 to 5.7, respectively. The ratios of the inside to outside periphery heat transfer coefficients were of the order of 2 and 4 for the coils with curvature ratios of 1/104 and 1/17, respectively. Seban and McLaughlin (1963) compared their average coefficients to the following relationship and found that there was no greater than 10 % and 15 % deviation for the coils with curvature ratios of 1/104 and 1/17:

$$\mathrm{Nu}\,\mathrm{Pr}^{-0.4} = \frac{f}{8}\mathrm{Re} \tag{2.7}$$

Heat transfer and pressure loss in steam heated helically coiled tubes were studied by Rogers and Mayhew (1964). They noticed that even for a steam heated apparatus, uniform wall temperature was not obtained, mainly due to the distribution of the steam condensate over the coil surface. They proposed the following relationship for the inner Nusselt number based on the film temperature:

$$\mathrm{Nu} = 0.021\,\mathrm{Re}^{0.85}\,\mathrm{Pr}^{0.4}(r/R)^{0.1} \tag{2.8}$$

Mori and Nakayama (1965) studied fully developed flow in a curved pipe with a uniform heat flux for large Dean numbers. Both theoretical and experimental flow and temperature fields were investigated. They assumed that the flow was divided into two sections, a small boundary layer near the pipe wall, and a large core region making up the remaining flow. In the core region, the secondary flow was assumed to be completely horizontal, transporting the fluid to the outside of the pipe. The fluid returned to the inner wall via the boundary layer. This pattern differed for that of small Dean numbers. Through their theoretical analysis, they deduced that the additional flow resistance of a curved pipe is caused by stress due to the secondary flow. They also developed a ratio between the thickness of the temperature and velocity boundary layers, expressed in terms of the Prandtl number. The Nusselt number ratio between straight and curved pipes was shown to be a function of the Dean number and the ratio between the thickness of the thermal and hydrodynamic boundary layers. Experiments performed with a curvature ratio of 1/40 were used to validate the theory. Profiles of both temperature and velocity supported the theoretical analysis.

Data on the pressure drop and heat transfer for laminar flow of glycerol was presented by Kubair and Kuloor (1966) for different types of coiled pipes, including helical and spiral configurations. Reynolds numbers were in the range of 80 to 6000 with curvature ratios in the range of 1/10.3 to 1/27. The number of turns ranged from 7 to 12. A steam bath was used to provide constant temperature wall conditions on the outside of the coil. The authors also noted that the results for the interaction between heat transfer rates and the Graetz number of Berg and Bonilla (1950) were opposite to those of Seban and McLaughlin (1963). The authors (Kubair and Kuloor, 1966) speculated that this difference might have been due to the fact that the two studies used different boundary conditions, one being constant wall temperature (Berg and Bonilla, 1950) and the other at constant heat flux (Seban and McLaughlin, 1963). One of the coils used by Kubair and Kuloor (1966) had the same curvature ratio as one of the coils used by Seban and McLaughlin (1963). The results of Kubair and Kuloor (1966) coincided with those of Seban and McLaughlin (1963) at low Graetz numbers, but deviated at higher Graetz numbers. The following Nusselt number relationship was developed based on the curvature ratio (r/R) and the Graetz number (Gz):

$$\mathrm{Nu} = [1.98 + 1.8(r/R)]\mathrm{Gz}^{0.7} \tag{2.9}$$

for the range of $10 < \mathrm{Gz} < 1000$, $80 < \mathrm{Re} < 6000$, and $20 < \mathrm{Pr} < 100$.

Mori and Nakayama (1967a) studied the flow field and heat transfer in a fully developed turbulent flow both theoretically and experimentally. Heat transfer was studied for the constant heat flux system and the variations of physical properties with temperature were not taken into account in the development. The analysis was performed assuming a thin boundary layer along the pipe wall, similar to the work of Mori and Nakayama (1965). Average Nusselt numbers around the periphery were calculated. It was shown that the difference between the Nusselt numbers for a straight and a curved pipe decreased slightly as the Prandtl number became large, which is opposite to the results found for laminar flow (Mori and Nakayama, 1965, 1967a). Experiments were performed with air flowing through curved pipes with curvature ratios of 1/18.7 and 1/40.

Mori and Nakayama (1967b) extend their earlier work to the theoretical analysis of uniform wall temperature rather than uniform heat flux. The results show that the formula for the Nusselt number of the uniform wall temperature is the same as that for uniform heat flux. The Nusselt number relationships developed in the previous work (Mori and Nakayama, 1965) for laminar flow were presented in a more practical form. The change of physical properties with temperature was studied for air, water, and oil. With the exception of laminar flow of water, the arithmetic mean temperature of the physical properties between the inlet and outlet could be used.

Both the outside-film and inside-film heat transfer coefficients in an agitated vessel were studied by Jha and Rao (1967). Five different coils were studied, along with different speeds and locations of the agitator. They developed an equation to predict the Nusselt number based on the geometry of the helical coil and the location of the agitator.

A method of series expansion was used by Ozisik and Topakoglu (1968) to solve the heat transfer for fully developed laminar flow with constant heat flux. The results showed that the heat transfer is dependent on three independent numbers, the curvature ratio of the pipe, Reynolds number, and Prandtl number.

Boiling of water was studied by Owhadi et al. (1968) in two different sized helical coils. Water was pumped through the coils and the coils were heated by direct current resistance in the wall of the tubes. They found that at lower vapour qualities (less then 80%), there were high heat transfer coefficients around the whole tube periphery. However, the highest coefficients were at the outer wall. At vapour qualities of 95% and higher, the top and bottom of the tube became dry.

Akiyama and Cheng (1971) numerically studied the condition of a steady fully developed laminar forced convection in uniformly heated curved pipes for a range of Dean numbers up to about 200. The solution employed a boundary vorticity method with a uniform wall heat flux and peripherally uniform wall temperature. A numerical approach was used as perturbation methods are known to diverge quickly as the Dean number increases (Akiyama and Cheng, 1971). Akiyama and Cheng (1971) showed that as the Dean number increased, the center of the secondary circulation moved towards the outer wall. However, in the horizontal direction, it first begins to move towards the outer wall, but with further increase in the Dean number, the center begins to move back towards the inner wall. From the streamlines produced at a Dean number of 196, Akiyama and Cheng (1971) suggested that the boundary layer approximation that has been used by other researchers (Barua, 1962; Mori and Nakayama, 1965) couldn't be applied. They also showed that when using the boundary layer approximation the predictions of the friction factor-Reynolds number value had the wrong trend for low Dean numbers. Akiyama and Cheng (1972) extended their work to include the thermal boundary condition of uniform wall temperature. They showed that the heat transfer results from the two different boundary conditions are quite similar, but distinct, for laminar flows. Some of their results contradicted Mori and Nakayama (1967b).

Numerical studies for uniform wall heat flux with peripherally uniform wall temperature for Dean numbers in the range of 1-1200, Prandtl numbers of 0.005-1600, and curvature ratios (r/R) of 1/10 to 1/100 for fully developed velocity and temperature fields were performed by Kalb and Seader (1972). An orthogonal toroidal coordinate system was used with the assumption that for small pitch a toroidal coordinate system can approximate a helical coordinate system. They found that the curvature ratio parameter had negligible effect on the average Nusselt number for any given Prandtl number. However, the curvature ratio did have an effect on the peripheral variation of the Nusselt number, though this effect was still not large. For Prandtl numbers greater than 0.7, it was shown that the local Nusselt number in the area of the inner wall was always less than that of a straight tube, and increasing less as the Dean number is increased till it reached a limiting value. The local Nusselt numbers on the outer wall continued to increase with increasing Dean number (Kalb and Seader, 1972). Kalb and Seader (1972) also noted that the fractional increase in heat-transfer coefficients is significantly greater than the fractional increase in friction losses, except for liquid metals. The following Nusselt relationship was developed for low Prandtl numbers (0.005 to 0.05) with Dean numbers in the range of 20 to 1200:

$$\overline{Nu} = 3.31 De^{0.115} Pr^{0.0108} \tag{2.10}$$

For Prandtl numbers in the range of 0.7 to 5 and Dean numbers of 80 to 1200, the following average Nusselt number relationship was developed:

$$\overline{Nu} = 0.913De^{0.476}\,Pr^{0.200} \tag{2.11}$$

Kalb and Seader (1974) furthered this work by applying the method to the case of a uniform wall-temperature boundary condition with Dean numbers up to 1200, Prandtl numbers and curvature ratios in the ranges of 0.05 to 1600 and 10 to 100, respectively. Their results showed that there is a slight effect of curvature on the peripheral variation of the Nusselt number. However, it did not affect the average Nusselt number. Like Akiyama and Cheng (1971), Kalb and Seader (1974) found that the thermal boundary condition had a significant effect on the temperature field.

Austin and Seader (1973) numerically solved the equations of fluid motion for the case of steady, fully-developed, isothermal, incompressible, viscous Newtonian flow in toroidal-type coiled-tube geometry. A finite-difference approach was used with first central-difference operators that were solved by a sequential application of a successive over-relaxation technique. However, the effect of coil pitch was not taken into consideration; Austin and Seader (1973) speculated that the pitch effect might become important as the radius of curvature approaches the radius of the tube. The ranges of Dean number, Reynolds Number, and curvature ratio were 1 to 1000, 10 to 4000, and 1/5 to 1/100, respectively. For low Dean numbers, the authors showed that the axial-velocity profile was essentially parabolic as in the straight tube case. As the Dean number is increased, the maximum velocity began to be skewed toward the outer periphery. It was shown that for Dean numbers greater than 10, the maximum axial velocity on the horizontal axis tends to move towards the outer periphery. Austin and Seader (1973) showed that the pressure distribution is dependant mainly on the Dean number and that the pressure increases smoothly from the inner to the outer periphery. The axial-pressure gradient was correlated to the friction factor, which showed a slight dependence on the curvature ratio. The numerical simulations of the secondary flow showed that at a Dean number of 1.0 and a curvature ratio of 1/100, the center of the secondary flow vortex was close to the center of the tube horizontally and situated slightly closer to the median than the upper tube wall in the vertical direction. The streamlines around the vortex were rather symmetrical. However, when the Dean number was increased the center of the vortex was seen to move upwards and inwards. The streamlines lost their symmetrical appearance. Changing the curvature ratio had a slight effect on the secondary flow streamlines for the same Dean number, indicating that the effect of curvature ratio was almost completely accounted for in the Dean number (recall that the Dean number is a function of the curvature ratio). The numerical results of Austin and Seader (1973) differed significantly from the model of Mori and Nakayama (1965).

The effects of buoyancy forces on fully developed laminar flow with constant heat flux were studied analytically by Yao and Berger (1978). Their studies were based on the Boussinesq approximation for the buoyancy forces and analyzed for both horizontally and vertically orientated curved pipes. Nusselt number relationships based on the Reynolds number, Raleigh number and Dean number are presented for both orientations.

Laminar convective heat transfer was studied both experimentally and numerically by Janssen and Hoogendoorn (1978) for both uniform heat flux and constant wall temperature. The thermal entry region was also studied and it was shown that the length of the thermal entry region was mainly dependent on a certain number of secondary flow circulations that were required to develop the temperature distribution. The effect of the different kind of boundary conditions was shown to be small (Janssen and Hoogendoorn, 1978).

Fully developed laminar flow and heat transfer was studied numerically by Zapryanov et al. (1980) using a method of fractional steps for a wide range of Dean (10 to 7000) and Prandtl (0.005 to 2000) numbers. Their work focused on the case of constant wall temperature and showed that the Nusselt number increased with increasing Prandtl numbers, even for cases at the same Dean number. They also presented a series of isotherms and streamlines for different Dean and Prandtl numbers.

Jensen and Bergles (1982) studied the effect of non-uniform circumferential heat flux distribution on forced convection boiling in helical coils. They stated that this non-uniformity can occur during the process of making the coils, which results in large heat flux distribution on the inner wall of the tube. Their work focused on the large heat flux distribution towards the outer wall, which is similar to solar energy concentrator, where there is a non-uniform distribution and the highest flux is located on the outside wall (Jensen and Bergles, 1982).

Temperature distribution and Nusselt numbers, both local and peripherally averaged, were determined by Rabadi et al. (1982) for fully developed pulsating laminar flow in a curved tube. The heat transfer boundary conditions of the tube wall were of axially uniform heat flux with a peripherally uniform wall temperature. They showed that the Nusselt number varied to a large degree both around the periphery of the tube as well as during cycles. These effects were higher for large Prandtl numbers and for low values of the frequency parameter.

Gaseous solid suspension flows in curved tubes was studied by Shimizu et al. (1984) with the intent to show the heat transfer increase due to the suspended solids. The use of suspend solids tends to break up the thermal boundary layer near the wall of the tubes. Since the suspend solids in the flow are at a heavier density than the gas, they do not travel along the same streamlines in curved pipe sections, and tend to travel further outward towards the outer wall and enter the viscous sublayer creating disturbance. They showed that increasing the solid loading ratio tended to increase the ratio of the suspension Nusselt number to the single phase Nusselt number.

The effect of buoyancy on the flow field and heat transfer was studied numerically by Lee et al. (1985) for the case of fully developed laminar flow and axially constant heat flux with a peripherally constant wall temperature. They found that buoyancy effects resulted in an increase in the average Nusselt number, as well as modifying of the local Nusselt number distribution. It was also found that the buoyancy forces result in a rotation of the orientation of the secondary flow patterns. Buoyancy forces were also studied for fully developed laminar flow by Futagami and Aoyama (1988) both numerically and experimentally. They produced an expression to predict the average Nusselt number for situations where both the secondary flow and buoyancy forces were important on the heat transfer coefficients. The experiments were conducted with uniform heat flux boundary conditions and were performed in the range where both centrifugal and buoyancy forces affected the secondary flow.

The heat transfer to a helical coil in an agitated vessel has been studied (Havas at al., 1987) and a correlation was developed for the outer Nusselt number based on a modified Reynolds number, Prandtl number, viscosity ratio, and the ratio of the diameter of the tube to the diameter of the vessel. In developing this correlation, the calculations of the heat transfer coefficient on the outside of the tube was done by taking the total heat flux, temperature difference, and the internal heat transfer coefficient; the value of the latter was taken from the literature.

The effect of the Prandtl number on the heat transfer in helical pipes was studied by Xin and Ebadian (1997) on both the average and local Nusselt numbers. In their studies, different torsions and curvature ratios were considered along with three different fluids, air, water and ethylene glycol. They concluded that the peripheral Nusselt numbers for laminar flow showed larger variation for higher Prandtl and Dean numbers.

Li et al. (1999) numerically investigated turbulent heat transfer in curved pipe for developing flow with water near the critical point using a control volume finite element method. In their work, buoyancy forces strongly affected the secondary flow, as these forces were much stronger than the centrifugal forces near the critical point. The heat transfer coefficient and the friction factor both increased significantly when the pressure approached the critical point. There was also an oscillatory behavior noted for the friction factor, similar to what has been seen with the Nusselt number in developing flows (Li et al., 1999).

Heat transfer enhancements due to chaotic particle paths were studied by Acharya et al. (1992, 2001) for coiled tubes and alternating axis coils. This chaotic stirring had been proposed by other authors (Jones et al., 1989) as a method for increasing stirring efficiency by non-mechanical means. The results of Acharya et al. (1992, 2001) showed that alternating the direction of the coil axis could increase the heat transfer rates of a coiled tube heat exchanger. They developed the following two correlations of the Nusselt number, for Prandtl numbers less than and greater than one, respectively.

$$Nu = 0.69\left(\frac{r}{R}\right)^{0.13} \mathrm{Re}^{0.5}\,\mathrm{Pr}^{0.43} \tag{2.12}$$

$$Nu = 0.67\left(\frac{r}{R}\right)^{0.13} \mathrm{Re}^{0.5}\,\mathrm{Pr}^{0.21} \tag{2.13}$$

Further studies were performed by Chagny et al. (2000) where the heat transfer rates between chaotic and helical coils (both with 33 bends) were studied for a Reynolds range of 30 to 30 000 and for different Prandtl numbers. Their results showed that there was a thermal advantage at low Reynolds numbers (<1000) as the heat transfer rates were higher in the chaotic system and it was more homogenous. At higher Reynolds numbers the effect was not as noticeable (Chagny et al., 2000). Lemenand and Peerhossaini (2002) developed a Nusselt number correlation based on the Reynolds number, Prandtl number and the number of bends in the pipe. For the same Reynolds and Prandtl numbers, their work showed that the Nusselt number slightly decreased with increasing number of bends (Lemenand and Peerhossaini, 2002). Yang et al. (2000) studied a system with periodically varying curvature, much like the chaotic systems developed above. Their findings showed that changing the amplitude or the wavelength of the curved pipe could increase the heat transfer rates.

Heat transfer for pulsating flow in a curved pipe was numerically studied by Chung and Hyun (1994) for strongly curved pipes with substantial pulsation amplitudes. Local Nusselt numbers were developed based on the Womersley number (ratio of transient inertial to viscous forces), which is a function of the pipe radius, the kinematic viscosity, and the frequency of the pulsation. It was found that the strength of the Womersley number affected the distribution of the Nusselt number around the periphery. Further work on pulsating flow was performed by Guo et al (1998) for fully developed turbulent flow in a helical coiled tube. In their work they studied both pulsating flow and steady state flow. They proposed the following correlation for steady turbulent flow for the Reynolds number range of 6000 to 180000 (Guo et al., 1998).

$$Nu = 0.328\,\mathrm{Re}^{0.58}\,\mathrm{Pr}^{0.4} \tag{2.14}$$

They noted that as the Reynolds number was increased to very large values (>140 000), the heat transfer coefficient for coils began to match the heat transfer coefficient for straight tubes. They also presented correlations of the peripheral local heat transfer coefficients as a function of the average heat transfer coefficients, Reynolds number, Prandtl number, and the location on the tube wall. Correlation of the Nusselt number as a function of the Womersley number were also given.

The combined effects of curvature and buoyancy on the heat transfer rates in fully developed laminar flow were numerically studied by Goering et al. (1997). They used a control volume approach to solve the Navier-Stokes equations and the energy equation, using the Boussinesq approximation to take the buoyancy into account. Two thermal boundary conditions were used, both of constant heat fluxes, but one was a constant peripheral heat flux while the other had a constant peripheral wall temperature. Regime maps were presented for both boundary conditions which split the heat transfer into three regimes; curvature dominant, buoyancy dominant, and an area where both factors were important. These areas can also be labeled as forced convection, mixed convection, and free convection, respectively (Goering et al., 1997).

Bai et al. (1999) experimentally studied turbulent heat transfer from horizontal helical coils. They concluded that as the Reynolds number is increased, the contribution of secondary flow to the heat transfer diminished and the heat transfer approaches that of a straight tube. This is due to the fact that as the Reynolds number increases the boundary layer becomes smaller. It is the large boundary layer that is shed off into the center of the tube by the secondary flow that increases the heat transfer coefficient, and this effect decreases with increasing Reynolds number (Bai et al., 1999). The local heat transfer coefficient on the outer wall can be 3 to 4 times that of the inner wall. They developed a correlation of the Nusselt number as a function of the location on the periphery. They also developed a Nusselt number correlation; however it did not contain the Dean number as only one size of coil was used in the experiment.

Comparisons for the heat transfer coefficients between straight tubes and helically coiled tubes immersed in a water bath were performed by Prabhanjan et al. (2002). Findings showed that the heat transfer coefficient were greater in the helically coiled system.

Inagaki et al. (1998) studied the outside heat transfer coefficient for helically coiled bundles for Reynolds numbers in the range of 6000 to 22 000 and determined that the outside Nusselt number could be described by the following relationship for their particular setup:

$$Nu = 0.78\,\mathrm{Re}^{0.51}\,\mathrm{Pr}^{0.3} \tag{2.15}$$

Sillekens et al. (1998) numerically studied the effects of buoyancy on the developing flow in a helical coil. Results showed that in general an increasing Grashoff number resulted in higher heat transfer and that there was a strong interaction between centrifugal and buoyancy effects, resulting in complex secondary flow. Strong buoyancy forces resulted in significant changes to the secondary flows normally described in literature for helical coils.

The combined effects of convective and thermal radiation heat transfer were studied numerically by Zheng et al. (2000) for laminar flow. For the range of parameters used in their study, they did not find any influence of the thermal radiation on the velocity field (both axial velocity and secondary flows) or on the temperature field. However, the heat transfer was significantly enhanced when the thermal radiation was taken into account.

Takahashi and Momozaki (2000) experimented with a two-phase mixture of air and mercury along with a magnetic field to determine the heat transfer characteristics of such a system. Their work studied the combined effect of the magnetic force and the centrifugal force on the flow of mercury and its effects on the heat transfer rates.

Two-phase flow of a steam-water mixture in a helical coil was studied experimentally by Guo et al. (2002) to determine the heat transfer rates for the transient case and with pulsating flow. Their results showed that the pulsating flow caused a significant variation in the peripherally time-averaged Nusselt numbers and the local Nusselt numbers. They also stated that the factors that affected oscillatory heat transfer were the Reynolds number, Prandtl number, and the oscillatory amplitude and frequency.

Boiling heat transfer in helical coils for steam-water was studied by Zhao et al. (2003) for a range of steam quality, mass fluxes, and heat fluxes. They presented a new correlation for pressure drop and found that the Lockhart-Martinelli type of correlations did not satisfactorily represent their experimental data. They proposed a new boiling heat transfer correlation for their data. Furthermore, they found that the boiling heat transfer was dependent on both the mass and heat fluxes.

Dry-out characteristics were studied experimentally by Kaji et al. (1995) for a two-phase flow through helical coils. Their work also studied wall temperature fluctuations and compared the results to straight tube experiments. Other works that describe dry-out in helical coils can be found in: Cumo et al. (1972), Unal et al. (1981), Styrikovich et al. (1984), Berthoud and Jayanti (1990).

Heat transfer studies of a helical coil immersed in a water bath was studied by Prabhanjan et al. (2004). A method to predicted outlet temperatures from the helical coil was proposed which took into consideration the flow rates and geometry of the coil. The heat transfer on the outside of the coils was from natural convection. In this type of system, neither constant wall temperature, nor constant wall heat flux, could be assumed.

3.8 Entry Flow

Dravid et al. (1971) numerically studied the entrance region laminar flow heat transfer for Dean numbers greater than 100. They assumed that the flow field was fully developed as it entered the coil. They showed that at very short distances into the tube inlet the secondary flow does not increase the heat transfer rate. Further along the tube the heat transfer coefficient did increase. They also observed the oscillatory action of the Nusselt number in the entry flow and it was shown to dampen out in the thermally developed region to an asymptotic value. The developing region is extremely short and for design purposes Dravid et al. (1971) suggest that the asymptotic Nusselt number should be used along the whole length of the coil. Dravid et al. (1971) proposed the following Nusselt number correlation for a Dean range of 50 to 2000 and a Prandtl range of 5 to 175:

$$Nu = [0.76 + 0.65\sqrt{\mathrm{De}}]\,\mathrm{Pr}^{0.175} \tag{2.16}$$

Akiyama and Cheng (1974a) studied the numerical solution of the Graetz problem (thermal entrance region) in curved pipes with uniform wall temperature for Dean numbers up to 100. A combination of the boundary vorticity method and a line iterative relaxation technique were used to solve the momentum equations. The development of the thermal boundary layer is not uniform around the circumference and the boundary layer develops quicker at the inner wall than at the outer wall. The distortion from concentric circles in the isotherms is the effect of the secondary flow. For low Prandtl numbers (Pr = 0.1), it was shown that the development of the Nusselt number along the axial length was similar to that of a straight pipe. The local Nusselt number would approach an asymptotic value. However, it was shown that an increase in the Dean number increased the Nusselt number and shortened the thermal entrance region (Akiyama and Cheng, 1974a). For larger Prandtl numbers (Pr = 0.7, 10, 500), the Nusselt number would decrease to a minimum and then increase again and level off to a constant value a certain distance downstream. It was also shown that both the Dean number and the Prandtl number increased the Nusselt number and decreased the thermal entrance length. The effect of Dean number was more evident at high Prandtl numbers. Akiyama and Cheng (1974a) also obtained fluctuating Nusselt number relations with the Graetz number as was observed by Dravid et al. (1971). However, Akiyama and Cheng (1974a, 1974b) proposed that these fluctuations were due to numerical instability rather than a physical phenomenon.

Singh (1974) studied the entry flow for both conditions of constant dynamic pressure at the entrance and for the uniform velocity entry condition. The theoretical findings were that the two different inlet conditions affected the development of the flow in the near-entry region; however it does not significantly affect the flow farther downstream.

Patankar et al. (1974) used a finite-difference method to solve for three-dimensional parabolic flow of fluid in a helically coiled pipe to determine the velocity and temperature fields for a torus. The study focuses on the developing entry flow (both thermodynamically and hydrodynamically) for large curvatures and axially constant heat flux with an isothermal periphery. They compared their results for both the temperature and velocity fields to other results cited in literature. To the most part, the results coincided with the literature data, except for the temperature profiles of Mori and Nakayama (1965) and suggested the error lie in the latter work, due to inaccuracy in measurement or in the setting of the boundary conditions (Patankar et al., 1974). They also confirmed that the oscillations of the wall temperature in the developing entry flow were due to the secondary flow as stated by Dravid (1971) and Seban and McLaughlin (1963). The authors expanded their work on curved tubes to study turbulent flow using the same numerical procedure (Patankar et al., 1975). A two-equation turbulence model was used, one equation for the kinetic energy of the turbulence and another one for its dissipation rate. A one-equation turbulence model was also tried but the results were not adequate. The predictions from this study were compared to experimental work and had reasonable agreement; however the fit was not as good as for the laminar study (Patankar et al, 1975).

A correlation of the entry region length for steady laminar flow as a function of the Dean number and the curvature ratio was developed by Austin and Seader (1974). In their work, the entry region length was noted to be anywhere between 90° and 245°. The smallest region was for the coil with the smallest Dean number and the largest curvature ratio, whereas the longest entry region (in terms of degrees) was with the largest Dean number and the smallest curvature ratio.

Kalb and Seader (1983) measured the Nusselt number for developing flow in a two-turn helical heat exchanger with uniform wall temperature boundary conditions. The fluid was in a gaseous state and entered with a Reynolds number such that the inlet flow (coming from a straight pipe) was turbulent; but would fall below the critical Reynolds number prior to leaving the outlet. Therefore, there was a transition from turbulent to laminar flow. Their results showed that there was a rapid transition from turbulent to laminar flow and that the Nusselt number also obtained the fully developed value well before the two turns of the coil.

The entry flow into curved pipes was studied by Padmanabhan (1987) for both axially constant heat flux and for axially constant wall temperature. Buoyancy effects were also studied in this work by using the Boussinesq approximation. The buoyancy was found to affect the secondary motion, and the effects were dependent on the type of thermal boundary conditions.

Steady, laminar flow with thermodynamically developing flow was studied numerically by Acharya et al. (1993). The flow was hydrodynamically fully developed with Prandtl numbers near unity. Acharya et al. (1993) identified four distinct regions in the thermodynamically developing flows based on the behavior of the Nusselt number.

Developing turbulent heat transfer was numerically studied by Lin and Ebadian (1997) using a control-volume finite element method. They studied the effects of pitch, curvature ratio and Reynolds number on the temperature fields and the Nusselt number. They found that the Nusselt number oscillated with distance downstream for developing flow. They also found that as the pitch, curvature or Reynolds was increased, these oscillations were stronger. Lin et al. (1997) studied the same effects as Lin and Ebadian (1997) but for the case of developing laminar flow and heat transfer. They found that the Nusselt number and the friction factor were oscillatory in the entrance region. They found that when the curvature ratio was decreased, the oscillations of both the Nusselt number and the friction factor were augmented. Lin and Ebadian (1999) numerically studied the effects of inlet turbulence intensity on the development of the turbulent flow and heat transfer in helically coiled pipes. Their findings were that increased inlet turbulence intensity tended to reduce the velocity gradient at the walls of the pipe though it had negligible effect on the maximum axial velocity. Increasing the intensity level also increased the intensity of the secondary flow but did not change its pattern. The thermal boundary layer developed quicker with increased inlet turbulence intensity.

Li et al. (1998) numerically studied the turbulent convective heat transfer in the entrance region of a curved pipe with a uniform wall temperature. At higher Grashof numbers, a third vortex due to the buoyancy forces became apparent. This affected the local Nusselt number. The buoyancy forces drastically improved the Nusselt number in the entrance region but its effect on the overall Nusselt number was negligible since the entrance region is so short (Li et al., 1998). Both the Nusselt number and the friction factor oscillated in the entrance region.

Developing heat transfer in a helical coil with a linear wall temperature was studied by Rindt et al. (1999). This boundary condition for the coil is different from the usual constant heat flux and constant wall temperature, though it would be identical to a constant heat flux for fully developed flow. They found that the Nusselt number oscillated along the axial position and attributed the phenomena to circulating secondary flow along the tube wall.

3.9 Non-Newtonian Fluid in Helical Flow and Heat Transfer

Jones (1960) performed a theoretical analysis of the flow of an incompressible non-Newtonian fluid in curved pipes and compared the results to Newtonian fluids. Jones showed that non-Newtonian fluids take longer or shorter angular distances for the fluid particles to traverse the central plane from the inner wall to the outer wall, depending on whether they exhibit negative or positive Weissenberg effects, respectively. Thomas and Walters (1963) showed that elastico-viscous liquids had a decreased curvature of their path through the central plane of the tube. These fluids also had increased flow rates through a curved tube for a given pressure gradient, compared to Newtonian fluids (Thomas and Walters, 1963). Barnes and Walters (1969) came to the same conclusion in their study of elastico-viscous fluids, and also noted that the effect of curvature on the transition from laminar flow to turbulent flow is less apparent for the elastico-viscous fluids than Newtonian fluids. However, their results for turbulent flow showed that the flow rates decreased compared to straight tubes, which was opposite to what was observed in the laminar region. Thomas and Walters (1965) extended their previous work of flow in curved tubes to the flow in curved tubes with elliptical cross-sections. Laminar flow in coiled pipes with non-Newtonian fluids was also studied by Rajasekharan et al. (1970) for both pseudo-plastic and dilatant fluids, modeled using a power-law model. They determined that the Nusselt number could be correlated to the curvature ratio, the flow behaviour index, and a modified Graetz number.

Numerical studies of laminar non-Newtonian flow and heat transfer in curved tubes using a finite difference method was performed by Hsu and Patankar (1982). Their results show that the axial velocity profiles become flatter for lower values of the power-law index. The friction factor increases with both the Dean number and with the power-law index (Hsu and Patankar, 1982). They also noted that the heat transfer coefficient varied significantly over the circumference of the tube, but the variation diminished with increasing Prandtl number.

Rao (1994) experimentally measured turbulent Fanning friction factors and Nusselt numbers for viscous power-law non-Newtonian fluids with curvatures in the range of 1/10 to 1/26 and power-law exponents (n) in the range of 0.78 to 1. The results indicated that the turbulent Nusselt number increases with decreasing n. It also indicates that the lower the n, the greater the secondary flow (Rao, 1994). Rao (1994) also mentioned that the relative performance of a helical coil to a straight tube may be described by the ratio $[(Nu_c/Nu_s)/(f_c/f_s)]$, where the subscripts c and s stand for curved and straight, respectively. Using this ratio as a basis, Rao (1994) stated that other than space saving, the helical coils do not have a heat transfer advantage over straight tubes for power-law non-Newtonian fluids. This point, however, seems too simplified as the design of the heat exchanger, including the economic benefits of using a helical coil would be determined based on more criteria than just the ratio proposed by Rao (1994).

The critical Reynolds number was found to be lower with the power-law fluids in the range of 0.78 to 1 than that of water, used as the Newtonian fluid in the study (Rao, 1994).

Robertson and Muller (1996) used a perturbation method to study the steady flow of Oldroyd-B fluids and for Newtonian fluids through curved pipes and curved annuli. Results were limited to the laminar flow regime. They studied both creeping flow ($Re \approx 0$) and non-creeping flow with a Reynolds number less then 25. For creeping flow, both the curved and annular tubes had secondary flows produced due to elasticity similar to those produced by inertia. However, the effects of elasticity and inertia were not found to be additive (Robertson and Muller, 1996).

Fan et al. (2001) used finite element computations to study the flow of both viscous and viscoelastic fluids through curved tubes. They quantified the intensity of the secondary flows by calculating two stream functions, one being the secondary volumetric flux per unit work consumption and the other as the secondary volumetric flux per unit axial volumetric flux. They showed that for both these parameters, the values first increased with the Reynolds number then decreased, for both the Newtonian and the non-Newtonian fluids.

3.10 Helical Flow with Solid Core (Curved Annular Flow)

Kapur et al. (1964) performed theoretical calculations for steady laminar flow of a Newtonian fluid through a curved annulus for cases with slight curvature. They showed graphical representations of the projected streamlines on the cross-section. Their work showed two vortices much like that of a normal curved pipe flow but the vortices were curved to fit the annulus. Topakoglu (1967) used an approximate solution to determine the secondary flow stream-lines for flow between two concentric torus shaped pipes. In the cases that were studied, there were four secondary flow vortices, with symmetry about the plane that cut the torus through the center. Of the two vortices on each side of the central plane, the direction of the secondary flows was opposite (Topakoglu, 1967).

The entrance flow into a curved annuls was studied numerically by Choi and Park (1992) for the case of an incompressible steady laminar flow. They tested numerous radius ratios and found that this parameter had a large effect on the secondary flow field. They also stated that unlike the case of a straight annular duct, the fully developed flow does not necessarily develop earlier when the radius ratio is larger. They followed up this work by publishing a paper on the mixed convective heat transfer in a curved annulus (Choi and Park, 1994). In this work they numerically solved the heat transfer for a constant wall temperature boundary condition with fully developed flow. They also invoked the Boussinesq approximation to take into account the effects of buoyancy. They compared the Nusselt number and friction factor in the flow to that of a straight annulus. They found that the Nusselt number ratio (curved to straight) and the friction factor ratio to be significantly affected by the radius ratio and the Dean number for small Grashof numbers (12.5) without changing much at high Grashof numbers (12 500), (Choi and Park, 1994).

Petrakis and Karahalios (1996) studied steady annular flow of an incompressible viscous fluid in a curved pipe with a coaxial core. Their findings show that the presence of a core affects the flow properties, especially at high Dean numbers. The same authors also developed analytical expressions for the axial velocity and for the stream function for exponentially decaying flow in a curved annular pipe (Petrakis and Karahalois, 1997). In both works it was shown that in some instances two additional secondary flow patterns developed resulting in a total of four vortices.

Xin et al. (1997) experimentally studied both single-phase and two-phase flow in helicoidal annular pipes to determine the pressure drop relationships. They developed a pressure drop correlation for single phase flow for laminar, transitional, and turbulent flow regimes. For the two-phase flow, they studied coils in both horizontal and vertical configurations and provided pressure drop correlations for each case.

Petrakis and Karahalios (1999) used a finite difference numerical method for the flow of a viscous, incompressible fluid in a curved annular conduit with a circular cross section. The Dean range was from 96 to 8000. Various core sizes were used. For small core sizes, changes in the Dean number significantly affect the flow properties, though this is not present for large core sizes. For the smaller core sizes, the velocity profile was skewed towards the outer wall, whereas for large core sizes the flow velocities approached parabolic flow.

Karahalois (1990) studied the heat transfer of a fluid flowing in a curved pipe with a solid core. The core and the curved pipe surface were both the same with a constant temperature gradient along the axial direction. Depending on the Dean number, a reversal of the flow was detected in the inner portion of the bend for significantly large cores (Karahalois, 1990). Ahn (2000) studied the heat transfer to a fluid in the annuli for a straight tube, with two conditions, either the outer tube or the core insulated and heat transfer through the opposite boundary. These were done for turbulent flow regimes and the outer wall had a rough surface. Different diameter ratios and wall roughness were used.

3.11 Applications

There are a fair number of publications that cite different uses for helical coils, some of these uses are discussed below.

Using a helical coil as a polymerization reactor is theoretically discussed by Mihail and Straja (1981). They developed a model that would predict the velocity profile, temperature profile, and the monomer conversion for polymerization in laminar flow. However, their results showed that there was no difference between monomer conversion in a helical coil and a straight tube at the levels of parameters that they tested.

The natural convection mass transfer from the outer surface of helical coils was studied by Sedahmed et al. (1985) for the purpose of using helical coils in electrochemical reactors, where the helical coils could be used simultaneously as both heat exchanger and electrode.

The pressure drop and heat transfer coefficients were measured for a tube and shell heat exchanger where the inner tube was replaced with a helical coil (Prasad et al., 1989). Correlations for Nusselt number on the tube side were developed for both laminar and turbulent flow. For the laminar flow the Nusselt number was correlated to the Dean number, whereas for the turbulent flow, correlations to the Reynolds number multiplied by the curvature squared, rather than the square root, as in the case of the Dean number were obtained. The coil was also tested in a waste heat recovery device (Prasad et al., 1989).

Taherian and Allen (1997) studied the natural convection from vertical helical coils in a cylindrical enclosure, while testing the tube diameter, coil surface area, and coil pitch on the heat transfer coefficient. They found that an increase in coil surface area resulted in a decrease in heat transfer coefficient. The purpose of these studies was for use in solar domestic hot water (SFHW) systems. Other work by Allen and Ajele (1994) indicated that the geometrical factor that had the most significant influence on the performance of a shell-and-coil heat exchanger was the dimensionless flow space defined as the ratio of the equivalent total flow space to an equivalent diameter of the coil.

Taherian and Allen (1998) studied the natural convection from single coils in a shell-and-coil heat exchanger. They found that the Nusselt number could not be correlated to the Rayleigh number based on the tube diameter. Their results showed that the most influential parameter on the heat transfer coefficient was the coil surface area, showing a decrease in the heat transfer coefficient as the heat transfer area was increased.

The application of helical coils for microfiltration of silica suspensions was studied and compared to straight tube filtration by Klunge et al. (1999). They studied the effect of changing viscosity, with the fluid viscosity increasing as the solution is concentrated by filtration. They found that the increasing viscosity changed the secondary flow formation and stability as well as the wall shear rate and the amount of backflow. Though they also found higher fluxes for the helical coil, the energy requirements to achieve these increases were also much higher.

Sahoo et al. (2002) designed an ultra-high temperature helical tube milk sterilizer using a triple tube design for the heating section. They tested the bacterial kill using the sterilizer. Sahoo et al. (2003) developed a method to predict the heat transfer coefficients in the system they designed in Sahoo et al. (2002). They used an iterative approach to predict the heat transfer coefficients. However, for the prediction of the annulus heat transfer coefficients, they took an equation for a straight tube annulus (from Chopey and Hicks, (1984)) and multiplied it by a correction factor determined by Jeschke (1925) for the relation between straight tube and helical tube heat exchangers. The accuracy of this approach is questionable, as annular tubes may behave differently than helical tubes, and the correction factor may not be appropriate.

Fleming et al. (2001) discussed the application of using a helical shell-in-tube heat exchanger in a metal-hydride-based hydrogen separation system. The helical tube was packed with Palladium deposited on kieselguhr with gas stream (hydrogen mixed with other inert gases) passing through the helical tube. In the outer shell, flow is cycled between hot and cold nitrogen gas to produce thermal cycling in the packed bed, resulting in hydrogen being adsorbed or desorbed from the Palladium, and hence creating a separation system (Fleming et al., 2001).

Gao et al. (2002) studied the phase separation phenomena in curved pipes in hopes of providing some light on the ability to develop a new type of curved pipe separator. Curved pipe separators were first used in the petroleum industry as sand is often part of the oil-water and natural gas streams (Gao et al., 2002). They studied the problem numerically, and also measured particle size and concentration profiles for two-phase flow. Based on the results of the particle size and distribution, along with the secondary flow effects, they made suggestions how separation efficiency could be improved.

The use of a helical coil as the evaporator section of a looped heat pipe was studied by Yi et al. (2002). They examined the characteristics of the flow and the heat transfer for different filling ratios and heat fluxes. They proposed correlations for the heat transfer rates based on experimental data.

Hameed and Muhammed (2003) studied the mass transfer of gases into falling liquid films in both straight inclined pipes and in helical coils with the goal to increase the mass transfer coefficients. They correlated their results for the mass transfer in the helical coil in terms of the Schmidt, Sherwood, Dean, and Gallileo numbers, for both laminar and turbulent flow (two separate correlations). Their results showed higher heat transfer coefficients for helical coils compared to straight falling tubes. Furthermore, they determined that increase in curvature also resulted in higher mass transfer coefficients.

The application of a helical coil in an ammonia-water vapour rectification process for absorption systems was studied numerically by Fernández-Seara et al. (2003). They discussed the effect of the heat and mass transfer coefficients on the performance of the rectifier.

The condensation of alternative refrigerant R-134a inside a helical coil was studied by Yu et al. (2003). Different mass fluxes of the refrigerant were passed through the helical coil. Cooling water was passed through a concentric annulus at flow rates that corresponded to Reynolds numbers in the range of 1500 to 10000. The helical coil was set up in vertical, horizontal, and inclined orientations, and these different orientations were shown to have a significant effect of the tube-side and the overall heat transfer coefficients.

3.12 Conclusions

Although a significant amount of research has been performed on the flow patterns and heat transfer in curved pipes and helically coiled pipes, there is still much that needs to be investigated. In particular the fluid-to-fluid heat transfer needs further study as the past work has mainly focused on the constant heat flux and constant wall temperature conditions. There is little information on a double-pipe helical heat exchanger existing in the literature. Information on annular flow in a helical pipe exists, but that is for fluid flow with a constant temperature gradient along the pipe and core. Hence, fluid flow and the heat transfer need to be studied for a double-pipe helically coiled heat exchanger.

IV. NUMERICAL STUDIES OF A DOUBLE-PIPE HELICAL HEAT EXCHANGER

4.1 Abstract

A double-pipe helical heat exchanger has been numerically modeled for fluid flow and heat transfer characteristics under different fluid flow rates and tube sizes. Dean numbers for the inner tube ranged from 38 to 350. For all cases, the mass flow rates in the annulus were either half, equal, or double the flow rate in the inner tube. Two different tube diameter ratios were used. The overall heat transfer coefficients were calculated for both parallel flow and counterflow. The three-dimensional governing equations for momentum, continuity, and heat transfer were solved using a finite volume based computational fluid dynamics (CFD) code. Validation of simulations were conducted by comparing the Nusselt numbers in the inner tube with those found in literature, the results fell within the range found in the literature. For the parameters tested in this study, the greatest thermal resistance was found in the annular region of the heat exchanger. The thermal resistance of this area could be decreased by increasing the inner tube diameter or by increasing the flow rate in the annulus. The Nusselt number in the annulus was correlated with a modified Dean number, and showed a strong linear relationship for the range of Dean numbers in this work.

4.2 Introduction

Helically coiled tubes can be found in many applications including food processing, nuclear reactors, compact heat exchangers, heat recovery systems, chemical processing, low value heat exchange, and medical equipment (Abdalla, 1994; Bai et al., 1999; Berger et al., 1983; Prabhanjan et al., 2002; Rabin and Korin, 1996; Rao, 1994; Sandeep and Palazoglu, 1999). There are numerous references dealing with fluid flow through helical coils. As the fluid flows through the tube, the curvature of the tube causes centrifugal forces to act on the fluid, resulting in a secondary flow pattern perpendicular to the axial direction. This secondary flow pattern generally consists of two vortices, which move fluid from the inner wall of the tube across the center of the tube to the outer wall. Upon reaching the outer wall it travels back to the inner wall following the wall. The secondary flow increases heat transfer rates as it moves fluid across the temperature gradient. Thus there is an additional convective heat transfer mechanism, perpendicular to the main flow, which does not exist in straight tube heat exchangers (except when produced by buoyancy forces). The majority of the work involving helically coiled heat exchangers has focused on either constant wall temperature or constant wall heat flux boundary conditions (Prabhanjan et al., 2004). These two boundary conditions are very useful in heat exchange applications, as the constant wall temperature relates to the heating of the coils by steam, and the constant wall heat flux can be achieved by equipping the coil with electric heating wires. However, there is a third common boundary condition that is often not explored, and that is for liquid-to-liquid heat exchangers (the tube wall separates the two fluids), where neither the heat flux, nor the wall temperature, is constant. This can be a problem for designing heat exchangers, especially when there is developing flow (hydrodynamic and/or thermal) in the heat exchanger, or when there are thermally dependant fluid properties. In these cases, the heat transfer coefficients are not constant and may be a function of the temperature. There are a few references that discuss designing shell-in-tube helical heat exchangers, however the calculation procedure is not based on data from helically coiled tubes, but rather assumes that a bank of tubes can be used as an approximation for calculating heat transfer coefficients, such as in Haraburda (1995).

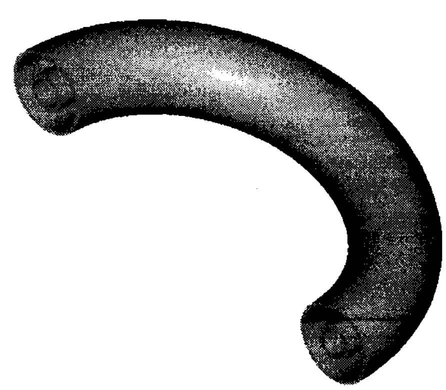

Figure 4.1: Section of a double-pipe helical heat exchanger.

Designing a double-pipe helical heat exchanger, such as in Figure 4.1, requires heat transfer coefficients for the two fluid flows (both sides of the tube), the flow rate in the helical tube and the flow rate in the annulus, along with design inlet and outlet temperatures. Some information exists on the heat transfer in a curved annulus, however this is also limited to constant wall temperature gradient in the axial direction (Karahalois, 1990), making it difficult to predict the heat transfer coefficients on the inner wall of the annulus.

4.3 Objective

The objective of this work was to determine the heat transfer characteristics for a double-pipe helical heat exchanger by varying the size of the inner tube and the mass flow rates (within the laminar region) in both the annulus and in the inner tube. These objectives were carried out for both parallel flow and counterflow heat exchangers. A computational fluid dynamics package (PHOENICS 3.3) was used to predict the flow and temperature profiles in a double-pipe helical heat exchanger.

4.4 Materials and Methods

4.4.1 CFD modeling

Geometries for the heat exchanger were created in AutoCAD 14 and exported as stereolithography files. Three different coils were created, one for the annulus, with inner and outer diameters of 0.1 and 0.115 m, respectively, and with a pitch of 0.115 m. The two other coils were created with outer diameters of 0.04 and 0.06 m, both with a pitch of 0.115 m and with a wall thickness that was 15% of the respective outer diameter. Each of the coils had a length of 2π (one full turn).

The coils were imported into PHEONICS 3.3, a commercial computational fluid dynamics software based on a control volume-finite difference formulation. A cylindrical coordinate system was used with a mesh size of 30 x 40 x 80 in the axial, horizontal, and vertical directions, respectively. The coils were orientated in the vertical position, though the results are also appropriate for horizontal coils as the buoyancy forces acting on the fluid were not activated. The radius of curvature for all the coils was 0.8 m, which resulted in curvature ratios of 0.0625, 0.0435, and 0.0261 for the inner diameters of each of the above-mentioned coils, respectively. Inlets and outlets were located at each end of the coil. The boundary conditions associated with the inlets specified the inlet velocities in the axial direction. Coil properties were set to those of stainless steel, with a thermal conductivity of 16 $W \cdot m^{-1} \cdot K^{-1}$, density of 7881.8 $kg \cdot m^{-3}$ and a specific heat of 502 $J \cdot kg^{-1} \cdot K^{-1}$. The outer coil was set to be adiabatic (representing an insulated tube) and the inner coil was set to allow conductive heat flow through the tube.

Simulations were performed using 4 different mass flows in the inner tube, $\dot{m}_i$, (0.00835, 0.02504, 0.04174, and 0.05843 $kg \cdot s^{-1}$). These resulted in inner Dean numbers in the range of 38 to 350. For each inner flow rate, 3 trials were performed with annulus mass flow rates that were ½, 1 and 2 times the inner flow rate. For example, the three annulus flow rates, $\dot{m}_o$, associated with the inner flow rate of 0.00835 $kg \cdot s^{-1}$ were 0.00418, 0.00835, and 0.0167 $kg \cdot s^{-1}$. These were chosen to keep the ratio of the mass flow rates similar, so that the temperature changes of each fluid are kept within a reasonable range of each other, otherwise, the temperature change of one fluid could be very high, and little change in the other fluid, making it more difficult to accurately calculate the heat transfer coefficients. Density, heat capacity and the thermal conductivity of the fluid were constant at 998.23 $kg \cdot m^{-3}$, 4181.8 $J \cdot kg^{-1} \cdot K^{-1}$, and 0.597 $W \cdot m^{-1} \cdot K^{-1}$, respectively.

The total number of simulations performed was 48 (2 tube diameters x 4 inner flow rates x 3 annulus flow rates x 2 flow directions). The output of the simulations included the inlet and outlet velocities, mass flow rates and enthalpy rates, as well as velocity, pressure, and temperature fields at 30 specified cross-sections.

4.4.2 Calculation of heat transfer coefficients

The inlet and outlet and temperatures allowed for the calculation of the overall heat transfer coefficient, U_o, using the following equation (White, 1984):

$$U_o = \frac{q}{A_o LMTD} \tag{4.1}$$

LMTD is the log mean temperature difference, calculated based on the inlet temperature difference, ΔT_1, and the outlet temperature difference, ΔT_2, and the following equation (White, 1984):

$$LMTD = \frac{(\Delta T_2 - \Delta T_1)}{\ln(\frac{\Delta T_2}{\Delta T_1})} \tag{4.2}$$

The overall heat transfer rates were based on the outer surface area, A_o, of the inner tube.

Heat transfer coefficients were calculated in a similar manner along the length of the tube using the data from each cross-section (30 cross-sections in total). This resulted in 29 heat transfer coefficients along the length of the heat exchanger (one at the midpoint between cross-sections). Heat transfer coefficients were calculated for both the inner tube and the annulus. For these calculations, average bulk temperatures and average temperature of the coil at each cross-section were used.

4.4.3 Calculations of effectiveness-*NTU*

An effectiveness-*NTU* (number of transfer units) approach was also employed. The effectiveness-*NTU* method is used to determine outlet temperatures for a heat exchanger when all other variables are known (inlet temperatures, mass flow rates, surface area, and overall heat transfer coefficient). The effectiveness is the ratio of the actual amount of heat transfer to the maximum possible heat transfer for the given heat exchanger. The maximum amount of heat transferred, q_{max}, is calculated by (White, 1984):

$$q_{\max} = C_{\min}(T_{hotin} - T_{coldin}) \tag{4.3}$$

C_{min} is the minimum between $\dot{m}_c c_{p_c}$ and $\dot{m}_h c_{p_h}$ (mass flow rate multiplied by specific heat), T_{hotin} is the inlet temperature of the hot fluid, and T_{coldin} is the inlet temperature of the cold fluid. The effectiveness is generally plotted versus the NTU_{max} to obtain graphs that contain curves of constant C_{min} to C_{max} ratios. NTU_{max} is defined as (White, 1984):

$$NTU_{\max} = \frac{A_o U_o}{C_{\min}} \tag{4.4}$$

The effectiveness-NTU was plotted for the cases of $C_{min}/C_{max} = 1$ and $C_{min}/C_{max} = 0.5$, as these were the two cases related to the flow rates used in the trials. The ratio of C_{min} to C_{max} of unity refers to the minimum effectiveness for the heat exchanger. A ratio of C_{min} to C_{max} of nil is the maximum effectiveness of the heat exchanger, and is given by the following equation for all heat exchangers (White, 1984):

$$\varepsilon = \varepsilon_{\max} = 1 - e^{-NTU} \tag{4.5}$$

Furthermore, the theoretical effectiveness, ε, for a parallel flow and counterflow heat exchangers are given by the following two equations, respectively (White, 1984):

$$\varepsilon = \frac{1 - \exp(1 - NTU(1 + \frac{C_{\min}}{C_{\max}}))}{1 + \frac{C_{\min}}{C_{\max}}} \tag{4.6}$$

$$\varepsilon = \frac{1 - \exp(-NTU(1 - \frac{C_{\min}}{C_{\max}}))}{1 - \frac{C_{\min}}{C_{\max}} \exp(-NTU(1 - \frac{C_{\min}}{C_{\max}}))} \tag{4.7}$$

4.4.4 Model validation

The numerical procedure was validated by comparing the results of the Nusselt numbers for the flow through the helical coil and comparing these to Nusselt numbers from literature. The validation trials were performed with both constant heat flux and constant wall temperature boundary conditions. There are a number of correlations in the literature for the Nusselt number as a function of the Dean number for both the uniform heat flux and the uniform wall temperature boundary conditions. Mori and Nakayama (1965, 1967) developed the following correlation and stated that it could be used for both boundary conditions:

$$Nu_{cur} = \frac{0.864}{\zeta} \sqrt{De}(1 + \frac{2.35}{\sqrt{De}}) \tag{4.8}$$

where ζ is the boundary layer thickness ratio for Pr > 1 and is given by:

$$\zeta = \frac{2}{11}\left\{1+\sqrt{\left(1+\frac{77}{4}\frac{1}{\mathrm{Pr}^2}\right)}\right\} \tag{4.9}$$

Akiyama and Cheng (1972, 1974b) determined the Nusselt number for uniform wall temperature and uniform heat flux using a parameter Q, defined as $Q = (De^{1/2}\mathrm{Pr})^{1/4}$. Their results for the uniform wall flux where applicable for $Q \geq 3.5$, $\mathrm{Pr} \geq 1$ and Nu_{asy} = 4.36 and produced the following correlation:

$$\frac{Nu_{cur}}{Nu_{asy}} = 0.234Q\left(1-1.15Q^{-1}+29.2Q^{-2}-164Q^{-3}+316Q^{-4}\right) \tag{4.10}$$

For the uniform wall temperature, the range of parameters was $Q \geq 3.0$, $\mathrm{Pr} \geq 1$, and Nu_{asy} = 3.66. The correlation was:

$$\frac{Nu_{cur}}{Nu_{asy}} = 0.270Q\left(1-1.48Q^{-1}+23.2Q^{-2}-120Q^{-3}+212Q^{-4}\right) \tag{4.11}$$

The values of 4.36 and 3.66 are the asymptotic Nusselt numbers for heat transfer in a straight pipe with uniform heat flux and uniform wall temperature boundary conditions, respectively.

4.5 Results and Discussion

4.5.1 Model validation

Figure 4.2 shows the results from this study for both a uniform heat flux and a uniform wall temperature for the two different coil diameters and the four different mass flow rates. On the Figure, the correlations of Mori and Nakayama (1965, 1967), Dravid et al. (1971), and Akiyama and Cheng (1972, 1974a) are shown for Pr = 7. There is significant variation between the results of these different correlations. The results from this study (Pr = 7.03) fall within the range of the correlations, fitting best with those of Akiyama and Cheng (1972, 1974a). The difference in the Nusselt numbers for the constant wall heat flux and the constant wall temperature, for all practical purposes are negligible, corresponding to the conclusions of Mori and Nakayama (1967). The Nusselt numbers shown in Figure 4.2 are the average of the Nusselt numbers along the first turn of the coil. Though this is a case of developing flow, the average Nusselt number is a decent approximation of the asymptotic Nusselt number in this work as little variation was noted along the length of the coil. Akiyama and Cheng (1974b) studied the thermal entrance region for a constant wall temperature and showed that as the Dean number and the Prandtl number increased the entrance region was shortened. The entrance region for a Dean number of 37.1 and a Prandtl number of 10 became asymptotic by a Graetz number of roughly 100. For the simulations used in this study, and under similar Dean (= 37) and Prandtl (= 7.03) numbers, the flow would become stable 14.1% around the first turn. Furthermore, the Nusselt number is not constant up to the asymptotic value, with part of the range with a Nusselt number above the asymptotic value and part below. As the Dean number is increased, the variation tends to be less.

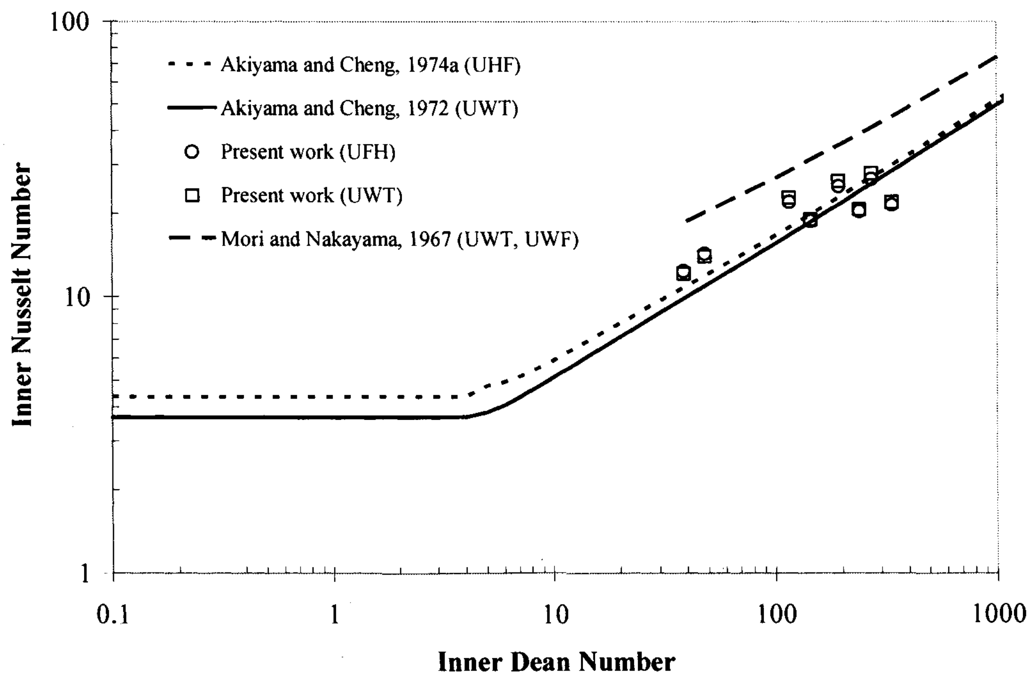

Figure 4.2: Nusselt number versus Dean number in the helical coil for uniform wall temperature (UWT) and uniform heat flux (UHF) thermal boundary conditions.

Furthermore, the effectiveness-NTU charts have been produced for both the parallel flow and the counterflow configurations (Figures 4.3 and 4.4). On these charts the theoretical curves are plotted for capacity ratios of 0.0, 0.5 and 1.0. As can be seen, the simulation data fits well with these curves. This result is expected for a heat

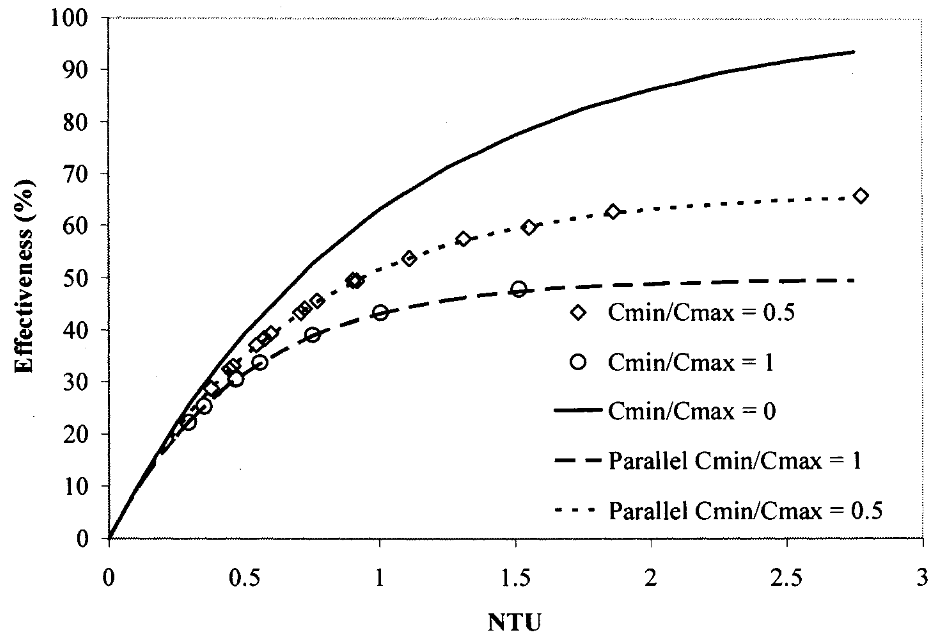

Figure 4.3: Effectiveness-NTU graph for parallel flow in the double-pipe helical heat exchanger. Experimental (symbols) and theoretical (lines) are shown.

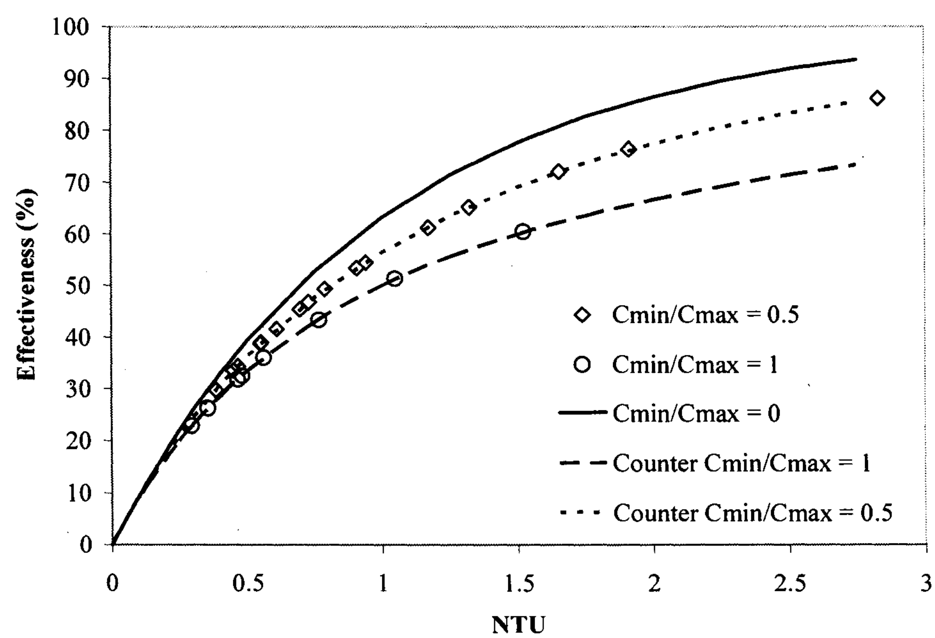

Figure 4.4: Effectiveness-NTU graph for counterflow in the double-pipe helical heat exchanger. Experimental (symbols) and theoretical (lines) are shown.

exchanger with a constant overall heat transfer coefficient. In the case presented here, there is a developing flow which results in non-uniform heat transfer coefficients along the length of the tube. The calculations for the effectiveness were done considering the average overall heat transfer coefficient, and there is little deviation from the theoretical predictions. This further validates the statements by Dravid et al. (1971) that the effects of developing flow are negligible on the overall heat transfer process in a helical heat exchanger, and furthermore these results show that this assumption is valid for double-pipe helical heat exchangers in both parallel flow and counterflow configurations.

4.5.2 Overall heat transfer coefficients

Figures 4.5 and 4.6 show the overall heat transfer coefficients versus the inner Dean number for the cases of parallel flow and counterflow, respectively. Both cases have overall heat transfer coefficients that are nearly similar, for the same given flow rates. The ratio of the overall heat transfer coefficients (parallel flow divided by counterflow) for a give case range from 0.94 to 1.07, with the majority of the ratios slightly above unity, in favor of the counterflow. The overall heat transfer coefficients increase with increasing inner Dean number. However, the significance of the increase is a function of the ratio of the mass flow rates. As can be seen in Figure 4.5, the ratio of the mass flow rates has a significant effect on the overall heat transfer coefficient, raising the overall heat transfer coefficient when the flow rate in the annulus is increased. The relationship between the overall heat transfer coefficient and the inner Dean number is correlated on the graphs in the form of a power law function:

$$U_o = aDe^b \tag{4.12}$$

The results of the correlations for these cases are shown in Table 4.1. From these relationships, it can be shown that increasing the inner Dean number has a greater effect on the overall heat transfer coefficients when the outer flow rate is higher. This is due to the outer heat transfer being more limiting than the inner heat transfer. When flow rates are increased, the overall heat transfer rate will also increase, but the significance of the increase is highly dependent on the ratio of the two flow rates. There is a difference between the overall heat transfer coefficients for the two different tube sizes. There are a

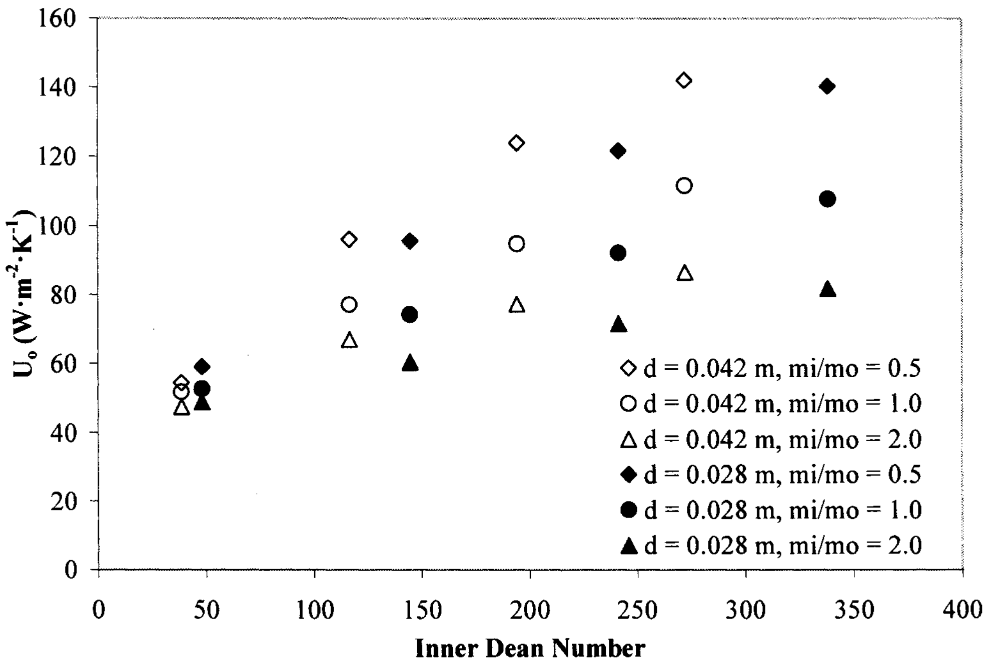

Figure 4.5: Overall heat transfer coefficient versus the inner Dean number for parallel flow.

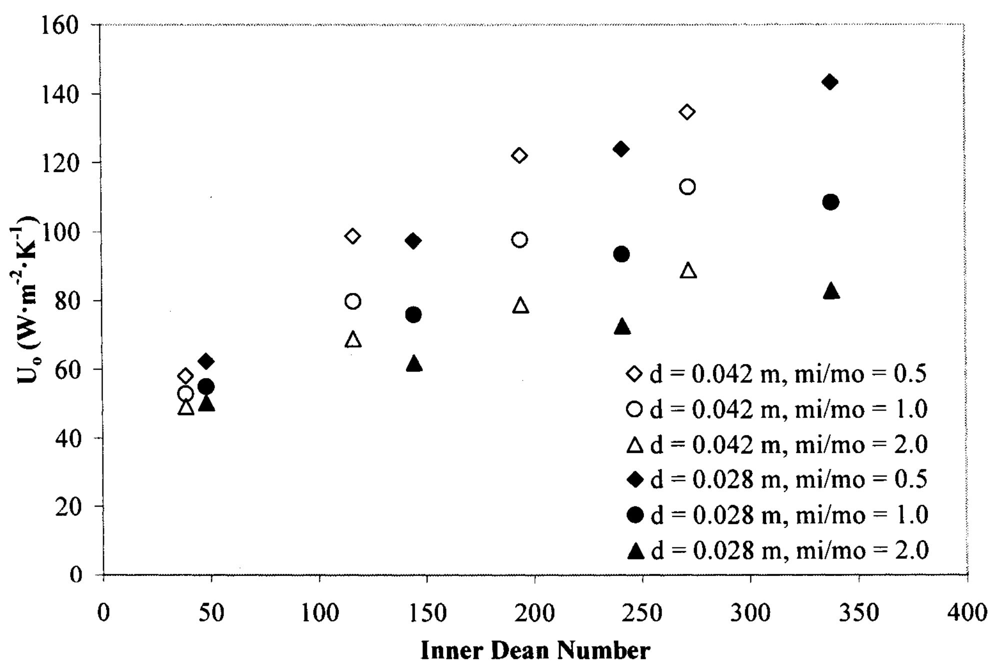

Figure 4.6: Overall heat transfer coefficient versus the inner Dean number for counterflow.

couple of reasons why this difference has been observed. The main reason is due to the difference in the annulus heat transfer coefficient, which would most likely be higher for a smaller gap size. Also, both tubes are curved with the same radius of curvature; hence the large tube is curved with a greater curvature ratio than the smaller tube, which could result in great secondary flow effects. Though these results are graphed with the Dean number as the independent variable, the Dean number may not fully describe the complexities of this flow. In fact, there are several relationships for heat transfer coefficients (in the form of Nusselt numbers) for helically coiled heat exchangers that are not developed solely on the Dean number. Seban and McLaughlin (1963) correlated the Nusselt number as a function of the friction factor and the Reynolds number, while Janssen and Hoogendoorn (1978) used correlations solely on the Reynolds number and Prandtl number for certain ranges of the Dean number. For higher Dean numbers ($100 < De < 8300$), Janssen and Hoogendoorn (1978) correlated the Nusselt number with the Reynolds number, Prandtl number and the curvature ratio, rather than combining the Reynolds number and the curvature ratio into the Dean number.

Table 4.1: Correlation results for overall heat transfer coefficients based on Equation 4.12.

Trial		Parallel flow			Counterflow		
d (m)	$\dot{m}_i / \dot{m}_o$	a	b	R^2	a	b	R^2
0.028	0.5	10.45	0.45	0.999	11.75	0.43	0.999
0.042	0.5	8.88	0.50	0.999	11.82	0.44	0.994
0.028	1.0	12.58	0.36	0.991	14.25	0.34	0.990
0.042	1.0	12.33	0.39	0.997	12.73	0.39	0.999
0.028	2.0	17.55	0.26	0.972	16.47	0.30	0.999
0.042	2.0	15.54	0.31	0.999	18.67	0.25	0.975

The advantage in using the heat exchanger in the counterflow configuration versus the parallel flow configuration is shown in Figure 4.7. The graph shows the percent increase in the heat transfer expected when the flow is changed from parallel flow to counterflow. The highest rates of increase are for low Dean numbers in the inner tube. As the flow rate is increased the relative advantage is significantly decreased. The cases where the inner flow is twice the annulus flow produced higher percent increases.

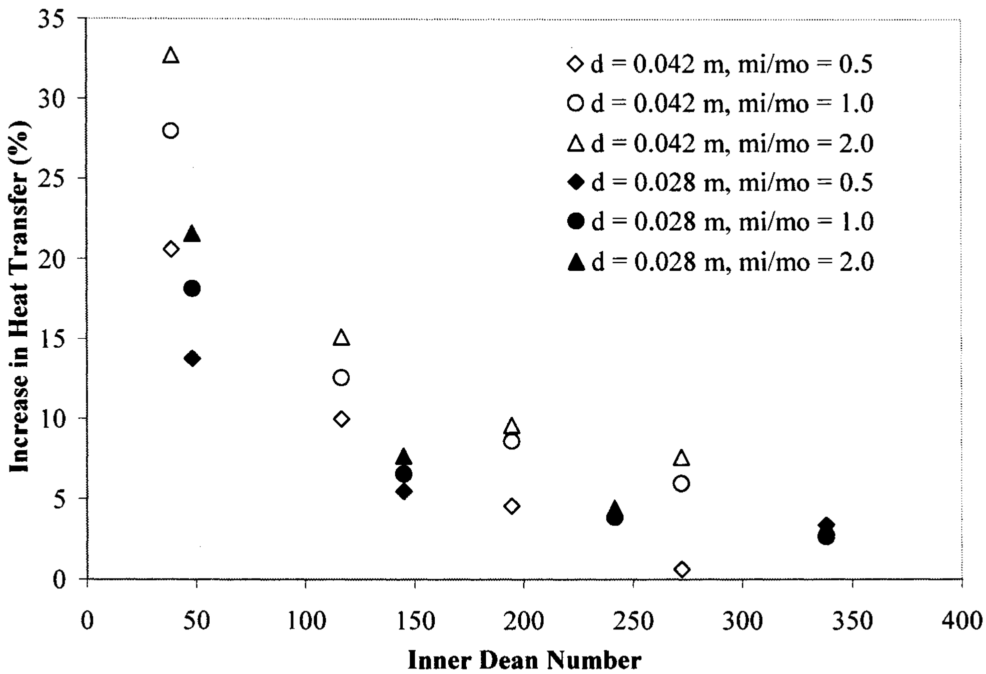

Figure 4.7: Percent increase in heat transfer when comparing parallel flow to counterflow configurations versus the inner Dean number.

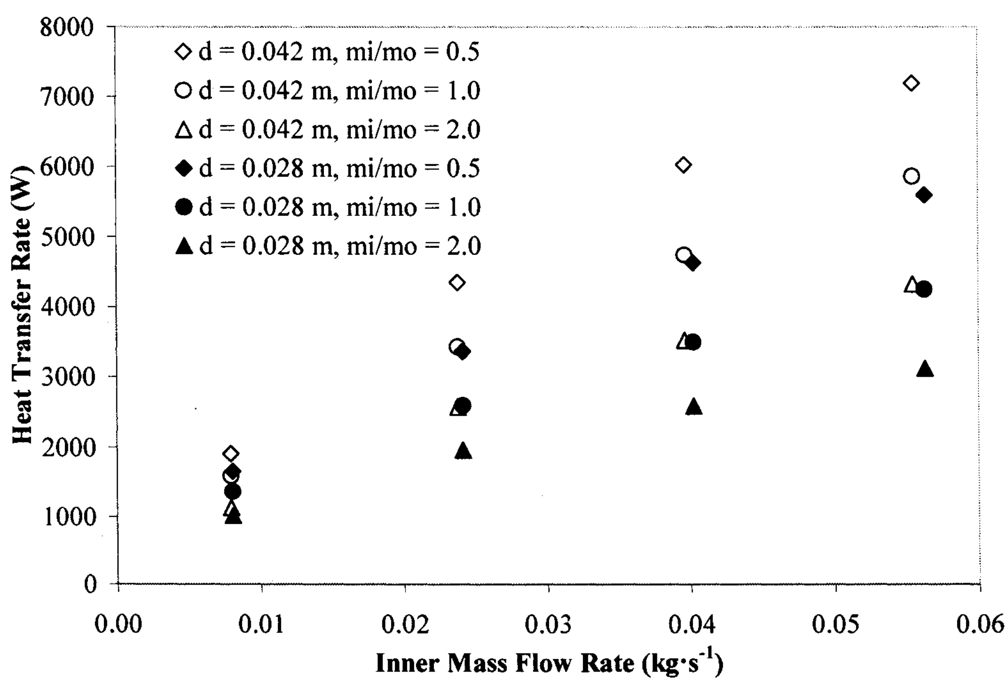

Figure 4.8: Heat transfer rate in the heat exchanger versus the mass flow rate in the inner tube.

Figure 4.8 shows the relationship between the heat transfer rate and the mass flow rate in the inner tube for the case of parallel flow. The data points are also divided into the three different mass flow ratios and the two different tube sizes. This allows for a more intuitive understanding of the effectiveness of the different mass flow ratios and tube sizes on the heat transfer rate than the plots of heat transfer coefficients versus the inner Dean number. For any given inner mass flow rate, there are six different values, corresponding to the different combinations of mass flow ratios and tube sizes. Increasing the tube size resulted in an increase in the total heat transfer rate. Increasing the inner tube diameter changes the flow pattern, flow intensity and available surface area for heat transfer. For the flow in the inner tube, the velocity is decreased which tends to result in a lower Reynolds number. At the same time, the curvature ratio is increased, which tends to increase secondary flows. However, for these changes, the inner Dean number decreases, which should result in lower heat transfer coefficients. The increase in the inner tube diameter (while keeping the outer tube the same diameter), increases the available heat transfer surface area for both fluids. Furthermore, increasing the tube size decreases the cross-sectional area for fluid flow in the annulus, resulting in an increased flow velocity, opposite to that found in the inner tube.

4.5.3 Inner Nusselt numbers

The Nusselt numbers for the inner tube are described in the section on model validation (4.5.1). This is an area that has been extensively studied and the results in this work are supported by other literature values. However, the inner Nusselt number is slightly affected by the flow in the annulus. The values quoted in the literature are for the most part either constant wall temperature or constant wall heat flux. In this work, neither of these boundary conditions is present. There is both hydrodynamically and thermodynamically developing flow before reaching a steady state. The extent of the thermodynamically developing flow could be affected by the unsteadiness of the boundary conditions. For the parallel flow case, increasing the flow rate in the annulus would tend to increase the inner Nusselt number, from anywhere from 0.5 to 2.5 % (Data not shown). However, for the counterflow case, the increase in the outer flow rate tends to decrease the Nusselt number for low inner Dean numbers, but had the opposite effect at higher inner Dean numbers, where the Nusselt number increased with increased flow rates in the annulus. For the counterflow case, increasing the outer flow rate resulted in a Nusselt number difference anywhere from -2.1 to 1.5 % (Data not shown).

4.5.4 Annulus Nusselt numbers

Nusselt numbers for the annulus have been calculated and correlated to a modified Dean number. The modified dean number for the annulus is calculated as it would be for a normal Dean number, except that the curvature ratio used is based on the ratio of the radius of the outer tube to the radius of curvature of the outer tube, and the Reynolds number based on the hydraulic radius of the annulus. Thus the modified Dean number is:

$$De = \frac{\rho V}{\mu}\left(\frac{D_o^2 - D_i^2}{D_o + D_i}\right)\left(\frac{D_o}{2R}\right)^{1/2} \tag{4.13}$$

The Nusselt number for the annulus is calculated using the hydraulic radius of the annulus as the characteristic length.

The correlation developed between the Nusselt number and the Dean number for the parallel and counterflow configurations are shown in Figures 4.9 and 4.10, respectively. For the range of Dean numbers tested, the best correlations were linear. The different tube sizes had a slight effect on the correlations, so separate correlations were performed.

The correlation was also performed using the modified Dean number with the ratio of the total gap of the annulus to the radius of curvature of the outer tube as the curvature ratio:

$$De = \frac{\rho V}{\mu}\left(\frac{D_o^2 - D_i^2}{D_o + D_i}\right)\left(\frac{D_o - D_i}{R}\right)^{1/2} \tag{4.14}$$

These results were better as the different tube sizes could be correlated together. These results are shown in Figure 4.11. The correlation shows much better fit than the previous methods.

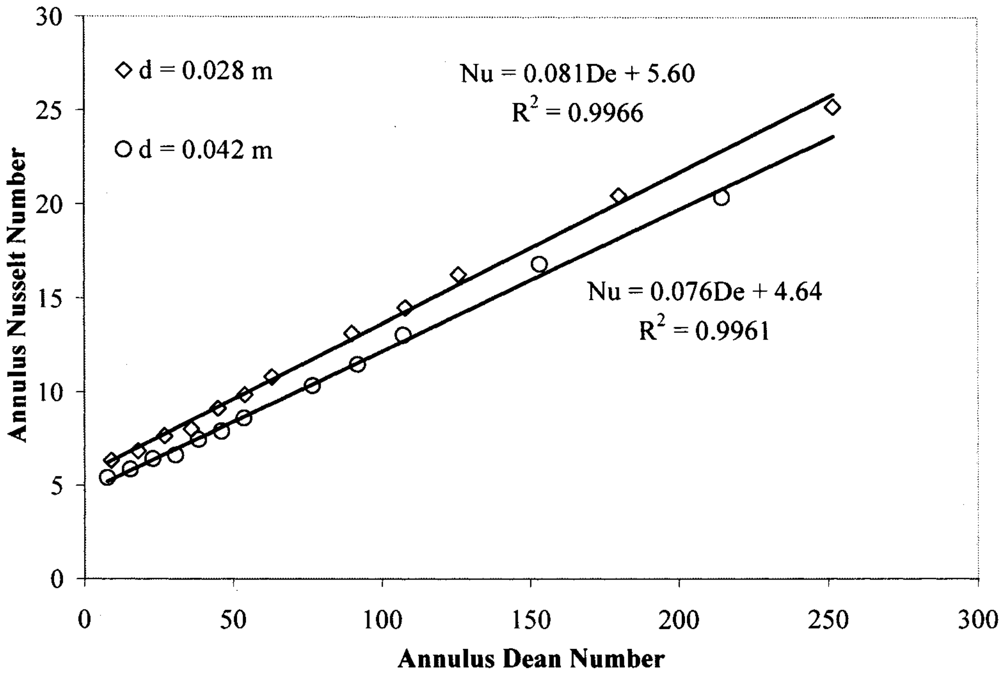

Figure 4.9: Nusselt number versus the annulus Dean number for parallel flow in the annulus.

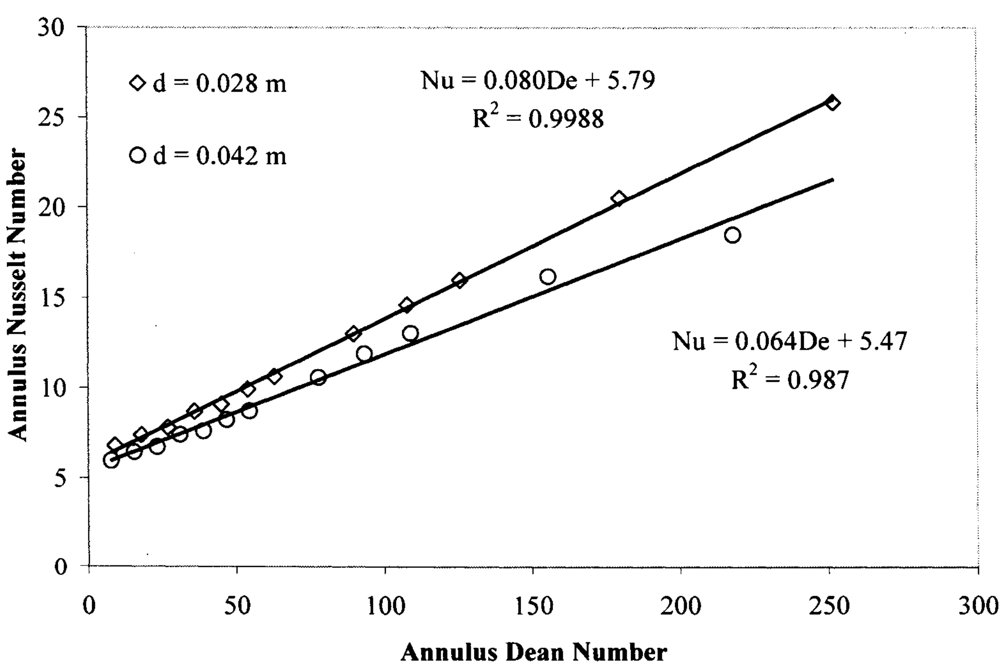

Figure 4.10: Nusselt number versus the annulus Dean number for counterflow in the annulus.

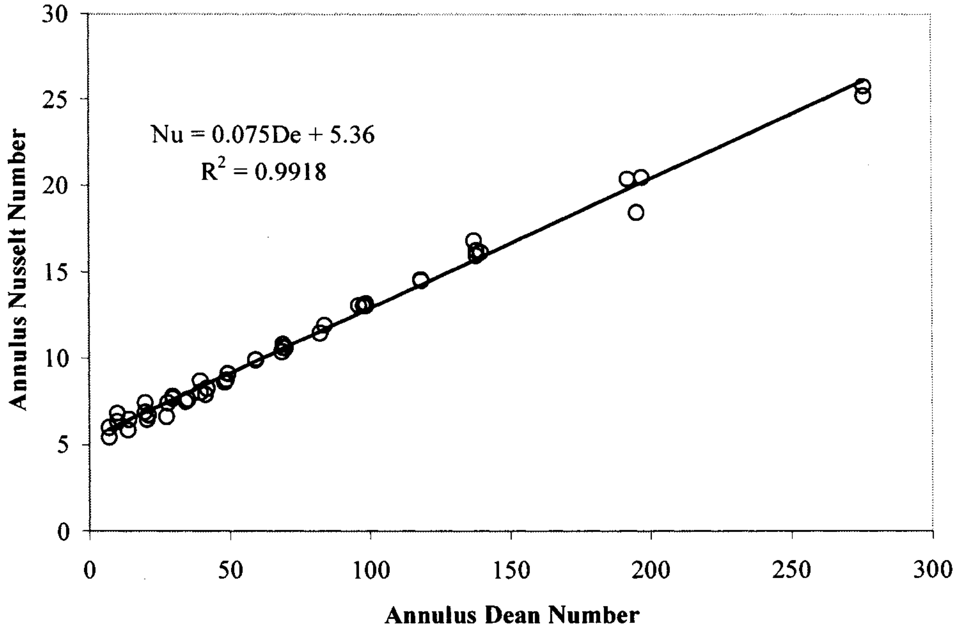

Figure 4.11: Nusselt number versus the annulus Dean number for parallel flow and counterflow using the annulus gap divided by the curvature of radius as the curvature ratio used in the Dean number.

4.5.5 Thermal resistances

It is important to look at the individual thermal resistances of the heat exchanger to determine where the largest resistances are, as decreasing these will have a much greater effect than trying to decrease resistances that are already quite low. The total thermal resistance (U_oA_o) of the heat exchanger is calculated by summing the reciprocals of all the individual thermal resistances (White, 1984):

$$U_oA_o = \frac{1}{\left[\dfrac{1}{A_ih_i} + \dfrac{\ln\left(r_o/r_i\right)}{2\pi kL} + \dfrac{1}{A_oh_o}\right]} \tag{4.15}$$

Figure 4.12 shows the thermal resistances versus the overall heat transfer coefficient. The overall heat transfer coefficient is highly dependent on decreasing the thermal resistance of the annulus, and is weakly affected by changes in the thermal resistance in the inner tube, especially for the case with the smaller tube size. For the most part the thermal resistance in the inner tube was fairly small and there is little trend between the inner thermal resistance and the overall heat transfer coefficient. For example, the thermal resistance for the inner tube with a diameter of 0.028 m stays practically constant for any overall heat transfer coefficient above 80 $W \cdot m^{-2} \cdot K^{-1}$. These data points are the ones with the highest inner Dean numbers, but there is little advantage in running at these higher Dean numbers if the thermal resistance in the annulus is the limiting factor for heat transfer. Therefore, in designing a heat exchanger, particular attention should be focused on decreasing the thermal resistance of the limiting condition, which has been shown to be the annulus region for the work in this study.

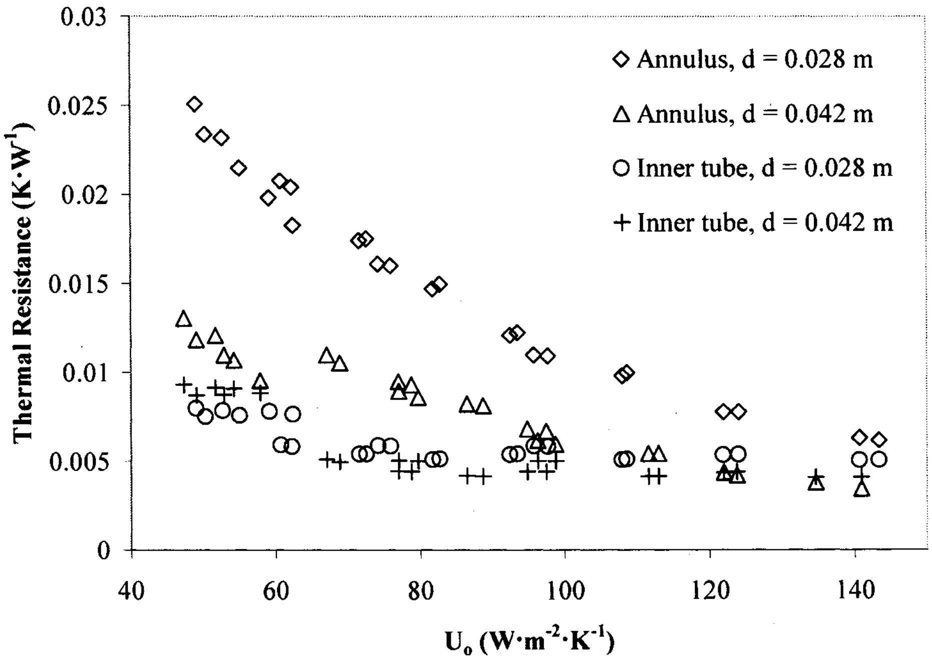

Figure 4.12: Thermal resistances versus the overall heat transfer coefficient for all simulations.

4.6 Conclusions

A computational fluid dynamics package (PHOENICS 3.3) was used to numerically study the heat transfer characteristics of a double-pipe helical heat exchanger for both parallel flow and counterflow. Validation runs were performed with the boundary conditions of constant wall temperature and constant heat flux. The results of these simulations were well within the range of results from the literature for helical coils. Effectiveness-NTU charts were presented for both the parallel flow and counterflow cases and the results showed that there is little difference between the theoretical calculations and the simulations.

Overall heat transfer coefficients were calculated for inner Dean numbers in the range of 38 to 350. The results show an increasing overall heat transfer coefficients as the inner Dean number is increased; however, flow conditions in the annulus had a stronger influence on the overall heat transfer coefficient. Thermal resistances were calculated for the annulus, inner tube and the coil. The total thermal resistance was, for the most part, highly dominated by the annulus, indicating that in the design of double-pipe helical heat exchangers, this is the area that should receive the most attention to effectively increase the overall heat transfer effectiveness. Furthermore, increasing the size of the inner tube resulted in lower thermal resistances in the annulus, though the thermal resistance in the inner tube remained fairly constant.

Nusselt numbers for the annulus were correlated with a modified Dean number, resulting in a strong linear relationship between the Nusselt number and the modified Dean number for the range of flow rates used in this study.

4.7 Acknowledgements

The authors are grateful to FCAR (Fonds pour la Formation de Chercheurs et l'Aide à la Recherche) and NSERC (Natural Sciences and Engineering Research Council of Canada) for the financial assistance for this study.

4.8 Nomenclature

a	Constant
A	Surface area of tube (m^2)
b	Constant
C	Capacity rate ($J \cdot s^{-1} \cdot K^{-1}$)
c_p	Specific heat ($J \cdot kg^{-1} \cdot K^{-1}$)
d	Diameter of inner tube (m)

D	Diameter of annulus (m)
De	Dean number, $De = \mathrm{Re}(d/2R)^{1/2}$
h	Heat transfer coefficient ($W \cdot m^{-2} \cdot K^{-1}$)
k	Thermal conductivity ($W \cdot m^{-1} \cdot K^{-1}$)
L	Length of heat exchanger (m)
$LMTD$	Log-mean temperature difference (K)
$\dot{m}$	Mass flow rate ($kg \cdot s^{-1}$)
NTU	Number of transfer units
Nu	Nusselt number, $Nu = hd/k$
Pr	Prandtl number, $\mathrm{Pr} = c_p \mu/k$
q	Heat transfer rate ($J \cdot s^{-1}$)
Q	Parameter defined by Akiyama and Cheng (1972, 1974b)
U	Overall heat transfer coefficient ($W^{-1} \cdot m^{-2} \cdot K^{-1}$)
R	Radius of curvature (m)
T	Temperature (K)
ΔT_1	Temperature difference at inlet (K)
ΔT_2	Temperature difference at outlet (K)
UHF	Uniform heat flux boundary condition
UWT	Uniform wall temperature boundary condition
V	Average velocity ($m \cdot s^{-1}$)
ε	Effectiveness
ζ	Boundary layer thickness ratio
ρ	Density ($kg \cdot m^{-3}$)
μ	Dynamic viscosity ($kg \cdot m^{-1} \cdot s^{-1}$)

Subscripts

asy	Asymptotic value
c	Cold
coldin	Cold fluid in
cur	Curved tube

h	Hot
hotin	Hot fluid in
i	Inside/inner
max	Maximum
min	Minimum
o	Outside/outer

4.9 References

Abdalla, M. A. 1994. A four-region, moving-boundary model of a once through, helical-coil steam generator. *Annals of Nuclear Energy*, Vol. 21(9):541-562.

Akiyama, M. and K. C. Cheng. 1972. Laminar forced convection heat transfer in curved pipes with uniform wall temperature. *International Journal of Heat and Mass Transfer*, Vol. 15:1426-1431.

Akiyama, M. and K. C. Cheng. 1974a. Graetz problem in curved pipes with uniform wall heat flux. *Applied Science Research*, Vol. 29:401-418.

Akiyama, M. and K. C. Cheng. 1974b. Laminar forced convection in the thermal entrance region of curved pipes with uniform wall temperature. *The Canadian Journal of Chemical Engineering*, Vol. 52:234-240.

Bai, B., L. Guo, Z. Feng, and X. Chen. 1999. Turbulent heat transfer in a horizontally coiled tube. *Heat Transfer-Asian Research*, Vol. 28(5):395-403.

Berger, S. A., L. Talbot, and L. S. Yao. 1983. Flow in curved pipes. *Ann. Rev. Fluid Mech.*, Vol. 15:461-512.

Dravid, A. N., K. A. Smith., E. W. Merrill, and P. L. T. Brian. 1971. Effect of secondary fluid motion on laminar flow heat transfer in helically coiled tubes. *AIChE Journal*, Vol. 17(5):1114-1122.

Haraburda, S. 1995. Consider helical-coil heat exchangers. *Chemical Engineering*, Vol. 102(7):149-151.

Janssen, L. A. M. and C. J. Hoogendoorn. 1978. Laminar convective heat transfer in helical coiled tubes. *International Journal of Heat and Mass Transfer*, Vol. 21:1197-1206.

Karahalios, G. T. 1990. Mixed convection flow in a heated curved pipe with core. *Physics of Fluids A*, Vol. 2(12):2164-2175.

Mori, Y. and W. Nakayama. 1965. Study on forced convective heat transfer in curved pipes (1st report, laminar region). *International Journal of Heat and Mass Transfer*, Vol. 8:67-82.

Mori, Y. and W. Nakayama. 1967. Study on forced convective heat transfer in curved pipes (3rd report, theoretical analysis under the condition of uniform wall temperature and practical formulae). *International Journal of Heat and Mass Transfer*, Vol. 10:681-695.

Prabhanjan, D. G., G. S. V. Raghavan, and T. J. Rennie. 2002. Comparison of heat transfer rates between a straight tube heat exchanger and a helically coiled heat exchanger. *International Communications in Heat and Mass Transfer*, Vol. 29(2):185-191.

Prabhanjan, D. G., T. J. Rennie, and G. S. V. Raghavan. 2004. Natural convective heat transfer from helical coiled tubes. *International Journal of Thermal Sciences*, Vol. 43(4):359-365.

Rabin, Y. and E. Korin. 1996. Thermal analysis of a helical heat exchanger for ground thermal energy storage in arid zones. *International Journal of Heat and Mass Transfer*, Vol. 39(5):1051-1065.

Rao, B. K. 1994. Turbulent heat transfer to power-law fluids in helical passages. *International Journal of Heat and Fluid Flow,* Vol. 15(2):142-148.

Sandeep, K. P. and T. K. Palazoglu. 1999. Secondary flow in coiled tubes. Presented at the *1999 ASAE Annual International Meeting*. Paper No. 996148. ASAE, 2950 Niles Rd., St. Joseph, MI 49085-9659 USA.

Seban, R. A. and E. F. McLaughlin. 1963. Heat transfer in tube coils with laminar and turbulent flow. *International Journal of Heat and Mass Transfer,* Vol. 6:387-395.

White, F. M. 1984. *Heat Transfer*. Addison-Wesley Publishing Company, Inc., 588 pp.

CONNECTING TEXT

The numerical investigation of the heat transfer characteristics of the double-pipe helical heat exchanger were presented in Chapter IV. Though the results were partially validated with literature data, an experimental investigation of the heat exchanger was needed to complete the validation. This is the topic of the following article.

V. EXPERIMENTAL STUDIES OF A DOUBLE-PIPE HELICAL HEAT EXCHANGER

5.1 Abstract

An experimental study of a double-pipe helical heat exchanger was performed. Two heat exchanger sizes and both parallel flow and counterflow configurations were tested. Flow rates in the inner tube and in the annulus were varied and temperature data recorded. Overall heat transfer coefficients were calculated and heat transfer coefficients in the inner tube and the annulus were determined using Wilson plots. Nusselt numbers were calculated for the inner tube and the annulus. The inner Nusselt number was compared to the literature values. Though the boundary conditions were different, a reasonable comparison was found. The Nusselt number in the annulus was compared to the numerical data. The experimental data fit well with the numerical for the larger heat exchanger. But, there were some differences between the numerical and experimental data for the smaller coil; however these differences may have been due to the nature of the Wilson plots. Overall, for the most part the results confirmed the validation of previous numerical work.

5.2 Introduction

Several studies have indicated that helically coiled tubes are superior to straight tubes when employed in heat transfer applications (Berger et al., 1983; Janssen and Hoogendoorn, 1978; Prabhanjan et al., 2002; Ruthven, 1971). The centrifugal force due to the curvature of the tube results in the development of secondary flows (flows perpendicular to the axial direction) which assist in mixing the fluid and enhance the heat transfer. In straight tube heat exchangers there is little mixing in the laminar flow regime, thus the application of curved tubes in laminar flow heat exchange processes can be highly beneficial. These situations can arise in the food processing industry for the heating and cooling of either highly viscous liquid food, such as pastes or purees, or for products that are sensitive to high shear stresses.

The majority of the studies involving helical coils and heat exchange have focused on two major boundary conditions; constant wall temperature and constant heat flux (Shah and Joshi, 1987; Prabhanjan et al., 2004). However, these boundary conditions are not present in most fluid-to-fluid heat exchangers. Haraburda (1995) described a method of calculating the shell side heat transfer coefficients for a coil-in-shell type heat exchanger; however, the calculations were based on empirical relations for flow over a bank of non-staggered circular tubes. Patil et al. (1982) describe a method for designing a coil-in-shell heat exchanger similar to that of Haraburda (1995).

The heat exchanger proposed in this work is unlike the coil-in-shell heat exchangers of Patil et al. (1982) and Haraburda (1995) in that the shell is replaced by a coiled tube. This changes the flows of the two fluids from being perpendicular to parallel flow or counterflow. This configuration results in secondary flows in both the inner tube and in the annulus, as both sections are curved and subjected to centrifugal forces. Furthermore, the coil-in-shell tube could, theoretically, have regions in the shell next to the coil where there is poor circulation. This problem could be avoided by using a double-pipe configuration. Karahalios (1990) and Petrakis and Karahalios (1996, 1997, 1999) have studied the fluid flow and heat transfer in a curved pipe with a solid core. They showed that the size of the core affected the flow in the annulus, with flows approaching parabolic for large cores and the flow being skewed towards the outer wall (Petrakis and Karahalios, 1999). Karahalios (1990) studied the heat transfer in a curved annulus; however, a constant temperature gradient on both the outer and inner walls of the annulus was used as the thermal boundary condition. These boundary conditions are not appropriate for the heat exchanger proposed in this work, where the temperature of the inner wall of the annulus will be dictated partly by the fluid temperature in the inner tube. Furthermore, the outer wall of the annulus will be insulated. This type of heat exchanger was numerically studied In Chapter IV, and was partly validated by using literature data. However, the wall boundary conditions for heat transfer were different from literature data, and there were no comparable annulus values. Thus the numerical results need to be validated with experiments using a double-pipe helical heat exchanger.

5.3 Objective

The objectives of this study were:

1. Design, build, and instrument two double-pipe helical heat exchangers, the difference between the two being the size of the inner tube.
2. Experimentally evaluate the heat transfer characteristics of a double-pipe helical heat exchanger for both parallel flow and counterflow configurations.
3. Compare the experimental results with the work of Chapter IV.

5.4 Materials and Methods

5.4.1 Heat exchanger

The heat exchanger was constructed from copper tubing and standard copper connections. The outer tube of the heat exchanger had an outer diameter of 15.9 mm and a wall thickness of 0.8 mm. The inner tube had an outer diameter of either 9.5 mm or 6.4 mm, both with wall thickness of 0.8 mm. The end connections are shown in Figure 5.1, which were constructed from standard copper tees and reducers. Each coil had a radius of curvature (measured from the center of the inner tube) of 235.9 mm. Small holes were drilled in the outer tube and tapped so that set screws could be used to ensure that the inner tube was centered prior to the final soldering of the end connections, which then held the inner tube in place. After soldering the set screws were removed and the holes covered so that the fluid flow in the annulus would not be disturbed. The heat exchanger consisted of one loop.

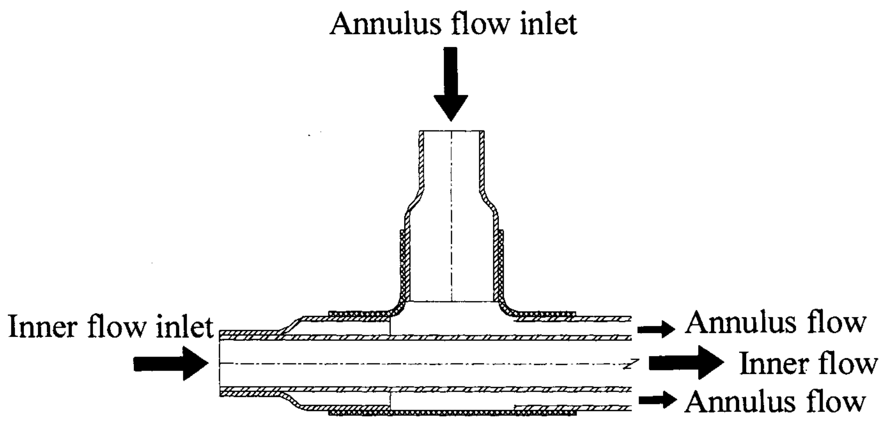

Figure 5.1: Cross-section of end connections used on the heat exchanger.

5.4.2 Experimental apparatus

The heat exchanger was tested in the setup show in Figure 5.2. Cold tap water (≈22.1°C) was used for the fluid flowing in the annulus. A large reservoir was used and a small submersible pump (#523086, Little Giant Pump Company, Oklahoma City, OK) was used to provide flow to the annulus. The water in the annulus was not circulated, and additional water was periodically added to the reservoir. However, this did not significantly change the depth of water in the reservoir and hence the flow rate was not compromised. The flow was controlled by a flowmeter (Model 4L53, Cole Parmer, Vernon Hills, IL) with an attached metering valve, allowing flows to be controlled and measured between 100 to 1500 $cm^3 \cdot min^{-1}$. Hot water for the inner tube was provided with an Isotemp Refrigerated Circulator (model 1013, Fisher Scientific, Pittsburgh, PA) set at 60°C. This water was circulated via the internal pump. The flow rate for the inner tube was controlled by an identical flowmeter and metering valve as described for the annulus flow. Flexible PVC tubing was used for all the connections. Type K thermocouples (Omega Engineering, Stanford, CT) were inserted into the flexible PVC tubing to measure the inlet and outlet temperatures for both fluids. Temperature data was recorded using a data acquisition/switch unit (Model 34970A, Agilent, Palo Alto, CA) connected to a computer.

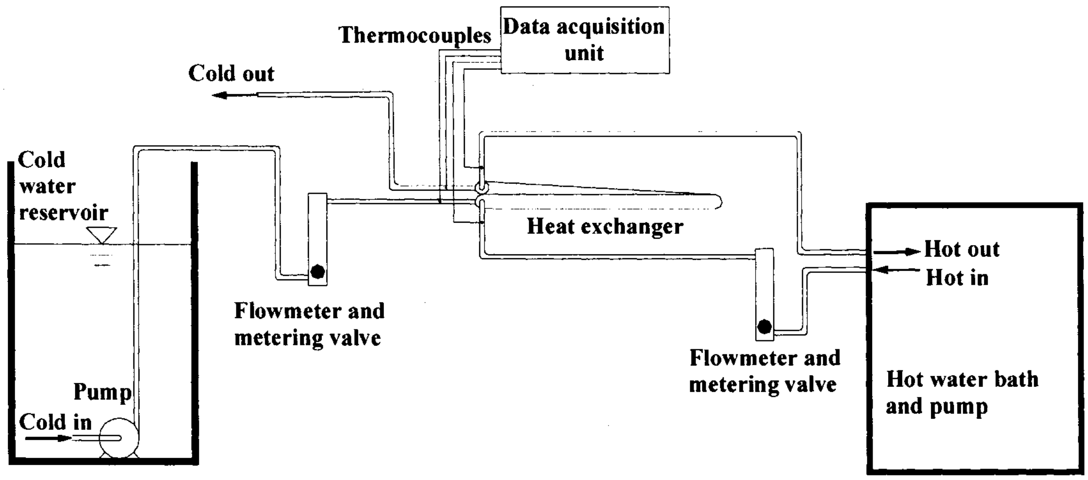

Figure 5.2: Schematic of the experimental setup.

5.4.3 Experimental procedure

Flow rates in the annulus and in the inner tube were varied. The following five levels were used: 100, 300, 500, 700, and 900 $cm^3 \cdot min^{-1}$. All possible combinations of these flow rates in both the annulus and the inner tube were tested. These were done for both coils, and in parallel flow and counterflow configurations. Furthermore, three replicates were done for every combination of flow rate, coil size and configuration. This resulted in a total of 300 trials. Temperature data was recorded every ten seconds. The data used in the calculations was from after the system had stabilized. Temperature measurements from the 120 seconds of the stable system were used, with temperature reading fluctuations within +/- 0.15°C. Though the type-K thermocouples had limits of error of 2.2°C, when placed in a common water solution the readings at steady state were all within +/- 0.1°C. All the thermocouples were constructed from the same roll of thermocouple wire, and hence the repeatability of temperature readings was high.

5.4.3 Calculation of heat transfer coefficients

The overall heat transfer coefficient, U_o, was calculated from the temperature data and the flow rates using the following equation (White, 1984):

$$U_o = \frac{q}{A_o LMTD} \tag{5.1}$$

LMTD is the log mean temperature difference, based on the inlet temperature difference,ΔT_1, and the outlet temperature difference, ΔT_2, using the following equation (White, 1984):

$$LMTD = \frac{(\Delta T_2 - \Delta T_1)}{\ln(\frac{\Delta T_2}{\Delta T_1})} \tag{5.2}$$

Heat transfer coefficients for the annulus side, h_o, and for the inner tube side, h_i, were calculated using traditional "Wilson plots" as described by Rose (2004). Wilson plots have been used in other heat exchanger studies (Briggs and Young, 1969; Shah, 1990). Wilson plots allow the heat transfer coefficients to be calculated based on the overall temperature difference and the rate of heat transfer, without the requirement of wall temperatures. This method was chosen to avoid the disturbance of flow patterns and heat transfer while attempting to measure wall temperatures. Wilson plots are generated by calculating the overall heat transfer coefficients for a number of trials where one fluid flow is kept constant and the other is varied. In this work, the flow in the inner tube was kept constant and the flow in the annulus was varied for the five different flow rates mentioned above. The overall heat transfer coefficient can be related to the inner and outer heat transfer coefficients by the following equation (White, 1984):

$$\frac{1}{U_o} = \frac{A_o}{A_i h_i} + \frac{A_o \ln(D_i/d_o)}{2\pi k L} + \frac{1}{h_o} \tag{5.3}$$

After calculating the overall heat transfer coefficients, the only variables in Equation 5.3 that are unknown are the heat transfer coefficients. By keeping the mass flow rate in the inner tube constant, it is then assumed that the inner heat transfer coefficient is constant. The outer heat transfer coefficient is assumed to behave in the following manner (Rose, 2004):

$$h_o = C v_o^n \tag{5.4}$$

Equation 5.4 was placed into Equation 5.3 and the values for the constant C and the exponent n were determined through curve fitting. The inner and outer heat transfer coefficients could then be calculated. This procedure was repeated for each inner flow rate, coil size, configuration, and replicate. This resulted in 60 Wilson plots, and 60 inner heat transfer coefficients. For each Wilson plot, five outer heat transfer coefficients were calculated, one for each of the flow velocities used.

5.5 Results and Discussion

5.5.1 Overall heat transfer coefficients

Overall heat transfer coefficients for parallel flow are presented in Figures 5.3 and 5.4 for the large coil and the small coil, respectively. The overall heat transfer coefficient is plotted against the inner Dean number for each of the flow rates in the annulus. The trends are typical for a fluid-to-fluid heat exchanger with the overall heat transfer coefficient increasing with both inner and annulus flows. For a given annulus flow rate, increasing the inner flow rate results in an eventual asymptotic overall heat transfer coefficient. It appears that this asymptotic value is reached at a lower Dean number for the large coil than the smaller coil.

The results from the counterflow configuration were similar to the parallel flow, as is expected, as changing the flow direction should have negligible effects on the heat transfer coefficients. Heat transfer rates, however, are much higher in the counterflow configuration, due the increased log mean temperature difference. The counterflow versus the parallel flow overall heat transfer coefficients are plotted in Figure 5.5, where the values plotted against each other are from the same experimental parameters. There is a reasonable agreement between the two values.

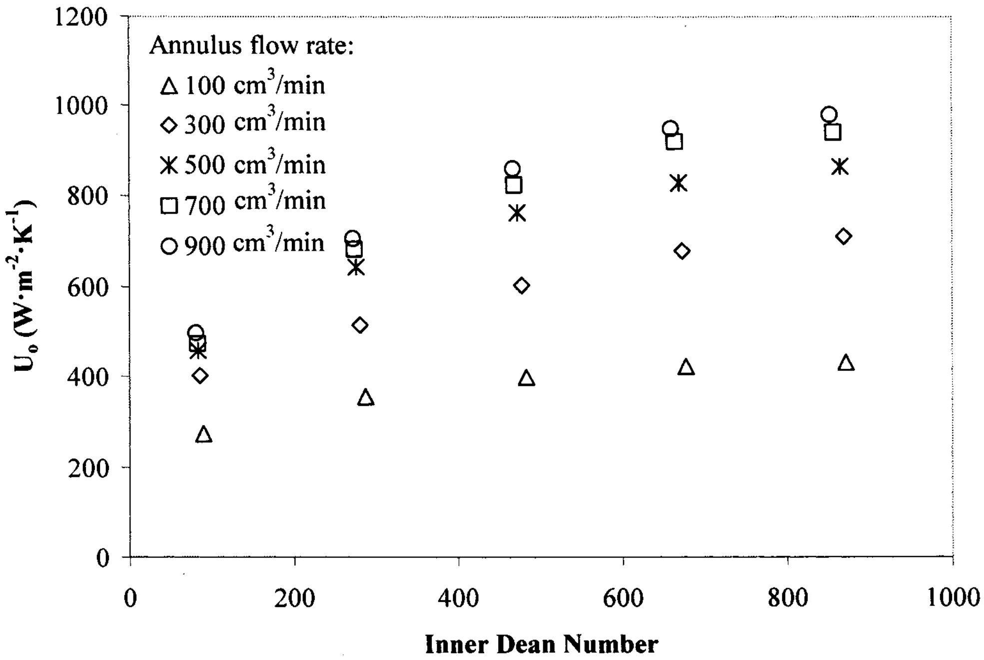

Figure 5.3: Overall heat transfer coefficient versus the inner Dean number for the large coil for each annulus mass flow rate.

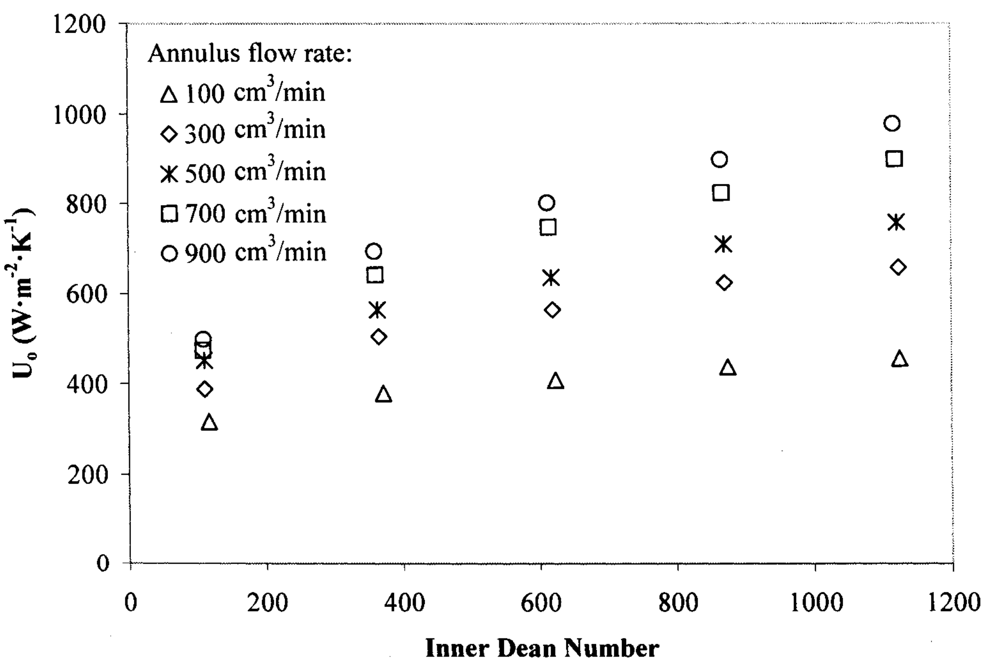

Figure 5.4: Overall heat transfer coefficient versus the inner Dean number for the small coil for each annulus mass flow rate.

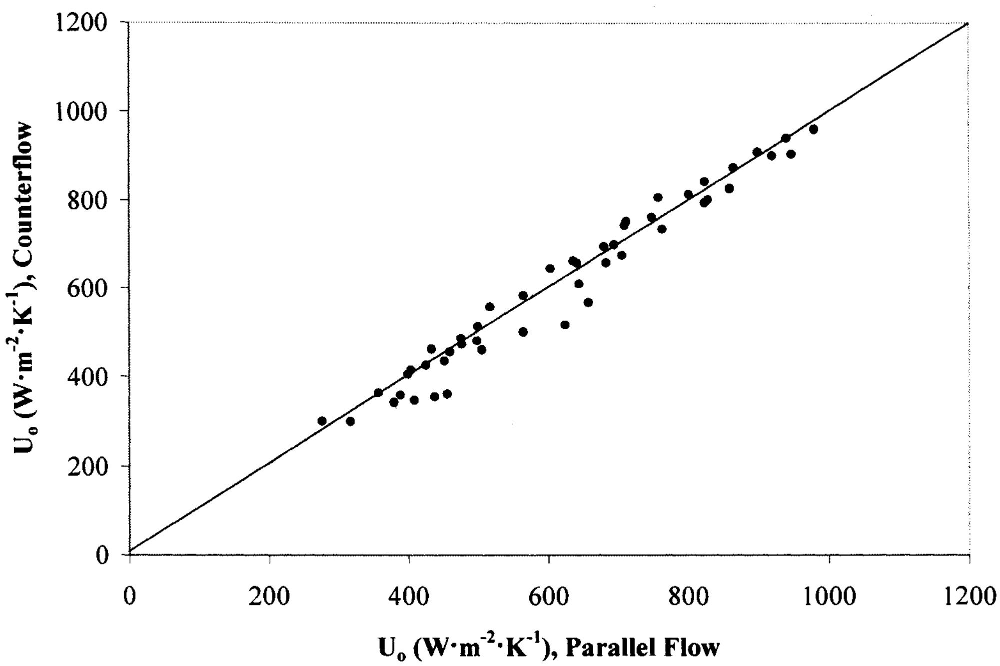

Figure 5.5: Counterflow overall heat transfer coefficient versus parallel flow overall heat transfer coefficient for all trials.

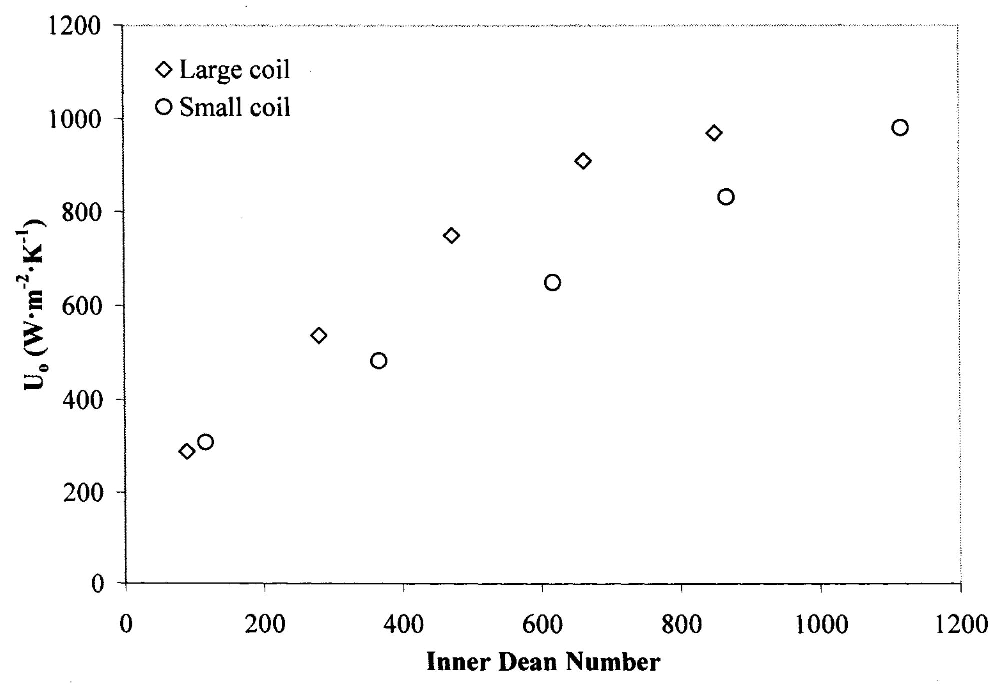

Figure 5.6: Overall heat transfer coefficient versus inner Dean number when mass flow rates are identical.

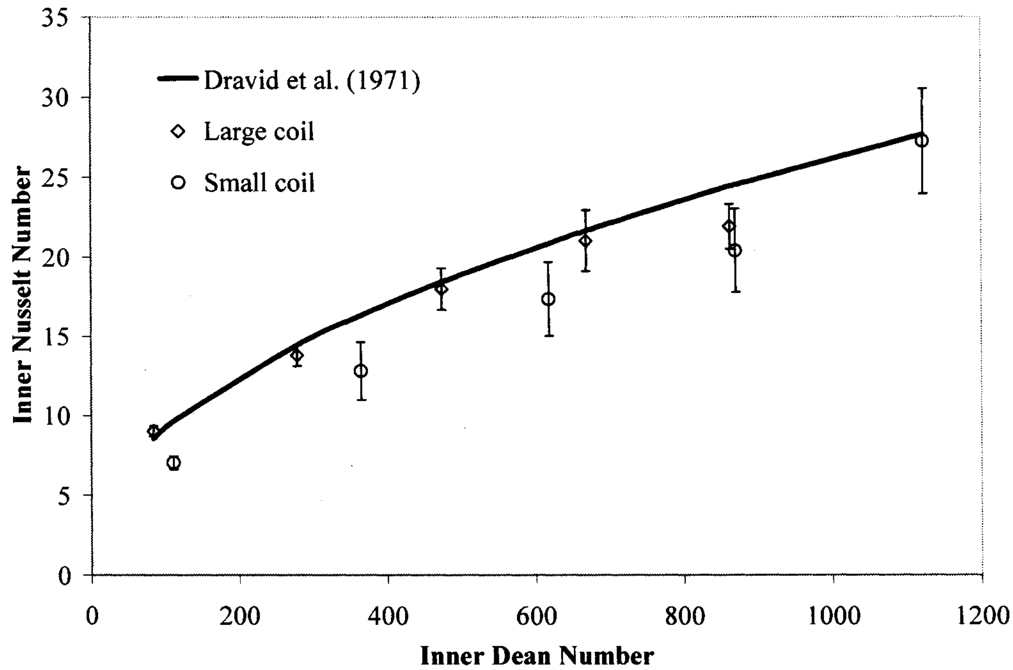

Figure 5.7: Inner Nusselt number versus inner Dean number.

Figure 5.6 shows the overall heat transfer coefficient versus the inner Dean number for the case when the mass flow rates in the inner tube and in the annulus are identical. For this case the overall heat transfer coefficient is higher for the large tube at the same inner Dean number, which is the same result as found in the numerical work of Chapter IV.

5.5.2 Inner Nusselt numbers

The inner Nusselt numbers are presented in Figure 5.7 (with ± 2 standard errors). These values are the average inner Nusselt number at each Dean number (average of parallel flow and counterflow values). The data are compared to the correlation of Dravid et al. (1971). Dravid et al. (1971) developed their correlation based on both numerical and experimental data with a constant wall heat flux. The Dean number range for Dravid et al. (1971) was from 50 to 2000 and the Prandtl number range was from 5 to 175. In order to calculate these correlations, Prandtl numbers were essential for the flow.

These were evaluated using the arithmetic mean temperature of the corresponding fluid (average of inlet and outlet temperatures). Decent agreement between the experimental and literature values indicate that the use of existing correlations for heat transfer in helical coils could be used to estimate inner heat transfer rate in a double-pipe helical heat exchanger. The experimental data fit close to the correlation of Dravid et al. (1971). However the Wilson plots did not work so well with the smaller coil, as there was more variance in the results.

5.5.3 Annulus Nusselt numbers

The Nusselt numbers in the annulus were calculated and correlated to the following modified Dean number:

$$De^* = \frac{\rho v}{\mu}\left(\frac{D_o^2 - D_i^2}{D_o + D_i}\right)\left(\frac{D_o - D_i}{R}\right)^{1/2} \tag{5.5}$$

The correlation developed numerically in Chapter IV is shown with the experimental data from this study in Figure 5.8 (with ± 2 standard errors). The data for the large coil fits well with the correlation; though the data for the small tube tends to diverge with increasing Dean number. This may indicate that the Nusselt number correlations need to take into account factors other than just the Dean number, or that the particular Dean number should be modified. In Chapter IV, the correlation of the data to a Dean number that used a different curvature ratio was also performed. However, in that case, separate correlations need to be made for each tube size, as could be done in here. Furthermore, the entrance region between the numerical and experimental heat exchanger were different. In the numerical work the inlet and outlet flows in the annulus were straight, whereas in this work the flow underwent a 90° bend at the entrance to the heat exchanger. It is difficult to predict the effect of the end connections of the Nusselt number. This could cause larger entrance effects which may not be applicable to heat exchangers with more than one loop. Furthermore, the data in this experimental work and the numerical data differ in Prandtl number, which was not considered in the correlation of the numerical data, as the numerical data used a Prandtl number for water at 20°C, and the average water temperature in the annulus in this work was higher. This should lower the correlation from Chapter IV bringing it closer to the small coil. Despite the differences between the two coil sizes, the Nusselt numbers for each coil size can be correlated to the modified Dean number linearly, as was done in Chapter IV. Further research needs to be performed on this entrance region to determine its effect on the heat transfer rates.

The low values for the small coil could also be due to the nature of the Wilson plots. It was noted that small changes in the coefficients used in the Wilson plots had a small effect on the inner Nusselt numbers, but much larger effects on the annulus Nusselt numbers. So the Wilson plots may be part of the reason for the divergence between the experimental and numerical results.

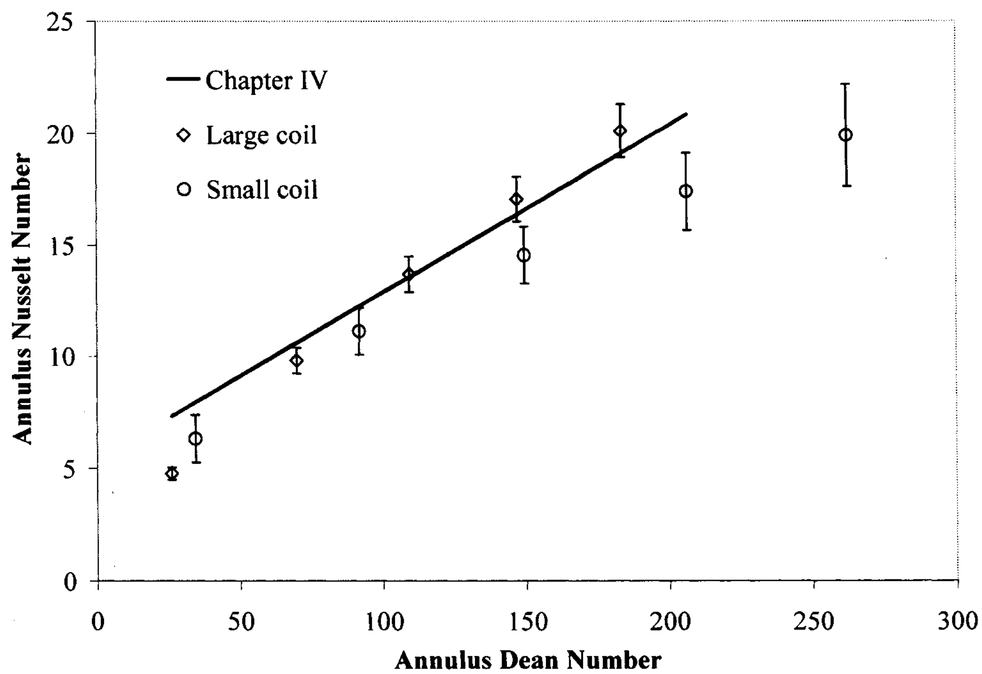

Figure 5.8: Annulus Nusselt number versus annulus Dean number.

5.6 Conclusions

An experimental study of a double-pipe helical heat exchanger was performed using two differently sized heat exchangers. The mass flow rates in the inner tube and in the annulus were both varied, as well as both parallel flow and counterflow configurations were tested. There were little differences between the overall heat transfer coefficients for the parallel flow and counterflow configurations. However, heat transfer rates were much higher in the counterflow configuration due to the larger average temperature difference between the two fluids.

The Nusselt number in the inner tube was compared to the literature values. Though the boundary conditions are different between the experimental data and the literature data, there was reasonable agreement between the two. The Nusselt number in the annulus was compared to the numerical work, and though the experimental data fit well with the numerical data for the larger coil, there was a deviation between the data for the small coil. There may be a cause for the difference in the Nusselt number as the entrance region was very different between the numerical and experimental setups. The 90° elbow used in the connection in the experimental setup could increase the Nusselt number significantly in the entrance region, further work needs to be done to quantify this effect.

5.7 Acknowledgements

The authors are grateful to FCAR (Fonds pour la Formation de Chercheurs et l'Aide à la Recherche) and NSERC (Natural Sciences and Engineering Research Council of Canada) for the financial assistance for this study.

5.8 Nomenclature

A	Surface area of tube (m^2)
C	Constant in Equation 5.4
d	Diameter of inner tube (m)
D	Diameter of annulus (m)
De^*	Modified Dean number
h	Heat transfer coefficient ($W \cdot m^{-2} \cdot K^{-1}$)
k	Thermal conductivity ($W \cdot m^{-1} \cdot K^{-1}$)
L	Length of heat exchanger (m)
$LMTD$	Log-mean temperature difference (K or °C)
n	Exponent in Equation 5.4

q	Heat transfer rate ($J \cdot s^{-1}$)
v	Velocity ($m \cdot s^{-1}$)
U	Overall heat transfer coefficient ($W \cdot m^{-2} \cdot K^{-1}$)
ΔT_1	Temperature difference at inlet (K)
ΔT_2	Temperature difference at outlet (K)
ρ	Density ($kg \cdot m^{-3}$)
μ	Dynamic viscosity ($kg \cdot m^{-1} \cdot s^{-1}$)

Subscripts

i	Inside/inner
o	Outside/outer

5.9 References

Berger, S. A., L. Talbot, and L. S. Yao. 1983. Flow in curved pipes. *Ann. Rev. Fluid Mech.*, Vol. 15:461-512.

Briggs, D. E. and E. H. Young. 1969. Modified Wilson plot techniques for obtaining heat transfer correlations for shell and tube heat exchangers. *Chem. Eng. Prog. Symp. Ser.* Vol. 65:35-45.

Dravid, A. N., K. A. Smith, E. W. Merrill, and P. L. T. Brian. 1971. Effect of secondary fluid motion on laminar flow heat transfer in helically coiled tubes. *AIChE Journal*, Vol. 17(5):1114-1122.

Haraburda, S. 1995. Consider helical-coil heat exchangers. *Chemical Engineering*, Vol. 102(7):149-151.

Janssen, L. A. M. and C. J. Hoogendoorn. 1978. Laminar convective heat transfer in helical coiled tubes. *International Journal of Heat and Mass Transfer*, Vol. 21:1197-1206.

Karahalios, G. T. 1990. Mixed convection flow in a heated curved pipe with core. *Physics of Fluids A*, Vol. 2(12):2164-2175.

Patil, R. K., Shende, B. W., and P. K. Ghosh. 1982. Designing a helical-coil heat exchanger. *Chemical Engineering*, Vol. 92(24):85-88.

Petrakis, M. A., and G. T. Karahalios. 1996. Technical note: steady flow in a curved pipe with a coaxial core. *International Journal for Numerical Methods in Fluids*, Vol. 22(12):1231-1237.

Petrakis, M. A., and G. T. Karahalios. 1997. Exponential decaying flow in a gently curved annular pipe. *International Journal of Non-Linear Mechanics*, Vol. 32(5):823-835.

Petrakis, M. A., and G. T. Karahalios. 1999. Fluid flow behaviour in a curved annular conduit. *International Journal of Non-Linear Mechanics*, Vol. 34(1):13-35.

Prabhanjan, D. G., G. S. V. Raghavan, and T. J. Rennie. 2002. Comparison of heat transfer rates between a straight tube heat exchanger and a helically coiled heat exchanger. *International Communications in Heat and Mass Transfer*, Vol. 29(2):185-191.

Prabhanjan, D. G., T. J. Rennie, and G. S. V. Raghavan. 2004. Natural convective heat transfer from helical coiled tubes. *International Journal of Thermal Sciences*, Vol. 43(4):359-365.

Rose, J. W. 2004. Heat-transfer coefficients, Wilson plots and accuracy of thermal measurements. *Experimental Thermal and Fluid Science*, Vol. 28:77-86.

Ruthven, D. M. 1971. The residence time distribution for ideal laminar flow in a helical tube. *Chemical Engineering Science*, Vol. 26:113-1121.

Shah, R. K. 1990. Assessment of modified Wilson plot techniques used for obtaining heat exchanger design data, in: *Heat Transfer 1990. Proceedings of the 9th International Heat Transfer Conference*, Vol. 5:51-56.

Shah, R. K. and S. D. Joshi. 1987. Convective heat transfer in curved ducts. In: Handbook of Single-Phase Convective Heat Transfer (eds. S. Kakac, R. K. Shah, W. Aung), Wiley Interscience, New York, pp 5.1-5.46.

White, F. M. 1984. *Heat Transfer*. Addison-Wesley Publishing Company, Inc., 588 pp.

CONNECTING TEXT

Upon completion of both the numerical and experimental investigations of the double-pipe heat exchanger, and finding reasonable agreement between the two models, further study is required into the effect of fluid properties on the heat transfer characteristics of the heat exchanger. Chapters IV and V were both conducted using water as the heating and cooling fluids. For industrial applications, one, if not both, of these fluids will be a liquid other than water, as well as being subjected to thermal effects. Thus Chapter VI deals with the effects of the Prandtl number and thermally dependent fluid thermal conductivities on the heat transfer characteristics of a double-pipe helical heat exchanger.

VI. EFFECT OF FLUID THERMAL PROPERTIES ON THE HEAT TRANSFER CHARACTERISTICS IN A DOUBLE-PIPE HELICAL HEAT EXCHANGER

6.1 Abstract

Heat transfer characteristics of a double-pipe helical heat exchanger were numerically studied to determine the dependency of the heat transfer on the thermal properties of the fluid. Two studies were performed; the first with three different Prandtl numbers and the second with thermally dependent thermal conductivities. The first study used Prandtl numbers of 7.0, 12.8, and 70.3, with four different flow rates in the inner tube and two tube sizes. For each inner tube flow rate, three different flow rates in the annulus were used. For the second study, two different flow rates were used in the inner tube, each with two different flow rates in the annulus. Both parallel flow and counterflow configurations were used. Thermal conductivities of the fluid were based on a linear relationship with the fluid temperature. Six different fluid dependencies were modeled.

Results from the first study showed that the inner Nusselt number was dependent on the Prandtl number, with a greater effect at low Dean numbers, this being attributed to changing hydrodynamic and thermal entry lengths and its effects. Correlations of the Nusselt number based on the Prandtl number and a modified Dean number are presented for the flow in the annulus. Results from the second part of the study showed that the Nusselt number was better correlated against a modified Dean number, for both flow in the inner tube and in the annulus. The counterflow configuration had higher heat transfer rates than the parallel flow, but the ratio of these differences was not different when comparing thermally dependent properties and thermally stable properties.

6.2 Introduction

Using correct and proper values for fluid properties are important when designing a heat exchanger for a particular process, especially for the heating and cooling of complex fluids, such as food products. These properties play a role in both the rate of heat transfer (and hence the required size of the heat exchanger) as well as the pressure drop across the heat exchanger, which is important for assuring that correct pumps are selected. Furthermore, temperature dependent properties complicate the design of heat exchangers for specific processes. The prediction of the developing hydrodynamic and thermal boundary layers can be quite complex and difficult. Numerical methods and/or experiments are often required.

For the most part, heat transfer characteristics for tube flow are described using dimensionless numbers, with the Nusselt number expressed as a function of the Reynolds number and the Prandtl number. However, for helical coils, the Reynolds number is often replaced by the Dean number (Mori and Nakayama, 1965; Kalb and Seader, 1972), which takes the curvature effect into consideration, though this is not always the case (Bai et al., 1999). Other correlations have been based on friction factors (Seban and McLaughlin, 1963) and the Graetz number (in the case of developing flow) (Kubair and Kuloor, 1966), and the curvature ratio (Ozisik and Topakoglu, 1968).

The majority of these cases are for thermal boundary conditions of constant wall temperature or constant wall flux, which is different from the boundary conditions found in a fluid-to-fluid heat exchanger (Prabhanjan et al., 2004). Under these conditions, changing the flow rate, fluid properties or fluid temperature on one side of the heat exchanger can affect the heat transfer and fluid flow characteristics on the other side of the heat exchanger. For example, increasing the flow rate tends to increase heat transfer rates, which result in an increase/decrease of the average temperature of the fluid on the other side of the barrier. Thus the fluid properties, such as thermal conductivity, density, and viscosity of the fluid may change. If the viscosity decreases, the average pressure drop will also decrease. Depending on the type of pump used, this could result in an increased flow rate. Thus it is important to investigate and understand the effects of thermally dependent fluid properties, and how flow rates and geometry can affect the heat transfer characteristics when dealing with thermally dependent properties.

6.3 Objective

The objective of this work is to study the effects of fluid thermal properties on the heat transfer characteristics for double-pipe helical heat exchangers. The work was performed using a computational fluid dynamics package (PHOENICS 3.3). The set goals were achieved in two stages:

1. Determination of the effects of the Prandtl number
2. Determination of the effects of thermally dependent thermal conductivity

6.4 Materials and Methods

6.4.1 CFD modeling

The method used to perform the computational fluid dynamics modeling of the double-pipe helical heat exchanger are outlined in Chapter IV, along with validation simulations. In this work, the same geometries were used as in Chapter IV: two different sized double-pipe heat exchangers. Both used an outer tube with an inner diameter of 0.1 m and a pitch of 0.115 m. The inner tubes had outer diameters of 0.04 and 0.06 m, both with wall thicknesses that were 15% of the diameter (inner diameters of 0.028 and 0.042 m) and a pitch of 0.115 m. The length of the heat exchangers from inlet to outlet is 2π. The radius of curvature of the tubes is 0.8 m. The properties of the inner tube were set to stainless steel, with a thermal conductivity of 16 $W{\cdot}m^{-1}{\cdot}K^{-1}$, density of 7881.8 $kg{\cdot}m^{-3}$ and a specific heat of 502 $J{\cdot}kg^{-1}{\cdot}K^{-1}$. The outer tube was set to have adiabatic boundary conditions; the inner tube was set to allow conductive heat flow through the tube. The flow regime for all trials was in the laminar region.

6.4.2 Prandtl numbers

In the first set of simulations, the Prandtl number was varied using three different levels, 7.03, 12.8, and 70.3. These different Prandtl numbers were achieved by changing the thermal conductivity of the fluid, using thermal conductivities of 0.597, 0.328, 0.0597 $W{\cdot}m^{-1}{\cdot}K^{-1}$, along with a dynamic viscosity of 1.004 x 10^{-3} $kg{\cdot}m^{-1}{\cdot}s^{-1}$, and a specific heat of 4181.8 $J{\cdot}kg^{-1}{\cdot}K^{-1}$. Four different mass flow rates were used in the inner tube (0.00835, 0.02504, 0.04174 and 0.05843 $kg{\cdot}s^{-1}$). For each of these flow rates, three simulations were performed, one with an annulus mass flow rate that has half the inner value, one with an equal value, and one that had double the inner mass flow rate, resulting in 12 different flow combinations. These combinations were performed using both coil sizes and the three Prandtl numbers resulting in a total of 72 trials.

6.4.3 Thermally dependent thermal conductivities

The second set of simulations focused on thermally dependent thermal conductivities. In this set, two different mass flow rates were used in the inner tube (0.00835 and 0.05843 $kg \cdot s^{-1}$), with flow rates in the annulus which were either half or double the value in the inner tube. This results in four different flow combinations. Six different model fluids were used. The thermal conductivities of these fluids were based on the following relationship:

$$k = \mathrm{A} + \mathrm{B}T_{abs} \tag{6.1}$$

This results in a linear relationship between the thermal conductivity of the fluid and the absolute temperature, T_{abs}, with a value of 0.597 $W \cdot m^{-1} \cdot K^{-1}$ for all fluids at 20°C. The particular values used for the constants, A and B, are given in Table 6.1, along with the percent change the fluid undergoes if heated from 20°C to 80°C. Fluids K4, K5, and K6 were also tested in a counterflow configuration, using the four different flow combinations and the two different tube sizes.

Table 6.1: Constants used in Equation 6.1 and percent change in thermal conductivity.

Fluid	A ($W \cdot m^{-1} \cdot K^{-1}$)	B ($W \cdot m^{-1} \cdot K^{-2}$)	% change
K1	0.451	0.000498	5
K2	0.306	0.000995	10
K3	0.0139	0.00199	20
K4	-0.569	0.00398	40
K5	-1.444	0.00697	70
K6	-2.318	0.00995	100

Table 6.2 shows a selection of some common food products along with the percent change of the thermal conductivity occurring between two temperatures. For the most part, these food products would have a relationship with temperature similar to fluid K2. Other thermal conductivity values have been added to adequately cover additional cases that could possibly occur in the food industry.

Table 6.2: Thermal conductivities of selected food products (ASHRAE, 1998).

Food product	Temperature (°C)	Thermal conductivity ($W \cdot m^{-1} \cdot K^{-1}$)	% change
Apple juice, 87% H_2O	20 80	0.559 0.631	12.9
Grape juice, 89% H_2O	20 80	0.567 0.639	12.7
Whole milk	20 80	0.550 0.614	11.6
Sucrose solution, 40% H_2O	20 80	0.404 0.454	12.4
Glucose solution, 89% H_2O	20 80	0.566 0.639	12.9
Honey, 80% H_2O	2 69	0.502 0.415	-17.3

6.5 Results and Discussion

6.5.1 Prandtl effects in the inner tube

Three different Prandtl numbers were used in the inner tube, 7.0, 12.8, and 70.3. Each of these was achieved by changing the thermal conductivity of the fluid, while the other fluid properties (density, specific heat) were not changed. A total of 72 simulations were performed (4 inner flow rates, 3 corresponding annulus flow rates, 2 tube diameters, and 3 Prandtl numbers). In this work, the difficulty to determine the appropriate effect of the Prandtl number is augmented by the developing hydrodynamic and thermal entrance regions. For each Dean number, the hydrodynamic entrance region is of different lengths, which also affects the thermal entrance region. Hence it is difficult to correlate the data to a simple power law equation, as the entrance effects can become large as the Prandtl number increases. However, there are 24 simulations that have corresponding simulations that only differ by the Prandtl numbers used. That is, for any given simulation, there are two other simulations that are operated under the same conditions; except for the Prandtl number (different Prandtl numbers are due only to different thermal conductivities of the fluid). In order to determine the effect of the Prandtl number on the Nusselt number, the ratio of the Nusselt numbers (for any two simulations with the same operating parameters) were calculated. Two different ratios were used, each were based on the Nusselt number for a given Prandtl number (12.8 or 70.3) divided by the Nusselt number with the lowest Prandtl number (7.0). Figure 6.1 shows a plot of the increase in Nusselt number versus the Dean number. The ratio of the Nusselt numbers tends to decrease with increasing Dean number, which could be attributed to the changing hydrodynamic entry length. For the most part, the effect of different Prandtl numbers on the Nusselt number is limited to low Dean numbers. However, this is not a general statement, as the hydrodynamic and thermal entrance regions are affected by the Dean number. Furthermore, the Prandtl number affects the developing thermal boundary layer, tending to increase the entry length as it is increased.

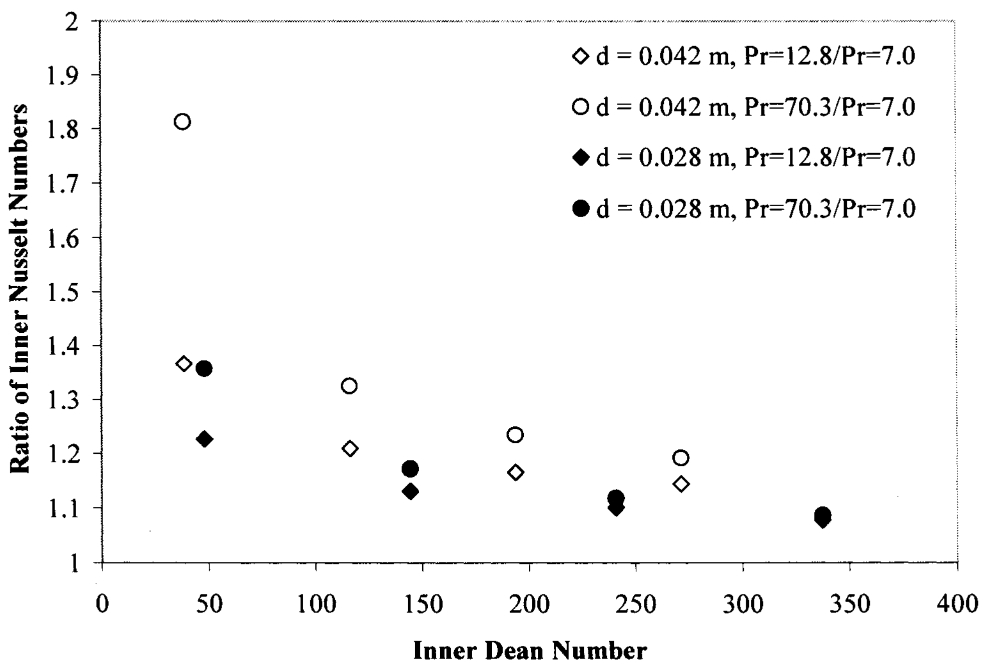

Figure 6.1: Ratio of inner Nusselt number when the Prandtl number is changed from 7.0 to 12.8 or from 7.0 to 70.3, versus the inner Dean number.

The effect of the Prandtl and Dean numbers on the Nusselt number is often presented as a power law equation, in the following form:

$$Nu = aDe^{b}\,\mathrm{Pr}^{c} \tag{6.2}$$

For any given set of flow conditions (flow rate, tube size) that only differs due to the Prandtl number, then the ratio of the Nusselt numbers can be expressed as:

$$\frac{Nu_2}{Nu_1} = \left(\frac{\Pr_2}{\Pr_1}\right)^c \tag{6.3}$$

The constant can be evaluated as follows:

$$c = \frac{\ln\left(\frac{Nu_2}{Nu_1}\right)}{\ln\left(\frac{\Pr_2}{\Pr_1}\right)} \tag{6.4}$$

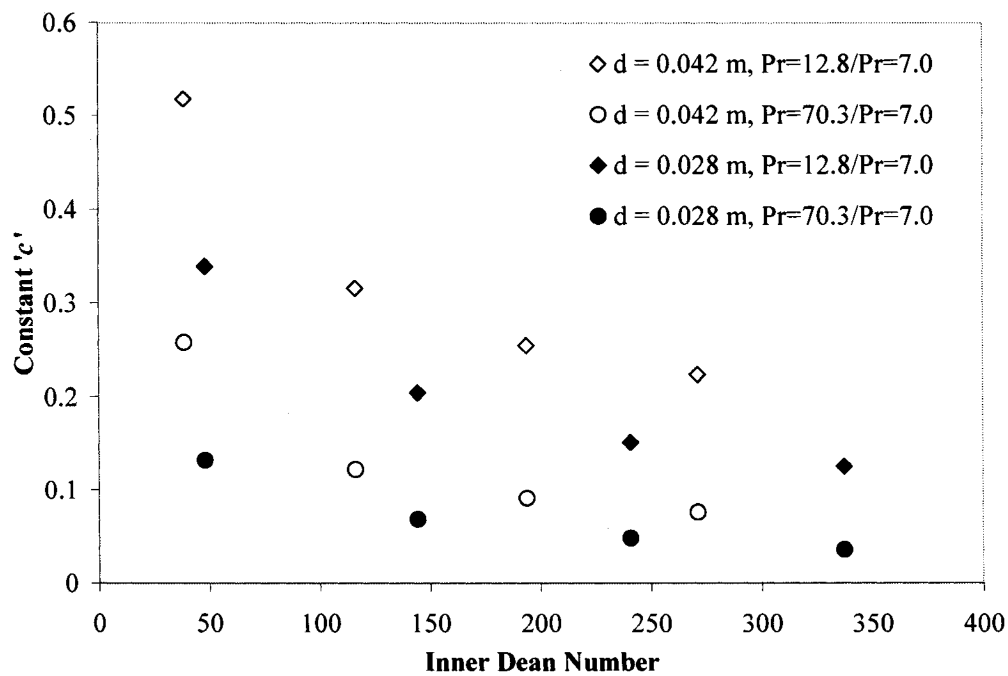

Figure 6.2: Constant '*c*' used in the inner Nusselt number correlations versus the inner Dean number. Plot shows when the Prandtl number is changed from 7.0 to 12.8 or from 7.0 to 70.3, with all other factors similar.

The values of the constant are plotted against the Dean number in Figure 6.2. There is a definite decrease in this constant as the Dean number is increased. Increasing the Dean number could result in larger entrance length. Generally, increasing the Reynolds number increases the entrance length, though the curvature effects this change.

The value of the constant ranged from 0 to 0.55. For helical coils, the Prandtl number effect on the heat transfer is often related to the Nusselt number in a power law formulation, along with the Reynolds number or the Dean number. Seban and McLaughlin (1963) found that for laminar flow the power is one-third. Dravid et al. (1971), found a relationship with an exponent of 0.175, for Dean numbers in the range of 50 to 2000 and Prandtl numbers from 5 to 175. Kalb and Seader (1972, 1974) found an exponent of 0.0108 for low Prandtl numbers (0.005 to 0.05) and a constant wall heat flux, whereas for Prandtl numbers in the range of 0.7 to 5 they reported exponents of either 0.1 or 0.2, for constant wall heat flux and constant wall temperatures, respectively. Janssen and Hoogendoorn (1978) found that an exponent of 0.167 worked well in their correlations in the fully developed thermal region, whereas the Nusselt number was proportional to the Prandtl number to the power of 0.333 in the thermal entry region. The work present here differs from the literature due to the boundary conditions and the pitch of the coil, which are usually not found in the literature, though there are conditions that are present in a double-pipe helical heat exchanger.

6.5.2 Prandtl effects in the annulus

Nusselt numbers were calculated for the annulus. These, unlike the flow in the inner tube, were less affected by entry effects. However, correlating the Nusselt number to the Prandtl and Dean numbers was limited to different ranges of $(De^2\mathrm{Pr})^{1/2}$. This is not unusual, as other authors have often used different correlations depending on the range of one or more of the variables. Janssen and Hoogendoorn (1978) used the variable $(De^2\mathrm{Pr})^{1/2}$ to describe ranges where certain correlations were applicable. Three distinct regions were observed. The highest range (with $(De^2\mathrm{Pr})^{1/2}$ above 500) were divided into two correlations, one for each pipe size, as they could not be correlated together. The following correlations were developed in this work:

$$Nu = 2.08 De^{0.20}\,\mathrm{Pr}^{0.28} \quad \text{for } 18 < (De^2\mathrm{Pr})^{1/2} < 100 \quad R^2 = 0.955 \tag{6.5}$$

$$Nu = 0.39 De^{0.58}\,\mathrm{Pr}^{0.46} \quad \text{for } 100 < (De^2\mathrm{Pr})^{1/2} < 500 \quad R^2 = 0.989 \tag{6.6}$$

$$Nu = 2.70 De^{0.30}\,\mathrm{Pr}^{0.29} \quad \text{for } 500 < (De^2\mathrm{Pr})^{1/2} < 2315,\ d = 0.4 \quad R^2 = 0.969 \tag{6.7}$$

$$Nu = 5.27 De^{0.20}\,\mathrm{Pr}^{0.19} \quad \text{for } 500 < (De^2\mathrm{Pr})^{1/2} < 1610,\ d = 0.6 \quad R^2 = 0.974 \tag{6.8}$$

For these ranges, the number of data points used was 16, 39, 10, and 7, respectively. The predicted values (from each corresponding equation) versus the simulated values for the Nusselt numbers are presented in Figure 6.3. The square of the correlation coefficient for all the correlations was close to unity. The Dean number used in these correlations is a modified Dean number for the curved annulus:

$$De = \frac{\rho V}{\mu}\left(\frac{D_o^2 - D_i^2}{D_o + D_i}\right)\left(\frac{D_o - D_i}{R}\right)^{1/2} \tag{6.9}$$

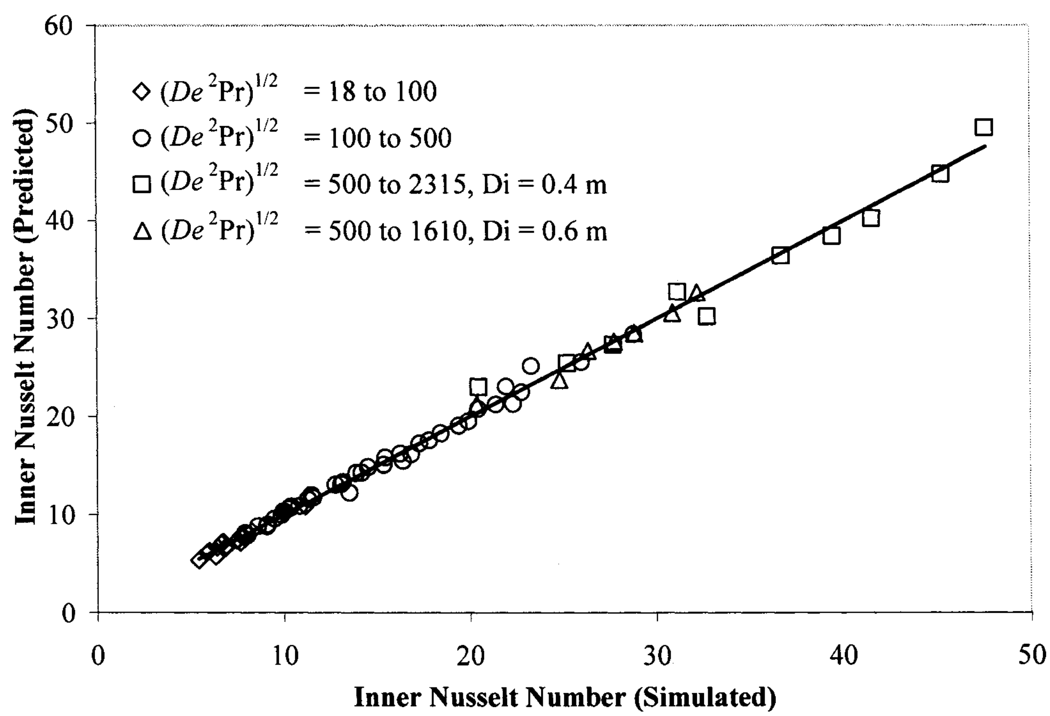

Figure 6.3: Annulus Nusselt number predicted by Equations 6.5 to 6.8 compared to the numerically determined annulus Nusselt number.

6.5.3 Thermally dependent thermal conductivity

In most calculations for heat transfer coefficients the fluid properties are assumed to be constant and taken at the mean temperature of the fluid. Even for basic systems this can pose a problem. If the outlet temperature is not known, then an iterative procedure is required to calculate the heat transfer coefficient and the temperature drop. This is further complicated if there are two fluids (such as a fluid-to-fluid heat exchanger) and if the fluid properties change with temperature. If the fluid properties are constant, then changing the flow properties on one side of the tube wall should not affect the Nusselt number on the other side of the tube wall for fully developed flow. However, this is not so if the fluid properties are temperature dependent. The effects of changing the flow rate in the annulus on the Nusselt number in the inner tube is shown in Figure 6.4. Here, the original Nusselt number is shown on the x-axis, and the percent increase in the Nusselt number is shown on the y-axis when the flow in the annulus is quadrupled. The data is broken up into 4 sections, one for each of the inner Reynolds numbers. The trials with the lower Reynolds numbers were affected more by the change than the trials with the larger Reynolds number.

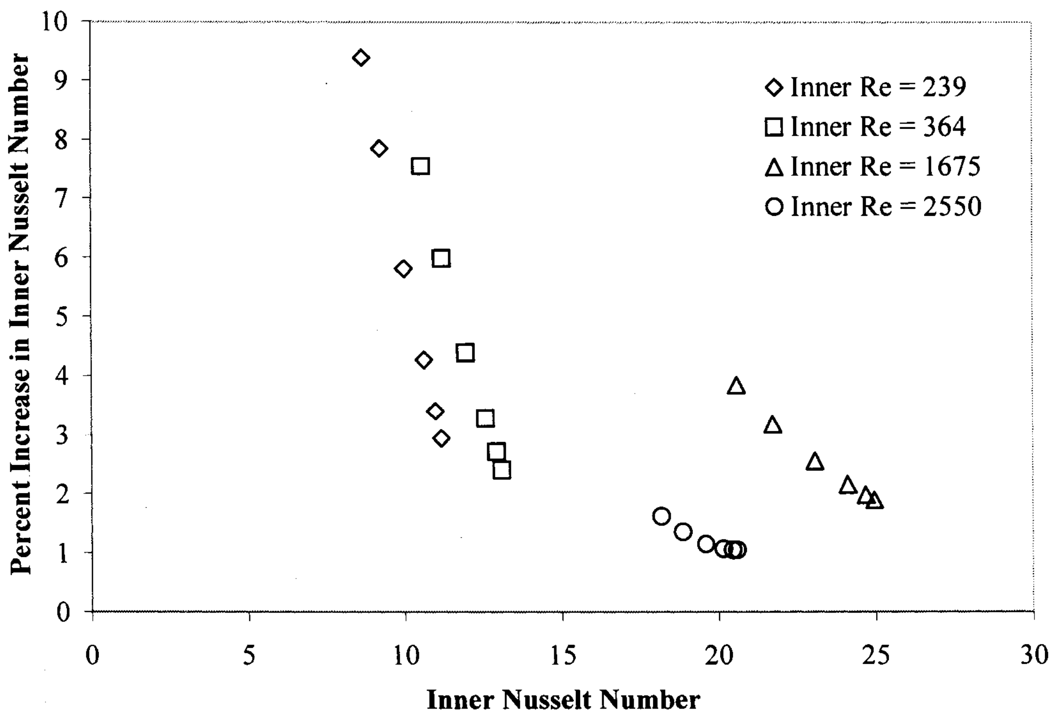

Figure 6.4: Percent increase of the inner Nusselt number when the flow rate in the annulus was quadrupled.

Increased flow rate in the annulus results in a larger temperature gradient for heat transfer. These increased temperature gradients result in higher heat transfer rates, which allow the inner fluid to cool down quicker, resulting in lower thermal conductivities in the fluid. This effectively increases the average Prandtl number (relative thickness of hydrodynamic and thermal boundary layers), and increases the Nusselt number. However, unlike the case of constant fluid properties, an increase in the Nusselt number for fluids with thermally dependent conductivities does not necessarily mean an increase in heat transfer coefficients. The Nusselt number is the ratio of the heat transfer coefficient (multiplied by a characteristic length) divided by the thermal conductivity. An increase in the Nusselt number and a decrease in the thermal conductivity do not necessarily result in a higher heat transfer coefficient. Figure 6.5 shows the percent increase in the inner heat transfer coefficient versus the inner heat transfer coefficient for the 4 different Reynolds numbers when the flow in the annulus is increased fourfold. It can be seen here that the increase in the heat transfer coefficient can be negative or positive, depending on the strength of the thermal dependence. The highest percent increases are for fluid K1, which has the least thermal dependency of all the fluids. With increasing thermal dependence (K1 to K6), the increase in heat transfer coefficient decreases.

The difficulty in determining the exact effect of the thermally dependent thermal conductivity on the heat transfer coefficients is complicated due to the fact that both fluids (in the inner tube and in the annulus) use a thermally dependent thermal conductivity. It would have been ideal to have one of them constant (no temperature effect). This would keep one of the entry regions constant, and the analysis could focus solely on the tube that had the thermally dependent thermal conductivity. However, the inner Nusselt numbers can be correlated to a modified Graetz number, Gz^*:

$$Gz^* = De\,\mathrm{Pr}\frac{d}{x} \tag{6.10}$$

where d is the diameter of the inner tube and x is the axial distance along the tube. The Reynolds number, which is usually present in the Graetz number, has been replaced with the Dean number. Two different correlations were performed, one for each of the tube sizes. The results are presented in Figure 6.6. The two correlation equations are:

$$Nu = 7.31 Gz^{*0.247} \quad \text{for } d = 0.28\text{ m} \quad \mathrm{R}^2 = 0.994 \tag{6.11}$$

$$Nu = 3.94 Gz^{*0.420} \quad \text{for } d = 0.42\text{ m} \quad \mathrm{R}^2 = 0.996 \tag{6.12}$$

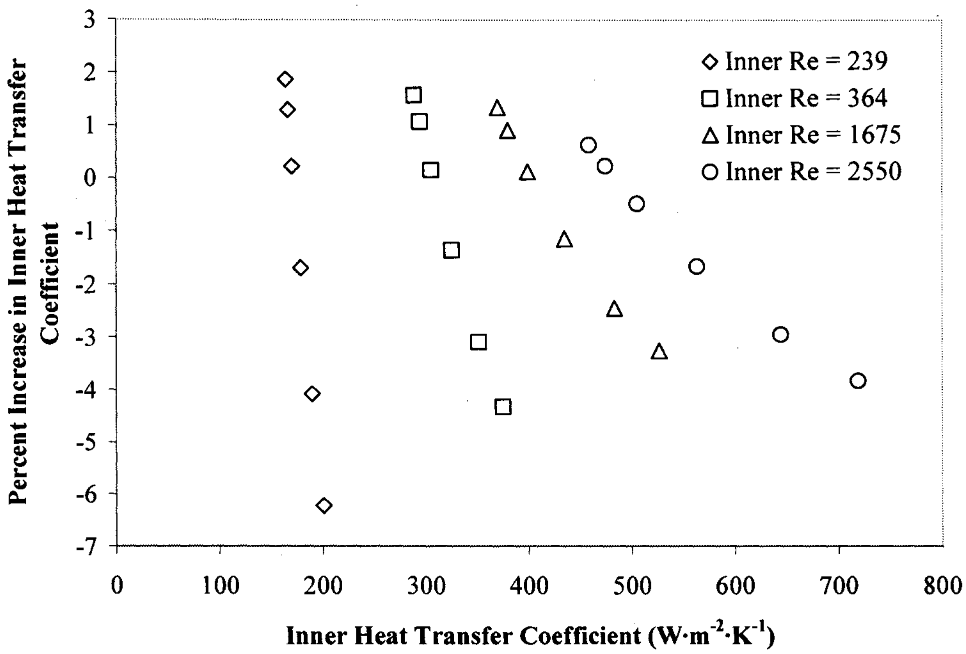

Figure 6.5: Percent increase of the inner heat transfer coefficient when the flow rate in the annulus is quadrupled.

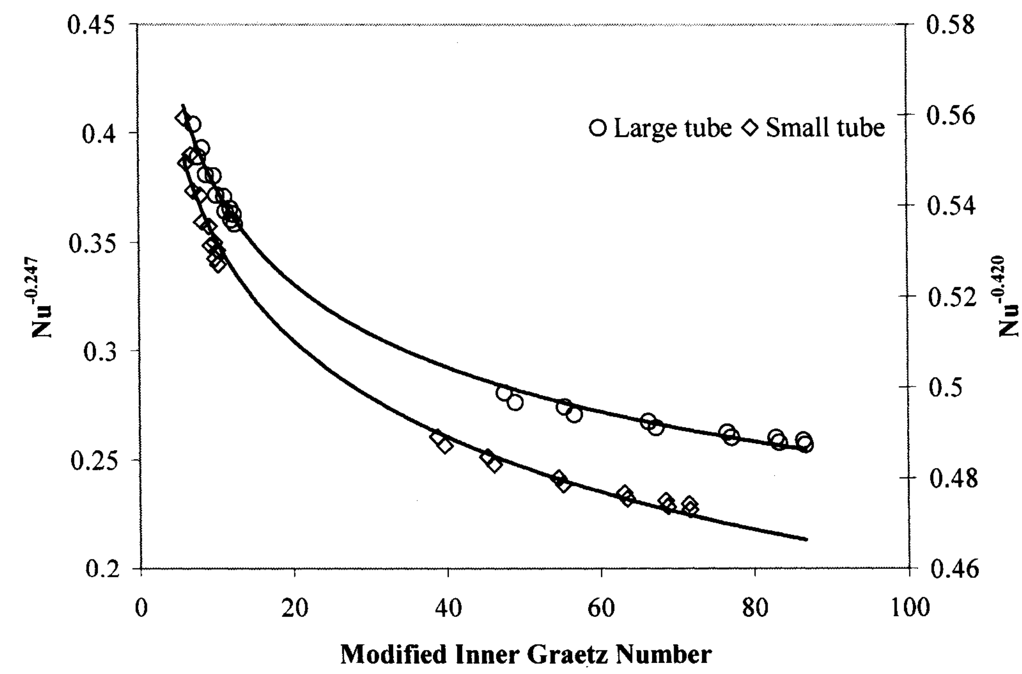

Figure 6.6: Inner Nusselt number to the exponent -0.247 (small tube) and to the exponent -0.420 (large tube) versus the modified inner Graetz number.

The same procedure was used to determine the Nusselt number in the annulus, but the Dean number used in the modified Graetz number was calculated with the following equation, rather than equation 6.9:

$$De = \frac{\rho V}{\mu}\left(\frac{D_o^2 - D_i^2}{D_o + D_i}\right)\left(\frac{D_o}{2R}\right)^{1/2} \tag{6.13}$$

The correlation equation developed was as follows:

$$Nu = 0.173Gz^* + 5.75 \qquad R^2 = 0.978 \tag{6.14}$$

The correlation is shown in Figure 6.7. This correlation gives an asymptotic Nusselt number of 5.75, whereas in Chapter IV, the asymptotic Nusselt number (for the Dean-Nusselt correlation) gave an asymptotic value of 5.36. However, the correlation in Chapter IV did not take into consideration thermally dependent thermal conductivities of the fluid.

Parallel flow versus counterflow heat exchangers were compared to determine the effects thermal dependent conductivities had on the heat transfer rates. The first, and obvious effect, is due to the nature of counterflow heat exchangers, they result in larger heat transfer rates, and hence larger temperature changes. This results in changes to the Graetz number in both the inner and the outer annulus (due to changes in average Prandtl number). However, with the two fluids having the same thermal dependence, one drops in average Prandtl number, while the other experiences an increase in the average Prandtl number. This situation exists for parallel flow and counterflow configurations. However, in a parallel flow heat exchanger, along the length of the heat exchanger, one fluid has an increasing thermal conductivity while the other has a decreasing thermal conductivity. Therefore, the thermal resistance will decrease on one side of the tube, and the resistance will increase on the other side, partially canceling each other out in the overall effect. For a counterflow heat exchanger, the highest thermal resistances will both be located at one end of the heat exchanger (at the cold inlet and hot outlet) and the lowest thermal resistances at the other end. This results in two very different distributions of thermal resistances, as well as temperature profiles. Figure 6.8 shows the heat transfer rates of counterflow versus parallel flow for both thermally stable and thermally dependent fluid thermal conductivities. The ratio between the two heat transfer rates is not affected by the changing thermal properties. Though the properties do change

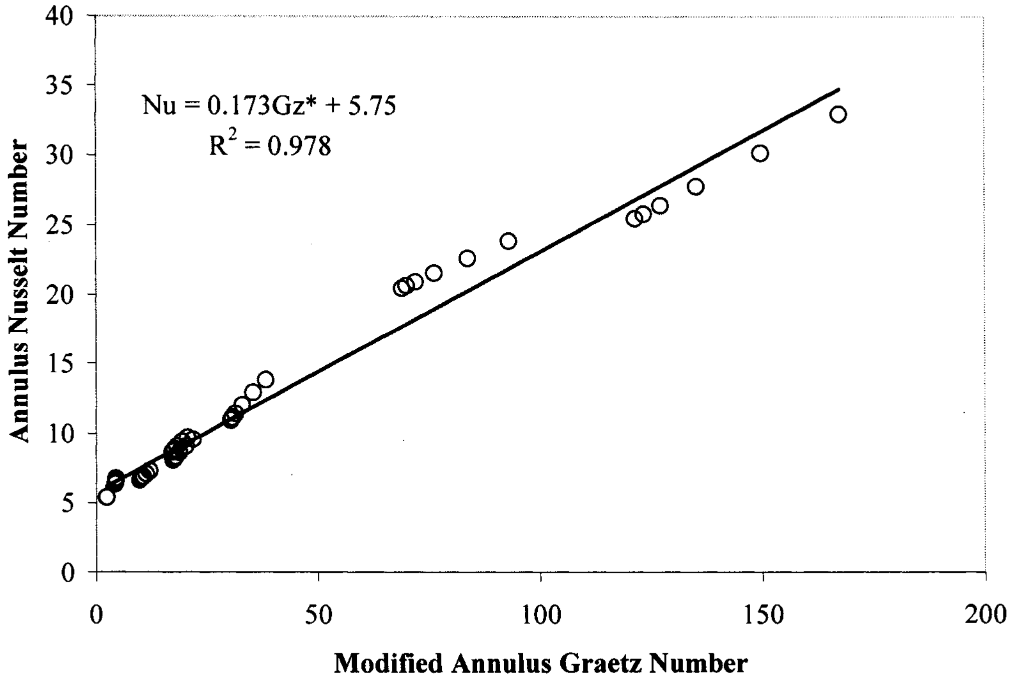

Figure 6.7: Annulus Nusselt number versus the modified annulus Graetz number.

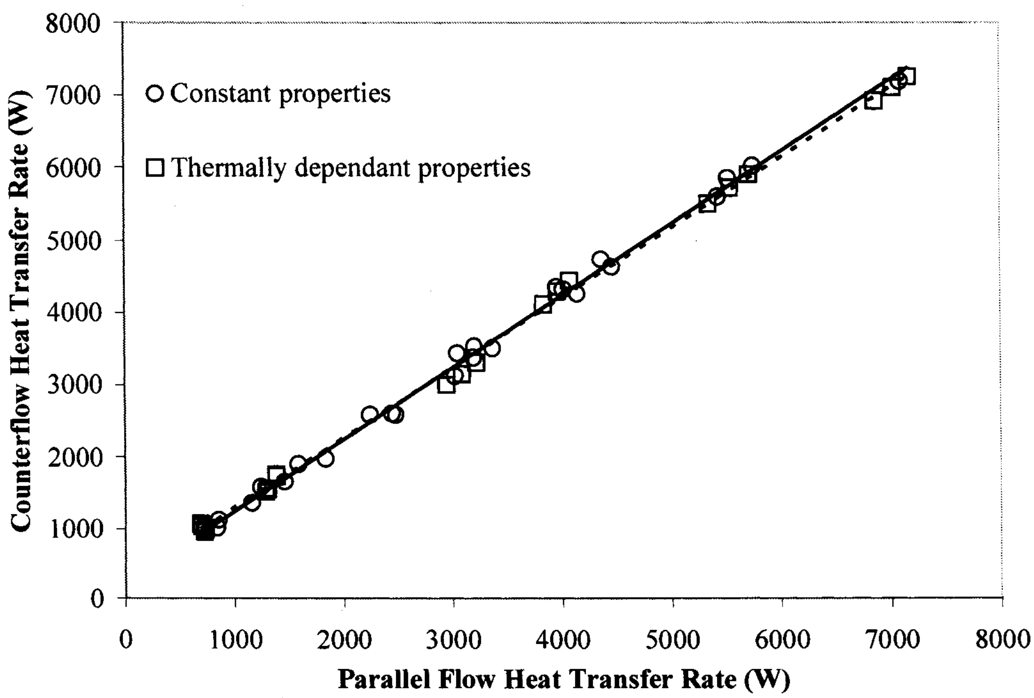

Figure 6.8: Counterflow heat transfer rate versus parallel flow heat transfer rate for either constant properties or thermally dependant properties.

more in a counterflow configuration, due to the large temperature changes, they did not have any additional effects.

6.6 Conclusions

A computational fluid dynamics package (PHOENICS 3.3) was used to numerically study the effects of fluid thermal properties on the heat transfer characteristics in a double-pipe helical heat exchanger. Three levels of Prandtl numbers were used; these were modified by changing the thermal conductivity. The Nusselt number was shown to be much more sensitive to changes in the Prandtl number at low Dean numbers than at higher Dean numbers. These changes were attributed to changes in the developing thermal and hydrodynamic boundary layers. The Nusselt number in the annulus was correlated as a function of a modified Dean number and the Prandtl number. However, regions of $(De^2\mathrm{Pr})^{1/2}$ were identified where multiple correlations were needed to adequately describe the relationship.

Thermally dependent thermal conductivities were studied using six different degrees of dependence. The results indicated that there can be significant changes in the Nusselt number based on the thermal dependency. Changing the flow rate in one tube can change the average thermal conductivity value to a fairly large degree, as well as changing the entry length for the developing thermal boundary layer. For both the inner tube and for the annulus, the Nusselt number correlated well with the Graetz number. The Graetz number used in this work, however, was not the standard Graetz number. It was modified by replacing the Reynolds number in the Graetz number calculation with the Dean number, for both the inner tube and the annulus. Though this worked well for the annulus, two different correlations were needed for the inner tube, one for each of the tube diameters, showing that further investigation needs to be made in this area.

Parallel flow versus countercurrent flow was studied to determine if the thermally dependent properties had any effect on the heat transfer rates. In counterflow conditions, greater heat transfer rates resulted in larger changes in fluid properties. When the ratio of the heat transfer rates for parallel flow versus counterflow were plotted against each other, there was no difference based on thermally dependent versus thermally stable fluid properties. This suggests that the location of the two developing flows is not relevant in the design of the heat exchanger. They can either be at the same end of the heat exchanger or at opposite ends, for the conditions observed in this study.

6.7 Acknowledgements

The authors are grateful to FCAR (Fonds pour la Formation de Chercheurs et l'Aide à la Recherche) and NSERC (Natural Sciences and Engineering Research Council of Canada) for the financial assistance for this study.

6.8 Nomenclature

a	Constant
A	Constant ($W \cdot m^{-1} \cdot K^{-1}$)
b	Constant
B	Constant ($W \cdot m^{-1} \cdot K^{-2}$)
c	Constant
d	Diameter of inner tube (m)
D_o	Outer diameter of annulus (m)
D_i	Inner diameter of annulus (m)
De	Dean number
Gz^*	Modified Graetz number
k	Thermal conductivity ($W \cdot m^{-1} \cdot K^{-1}$)
Nu	Nusselt number
Pr	Prandtl number
R	Radius of curvature (m)
T_{abs}	Absolute temperature (K)
V	Average velocity ($m \cdot s^{-1}$)
x	Axial distance (m)
ρ	Density ($kg \cdot m^{-3}$)
μ	Viscosity ($kg \cdot m^{-1} \cdot s^{-1}$)

6.9 References

ASHRAE. 1998. Ch. 8: Thermal Properties of Foods. In: *Refrigeration Handbook*, American Society of Heating, Refrigeration and Air-Conditioning Engineers, Inc., Atlanta, GA.

Bai, B., L. Guo, Z. Feng, and X. Chen. 1999. Turbulent heat transfer in a horizontally coiled tube. *Heat Transfer-Asian Research*, Vol. 28(5):395-403.

Dravid, A. N., K. A. Smith, E. W. Merril, and P. L. T. Brian. 1971. Effect of Secondary fluid motion on laminar flow heat transfer in helically coiled tubes. *AIChE Journal*, Vol. 17(5):1114-1122.

Janssen, L. A. M. and C. J. Hoogendoorn. 1978. Laminar convective heat transfer in helical coiled tubes. *International Journal of Heat and Mass Transfer*, Vol. 21: 1197-1206.

Kalb, C. E. and J. D. Seader. 1972. Heat and mass transfer phenomena for viscous flow in curved circular tubes. *International Journal of Heat and Mass Transfer*, Vol. 15:801-817.

Kalb, C. E. and J. D. Seader. 1974. Fully developed viscous-flow heat transfer in curved circular tubes with uniform wall temperature. *AIChE Journal*, Vol. 20(2):340-346.

Kubair, V. and N. R. Kuloor. 1966. Heat transfer to Newtonian fluids in coiled pipes in laminar flow. *International Journal of Heat and Mass Transfer*, Vol. 9:63-75.

Mori, Y. and W. Nakayama. 1965. Study on forced convective heat transfer in curved pipes (1st report, laminar region). *International Journal of Heat and Mass Transfer*, Vol. 8:67-82.

Ozisik, M. N., and H. C. Topakoglu. 1968. Heat transfer for laminar flow in a curved pipe. *Journal of Heat Transfer*, Vol. 90:313-318.

Prabhanjan, D. G., T. J. Rennie, and G. S. V. Raghavan. 2004. Natural convection heat transfer from helical coiled tubes. *International Journal of Thermal Sciences*, Vol. 43:359-365.

Seban, R. A. and E. F. McLaughlin. 1963. Heat transfer in tube coils with laminar and turbulent flow. *International Journal of Heat and Mass Transfer*, Vol. 6:387-395.

CONNECTING TEXT

Chapter VI dealt with the effects of the fluid thermal properties on the heat transfer characteristics of the double-pipe helical heat exchanger. Chapter VII will deal with the hydrodynamic property of the fluid, viz., the viscosity. To adequately cover this, both thermally dependent viscosities and non-Newtonian fluids are studied. The effects of these on the heat transfer and pressure drop characteristics are investigated.

VII. THERMALLY DEPENDENT VISCOSITY AND NON-NEWTONIAN FLOW IN A DOUBLE-PIPE HELICAL HEAT EXCHANGER

7.1 Abstract

A double-pipe helical heat exchanger was numerically studied to determine the effects of thermally dependent viscosity and non-Newtonian flows on the heat transfer coefficients and the pressure drop. Thermally dependent viscosities were found to have very little effect on the Nusselt number correlations; however it did have a significant effect on the pressure drop in the heat exchanger. Changing the flow rate in the annulus could significantly affect the pressure drop in the inner tube, since the average viscosity of the fluid in the inner tube would change due to the change in the average temperature.

The effect of non-Newtonian power law fluids on the heat transfer and the pressure drop were determined for both the flow in the inner tube and in the annulus. The Nusselt number was correlated with the Péclet number for both of these regions. For the annulus, the curvature ratio was also incorporated into the correlation. Pressure drop data were compared by using ratios of the pressure drop of the non-Newtonian fluid to a Newtonian fluid at identical mass flow rates. These values were presented over a range of mass flow rates.

7.2 Introduction

Heat treatment of biological materials, whether they are in solid or liquid form, is generally a very complex process as material properties are often intricate in nature and can be affected by temperature changes. This applies to liquid foods (milk, juices, pastes, purees, and so forth) that need to be pasteurized, sterilized, or undergo other types of heat treatment. Changes in temperature of the food product can affect both the fluid properties (density, viscosity) as well as its thermal properties (thermal conductivity, specific heat). Furthermore, many of these food products are non-Newtonian fluids (Simpson and Williams, 1974) which complicates the design of heat exchangers.

During heating and cooling operations, the viscosity of many food products can change appreciably. Table 7.1 lists some common food products with their viscosity at different temperatures along with the percent change in viscosity when heated from the low to the high temperatures.

Table 7.1: Viscosities of selected liquid foods (from Singh and Heldman, 1993).

Product	Temperature (°C)	Viscosity (Pa·s)	% change
Cream, 10% fat	40 80	0.00148 0.00083	-43.9
Homogenized milk	20 80	0.0020 0.0006	-70.0
Corn oil	25 38	0.0565 0.0317	-43.9
Cottonseed oil	20 38	0.0704 0.0306	-56.5
Peanut oil	25 38	0.0656 0.0251	-61.7
Safflower oil	25 38	0.0522 0.0286	-45.2

It is important to understand the effect of these fluids on the heat transfer characteristics in a heat exchanger, along with the changes in the pressure drop across the heat exchanger for design purposes. Non-Newtonian fluids do not have a linear relationship between shear stress, τ, and strain rate, u'. The shear stress for a one dimensional flow is:

$$\tau = K(u')^n \tag{7.1}$$

In this work, the non-Newtonian fluids are based on a power-law equation (Equation 7.1), where K is the consistency index and n is the flow behaviour index. Values of $n < 1$ are pseudo-plastic and those with $n > 1$ are dilatant substances. Newtonian fluids have n equal to unity and the shear stress and shear strain is proportional by the factor, μ, the fluid viscosity.

Many works involving non-Newtonian viscous power-law fluids use a universal Reynolds number, Re*, rather than the general Reynolds number formulation (Kozicki et al., 1966; Rao, 1994):

$$\mathrm{Re}^* = \frac{\rho v^{2-n} D_h^n}{K\left[\frac{a+bn}{n}\right]^n 8^{n-1}} \tag{7.2}$$

This equation is applicable to ducts of different geometries, with the geometry being taken into account through the use of the hydraulic diameter, D_h, and the parameters a and b. For a circular geometry, the values of a and b are 0.25 and 0.75, respectively (Rao, 1994). For the case of n = 1, and a circular geometry, the above equation collapses to the standard Reynolds number (Rao, 1994), with K equal to the dynamic viscosity.

Very little work has been done in the study of thermally dependent viscosities and non-Newtonian fluids in double-pipe helical heat exchangers. However, some studies have been performed with non-Newtonian fluids in helical coils. Jones (1960) showed that the angular distance required for fluid particles to cross from the inner wall to the outer wall was dependent on the properties of the non-Newtonian fluid, and could be longer or shorter in comparison with a Newtonian fluid. Visco-elastic liquids were numerically studied by Thomas and Walters (1963) for the flow through a helical coil. The general motion of the fluid was similar to Newtonian fluids; however, increasing the elasticity of the fluid resulted in a decrease in the curvature of the streamlines. Furthermore, for a given pressure drop, the volumetric flow rate was increased for visco-elastic fluids. Rajasekaran et al. (1966) studied the secondary flow of non-Newtonian fluids in helical coils by measuring the diametrical pressure drop at different locations along the coil. Laminar flow in coiled pipes with pseudo-plastic and dilatant fluids (power-law models) was studied experimentally by Rajasekharan et al. (1970). The Nusselt number was correlated to the curvature ratio, the flow behaviour index, and a modified Graetz number. Further heat transfer and pressure drop studies for power-law fluids was studied numerically by Hsu and Patankar (1982). They showed that the friction factor increased with an increase in the flow behaviour index. Rao (1994) studied the friction factors and heat transfer for turbulent flow with power-law fluids having a flow behaviour index in the range of 0.78 to 1.0. For turbulent flow, it was found that the Nusselt number increased with decreasing flow behaviour indices.

7.3 Objectives

The objectives of this study are to determine the effects of thermal dependent viscosities and non-Newtonian fluids on the heat transfer characteristics and pressure drop relations in double-pipe helical heat exchangers.

7.4 Materials and Methods

7.4.1 CFD modeling

The method used to perform the computational fluid dynamics modeling of the double-pipe helical heat exchanger have been discussed in detail in Chapter IV, along with the validation simulations. The same heat exchanger dimensions were used in this work. The difference between the modeling in Chapter IV and this work is the fluid properties, as discussed in sections 7.4.2 and 7.4.3.

The outer tube had an inner diameter of 0.1 m and a pitch of 0.115 m. The outer diameters of the inner tubes were 0.04 and 0.06 m, both with wall thicknesses that were 15% of the diameter and a pitch of 0.115 m. The length of the heat exchangers from inlet to outlet is 2π. The radius of curvature of the tubes is 0.8 m. The properties of the inner tube were set to stainless steel, with a thermal conductivity of 16 $W \cdot m^{-1} \cdot K^{-1}$, density of 7881.8 $kg \cdot m^{-3}$ and a specific heat of 502 $J \cdot kg^{-1} \cdot K^{-1}$. The outer tube was set to have adiabatic boundary conditions; the inner tube was set to allow conductive heat flow through the tube.

7.4.2 Effect of thermally dependent viscosities

The first set of simulations focused on thermally dependent viscosities. Mass flow rates in the inner tube were set to 0.00835, 0.02504, 0.04174, and 0.05843 $kg \cdot s^{-1}$. These trials were performed at two different thermal conductivities, 0.597 or 0.0597 $W \cdot m^{-1} \cdot K^{-1}$. The function used to describe the temperature effects on the viscosity, μ, was:

$$\mu = \rho(\mathrm{A} + \mathrm{B}T_{abs}) \tag{7.3}$$

The values used for the constants in this equation are listed in Table 7.2, along with the percent change in viscosity when heated from 20°C to 80°C. These values result in a reduction of viscosity to one-half, one-third, or one-fifth of their value for fluids V1, V2, and V3, respectively, when heated from 20°C to 80°C. The values were chosen so that they covered the basic range of thermally dependent viscosities as would be found in the food industry, based on the data in Table 7.1

Table 7.2: Constants used in Equation 7.3 and percent change in viscosity.

Fluid	A ($m^2 \cdot s^{-1}$)	B ($m^2 \cdot s^{-1} \cdot K^{-1}$)	% change
V1	3.46 x 10^{-6}	-8.38 x 10^{-9}	-50
V2	4.28 x 10^{-6}	-1.12 x 10^{-8}	-66.7
V3	4.94 x 10^{-6}	-1.34 x 10^{-8}	-80

7.4.3 Non-Newtonian fluids

The second set of simulations was with non-Newtonian fluids. The values of n used were 0.5, 0.75, and 2.0. Simulations with n equal to unity were also performed for comparison. In all cases, the value of the consistency index, K, remained the same at 1.004×10^{-3} $kg \cdot m^{-1} \cdot s^{n-2}$. Note that for n of unity, the consistency index is the viscosity.

For the flow in the annulus, the geometric parameters, a and b, used in the calculation of Re* were 0.4890 and 0.9911 (small tube) and 0.4965 and 0.9972 (large tube), respectively. These values were obtained from Kozicki et al. (1966).

In a similar manner, the Dean number for both the inner tube and the annulus needs to be modified for the non-Newtonian fluid. This can be done by replacing the general expression of the Reynolds number by the universal Reynolds number, for both the inner tube (Hsu and Patankar, 1982) and the annulus, respectively:

$$De^* = \mathrm{Re}^*\left(\frac{r}{R}\right)^{1/2} \tag{7.4}$$

$$De^* = \mathrm{Re}^*\left(\frac{D_o - D_i}{R}\right)^{1/2} \tag{7.5}$$

Furthermore, the Prandtl number is no longer purely a fluid property for non-Newtonian fluids, but is also a flow property, since the reference viscosity used in the formulation of the Prandtl number is a function of the velocity (Hsu and Patankar, 1982). The modified Prandtl number is (Hsu and Patankar, 1982):

$$\mathrm{Pr}^* = \frac{c_p}{k} K \left(\frac{v}{d}\right)^{n-1} \tag{7.6}$$

In total, this section comprised of 120 simulations, using 5 values for n (0.5, 0.75, 1.0, and 2.0), 4 inner mass flow rates (0.00835, 0.0125, 0.0209, and 0.0584 $kg \cdot s^{-1}$), 3 corresponding annulus mass flow rates (1/2, 1, and 2 times the inner mass flow rate), and 2 inner tube diameters (0.04 and 0.06 m outer diameters). All possible combinations of these factors were used.

7.5 Results and Discussion

7.5.1 Thermally dependent viscosity

Effects of thermally dependent viscosity were studied in a double-pipe helical heat exchanger. Heat transfer coefficients were calculated along with the change in pressure drop along the length of the heat exchanger. It is not expected that a thermally dependent viscosity will greatly change the heat transfer rates, as the viscosity affects both the Reynolds number (and hence Dean number) and the Prandtl number in an inverse manner. Furthermore, the entry flow is a function of the Graetz number, which is based on the product of the Reynolds number and the Prandtl number. Since the Reynolds number is proportional to the viscosity, and the Prandtl number is inversely proportional to the viscosity, the product of these two terms is independent of the dynamic viscosity. Therefore, entry effects should not be changed for a thermally dependent viscosity. In general, the Nusselt number is generally not strongly affected by the viscosity. Most correlations for the Nusselt number are in the form of equation:

$$Nu = a \mathrm{Re}^b \mathrm{Pr}^c \tag{7.7}$$

If all other variables remain constant, then the Nusselt number is basically a function of the viscosity to the power (c-b). In general, this is a weak relationship. Based on the work of Kalb and Seader (1972), the power would be -0.276. Furthermore, the

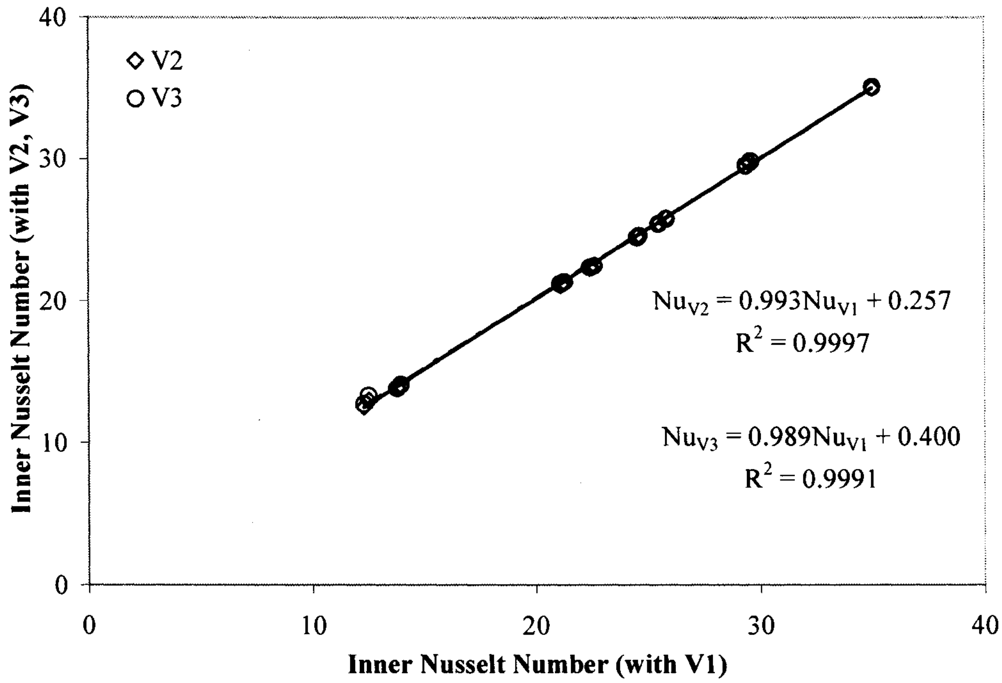

Figure 7.1: Inner Nusselt number (with fluid V1) versus the inner Nusselt number (with fluids V2 and V3).

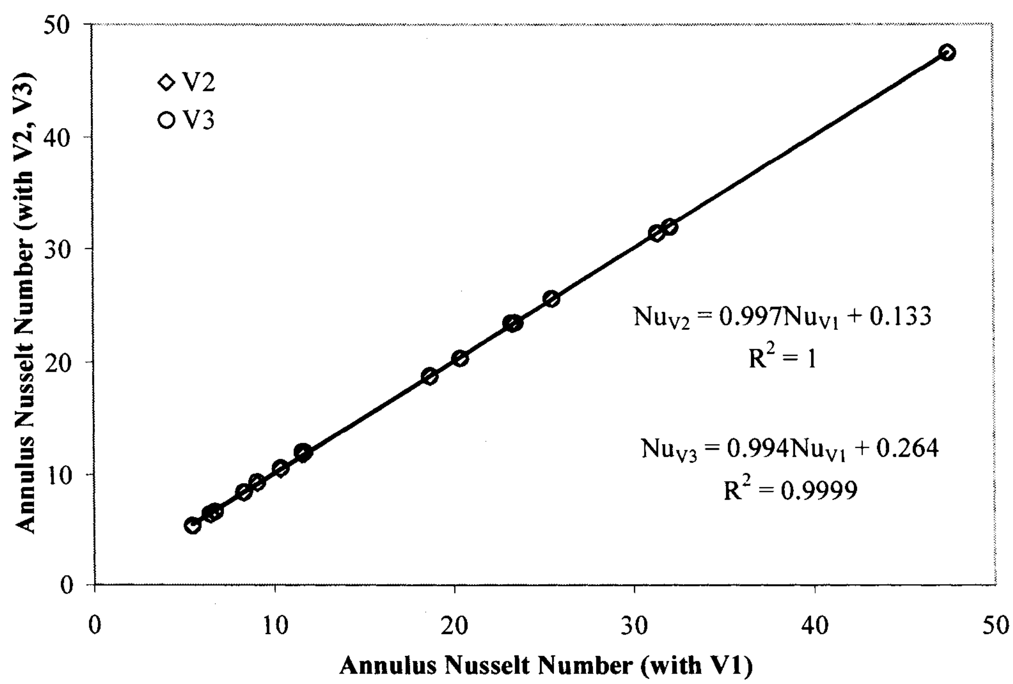

Figure 7.2: Annulus Nusselt number (with fluid V1) versus the annulus Nusselt number (with fluids V2 and V3).

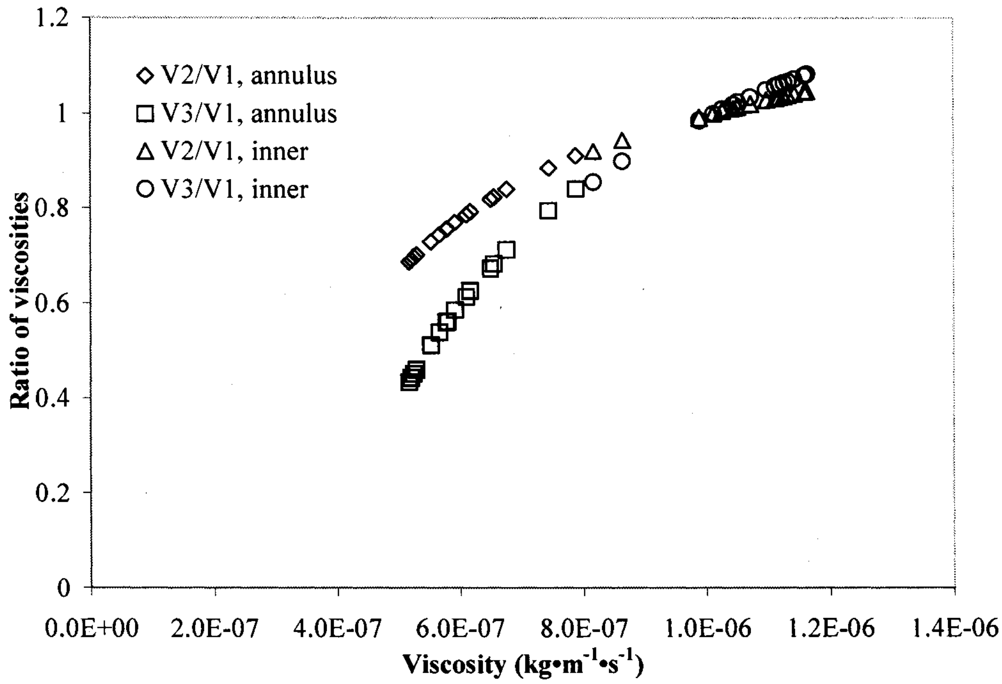

Figure 7.3: Ratio of viscosities (V2/V1 and V3/V1) for a given flow rate versus the viscosity for V1, for both the annulus and the inner tube.

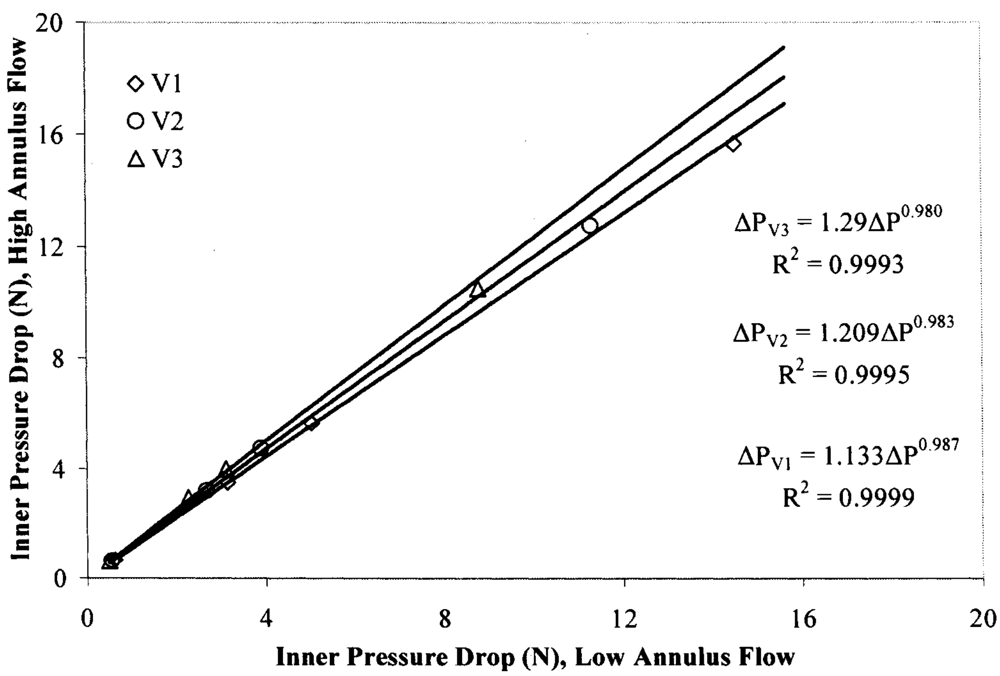

Figure 7.4: Pressure drop (N) in the inner tube with a high flow rate in the annulus versus the pressure drop (N) in the inner tube with a low flow rate in the annulus.

calculation of local Nusselt numbers with variable viscosity is normally done with the Sieder-Tate viscosity ratio (Sieder and Tate, 1936; Shah and Joshi, 1987), which is the ratio of the viscosity taken at the mean fluid temperature and the wall temperature, to the power of 0.14. However, this is for straight tubes and not for helical coils or curved annuli. Figures 7.1 and 7.2 show the Nusselt number calculated (for the inner tube and the annulus, respectively) using fluids V2 and V3 versus fluid V1, given the same values for all other variables. For both these cases, there is very little variation in the Nusselt number due to the different fluids. It should be noted, that at 20°C, all these fluids have the same viscosity. However, the viscosity does change slightly for any given situation, since the average temperature is different. Figure 7.3 shows the ratio of the viscosities for any given situation (with all other parameters identical) versus the average viscosity of fluid V1. There can be a significant difference in fluid viscosity between any two trials (with all other parameters identical), yet these difference do not appear in the ratio of the Nusselt numbers (Figures 7.1 and 7.2).

Pressure drop data are presented in Figure 7.4. The pressure drop on the *y*-axis is the pressure drop in the inner tube when the corresponding mass flow rate in the annulus is double the value of the inner tube. The pressure drop on the *x*-axis is the inner pressure drop when the mass flow rate in the annulus is half the value of the inner tube. The data is divided into 3 sets, one for each of the different thermally dependent viscosities as described in Table 7.2. The data presented are for those with a thermal conductivity of 0.597 $W \cdot m^{-1} \cdot K^{-1}$. Changing the mass flow rate in the inner tube results in higher heat transfer rates, and hence a greater change in the fluid viscosity and increase in the pressure drop due to the enhanced temperature change. For the trials with the lower thermal conductivity, the differences in pressure drop were negligible. The difference in temperature drop was much less, leading to very small changes in the viscosity.

7.5.2 Non-Newtonian flow

The effect of non-Newtonian fluid on the heat transfer characteristics in a double-pipe helical heat exchanger was studied. The results for the inner Nusselt number of the non-Newtonian flow were correlated with the Péclet number. The correlation was based on the following logarithmic equation:

$$Nu = C_1 \ln(Pe) + C_2 \tag{7.8}$$

The results for the constants, C_1 and C_2, are presented in Table 7.3 for each of the different values of the power-law exponent and for the different tube diameters. It should also be noted, that the Péclet number used in these calculations is a function of the geometry of the coil. Generally, the Péclet number is the product of the Reynolds number and the Prandtl number, resulting in a quantity that is independent of the viscosity, and one correlation should be adequate for all values of the flow behaviour index, *n*. However, using the Prandtl number as defined in Equation 7.6 and the Reynolds number in Equation 7.2, both for non-Newtonian flows, the Péclet number become a function of the geometrical correction factor and the flow behaviour index. The values for C_1 remain fairly constant over the whole range of *n* values in the smaller tube. Increasing the value of *n* tends to increase the value of C_2. This is shown on Figure 7.5 where the Nusselt number is plotted versus the Péclet number for the small tube.

Table 7.3: Correlation results for Equation 7.8.

Diameter (m)	n	C_1	C_2	R^2
0.014	0.5	3.92	-20.30	0.983
	0.75	3.89	-18.34	0.993
	1.0	3.82	-16.34	0.996
	1.5	3.90	-13.96	0.981
0.021	0.5	9.91	-73.29	0.999
	0.75	9.54	-65.07	0.999
	1.0	7.31	-42.42	0.986
	1.5	7.89	-39.82	0.998

For the larger tube, the fluid behaviour index has an effect on both the C_1 and C_2 values. The plot of inner Nusselt number versus Péclet for the large tube is shown in Figure 7.6. In these results there is a slight difference in the Nusselt number versus Péclet number for the two different tube sizes. Comparing Figures 7.5 and 7.6, the values in Figure 7.6 tend to follow a straighter line than in Figure 7.5. Note that the *x*-axis is a logarithmic scale, so the fact that the data is straight in Figure 7.6 does not mean that

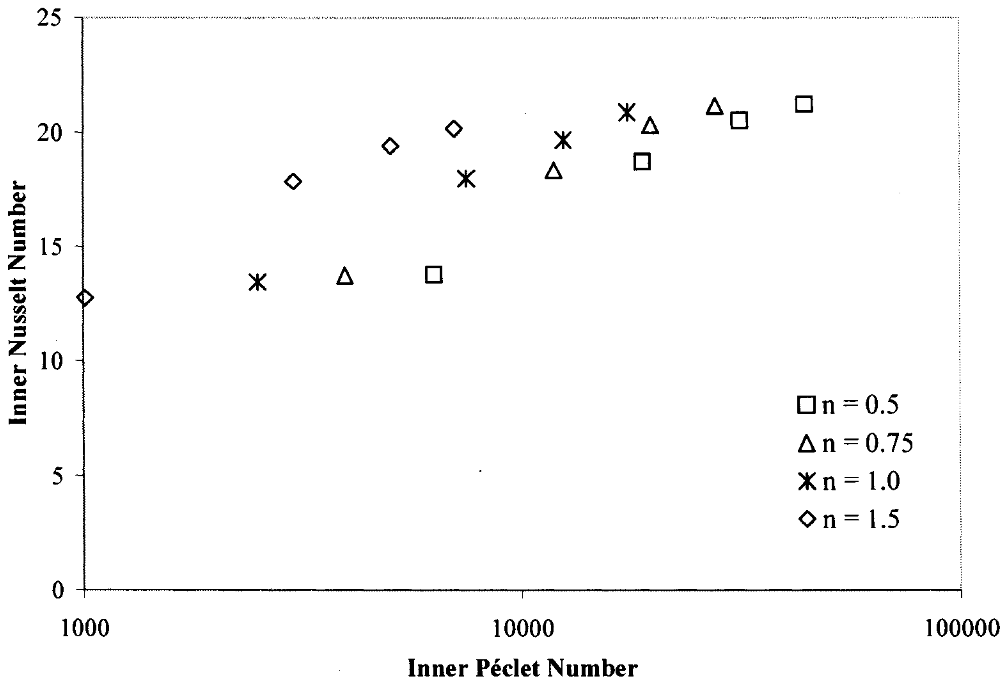

Figure 7.5: Inner Nusselt number versus inner Péclet number (function of geometry and flow behaviour index) for non-Newtonian fluids for the small tube.

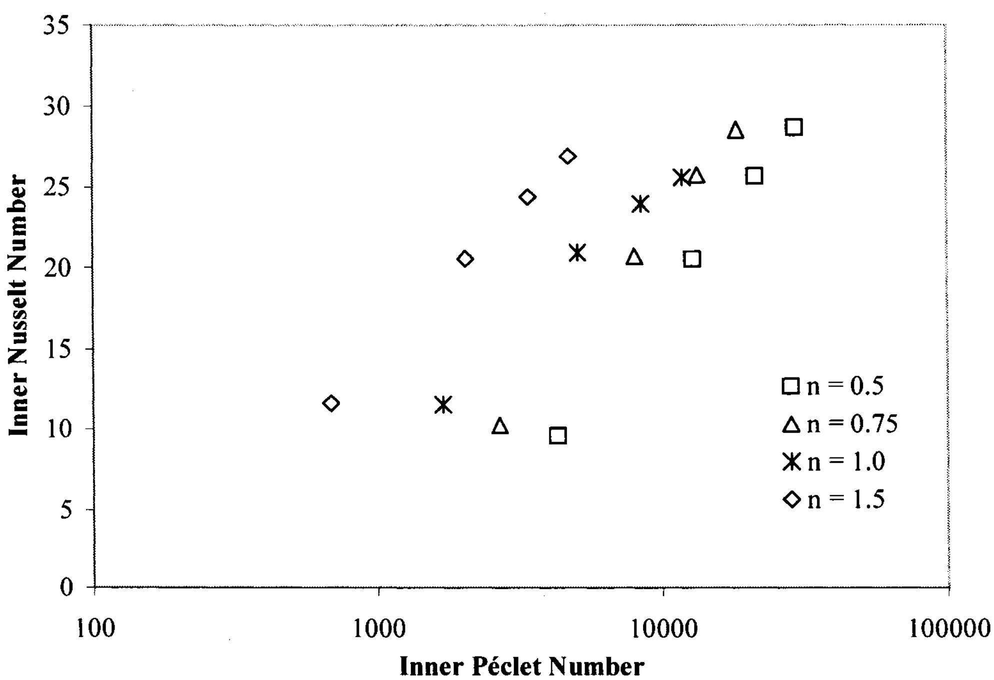

Figure 7.6: Inner Nusselt number versus inner Péclet number (function of geometry and flow behaviour index) for non-Newtonian fluids for the large tube.

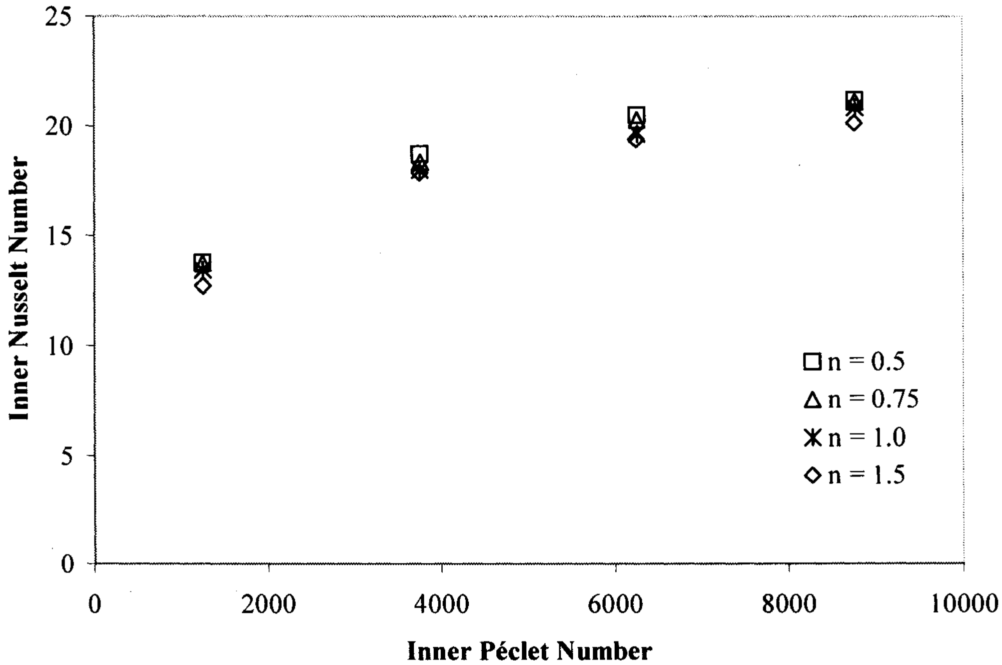

Figure 7.7: Inner Nusselt number versus inner Péclet number (independent of geometry and flow behaviour index) for non-Newtonian fluids for the small tube.

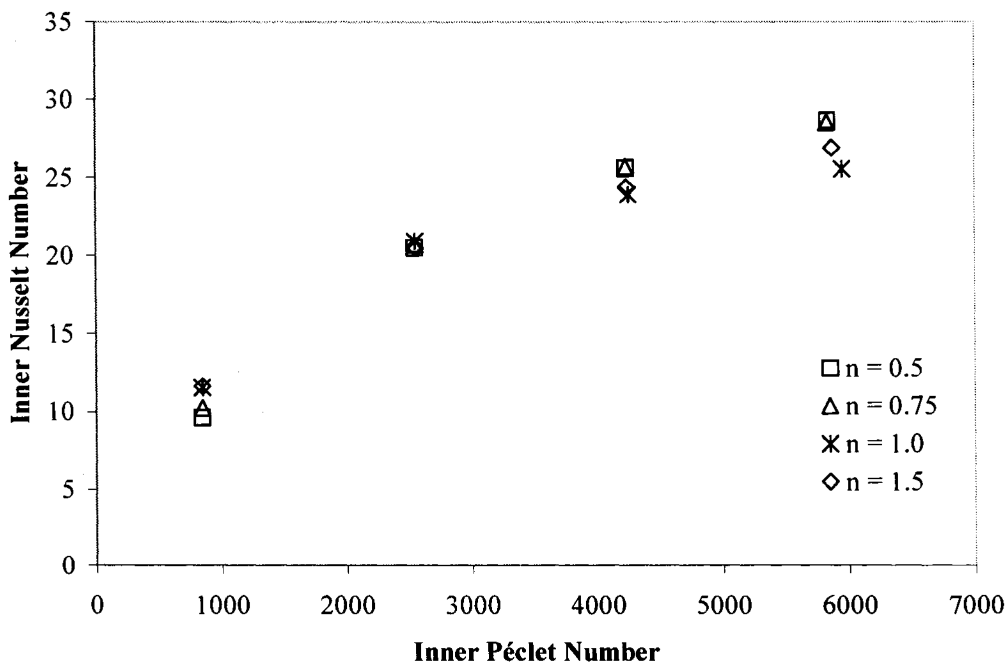

Figure 7.8: Inner Nusselt number versus inner Péclet number (independent of geometry and flow behaviour index) for non-Newtonian fluids for the large tube.

there is a linear relationship between the Nusselt number and the Péclet number. Furthermore, with the data appearing straighter in Figure 7.6 also corresponds to the better logarithmic (Equation 7.8).

Though Hsu and Patankar (1982) defined the Prandtl number using Equation 7.6, they also stated that the appropriate characteristic viscosity for tube flow is the flow consistency index multiplied by the geometrical correction factor (as used in the modified Reynolds number). Thus, if this characteristic viscosity were to be used in the both the Prandtl and Reynolds number expressions it should cancel out. The calculation of the Péclet number would then result in the following form, which is also the general form for flow of a non-Newtonian fluid:

$$Pe = \frac{\rho c_p v d}{k} \tag{7.9}$$

Figures 7.5 and 7.6 have been reproduced using this Péclet number and the results are shown in Figures 7.7 and 7.8, respectively. The data come closer together and a single correlation could be used for this data. The data was correlated for each behaviour index and tube diameter, and a general correlation without separating the data by the flow behaviour index was also performed. These results are shown in Table 7.4. Comparing Table 7.3 and 7.4, the only difference in the correlations are the values of the constant C_2. Therefore, the differences between these graphs are simply a multiplication factor due to the fluid behaviour constant. Though this may seem like a moot point, it does illustrate that the Figures 7.5 and 7.6 can be misleading, as they appear to show that the flow behaviour index greatly affects the Nusselt number. However, this is not the case, as Figures 7.7 and 7.8 show the real effects of the behaviour index, which are minimal. The data for the smaller tube diameter are very tight, leaving very little variation in the constants due to the flow behaviour index, and the data can easily be correlated together. However, the data for the large coil, which was a smaller radius of curvature, and hence increased secondary flow, indicate that there may be a slight effect of the flow behaviour index on the developing Nusselt number. Though the data for the correlation coefficients for the larger tube (Table 7.4) seem to indicate that there are large effects due to the flow behaviour index (values of C_1 and C_2 change appreciably), Figure 7.8 shows that the effects are fairly minimal and a general correlation for all the data should suffice for most engineering applications. Rao (1994) stated in his general introduction that the heat transfer of a power-law fluid in a straight tube is not significantly different from that of a Newtonian fluid. The present results seem to indicate that this also holds for laminar flow in a curved tube.

Table 7.4: Correlation results for Equation 7.8 using Péclet number from Equation 7.9.

Diameter (m)	n	C_1	C_2	R^2
0.014	0.5	3.92	-13.95	0.983
	0.75	3.89	-13.85	0.993
	1.0	3.82	-13.69	0.996
	1.5	3.90	-14.805	0.981
	All	3.88	-14.08	0.970
0.021	0.5	9.91	-57.21	0.999
	0.75	9.54	-54.07	0.999
	1.0	7.31	-37.35	0.986
	1.5	7.89	-41.52	0.998
	All	8.66	-47.48	0.978

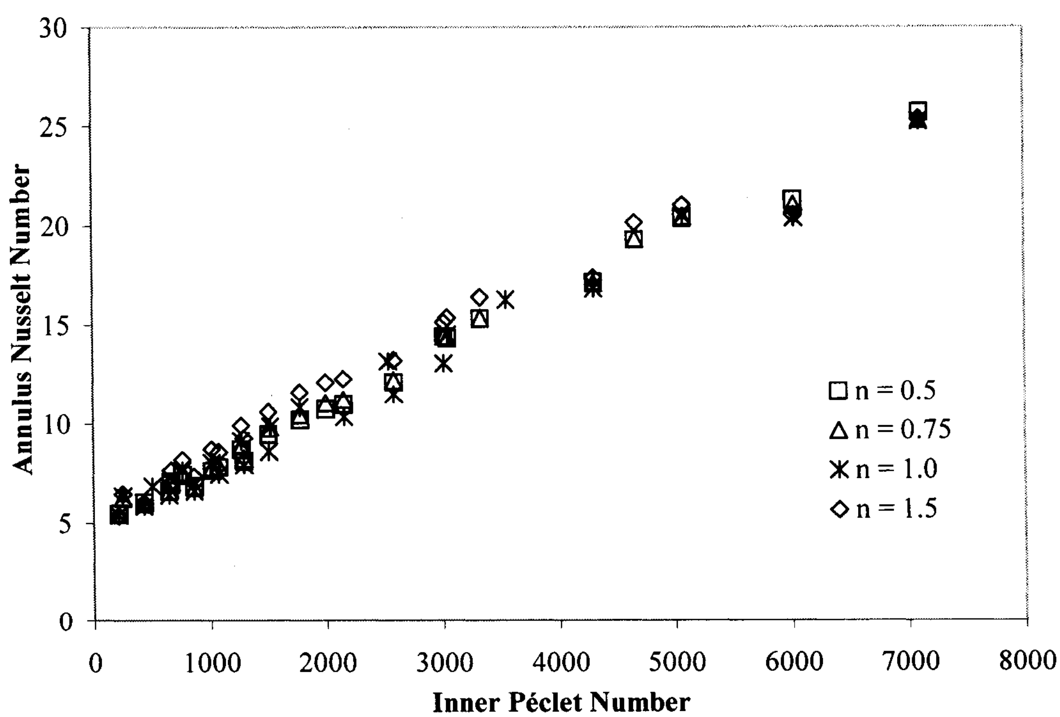

Figure 7.9: Annulus Nusselt number versus annulus Péclet number (independent of geometry and flow behaviour index) for non-Newtonian fluids.

The Nusselt number for the annulus is plotted against the Péclet number in Figure 7.9. This Péclet number is based on equation 7.9 with the exception that the diameter has been replaced with the hydraulic diameter. Therefore this Péclet number does not take into account the flow behaviour index, nor does it take into consideration the curvature. Correlations were also performed with a Péclet number that was a function of the curvature (the Reynolds number was replaced with the Dean number), and though it gave better results for a direct correlation between the Péclet number and the Nusselt number, the correlations were better when the curvature ratio was treated as a separate variable, rather than fixing it in the Dean number. The data were correlated using the following equation:

$$Nu = C_1 Pe^{C_2} \left(\frac{D_o - D_i}{2R} \right)^{C_3} + C_4 \tag{7.10}$$

The results of the correlation are reported in Table 7.5. Correlations were performed for each of the non-Newtonian fluids separately, and the standard Newtonian fluid, as well as one correlation that took all the data into consideration. Based on Figure 7.9, the variation between different flow behaviour indices is minimal, and one correlation should suffice to describe the heat transfer characteristics. However, Hsu and Patankar (1982) reported that the flow behavior index affects the Nusselt number ratio between curved and straight tubes. They produced a series of graphs showing the ratio of the Nusselt numbers versus the modified Dean number (which was a function of the flow behaviour index). It is possible that if their data was compared to a modified Dean number that was not a function of the flow behaviour index that similar results would be found as in this study, and one correlation for all flow indices could be made.

Table 7.5: Correlation results for Equation 7.10 using Péclet number from Equation 7.9.

n	C_1	C_2	C_3	C_4	R^2
0.5	0.034	0.91	0.55	4.35	0.998
0.75	0.046	0.89	0.59	4.42	0.996
1.0	0.272	0.89	1.18	4.45	0.995
1.5	0.424	0.72	0.81	3.65	0.995
All	0.116	0.85	0.79	4.29	0.991

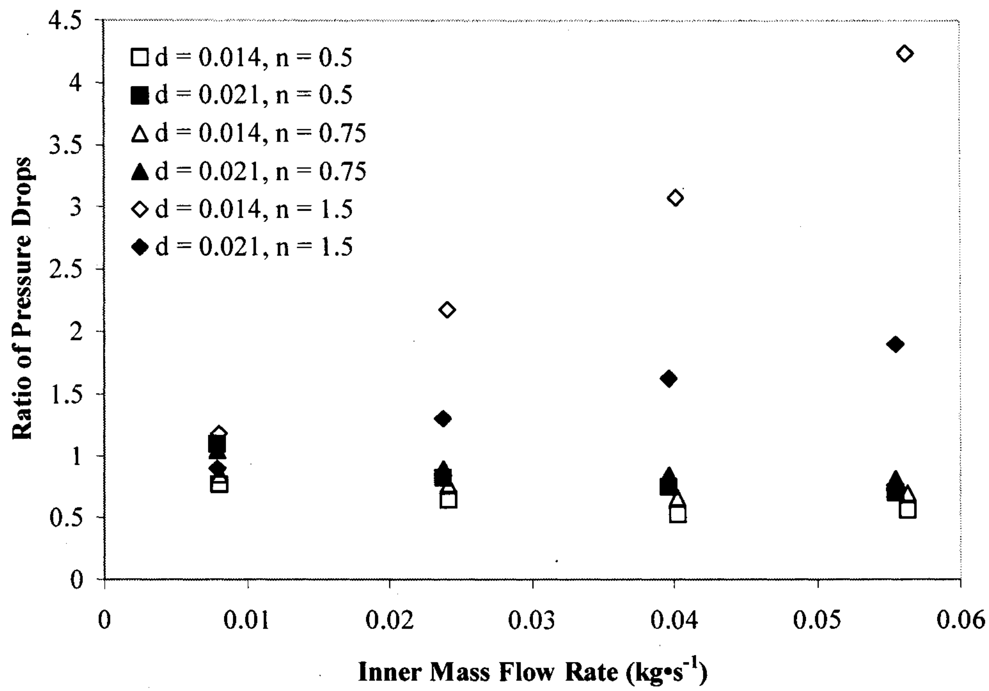

Figure 7.10: Ratio of pressure drops (non-Newtonian to Newtonian at same mass flow rate) versus the mass flow rate (kg·s^{-1}) for the inner tube.

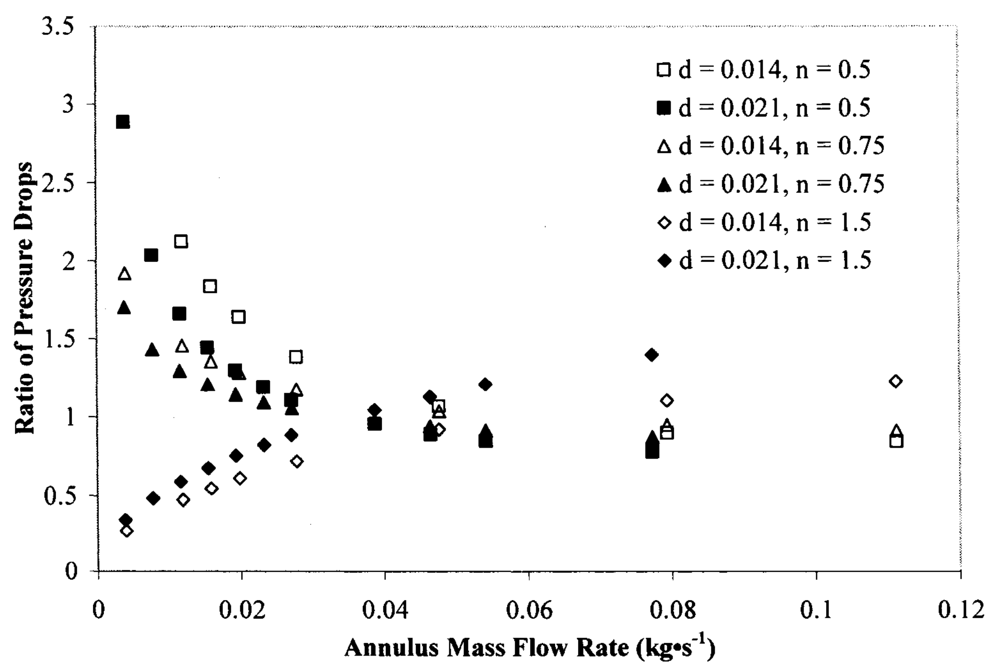

Figure 7.11: Ratio of pressure drops (non-Newtonian to Newtonian at same mass flow rate) versus the mass flow rate (kg·s^{-1}) for the annulus.

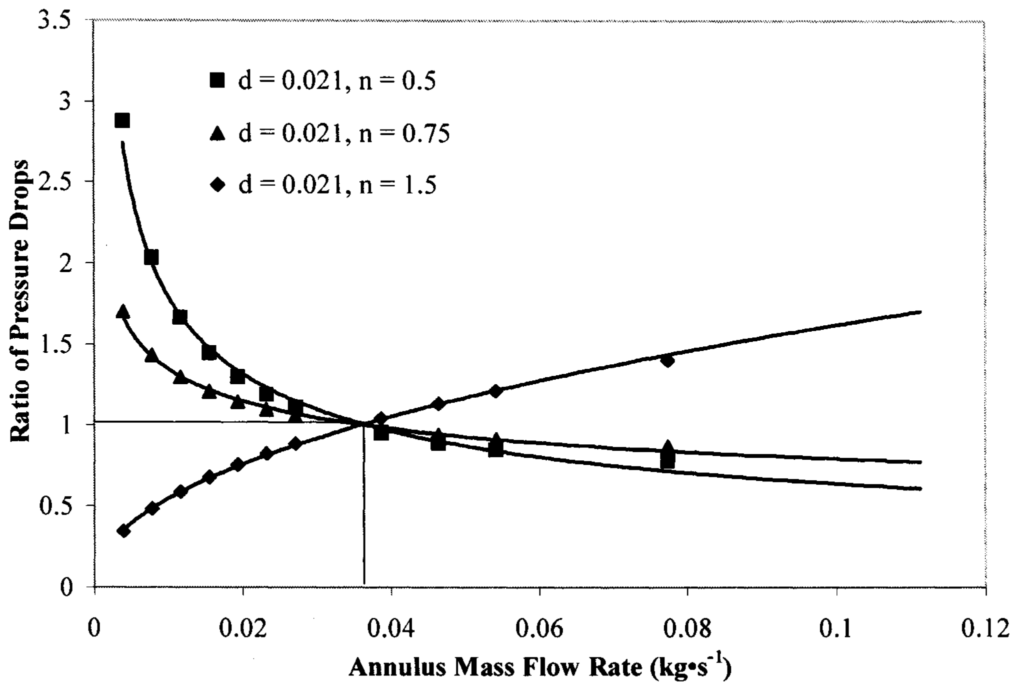

Figure 7.12: Ratio of pressure drops (non-Newtonian to Newtonian at same mass flow rate) versus the mass flow rate ($kg{\cdot}s^{-1}$) for the annulus with the large tube. Location of a strain rate of unity is shown.

Pressure drop results for the non-Newtonian flow are presented in Figures 7.10 and 7.11 for the inner tube and the annulus, respectively. In both Figures, the ratio between the pressure drops of the non-Newtonian fluid to the Newtonian fluid (for a given flow rate) are plotted versus the mass flow rate. The data is broken down into 6 conditions, three flow behavior indices and two tube sizes. In Figure 7.10, for flow behavior indices below unity, the ratio of the pressure drops decrease with increasing flow rate, though the significance of the decrease is rather minor. However, for the flow behaviour index above unity, the ratio increases substantially with increasing flow rate. These behaviors indicate that the effective strain rate of the fluid is above unity. Using the same mass flow rate, but in the large tube, reduces the strain rate, and hence causes the ratio of the pressure drops to become closer to unity. However, this is not the case for the annulus (Figure 7.11) where the strain rate for low mass flow rates is below unity and for higher flow rates it is above unity. Figure 7.12 is a recreation of Figure 7.11, but limits the data for the larger tube and presents trend lines for the three different flow behaviour indices. The three trend lines all intersect at the same value, which also corresponds to a pressure ratio of unity. This, in fact, would be the location where the strain rate is also unity. For the larger tube (smaller annulus gap), this occurs (by inspection) at a mass flow rate of 0.036 $kg \cdot s^{-1}$. The same procedure applied to the smaller tube results in a mass flow rate of 0.063 $kg \cdot s^{-1}$. The average velocities for these mass flow rates are 0.0072 and 0.0096 $m \cdot s^{-1}$, for the large and small tube sizes, respectively. However, with only two data points it is difficult to determine a correlation for the effective strain rate. Interestingly though, is that the ratio between the two velocities mentioned above, and the ratio between the two annulus cross sectional area are nearly identical, with values of 0.75 and 0.76, respectively. Data from other tube sizes needs to be obtained to determine if there is a linear correspondence between the velocity (where the value of the strain rate is unity) and the cross-sectional area, or if this is just a coincidence.

7.5.3 Industrial importance and consequences

For the design of double-pipe heat exchangers, this work demonstrates that thermally dependent viscosities need to be taken into consideration only for the pumping requirements, as there was little effect on the heat transfer coefficients. If a centrifugal pump is used to pump the fluids, then mechanisms may need to be used to ensure that the flow rates stay constant, as changing the flow rate in either the inner tube or the annulus can effected the pressure drop in the other section, leading to changes in the flow rate if the pump capacity is affected by pressure drops. This is especially important in food processing applications, where changes in flow rates can result in lower residence times, which may be detrimental to the effectiveness of some thermal processes.

This work also shows that non-Newtonian effects can be significant for the pumping requirements, especially at higher flow rates, where the pressure drop may increase or decrease significantly compared to Newtonian fluids. It is advised to take these into consideration when considering the pumping power requirements. However, there is still a lot of work that needs to be done for determining the non-Newtonian effects on heat transfer rates.

7.6 Conclusions

Flow and heat transfer in a double-pipe helical heat exchanger was solved numerically for two cases of interest; thermally dependent viscosity and non-Newtonian flow. For the thermally dependent viscosity, there were little effects on the Nusselt number correlations, as the Nusselt number was very weakly correlated to the viscosity. However, there can be a significant increase or decrease in the fluid viscosity as it heats or cools, and though it may not have a great effect on the heat transfer rates, it does affect the pressure drop. Changing the flow velocity in the annulus could significantly increase the pressure drop in the inner tube. The degree of severity of these changes was also affected by the thermal conductivity of the fluid.

For non-Newtonian flows, the Nusselt number was correlated with the Péclet number. These correlations were performed with two different versions of the Péclet number, one that was a function of the flow behaviour index (and hence a geometrical correction factor) and another that was not a function of this parameter. The data were better correlated with the latter Péclet number, which is also the general Péclet number used for non-Newtonian flows. This was done for both flows in the inner tube and in the annulus. Separate correlations had to be performed for the different tube sizes. However, the Nusselt number in the annulus was correlated to the Péclet number and the curvature ratio, resulting in a single correlation for all the data.

Pressure drop data were presented for the non-Newtonian flow for both the inner tube and the annulus. For the inner pipe, increasing the flow rate resulted in the ratio of the pressure drops to diverge from unity; however, this divergence was much stronger for the flow behaviour index of 1.5. In the annulus the strain rate ranged from below unity to above unity. The location of a strain rate of unity was determined for the two different annuli sizes. However, further annulus sizes need to be tested to determine what the effective correlation for strain rate is appropriate for the curved annulus.

7.7 Acknowledgements

The authors are grateful to FCAR (Fonds pour la Formation de Chercheurs et l'Aide à la Recherche) and NSERC (Natural Sciences and Engineering Research Council of Canada) for the financial assistance for this study.

7.8 Nomenclature

a	Constant
A	Constant ($m^2 \cdot s^{-1}$)
b	Constant
B	Constant ($m^2 \cdot s^{-1} \cdot K^{-1}$)
c	Constant
C	Constant
c_p	Specific heat ($J \cdot kg^{-1} \cdot K^{-1}$)
d	Inner diameter of the tube (m)
De^*	Modified Dean number
D_i	Inner diameter of annulus (m)
D_h	Hydraulic diameter (m)
D_o	Outer diameter of annulus (m)
k	Thermal conductivity ($J \cdot s^{-1} \cdot m^{-1} \cdot K^{-1}$)
K	Consistency index ($kg \cdot s^{n-2} \cdot m^{-1}$)
n	Flow behaviour index
Nu	Nusselt number
Pe	Péclet number
Pr*	Modified Prandtl number
r	Radius of inner tube (m)
R	Radius of curvature (m)
Re*	Universal Reynolds number
T_{abs}	Absolute temperature (K)
u'	Strain rate (s^{-1})
v	Average axial velocity ($m \cdot s^{-1}$)

ρ	Density ($kg \cdot m^{-3}$)
τ	Shear stress ($kg \cdot m^{-1} \cdot s^{-2}$)
μ	Viscosity ($m^2 \cdot s^{-1}$)

7.9 References

Hsu, C.-F., and S.V. Patankar. 1982. Analysis of laminar non-Newtonian flow and heat transfer in curved tubes. *AIChE Journal*, Vol. 28(4):610-616.

Jones, J. R. 1960. Flow of a non-Newtonian liquid in a curved pipe. *Quarterly Journal of Mechanics and Applied Mathematics*, Vol. 13(4):428-443.

Kalb, C. E. and J. D. Seader. 1972. Heat and mass transfer phenomena for viscous flow in curved circular tubes. *International Journal of Heat and Mass Transfer*, Vol. 15:801-817.

Kozicki, W., C. H. Chou, and C. Tiu. 1966. Non-Newtonian flow in ducts of arbitrary cross-sectional shape. *Chemical Engineering Science*, Vol. 21:665-769.

Rajasekharan, S., V. G. Kubair, and N. R. Kuloor. 1966. Secondary flow of non-Newtonian fluids in helical coils. *Indian Journal of Technology*, Vol. 4:33-35.

Rajasekharan, S., V. G. Kubair, and N. R. Kuloor. 1970. Heat transfer to non-Newtonian fluids in coiled pipes in laminar flow. *International Journal of Heat and Mass Transfer*, Vol. 13:1583-1594.

Rao, B. K. 1994. Turbulent heat transfer to power-law fluids in helical passages. International Journal of Heat and Fluid Flow, Vol. 15(2):142-148.

Shah, R. K. and S. D. Joshi. 1987. Chapter 5: Convective heat transfer in curved ducts. In: *Handbook of Single-Phase Convective Heat Transfer*, S. Kakac, R. K. Shah, and W. Aung, eds., Wiley-Interscience, NY, pp 5.1-5.46.

Sieder, E. N. and G. E. Tate. 1936. Heat transfer and pressure drops of liquid in tubes. *Ind. Eng. Chem.*, Vol. 28:1429-1435.

Simpson, S. G. and M. C. Williams. 1974. An analysis of high temperature/short time sterilization during laminar flow. *Journal of Food Science*, Vol. 39:1047-1054.

Singh, R. P. and D. R. Heldman. 1993. *Introduction to Food Engineering, second edition.* Academic Press, Inc., San Diego, CA, 499 pp.

Thomas, R. H. and K. Walters. 1963. On the flow of an elastico-viscous liquid in a curved pipe under a pressure gradient. *Journal of Fluid Mechanics*, Vol. 16:228-242.

CONNECTING TEXT

Chapters VI and VII dealt with the effects of fluid properties on the heat transfer characteristics of a double-pipe heat exchanger. For food processing applications, there are additional considerations to be met, on top of the fluid properties. These involve the residence time and temperature distributions. Furthermore, the uniformity of the heating/cooling process is important, especially to maximize product quality and to ensure adequate thermal treatment. Chapter VIII deals with these issues in a double-pipe helical heat exchanger.

VIII. RESIDENCE TIME, TEMPERATURE, AND HEATING UNIFORMITY IN A DOUBLE-PIPE HELICAL HEAT EXCHANGER

8.1 Abstract

A numerical study of a double-pipe helical heat exchanger was performed to ascertain the residence time distribution, temperature distribution and heating uniformity for food processing applications. Two different ratios of inner tube to outer tube diameters were simulated. A range of laminar flow rates were used, with both parallel flow and counterflow configurations. Both heating and cooling in the inner tube were studied. Furthermore, the use of a double-pipe heat exchanger as a holding tube was tested. Heating/cooling uniformity among different conditions was compared by using a first order kinetics model for sterilization.

Residence time distributions became more uniform with increased flow rates in both the inner tube and in the annulus, though the effect was more notable in the inner tube. Temperature uniformity in the inner tube increased with increasing flow rate. However, changing the flow rate in the annulus, for a constant flow rate in the inner tube, affected the uniformity. Similar results were found for the annulus. Heating uniformity in the inner tube tended to increase with increased flow rates. At higher flow rates, the differences between parallel and counterflow configurations were negligible. The cooling processes had much more uniformity than heating processes, due to the nature of the temperature and velocity profiles.

8.2 Introduction

Aseptic processing of liquid foods is often performed as a continuous operation where the liquid food undergoes heating, holding, and cooling operations just prior to packaging. It is of utmost importance to guarantee that the liquid product has been sterilized/pasteurized by the time that it is packaged, or in other words, that the required microbial lethality has been achieved for the targeted microorganisms. Lethality is affected by both temperature and time of the process, and lethality occurs in all three of the thermal stages of the aseptic processing system. Though obtaining the required lethality is essential, it is not desirable to go beyond the required lethality, as it can result in the quality reduction of the food product, from a nutritive and flavor standpoint. However, the calculations for the lethality must be based on the coldest temperature and the fastest moving particle (Simpson and Williams, 1974, Dignan et al., 1989; Heldman, 1989). Therefore, with the exception of the portion of the liquid food which is the coldest and fastest moving, the remaining fluid is undergoing additional heat treatment that is not necessary. Furthermore, Dignan et al. (1989) recommend that the heat treatment in the cooling section should not be included in the lethality calculation for liquids containing particulates, as these particulates may break up during the cooling section, and hence the cores of the particulates would cool faster than predicted, and the required lethality may not be achieved. Heldman (1989) suggested that this section should be included, since there can be significant heat treatment in the center of particulates as they cool much slower than the surrounding liquid. Despite the fact that the cooling section is not included in the calculations does not signify that it is not important, as there can be quality degradation if the product is not cooled quickly or in a uniform manner.

To optimize the quality of the product, it is necessary to reduce the amount of excess heat treatment that the liquid food experiences. The ideal situation is plug flow and uniform temperature, where every part of the fluid undergoes an identical time-temperature profile, resulting in the same lethality for the whole product, and therefore minimization of quality degradation. The residence time distribution (RTD) in the holding tube is of importance in calculating the lethality and the quality degradation. In the heating and cooling sections, the importance for minimizing quality degradation is based on the time-temperature profiles, and to harmonize this profile for all streamlines.

Helical coils offer advantages over straight tubes for the heating, holding, and cooling sections of an aseptic processing system. The increased mixing due to secondary flow result in higher heat transfer coefficients; resulting in quicker heating of the fluid than in a straight tube with the same diameter and mass flow rate (Prabhanjan et al., 2002). Furthermore, the secondary flows distribute the heat more evenly (Ruthven, 1971), and the velocity profiles tend to be flatter than in straight tubes, for both laminar and turbulent flow (Koutsky and Adler, 1964). Furthermore, the RTD in helical coils are narrower than those in straight tubes (Ruthven, 1971; Liu and Zuritz, 1995; Son and

Singh, 2002). RTD for particulate flow in helical coils has been studied for food processing applications and has further demonstrated the narrowing of the distribution (Salengke and Sastry, 1994; Salengke and Sastry, 1996; Sandeep et al., 1997).

RTD is usually measured by injecting a tracer into the inlet of the system and then measuring the concentration in the output over time (Janssen, 1994). The concentration is plotted versus time, and is normalized by dividing the concentration values by the area under the curve, resulting in values that are defined as $E(t)$. Integrating with respect to time, t, yields a value of unity (Heppell, 1985). The mean residence time can be calculated by integrating the product of time and the $E(t)$ values, or it can be calculated by dividing the volume of the equipment by the volumetric flow rate (Heppell, 1985; Ramaswamy et al., 1995),

$$\tau_m = \int_0^\infty tE(t)dt = \frac{Vol}{Q} \tag{8.1}$$

Rather than comparing actual RTD curves, the RTD can be compared by calculating the second moment about the mean, σ^2 (Heppell, 1985; Sancho and Rao, 1992),

$$\sigma^2 = \int_0^\infty t^2 E(t)dt - \tau_m^2 \tag{8.2}$$

The proportion of surviving spores from a sterilization process can be calculated based on the $E(t)$ distribution and the decimal reduction time, DRT. When the population of microorganisms, such as *E. coli* or *Salmonella*, is heat treated, the population will decrease in a logarithmic manner with respect to time (Singh and Heldman, 1993). The DRT is the time required for a 90% decrease in the population (a one log-cycle reduction). Using the DRT, the proportion of surviving spores can be calculated as (Heppell, 1985),

$$\frac{N}{N_0} = \int_0^\infty E(t)10^{-t/DRT}dt \tag{8.3}$$

The DRT, however, is a function of the temperature. This complicates matters for calculating the lethality in the heating and cooling sections of the aseptic processing system as the time-temperature profile is required. The DRT logarithmically decreases with temperature for bacterial spores and the dependency of the DRT on temperature is generally described by the thermal resistance constant, z (Singh and Heldman, 1993).

The thermal resistance constant is the necessary temperature increase to result in a 90% decrease in the *DRT*. Given a reference *DRT*, reference temperature, and a thermal resistance constant, the *DRT* at a given temperature can be calculated based on (Singh and Heldman, 1993),

$$DRT = DRT_{ref} 10^{\left(\frac{T_{ref} - T}{z}\right)} \tag{8.4}$$

In many processes, the standard heat treatment is for a 12 log-cycle reduction (12*DRT*) using a *DRT* value for *Clostridium botulinum* (Singh and Heldman, 1993).

Several studies have been performed to optimize the uniformity of sterilization processes for viscous foods. Simpson and Williams (1974) study a high temperature/short time for non-Newtonian foods and modeled the denaturation of bacterial spores and vitamin B_1 (thiamin) for laminar flow in a straight tube sterilizer. Kelder et al. (2002) numerically studied power-law fluids in coiled sterilizers, and like Simpson and Williams (1974) used thiamin retention as a measure of the quality of the product. Kelder et al. (2004) studied starch gelatinization in helical coils and found that both heat transfer and gelatinization rates were higher for more tightly curved coils.

8.3 Objectives

The objective of this work is to study the residence time, residence time distribution, and heating uniformity in a double-pipe helical heat exchanger, and to determine, if possible, the best operating conditions to maximize the heating uniformity.

8.4 Materials and Methods

8.4.1 CFD Modeling

The method used to perform the computational fluid dynamics modeling of the double-pipe helical heat exchanger are outlined in Chapter IV, along with the validation simulations. The outer tube had an inner diameter of 0.1 m and a pitch of 0.115 m. The outer diameters of the inner tubes were 0.04 and 0.06 m, both with wall thicknesses that were 15% of the diameter and a pitch of 0.115 m. The length of the heat exchangers from inlet to outlet is 2π radians. The radius of curvature of the tubes is 0.8 m. The properties of the inner tube were set to stainless steel, with a thermal conductivity of $16\ W\cdot m^{-1}\cdot K^{-1}$, density of $7881.8\ kg\cdot m^{-3}$ and a specific heat of $502\ J\cdot kg^{-1}\cdot K^{-1}$. The outer tube was set to have adiabatic boundary conditions; the inner tube was set to allow conductive heat flow through the tube.

Four different mass flow rates in the inner tube were used: 0.0084, 0.0250, 0.0417, and $0.0584\ kg\cdot s^{-1}$. For each of these mass flow rates, the flow rate in the annulus was set at either half, full, or double the value. This results in 12 different combinations, used over the two different tube sizes. Both parallel flow and countercurrent flows were tested. The inlet temperatures in the inner tube were 0°C or 80°C, the inlet temperature to the annulus would be either 80°C or 0°C, respectively. This allowed the differences between heating and cooling to be studied in both the inner tube and the annulus. This resulted in a total of 96 simulations.

8.4.2 Calculation of residence time and residence time distribution

The calculation for the residence time and residence time distribution could not be performed in the same manner as described in the introduction, as the results obtained are flow velocities and not concentration profiles over time. However, these two parameters can still be calculated. The residence time was calculated for the total flow, and for the flow in each individual cell, however, mixing between cells was not taken into consideration. The local residence time, τ_{loc}, for any given cell, was calculated by dividing the volume of the cell by the axial volumetric flow rate,

$$\tau_{loc} = \frac{L_{loc} A_{x,loc}}{v_{loc} A_{x,loc}} = \frac{L_{loc}}{v_{loc}} \tag{8.5}$$

The average residence time, τ, of the whole tube, or annulus, is a weighted average of all the local residence times. The weighted average is based on the proportion of the total flow that is flowing through each particular cell, hence,

$$\tau = \sum \tau_{loc} \frac{v_{loc} A_{x,loc}}{v A_x} \tag{8.6}$$

The variance of the residence times was calculated to describe the residence time distribution at each cross-section along the length of the heat exchanger. Furthermore, the coefficient of variation, *CV*, was calculated at each cross-section. The coefficient of variation is the standard deviation divided by the mean.

8.4.3 Calculation of heating uniformity

The heating uniformity was determined by using a model similar to that used in the calculation of the thermal kill of microorganisms. Although there is some debate if the model described in the introduction, that is, first order kinetics, is the best method to use in unsteady thermal processes (Anderson et al., 1996), it has been chosen because it is highly common in the industry and fairly straight forward. Furthermore, nutrients such as vitamin B_1 (thiamin) have been modeled with first order kinetics (Simpson and Williams, 1974, Liao et al., 2000; Kelder et al., 2002). The local proportion of surviving microorganisms, λ_{loc}, was calculated for each cell as,

$$\lambda_{loc} = 10^{-\tau_{loc}/DRT} \tag{8.7}$$

The value for *DRT* was calculated using Equation 8.4. Originally, it was desired to use the values based on those of *Clostridium botulinum* (strain 213B) at 121°C from Anderson et al. (1996) with values of DRT_{ref} = 11.4 s and z = 9.79°C. However, it was found that using these values made it difficult to adequately compare simulations as the temperature differences from one end of the heat exchanger to the other was quite large, resulting in some thermal kills to be negligible. Though this would represent the real situation for that particular case, it will not give general results that could be extrapolated to other conditions. Therefore, the values for DRT_{ref}, T_{ref}, and *z*, were based on the average residence time, average fluid temperature, and 10.0°C, respectively. A different DRT_{ref} and T_{ref} were calculated for each cross-section in the flow. The T_{ref} was the average temperature in the cross-section. Using these values, for any fluid that was at the average residence time and average temperature, it would undergo a one log reduction thermal kill. It must be emphasized that using this data does not indicate that the objective of this work is to study the reduction of microorganisms in the heat exchanger. The above model is being used solely as a technique to give some insight into the best operating parameters for uniform heat treatment to maximize heating uniformity, not only for sterilization, but for retention of quality.

The total proportion of surviving microorganisms was based on a weighted average, similar to that used in calculating the average residence time,

$$\lambda = \sum \lambda_{loc} \frac{v_{loc} A_{x,loc}}{v A_x} \tag{8.8}$$

The maximum and minimum proportions were also calculated, along with the variance and the coefficient of variation. Furthermore, the mean, maximum, and minimum temperatures were determined at each cross-section of the flow. The variance and the coefficient of variation were also calculated at each cross-section.

8.5 Results and Discussion

8.5.1 Residence time distributions

Residence time distributions were calculated for flows in the inner tube and the annulus. The coefficient of variation for the residence time distributions was also calculated. For a given tube diameter, the coefficient of variation of the residence time should remain constant if the distribution remains proportional. A decrease in the coefficient of variation would indicate that the profile is becoming more uniform.

Table 8.1: Coefficient of variation of the residence time for the inner tube and the annulus.

Mass Flow Rate	Coefficient of Variation of Residence Time			
	Inner		Annulus	
($kg \cdot s^{-1}$)	Small tube	Large tube	Small tube	Large tube
0.0084	0.51	0.66	0.63	0.51
0.0250	0.39	0.51	0.61	0.49
0.0427	0.31	0.44	0.58	0.47
0.0584	0.22	0.39	0.55	0.45

Table 8.1 shows the coefficient of variation of the residence times at different mass flow rates, for the inner tube and the annulus. In both cases, the coefficient of variation decreases with increasing mass flow rate, indicating that the velocity

distribution is becoming more uniform with increasing flow rate. This effect is most likely due to the centrifugal forces that are stronger for the higher mass flow rates. For the same mass flow rate in the inner tube, the larger tube has a higher coefficient of variation. In the annulus, the larger gap size (smaller inner tube) has the higher coefficient of variation. The following two correlations were made for the coefficient of variation for the inner tube and the annulus, respectively:

$$CV = 0.4278 - 0.000145\,\mathrm{Re} + 7.967\left(\frac{d}{2R}\right) \qquad \mathrm{R}^2 = 0.955 \tag{8.9}$$

$$CV = 0.0296 - 0.000174\,\mathrm{Re} + 13.587\left(\frac{D_o - D_i}{2R}\right) \qquad \mathrm{R}^2 = 0.999 \tag{8.10}$$

These correlations, though not useful in the design of a heat exchanger, give some insight into the expected uniformity of the velocity profile. However, these correlations were only based on 2 tube sizes, so caution needs to be exerted when using them. Salengke and Sastry (1994) showed that the standard deviation of the normalized residence time for particles decreased for increasing flow rate in a curved holding tube. Salengke and Sastry (1996) also found that the standard deviation of the normalized residence time tended to increase with increasing curvature ratio, which is similar to the results from Equation 8.9.

8.5.2 Temperature distributions in the inner tube

Temperature and coefficient of variation of temperature data were gathered for various configurations of the double-pipe helical heat exchanger. Both parallel flow and counterflow configurations were used, with the fluid in the inner tube being either heated or cooled. Figure 8.1 shows the average bulk temperature of the fluid in the inner tube along the length of the tube for the small tube and a mass flow rate of 0.0084 $\mathrm{kg \cdot s^{-1}}$. The mass flow rates in the annulus were either half, full, or double the value of the inner tube. Changing the flow rate in the annulus affected both the temperature drop, as well as the coefficient of variation of the temperature. The coefficient of variation increased with higher flow rates in the annulus. There was a tendency for the coefficient of variation to first increase then decrease along the length of the tube. When the fluid first enters the heat exchanger, it is at a uniform temperature, and hence the coefficient of variation is nil, but then quickly increases as the fluid near the tube wall suddenly starts to change temperature. The coefficient will then start dropping as the temperature profile begins developing and the secondary flow mixes the fluid.

Figure 8.2 shows the average bulk temperature profiles along the length of the heat exchanger for all four different inner mass flow rates, in both the small and large tubes, where the flow rate is the same in the inner tube and in the annulus. Figure 8.3 shows the coefficient of variation of the temperature for the temperatures presented in Figure 8.2. As expected, an increase of the flow rate in the inner tube results in a decrease of the temperature drop. Temperature drops were also much higher for the

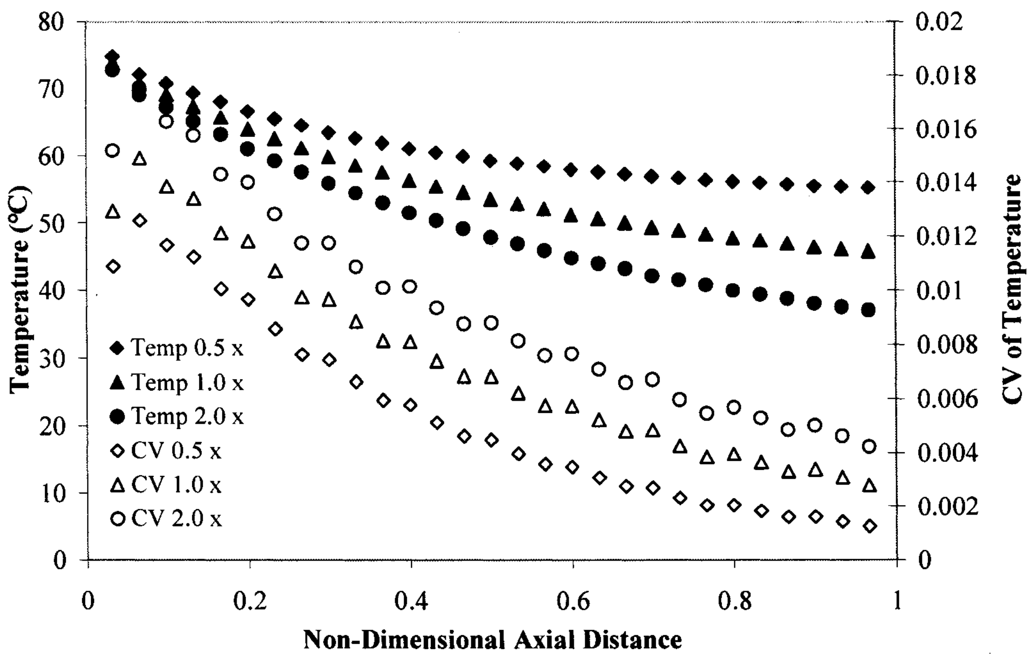

Figure 8.1: Fluid temperature and coefficient of variation of temperature along the length of the heat exchanger for an inner mass flow rate of 0.0084 $kg \cdot s^{-1}$.

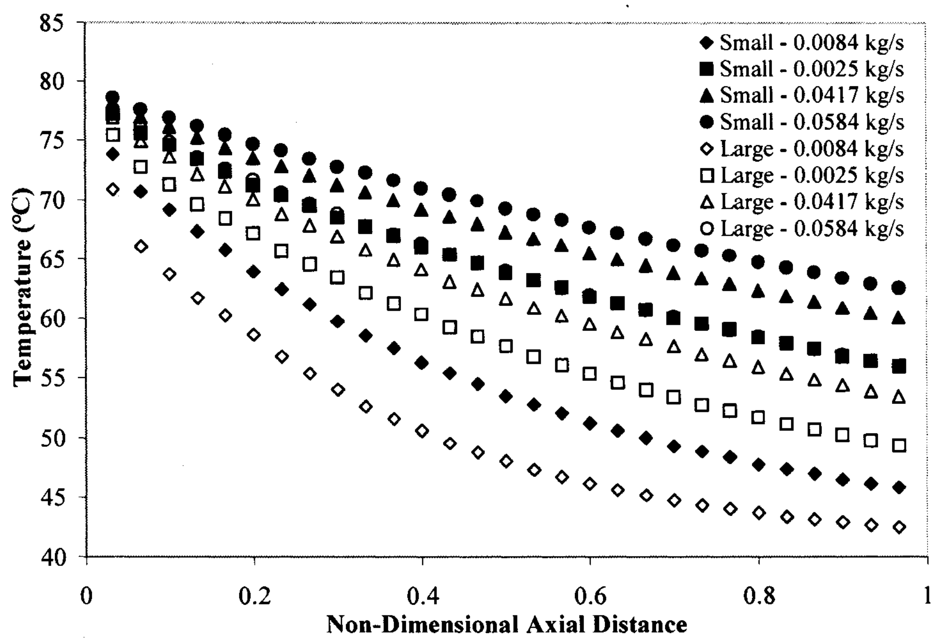

Figure 8.2: Fluid temperature along the length of the heat exchanger when mass flow rates were the same in the inner tube and in the annulus (both tube sizes).

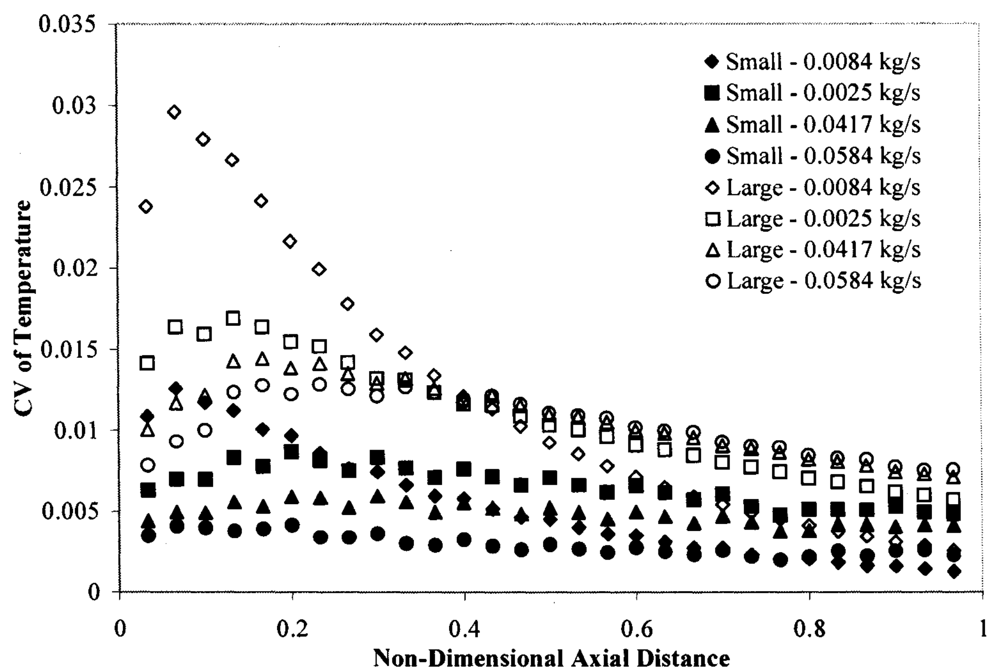

Figure 8.3: Coefficient of variation of fluid temperature along the length of the heat exchanger when mass flow rates were the same in the inner tube and in the annulus (both tube sizes).

flows in the large tube, due to the increased residence time, larger surface area, and higher heat transfer coefficients (as noted in Chapter IV). The coefficient of variation, however, tended to be greater in the large tube. Except for the smallest flow, the coefficient of variation of the temperature was not that different between the different flow rates, especially in the larger tube. In the smaller tube, the coefficient of variation did not differ largely over the length of the heat exchanger at the higher flow rates. It is expected that this deviation in the smaller tube is due to the long residence time, where it comes close to thermal equilibrium near the end of the heat exchanger, and hence the variation in the temperature decreases.

Table 8.2: Coefficient of variation of the temperature for the inner tube.

Mass Flow Rate	Coefficient of Variation of Temperature							
	Cooling				Heating			
	Small Tube		Large Tube		Small Tube		Large Tube	
($kg \cdot s^{-1}$)	parallel	counter	parallel	counter	parallel	counter	parallel	counter
0.0084	0.0075	0.0085	0.0120	0.0148	0.0102	0.0115	0.0166	0.0192
0.0250	0.0065	0.0069	0.0109	0.0119	0.0099	0.0103	0.0156	0.0168
0.0427	0.0048	0.0049	0.0108	0.0115	0.0076	0.0077	0.0162	0.0167
0.0584	0.0029	0.0029	0.0103	0.0108	0.0046	0.0046	0.0151	0.0153

Average coefficients of variation of temperature over the length of the heat exchanger were calculated for all simulations. Those for the inner tube are shown in Table 8.2 for both parallel flow and counterflow configurations when the fluid is being cooled or heated. In these cases, the mass flow rate in the annulus was equal to the mass flow rate in the inner tube. The counterflow tended to have greater coefficients of variation than the parallel flow at low flow rates, though this difference decreased with increasing flow rate, and was not appreciable at high flow rates. Also, the trends were the same for both the cases of heating and cooling. It is further postulated that the coefficient of variation of temperature is not the best method to compare temperature profiles, as the temperature changes from trial to trial, and they do not have the same basis of comparison. For example, two temperature profiles that are identical, but with all values simply shifted by the same temperature difference will not have the same coefficient of variation. Therefore, for temperature profiles, the variance may be a better indicator of the temperature profile for a given cross-sectional area. Table 8.3 shows the same trials as Table 8.2 but with the variance of the temperature rather than the coefficient of variation. It shows that for counterflow and parallel flow there is negligible difference in the average variance of the temperature, even though the rates of heat transfer are higher. This indicates that the profile is developing in a similar manner. However, as the mass transfer rate is increased, the variances decrease, most likely due to flattened temperature profiles due to the increased mixing caused by the stronger secondary flows. Furthermore, the data for the variance of temperature for the case of heating is identical as that for cooling for any given set of identical parameters.

Table 8.3: Variance of the temperature for the inner tube.

	Variance of Temperature							
	Cooling				Heating			
Mass Flow Rate	Small Tube		Large Tube		Small Tube		Large Tube	
($kg \cdot s^{-1}$)	parallel	counter	parallel	counter	parallel	counter	parallel	counter
0.0084	7.76	7.99	23.75	23.39	7.76	7.99	23.75	23.39
0.0250	5.10	5.62	14.82	15.86	5.10	5.62	14.82	15.86
0.0427	2.77	2.90	13.87	15.17	2.77	2.90	13.87	15.17
0.0584	1.07	0.98	12.70	13.65	1.07	0.97	12.70	13.65

8.5.3 Temperature distributions in the annulus

Temperature data was available for 12 different annulus mass flow rates, as each of the 4 different mass flow rates of the inner tube had 3 corresponding flow rates in the annulus. As expected, the lower flow rates for any tube size results in a greater temperature change since the residence time is increased. However, the results in the larger tube have a greater temperature increase than those with the smaller tube for the same mass flow rate. This is in contradiction with the results of the inner tube. The large tube has a smaller gap, and hence a larger velocity in the annulus. This generally results in a smaller temperature difference as the residence time of the fluid is decreased. However, due to the nature of a fluid-to-fluid heat exchanger, the rate of heat transfer from one fluid to the other is dependent on the flow rates in the other section of the heat exchanger. In this case, the limiting heat transfer rate is on the annulus side, so decreasing the gap size greatly increases the overall heat transfer coefficients.

Furthermore, the area available for heat transfer increased more than the residence time decreased.

The variance of temperature data are presented in Figures 8.4 and 8.5 for the small tube and the large tube, respectively. For the smaller tube (larger gap size), the peak in the variance decreased with increasing flow rate. For the lowest flow rate, the variance dropped the most, even though it had the highest peak. At this flow rate, the temperature began leveling off the most near the end of the heat exchanger, and the uniformity increased. At higher flow rates the temperatures did not get as close to an equilibrium temperature, and hence the variances were higher. However, for the other three flow rates, the higher variances were always associated with the lower flow rates. For the large tube, the lowest flow rate had variances that were similar to those with the smaller tube, but the peak variance in this case was not the highest peak. For the other flow rates, the lower flow rates resulted in the higher variances, except near the end of the heat exchanger, where there was a cross-over. However, on average, the variance was higher for the lower flow rates, indicating that as the flow rate increased, the secondary flows increased the mixing of the fluid leading to better temperature uniformity.

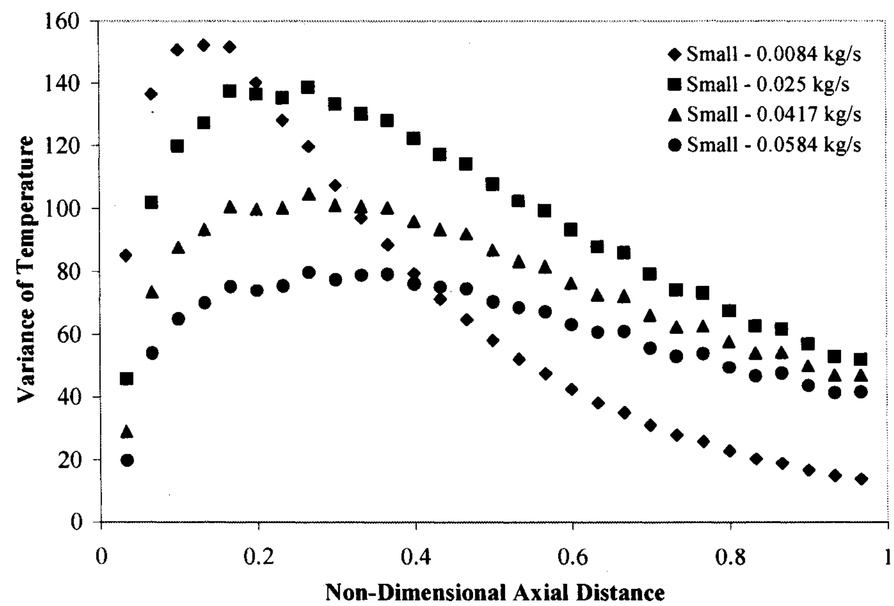

Figure 8.4: Variance of temperature in the annulus along the length of the heat exchanger when the mass flow rates in the inner tube and the annulus are the same (small tube).

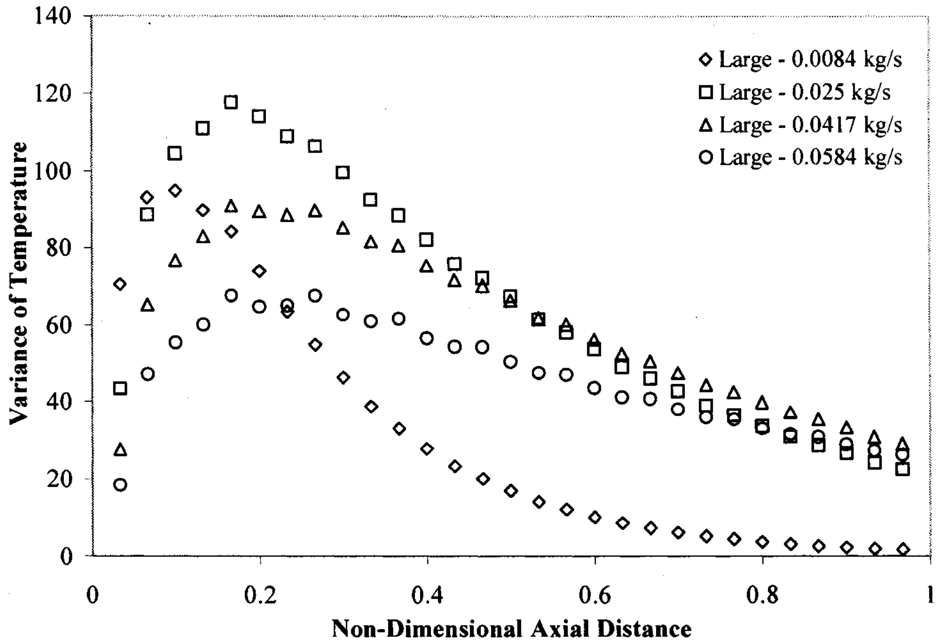

Figure 8.5: Variance of temperature in the annulus along the length of the heat exchanger when the mass flow rates in the inner tube and the annulus are the same (large tube).

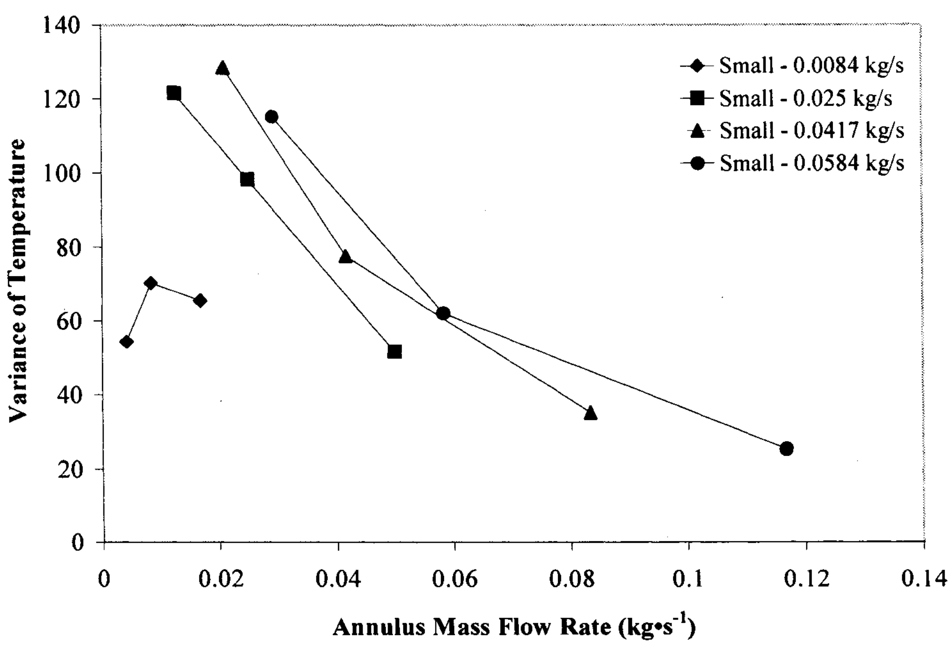

Figure 8.6: Variance of temperature in the annulus versus the annulus mass flow rate. Mass flow rates in the annulus and inner tube are the same (small tube).

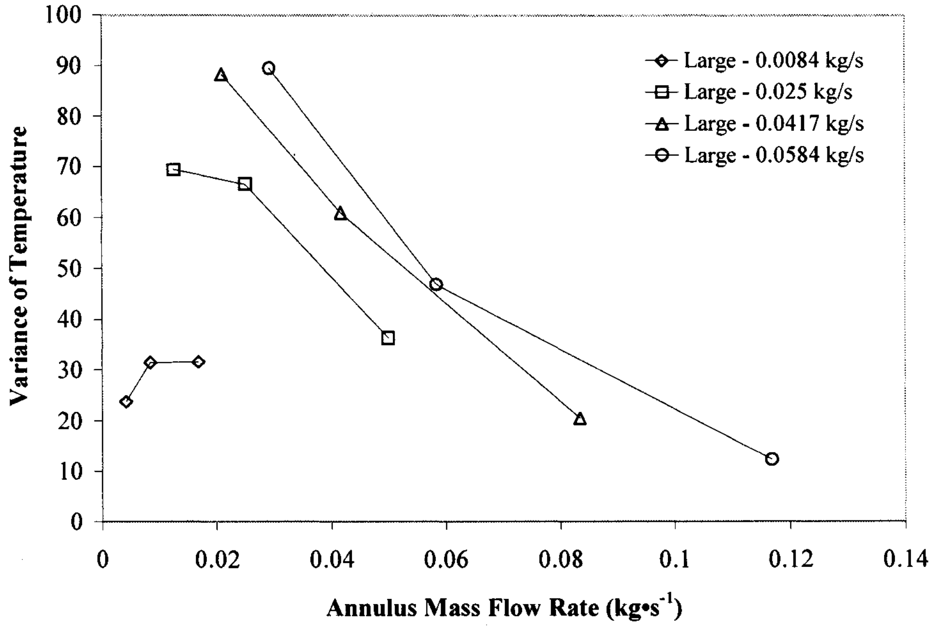

Figure 8.7: Variance of temperature in the annulus versus the annulus mass flow rate. Mass flow rates in the annulus and inner tube are the same (large tube).

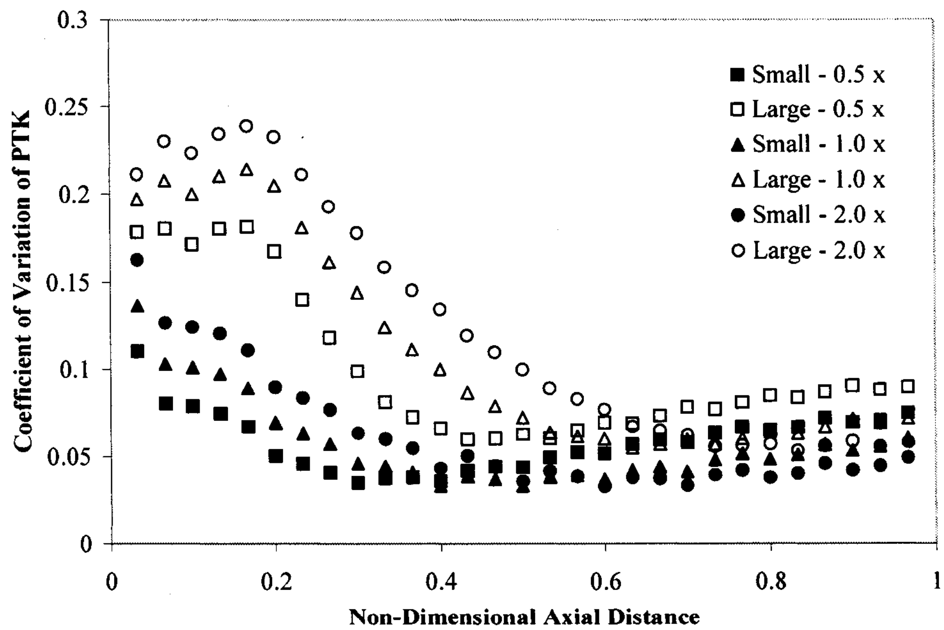

Figure 8.8: Coefficient of variation of the proportion of thermal kill (PTK) along the length of heat exchanger for the inner tube with a flow rate of 0.0084 kg·s^{-1}. Three annulus mass flow rates were used, half, full and double the inner tube mass flow rate; fluid is being cooled.

The variance of temperature versus the annulus mass flow rate is shown in Figures 8.6 and 8.7. The data is divided up based on the flow rate in the inner tube, as this had an affect on the average variance of the temperature in the annulus. Increasing the mass flow rate in the annulus, for a given flow rate in the inner tube resulted in a decrease in the variance, with exception of the lowest inner flow rate, where it first increased and then decreased (for the case with the smaller tube). For mass flow rates in the annulus that were similar, the variance was higher when the flow rate in the inner tube increased. These are cases where the heat transfer rates increased due to a reduction in the resistance on the inner tube side, and resulted in more heat being transferred away by the fluid in the annulus. Since the flow rate has not changed, there is no change in the secondary flow, so there is a greater temperature gradient across the fluid.

There were no differences in variance of the temperature when comparing heating versus cooling in the annulus. There were also negligible differences between the variance of temperature when comparing parallel flow versus counterflow.

8.5.4 Proportion of thermal kill in the inner tube

In order to provide insight to the thermal effectiveness of a double-pipe heat exchanger for pasteurization and sterilization processes during heating and cooling, the combination of the velocity and temperature profiles need to be merged in an appropriate manner. In this work a thermal kill model was used to gauge this effectiveness. For the flow rate in the inner tube of 0.0084 $kg{\cdot}s^{-1}$, the coefficient of variation of the proportion of thermal kill (PTK) is shown in Figure 8.8 for each of the three corresponding flow rates in the annulus. In all cases, the coefficient of variation was high at the entry of the heat exchanger and dropped along the length of the heat exchanger. When being cooled, the temperature profile of the inner fluid first starts off flat, and begins developing a quasi-parabolic profile as the temperature near the wall decreases. As it starts reaching the end of the heat exchanger it starts becoming flat again. The coefficient of variation of PTK tends to increase near the exit again, where the temperature profile began to flatten. The location of minimum variation is ideal for food processing applications. At this condition, the temperature is the highest where the mass flow rate is the highest, and the temperature is lower where the residence time is less, resulting in uniform thermal processing. The coefficient of variation tends to drop more rapidly when the flow rate in the annulus is lower. This is most likely due to the higher heat transfer resistance in the annulus at low flows, resulting in lower heat transfer rates. Since the fluid in the inner tube would not receive heat as fast, the temperature is more uniform. The coefficient of variation becomes stable in less distance in the smaller tube than in the larger tube. This may be because in the larger tube, there is a greater distance for the heat to penetrate into the center of the fluid, and the curvature ratio is smaller, resulting in weaker secondary flows. Figure 8.9 is for the same flow rates as Figure 8.8 except that it is the case of the fluid being heated rather than cooled. The coefficient of variation of PTK decreases as the flow (including secondary flow) and temperature profiles develop. The coefficient of variation of PTK decreases smoothly to a stable value, unlike the case where the fluid is being cooled. When the fluid first enters the heating stage, the slow moving fluid near the surface is quickly heated up, resulting in a large thermal kill near the walls but little in the center. As the fluid moves down the tube, heat begins penetrating the inner area and the development of the secondary flows helps this penetration so that the thermal kill becomes more uniform. In both heating and cooling, the coefficient of variation of the PTK should approach the same value, as the temperature becomes constant and the thermal kill is only dependent on the velocity profile.

Table 8.4 shows the average coefficient of variation of the thermal kill in the inner tube versus the mass flow in the inner tube for both the parallel flow and counterflow configurations, as well as for cooling and heating. For the most part, there are negligible differences between the two configurations, except at the low flow rate in the smaller tube, where the coefficient of variation of PTK is larger for the parallel flow. This deviation may be attributed to the patterns as to how the temperature develops for low flows. When the flow rate in the inner tube is low, the increase in rate of heat transfer can be quite appreciable if the configuration is changed from parallel flow to counterflow. However, the temperature difference is very large at the entrance of the parallel flow, but decreases near the end. In the case of counterflow, the temperature difference remains fairly stable throughout; therefore the large temperature difference at the entrance of the parallel flow can result in large temperature gradients in the profile near the beginning, resulting in very non-uniform thermal kill.

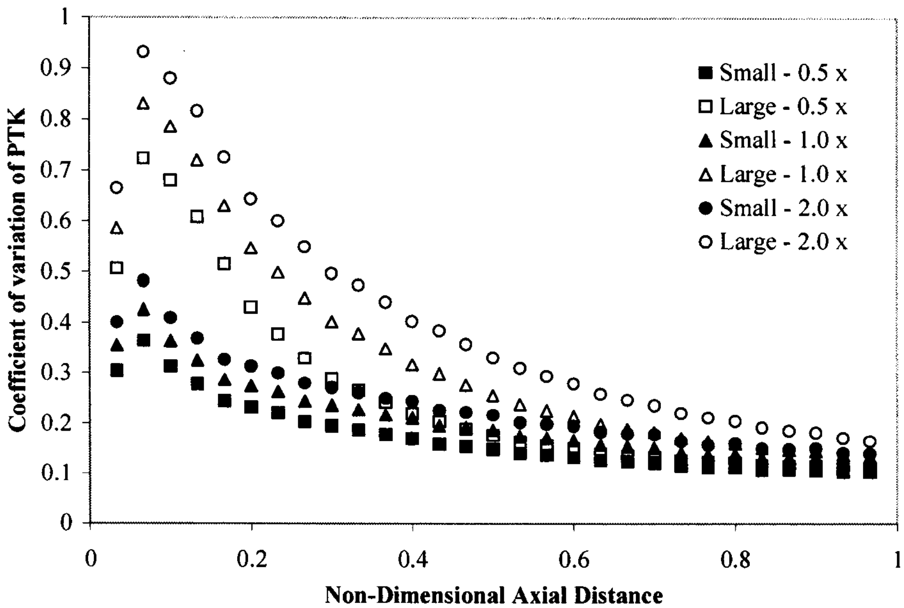

Figure 8.9: Coefficient of variation of the proportion of thermal kill (PTK) along the length of heat exchanger for the inner tube with a flow rate of 0.0084 kg·s^{-1}. Three annulus mass flow rates were used, half, full and double the inner tube mass flow rate; fluid is being heated.

Table 8.4: Coefficient of variation of the PTK for the inner tube.

Mass Flow Rate (kg·s^{-1})	Coefficient of Variation of the PTK							
	Cooling				Heating			
	Small Tube		Large Tube		Small Tube		Large Tube	
	parallel	counter	parallel	counter	parallel	counter	parallel	counter
0.0084	0.057	0.040	0.110	0.107	0.208	0.220	0.337	0.388
0.0250	0.034	0.033	0.081	0.087	0.123	0.124	0.229	0.240
0.0427	0.021	0.021	0.079	0.084	0.089	0.089	0.189	0.194
0.0584	0.024	0.023	0.077	0.080	0.064	0.063	0.165	0.166

8.5.5 Proportion of thermal kill in the annulus

The coefficient of variation of the proportion of thermal kill for flow in the annulus is shown in Figures 8.10 and 8.11 for the case of the fluid being heated, for the small tube and the large tube, respectively. For each trial shown, the flow rate in the annulus is equal to the flow rate in the inner tube. For the most part, the results are similar to those for the inner tube. The coefficient tends to rise to a peak and then decreases. One turn of the heat exchanger is not long enough for the coefficient to become stable. In general, the coefficient is lower for higher flow rates, except for the lowest flow, which peaks high but decreases below the other values along the length. The uniformity of the thermal kill in the annulus is expected to be less than in the inner tube, since the heat only penetrates from one wall, and thus it takes a while for the heat to penetrate all the way to the outer wall. The lower annulus flow rate shows the greatest rate of drop of the coefficient of variation of the PTK along the length of the heat exchanger. This would be due to the temperature profile becoming flatter as the temperature in the heat exchanger approaches equilibrium.

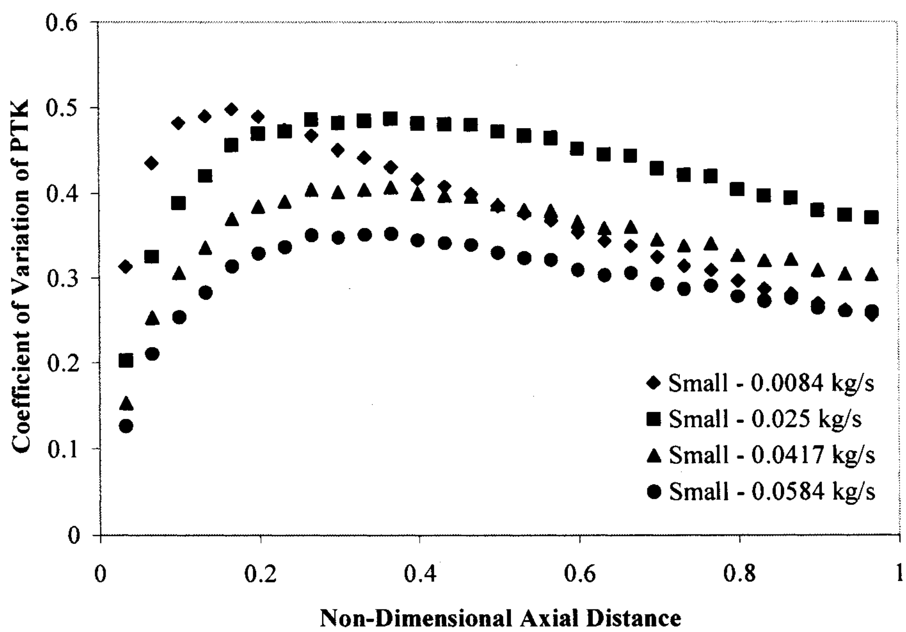

Figure 8.10: Coefficient of variation of the proportion of thermal kill (PTK) along the length of the heat exchanger for the annulus. Fluid is being heated and the mass flow rates in the annulus and the inner tube are the same (small tube).

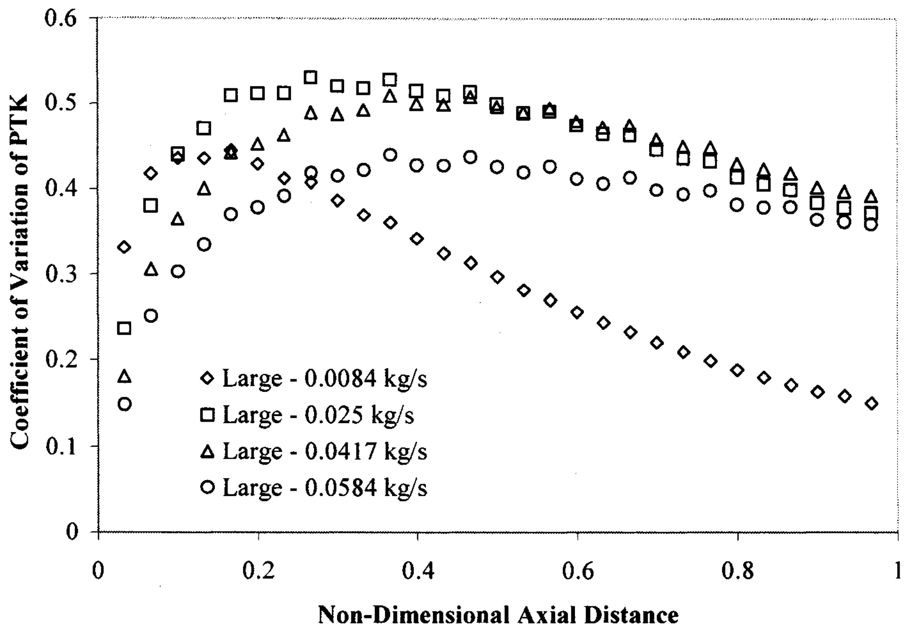

Figure 8.11: Coefficient of variation of the proportion of thermal kill (PTK) along the length of the heat exchanger for the annulus. Fluid is being heated and the mass flow rates in the annulus and the inner tube are the same (large tube).

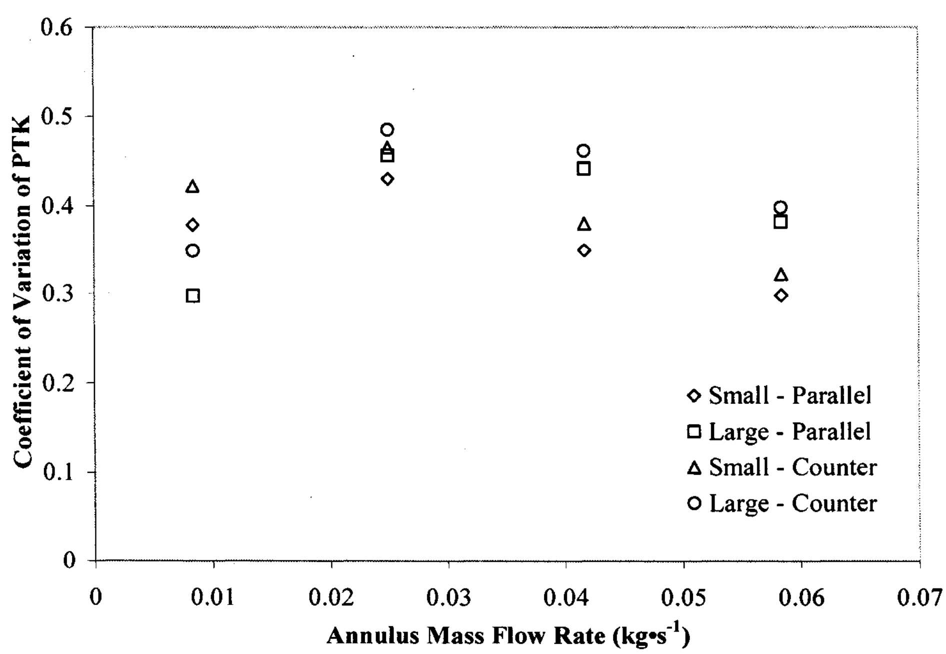

Figure 8.12: Coefficient of variation of the proportion of thermal kill (PTK) versus the mass flow rate in the annulus. Flow rates in the annulus are the same as in the inner tube; fluid is being heated (parallel and counterflow are compared).

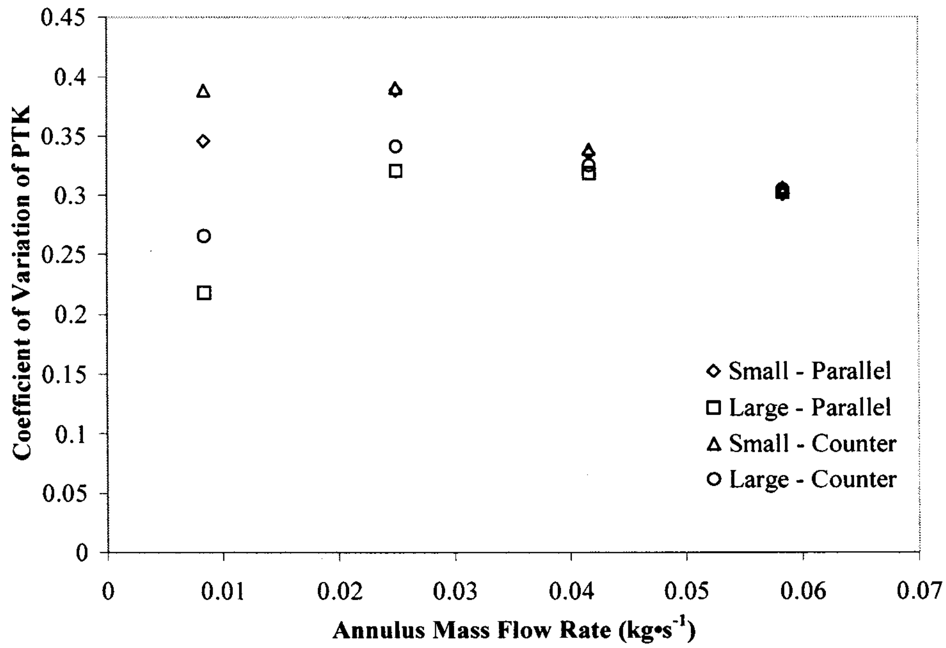

Figure 8.13: Coefficient of variation of the proportion of thermal kill (PTK) versus the mass flow rate in the annulus. Flow rates in the annulus are the same as in the inner tube; fluid is being cooled (parallel and counterflow are compared).

Figures 8.12 and 8.13 show the average coefficient of variation of the PTK versus the annulus mass flow rate for heating and cooling, respectively. The flow rates in the annulus and in the inner tube are equal in all cases. In the case of heating, the configuration of the flow and the mass flow rates have an effect on the heating uniformity. For the most part, increasing the annulus mass flow rate decreases the *CV* of the PTK. The exception to this is with the lowest flow rate. It is expected that this is because with the low flow rate, the residence time in the tube is long enough that the outlet temperature at the end of one turn is close to its equilibrium value, so the temperature profile is quite flat. This is not quite the case with the counterflow, which does not come close to equilibrium. Thus the uniformity is not as good in the counterflow configuration. This is seen for both the heating and cooling situations.

8.5.6 Holding tube uniformity

The holding tube portion of an aseptic process is the most important section. This is where the liquid food has reached the target temperature and is held until the required thermal treatment is achieved. In this section, the temperature should remain constant, and the uniformity of the thermal treatment should be dependent only on the velocity distribution, with plug flow being ideal. The proportion of thermal kill in the holding tube was also simulated for all the different flow rate combinations that were used in the above analysis. In these cases, the thermal kill in the inner tube was independent of the flow conditions in the annulus, and vice versa, since a uniform temperature was used throughout the heat exchanger. Furthermore, the coefficients of variation of the PTK were independent of the temperature used. These values of the coefficients are the expected equilibrium values that the heating and cooling cases are expected to reach once temperature uniformity is established. Table 8.5 shows the coefficient of variation of the PTK for the inner tube and the annulus. For the inner tube there is increased uniformity as the mass flow rate is increased. The following correlations were developed for the coefficient of variation as a function of the Reynolds number for the large and small tubes, respectively:

$$CV = -0.0261\ln(\mathrm{Re}) + 0.2435 \qquad R^2 = 0.996 \qquad (8.11)$$

$$CV = -0.0306\ln(\mathrm{Re}) + 0.268 \qquad R^2 = 0.999 \qquad (8.12)$$

For the annulus, there is very little effect of mass flow rate on the uniformity. Furthermore, the difference in the tube diameter does not have a very strong effect on the coefficient of variation.

Table 8.5: Coefficient of variation of PTK for inner tube and annulus as holding tubes.

Mass Flow Rate ($kg \cdot s^{-1}$)	Coefficient of Variation of the PTK: Inner, Small tube	Inner, Large tube	Annulus, Small tube	Annulus, Large tube
0.0084	0.087	0.100	0.078	0.084
0.0250	0.053	0.074	0.076	0.083
0.0427	0.038	0.058	0.076	0.081
0.0584	0.027	0.049	0.076	0.078

8.5.7 Industrial importance and consequences

For aseptic heat treatment operations, the objective is to provide the necessary sterility to the particles/fluid which undergoes the least sterility. In general, the narrowing of the residence time distribution is the first step in providing a sterile product that has the most uniform product quality (Liu and Zuritz, 1995). This work shows that the uniformity of the residence time in the inner tube increases with an increasing flow rate and a lower radius of curvature. However, this advantage is in opposition to the required pressure drop to obtain the desired flow rate, as the pressure drop increases with increasing flow rate and curvature (Berger et al., 1983). Increasing the Reynolds number results in a more uniform lethality, and the differences between counterflow and parallel flow configurations decrease. Thus, in general, as long as the pressure drop is not too large, it is better for both the heat transfer rate and the heating uniformity. Furthermore, the inner tube is ideal for cooling, as there seems to be more uniformity in the thermal kill than when heating. The inner tube seems to be a better choice for the heating/holding/cooling operations than the annulus, as increasing the flow rate in the inner tube can drastically increase the uniformity of the thermal process. The annulus, however, does not respond as well to changes in the mass flow rates. For the holding section, changing the mass flow rates had very little effect on the uniformity. This, however, may be very different if the heat transfer was occurring on both walls of the annulus, allowing heat to penetrate the center from both sides.

Flow rates in the annulus have significant effects on the uniformity of the proportion of thermal kill in the inner tube. There is a trade off between higher heat transfer rates and uniformity in this case. Furthermore, increased annulus flow rates result in great pressure drops.

8.6 Conclusions

The residence time distribution, temperature distribution, and heating uniformity were determined numerically for a double-pipe helical heat exchanger. Residence times were calculated along with the coefficient of variation of the residence time. The uniformity of the residence times increased with increasing flow rate in the inner tube. The uniformity was better in the smaller tube than the larger tube for the same mass flow rate. In the annulus, the uniformity was better for the larger tube than the smaller tube; in other words, more uniform for a smaller gap size.

Temperature distributions in the inner tube were much more uniform in the smaller tube than the large tube at the same mass flow rate, and became more uniform with increasing flow rate. The uniformity, however, was affected by the mass flow rate in the annulus, with large flow rates resulting in less uniformity. Parallel flow versus counterflow did not produce any significant differences in the temperature uniformity in the inner tube. The uniformity of the temperature distribution in the annulus was affected by the annulus mass flow rate, the inner tube flow rate and the size of the tube. Uniformity tended to increase as the mass flow rate in the annulus was increased. Increasing the flow rate in the inner tube tended to decrease the uniformity.

Heating uniformity in the inner tube tended to increase with increasing mass flow rate in the inner tube. The differences between parallel flow and counterflow became negligible with increased flow rates. Cooling processes had much more uniformity than the heating processes. However, in the annulus, the heating/cooling processes did not show any predictable trends in the uniformity. The heating uniformity in the inner tube for a holding operation increased with increasing flow rates, but remained fairly constant for the annulus.

8.7 Acknowledgements

The authors are grateful to FCAR (Fonds pour la Formation de Chercheurs et l'Aide à la Recherche) and NSERC (Natural Sciences and Engineering Research Council of Canada) for the financial assistance for this study. The authors also thank Peter Alvo, posthumously, for his insight and discussions of the topic.

8.8 Nomenclature

A	Area (m^2)
CV	Coefficient of variation

d	Inner diameter of inner tube (m)
D	Diameter of annulus (m)
DRT	Decimal reduction time (s)
$E(t)$	Residence time distribution function (s^{-1})
L	Length (m)
N	Population
PTK	Proportion of thermal kill
Q	Volumetric flow rate ($m^3 \cdot s^{-1}$)
R	Radius of curvature (m)
Re	Reynolds number
t	Time (s)
T	Temperature (°C)
v	Average velocity ($m \cdot s^{-1}$)
Vol	Volume (m^3)
z	Thermal resistance constant (°C)
λ	Proportion of surviving microorganisms
σ^2	Second moment about the mean
τ	Residence time (s)

subscripts

i	Inner
loc	Local
m	Mean
o	Initial/Outer
ref	Reference
x	Cross-section

8.9 References

Anderson, W. A., P. J. McClure, A. C. Baird-Parker, and M. B. Cole. 1996. The application of a log-logistic model to describe the thermal inactivation of *Clostridium* *botulinum* 213B at temperatures below 121.°C. *Journal of Applied Bacteriology*, Vol. 80:283-290.

Berger, S. A., L. Talbot, and L. S. Yao. 1983. Flow in curved pipes. *Annual Review of Fluid Mechanics*, Vol. 15:461-512.

Dignan, D. M., M. R. Berry, I. J. Pflug, and T. D. Gardine. 1989. Safety considerations in establishing aseptic processes for low-acid foods containing particulates. *Food Technology*, Vol. 43(3):118-121, 131.

Heldman, D. R. 1989. Establishing aseptic thermal processes for low-acid foods containing particulates. *Food Technology*, Vol. 43(3):122-123, 131.

Heppell, N. J. 1985. Comparison of the residence time distributions of water and milk in an experimental UHT sterilizer. *Journal of Food Engineering*, Vol. 4:71-84.

Janssen, P. W. M. 1994. Measurement of residence time distribution of processing plant using a cross correlation technique. *Journal of Food Engineering*, Vol. 21:215-223.

Kelder, J. D. H., K. J. Ptasinski, and P. J. A. M. Kerkhof. 2002. Power-law foods in continuous coiled sterilizers. *Chemical Engineering Science*, Vol. 57:4605-4615.

Kelder, J. D. H., K. J. Ptasinski, and P. J. A. M. Kerkhof. 2004. Starch gelatinization in coiled heaters. *Biotechnol. Prog.*, Vol. 20:921-929.

Koutsky, J. A. and R. L. Adler. 1964. Minimization of axial dispersion by use of secondary flow in helical tubes. *The Canadian Journal of Chemical Engineering*, Vol. 42:239-245.

Liao, H-J., M. A. Rao, and A. K. Datta. 2000. Role of thermo-rheological behaviour in simulation of continuous sterilization of a starch dispersion. *IChemE Transactions Part C – Food and Bioproducts Processing*, Vol. 78(C1):48-56.

Liu, Y. and C. A. Zuritz. 1995. Mathematical modeling of particulate two-phase flow in a helical coil. *Journal of Food Engineering*, Vol. 18:321-341.

Prabhanjan, D. G., G. S. V. Raghavan, and T. J. Rennie. 2002. Comparison of heat transfer rates between a straight tube heat exchanger and a helically coiled heat exchanger. *International Communications in Heat and Mass Transfer*, Vol. 29(2):185-191.

Ramaswamy, H. S., K. A. Abdelrahim, B. K. Simpson, and J. P. Smith. 1995. Residence time distribution (RTD) in aseptic processing of particulate foods: a review. *Food Research International*, Vol. 28(3):291-310.

Ruthven, D. M. 1971. The residence time distribution for ideal laminar flow in a helical tube. *Chemical Engineering Science*, Vol. 26(7):1113-1121.

Salengke, S. and S. K. Sastry. 1994. Residence time distribution of cylindrical particles in a curved section of a holding tube: the effect of particle size and flow rate. *Journal of Food Process Engineering*, Vol. 18:363-381.

Salengke, S. and S. K. Sastry. 1996. Residence time distribution of cylindrical particles in a curved section of a holding tube: the effect of particle concentration and bend radius of curvature. *Journal of Food Engineering*, Vol. 27:159-176.

Sancho, M. F. and M. A. Rao. 1992. Residence time distribution in a holding tube. *Journal of Food Engineering*, Vol. 15:1-19.

Sandeep, K. P., C. A. Zuritz, and V. M. Puri. 1997. Residence time distribution of particles during two-phase non-Newtonian flow in conventional as compared with helical holding tubes. *Journal of Food Science*, Vol. 62(4):647-652.

Simpson, S. G. and M. C. Williams. 1974. An analysis of high temperature/short time sterilization during laminar flow. *Journal of Food Science*, Vol. 39:1047-1054.

Singh, R. P. and D. R. Heldman. 1993. *Introduction to Food Engineering, second edition.* Academic Press, Inc., San Diego, CA, 499 pp.

Son, S. M. and R. K. Singh. 2002. Turbulence modeling and verification for aseptically processed soybean milk under turbulent flow conditions. *Journal of Food Engineering*, Vol. 52:177-184.

GENERAL SUMMARY AND CONCLUSIONS

9.1 General Summary and Conclusions

The purpose of this study was to investigate the heat transfer and fluid flow characteristics of a double-pipe helical heat exchanger. The majority of the work was done numerically, using a commercial computational fluid dynamics package. A physical model of the heat exchanger was built and tested. In both the numerical and the experimental work, different coil sizes were used, along with comparisons of parallel flow and counterflow, over a wide range of the laminar flow regime.

The numerical work was carried out using two differently sized heat exchangers. Both used the same outer tube geometry, but the inner tube size was varied. Simulations were performed using different flow rates in the inner tube and in the annulus. Validation of the model was performed with the boundary conditions of constant wall temperature and constant heat flux. The results of the inner Nusselt number from these trials were compared to literature data and showed a reasonable fit. Overall heat transfer coefficients were calculated, along with inner and annulus Nusselt numbers for both parallel flow and counterflow configurations. Correlations for the annulus Nusselt number were made using a modified Dean number. The Nusselt numbers in the inner tube were not very different from the ones with the constant heat flux and the constant wall temperature, indicating that existing correlations for these two boundary conditions can be used with negligible error in calculating the inner Nusselt number. Thermal resistances were calculated and indicated that the limiting factor for heat transfer was the resistance in the annulus, which could be reduced by increasing the inner tube diameter and increasing the flow rate in the annulus.

Two physical double-pipe helical heat exchangers were built and instrumented to study the heat transfer characteristics. The difference between the two heat exchangers was the size of the inner tube. The size of the outer tube was the same for both. Several mass flow rates were tested (laminar regime) for both parallel flow and counterflow configurations. There were little difference between the overall heat transfer coefficients for parallel flow and counterflow, as expected. Inner and outer heat transfer coefficients were determined using Wilson plots. The inner Nusselt number was comparable to literature data. The annulus Nusselt number was compared to the data in the numerical study. The data for the small tube diverged from the numerical, but was attributed to the nature of the Wilson plots. Furthermore, the developing flow between the numerical and the experimental trials was quite different, and may have affected the heat transfer coefficients.

The effects of fluid thermal properties on the heat transfer characteristics were studied numerically. Different Prandtl numbers were used by varying the thermal conductivity of the fluid in both the inner tube and in the annulus. The Nusselt number was much more sensitive to these changes at low Dean numbers, but rather insensitive at high Dean numbers. These differences were attributed to the difference in the developing thermal and hydrodynamic boundary layers. Thermally dependent thermal conductivities were also studied. The results correlated well with a modified Graetz number, which took the curvature ratio into consideration. Parallel flow and counterflow were studied with the thermally dependent thermal properties to see if there would be any effects. However, no effects were detected.

The effects of viscosity on the heat transfer and pressure drop characteristics in the heat exchanger were studied numerically. This was done in two sections, the first consisting of thermally dependent viscosities and the second on non-Newtonian fluids. Several thermally dependent viscosities were tested that covered the range expected in food processing applications. Thermally dependent viscosities had little effect on the Nusselt number, however, there were significant effects on the pressure drop in the heat exchanger. It was also shown that changing the velocity in either the inner tube or the annulus affected the pressure drop in the other section, as the average temperature, and hence the average viscosity was affected. Simulations were performed using non-Newtonian fluids with a power law relationship between the shear stress and the shear strain. The Nusselt numbers were calculated and correlated with the Péclet number and curvature ratio.

The residence time distribution, temperature distribution, and the heating uniformity were determined numerically for the heat exchanger, for both parallel flow and counterflow configurations. The uniformity of the residence time was shown to increase with increased flow rates in the inner tube. The smaller gap size in the annulus had better residence time uniformity than the large gap size. Temperature distributions in the inner tube were effected by the mass flow rate in the annulus, as this changed the rate of heat transfer. In both the inner tube and in the annulus, increasing the mass flow rate decreased the temperature uniformity in the other section. The heating uniformity was estimated by using thermal kill model for microorganisms. The use of this model was to give some insight into the heating/cooling uniformity, and was not intended to model real microorganisms. There were differences in heating uniformity when comparing parallel flow to counterflow, though these decreases with increasing flow rates. The cooling process was more uniform than the heating process for the inner tube. This was due to the difference when combing the temperature distribution with the velocity distribution. The uniformity in a holding tube was also studied, where the temperature was constant. In this case the heating uniformity increased with increasing flow rates in the inner tube; however the uniformity was fairly constant in the annulus, regardless of the flow rate.

9.2 Contributions to Knowledge

The work presented here provides original contribution to the body of knowledge concerning the heat transfer and the hydrodynamic characteristics of a double-pipe helical heat exchanger. The main contributions are as follows:

1. Nusselt numbers in the inner tube were determined to be negligibly different from Nusselt numbers from literature data, indicating that there are relatively small differences due to the boundary conditions.
2. Nusselt number correlations for the annulus were determined. These will provide important design information for double-pipe helical heat exchangers.
3. A method to estimate the heating uniformity was developed. This was used to estimate the heating uniformity in the annulus and the inner tube for both parallel flow and counterflow configurations, and for heating/holding/cooling operations. The results are useful for the food processing industry to aid in determining the optimum configuration and size of a double-pipe helical heat exchanger to maximize product quality and thermal efficiency.

Several sub-contributions can be identified in this research. The overall heat transfer coefficients were determined both numerically and experimentally for a double-pipe helical heat exchanger. It was shown that the large tube size increased heat transfer rates. The effects of viscosity (thermally dependent and non-Newtonian) on heat transfer and pressure drop were studied. These effects are common in food processing and the results presented here should provide useful insight into the design of double-pipe helical heat exchangers for food processing applications, as well as in other fields. Furthermore, the effects of the Prandtl number (by varying the thermal conductivity) and thermally dependent thermal conductivity on heat transfer characteristics were determined. Implications of these effects were discussed in the relevant chapter. A final contribution was the investigation of the residence time and temperature distributions for the inner tube and the annulus as well as for both parallel flow and counterflow configurations of the heat exchanger.

9.3 Recommendations for Further Research

The work presented in this thesis provides the foundation of the heat transfer and hydrodynamic characteristics of a double-pipe helical heat exchanger. There are several areas where further research is required:

The effects of Prandtl number should be further studied by taking into consideration changes in the other properties that compose the Prandtl number, other than the thermal conductivity. It would be beneficial if the Prandtl number in one section of the heat exchanger could be kept constant while the other is changing, to simplify the investigation. This also applies to the thermally dependent properties and the non-Newtonian flow.

The ratios of the inner tube diameter to the outer tube diameter should be studied more extensively. This work showed that the larger size of the two used was better for heat transfer rates; however, further investigation needs to be performed to determine the heat transfer coefficients for any tube ratio, as well as the pressure drop at any tube ratio.

The method used to determine the heating uniformity should be experimentally tested and to the quality of processed foods using different heat exchanger configurations and dimensions should be studied. Furthermore, research into heating liquid foods with particles in double-pipe helical heat exchangers is needed. Some work has been performed in helical coils for this, but not in the type of heat exchanger in this study.

GENERAL REFERENCES

Abdalla, M. A. 1994. A four-region, moving-boundary model of a once through, helical-coil steam generator. *Annals of Nuclear Energy*, Vol. 21(9):541-562.

Acharya, N., Sen, M., and H. C. Chang. 1992. Heat transfer enhancement in coiled tubes by chaotic mixing. *International Journal of Heat and Mass Transfer*, Vol. 35(10):2475-2489.

Acharya, N., Sen, M., and H. C. Chang. 1993. Thermal entrance length and Nusselt numbers in coiled tubes. *International Journal of Heat and Mass Transfer*, Vol. 37(2):336-340.

Acharya, N., Sen, M., and H. C. Chang. 2001. Analysis of heat transfer enhancement in coiled-tube heat exchangers. *International Journal of Heat and Mass Transfer*, Vol. 44: 3189-3199.

Ahn, S. W. 2000. Prediction of turbulent heat transfer in concentric annuli with outer rough wall. *International Communications in Heat and Mass Transfer*, Vol. 27(5):677-688.

Akagawa, K., T. Sakaguchi, and M. Ueda. 1971. Study on a gas-liquid two-phase flow in helically coiled tubes. *Bulletin of the JSME*, Vol. 14(72):564-571.

Akiyama, M. and K. C. Cheng. 1971. Boundary vorticity method for laminar forced convection heat transfer in curved pipes. *International Journal of Heat and Mass Transfer*, Vol. 14:1659-1975.

Akiyama, M. and K. C. Cheng. 1972. Laminar forced convection heat transfer in curved pipes with uniform wall temperature. *International Journal of Heat and Mass Transfer*, Vol. 15:1426-1431.

Akiyama, M. and K. C. Cheng. 1974a. Laminar forced convection in the thermal entrance region of curved pipes with uniform wall temperature. *The Canadian Journal of Chemical Engineering*, Vol. 52:234-240.

Akiyama, M. and K. C. Cheng. 1974b. Graetz problem in curved pipes with uniform wall heat flux. *Applied Science* Research, Vol. 29:401-418.

Ali, M. E. 1994. Experimental investigation of natural convection from vertical helical coiled tubes. *International Journal of Heat and Mass Transfer*, Vol. 37, No. 4:665-671.

Ali, M. E. 1998. Laminar natural convection from constant heat flux helical coiled tubes. *International Journal of Heat and Mass Transfer*, Vol. 41, No. 14:2175-2182.

Ali, S. 2001. Pressure drop correlations for flow through regular helical coil tubes. *Fluid Dynamics Research*, Vol. 28:295-310.

Allen, P. L. and O. J. Ajele. 1994. Optimum configuration of natural convection shell-and-coil heat exchanger with respect to thermal performance. *Proceedings of the 1994 Annual Conference, June 27-30, San Jose, California, American Solar Energy Society*, 292-297.

Anderson, W. A., P. J. McClure, A. C. Baird-Parker, and M. B. Cole. 1996. The application of a log-logistic model to describe the thermal inactivation of *Clostridium botulinum* 213B at temperatures below 121.°C. *Journal of Applied Bacteriology*, Vol. 80:283-290.

Anwer, M., R. and M. C. So. 1993. Swirling turbulent flow through a curved pipe. Part I: Effect of swirl and bend curvature. *Experiments in Fluids*, Vol. 14:85-96.

Anwer, M., R. M. C. So and Y. G. Lai. 1989. Perturbation by and recovery from bend curvature of a fully developed turbulent pipe flow. *Physics of Fluids A* Vol. 1(8):1387-1397.

ASHRAE. 1998. Ch. 8: Thermal Properties of Foods. In: *Refrigeration Handbook*, American Society of Heating, Refrigeration and Air-Conditioning Engineers, Inc., Atlanta, GA.

Austin, L. R. and J. D. Seader. 1973. Fully developed viscous flow in coiled circular pipes. *AIChE Journal*, Vol. 19(1): 85-94.

Austin, L. R. and J. D. Seader. 1974. Entry region for steady viscous flow in coiled circular pipes. *AIChE Journal*, Vol. 20: 820-822.

Austen, D. S., and H. M. Soliman. 1988. Laminar flow and heat transfer in helically coiled tubes with substantial pitch. *Experimental Thermal and Fluid Science*, Vol. 1:183-194.

Awwad, A., R. C. Xin, Z. F. Dong, M. A. Ebadian, and H. M. Soliman. 1995. Measurement and correlation of the pressure drop in air-water two-phase flow in horizontal helicoidal pipes. *International Journal of Multiphase Flow*, Vol. 21(4):607-619.

Bai, B., L. Guo, Z. Feng, and X. Chen. 1999. Turbulent heat transfer in a horizontally coiled tube. *Heat Transfer-Asian Research*, Vol. 28(5):395-403.

Barnes, H. A. and K. Walters. 1969. On the flow of viscous and elastico-viscous liquids through straight and curved pipes. *Proc. R. Soc. London Ser. A* 315:85-109.

Barua, S. N. 1962. On secondary flow in stationary curved pipes. *Quarterly Journal of Mechanics and Applied Mathematics*, Vol. XVI:61-77.

Berg, R. R. and C. F. Bonilla. 1950. *Trans. N. Y. Acad. Sci.* Vol. 13:12 (as cited in Kubair and Kuloor, 1966).

Berger, S. A., Talbot, L., and L. S. Yao. 1983. Flow in curved pipes. *Ann. Rev. Fluid Mech.*, Vol. 15:461-512.

Berthoud, G. and S. Jayanti. 1990. Characterization of dryout in helical coils. *International Journal of Heat and Mass Transfer*, Vol. 33(7):1451-1463.

Boersma, B. J. and F. T. M. Nieuwstadt. 1996. Large-eddy simulation of turbulent flow in a curved pipe. *International Journal of Fluid Engineering, Transactions of the ASME*, Vol. 118(2):248-254.

Bolinder, C. J. and B. Sunden. 1996. Numerical prediction of laminar flow and forced convective heat transfer in a helical square duct with finite pitch. *International Journal of Heat and Mass Transfer*, Vol. 39(15):3101-3115.

Briggs, D. E. and E. H. Young. 1969. Modified Wilson plot techniques for obtaining heat transfer correlations for shell and tube heat exchangers. *Chem. Eng. Prog. Symp. Ser.* Vol. 65:35-45.

Castelain, C., Mokrani, A., Legentilhomme, P., and H. Peerhossaini. 1997. Residence time distribution in twisted pipe flows: helically coiled system and chaotic system. *Experiments in Fluids*, Vol. 22:359-368.

Chagny, C., C. Castelain, and H. Peerhossaini. 2000. Chaotic heat transfer for heat exchanger design and comparison with a regular regime for a large range of Reynolds numbers. *Applied Thermal Engineering*, Vol. 20:1615-1648.

Chandratilleke, T. T. and Nursubyakto. 2003. Numerical prediction of secondary flow and convective heat transfer in externally heated curved rectangular ducts. *International Journal of Thermal Sciences*, Vol. 42:187-198.

Chen, X. and L. Guo. 1999. Flow patterns and pressure drop in oil-air-water three-phase flow through helically coiled tubes. *International Journal of Multiphase Flow*, Vol. 25:1053-1072.

Choi, H. K. and S. O. Park. 1992. Laminar entrance flow in curved annular ducts. *International Journal of Heat and Fluid Flow*, Vol. 13(1):41-49.

Choi, H. K. and S. O. Park. 1994. Mixed convection flow in curved annular ducts. *International Journal of Heat and Mass Transfer*, Vol. 37(17):2761-2769.

Chopey, N. P. and T. G. Hicks. 1984. *Handbook of Chemical Engineering Calculations*. McGraw-Hill Book Company, NY (as cited in Sahoo et al., 2003).

Chung, J. H. and J. M. Hyun. 1994. Heat transfer from a fully-developed pulsating flow in a curved pipe. *International Journal of Heat and Mass Transfer*, Vol. 37(1):43-52.

Cumo, M., G. E. Farello, and G. Ferrari. 1972. The influence of curvature in post dry-out heat transfer. *International Journal of Heat and Mass Transfer*, Vol. 15:2045-2062.

Czop, V., D. Barbier, and S. Dong. 1994. Pressure drop, void fraction and shear stress measurements in an adiabatic two-phase flow in a coiled tube. *Nuclear Engineering and Design*, Vol. 149:323-333.

Dean, W. R. 1927. Note on the motion of fluid in a curved pipe. *Philosophical Magazine*, Series 7, Vol. 4(20):208-23

Dean, W. R. 1928. The streamline motion of fluid in a curved pipe. *Philosophical Magazine*, Series 7, Vol. 5(30):673-95

Dennis, S. C. R. and M. Ng. 1982. Dual solutions for steady laminar flow through a curved tube. *Quarterly Journal of Mechanics and Applied Mathematics*, Vol. 35(3):305-324.

Dennis, S. C. R. and N. Riley. 1991. On the fully developed flow in a curved pipe at large Dean number. *Proc. R. Soc. London Ser. A* 434(1891):473-478.

Dignan, D. M., M. R. Berry, I. J. Pflug, and T. D. Gardine. 1989. Safety considerations in establishing aseptic processes for low-acid foods containing particulates. *Food Technology*, Vol. 43(3):118-121, 131.

Downing, R. S., and G. Kojaysoy. 2002. Single and two-phase pressure drop characteristics in miniature helical channels. *Experimental Thermal and Fluid Science*, Vol. 26:535-546.

Dravid, A. N., K. A. Smith, E. W. Merrill, and P. L. T. Brian. 1971. Effect of Secondary fluid motion on laminar flow heat transfer in helically coiled tubes. *AIChE Journal*, Vol. 17(5):1114-1122.

Eagles, P. M. 2003. On the evolution of the time-dependent localized disturbances to Dean flow in a channel with slowly varying curvature and Gap width. *Quarterly Journal of Mechanics and Applied Mathematics*, Vol. 56(1):93-104.

Eason, R. M., Y. Bayazitoglu, and A. Meade. 1994. Enhancement of heat transfer in square helical ducts. *International Journal of Heat and Mass Transfer*, Vol. 37(14):2077-2087.

Eustice, J. 1910. Flow of water in curved pipes. *Proc. R. Soc. London Ser. A* 84:107-18

Eustice, J. 1911. Experiments of streamline motion in curved pipes. *Proc. R. Soc. London Ser. A* 85:119-31.

Fan, Y., R. I. Tanner, and N. Phan-Thien. 2001. Fully developed viscous and viscoelastic flows in curved pipes. *Journal of Fluid Mechanics*, Vol. 440:327-357.

Fernández-Seara, J., J. Sieres, and M. Vazquez. 2003. Heat and mass transfer analysis of a helical coil rectifier in an ammonia-water absorption system. *International Journal of Thermal Sciences*, Vol. 42:783-794.

Fleming, W. H., J. A. Khan, and C. A. Rhodes. 2001. Effective heat transfer in a metal-hydride-based hydrogen separation process. *International Journal of Hydrogen Energy*, Vol. 26:711-724.

Futagami, K. and Y. Aoyama. 1988. Laminar heat transfer in a helically coiled tube. *International Journal of Heat and Mass Transfer*, Vol. 31(2):387-396.

Galier, S., S. Issanchou, P. Moulin, M. J. Clifton, and P. Aptel. 2003. Electrochemical measurement of velocity gradient at the wall of a helical tube. *AIChE Journal*, Vol. 49(8):1972-1979.

Gammack, D. and P. E. Hydon. 2001. Flow in pipes with non-uniform curvature and torsion. *Journal of Fluid Mechanics*, Vol. 433:357-382.

Gao, H., Guo, L., and X. Zhang. 2002. Liquid-solid separation phenomena of two-phase turbulent flow in curved pipes. *International Journal of Heat and Mass Transfer*, 45:4995-5005.

Genssle, A. and K. Stephan. 2000. Analysis of the process characteristics of an absorption heat transformer with compact heat exchangers and the mixture TFE-E181. *International Journal of Thermal Sciences*, Vol. 39:30-38.

Germano, M. 1982. On the effect of torsion on a helical pipe flow. *Journal of Fluid Mechanics*, Vol. 125:1-8.

Germano, M. 1989. The Dean equations extend to a helical pipe flow. *Journal of Fluid Mechanics*, Vol. 203:289-305.

Goering, D. J., J. A. C. Humphrey, and R. Greif. 1997. The dual influence of curvature and buoyancy in fully developed tube flows. *International Journal of Heat and Mass Transfer*, Vol. 40(9):2187-2199.

Grabowski, S. and H. S. Ramaswamy. 1998. Bend-effects on the residence time distribution of solid food particles in a holding tube. *Canadian Agricultural Engineering*, Vol. 40(2):121-126.

Guo, L., Chen, X., Feng, Z., and B. Bai. 1998. Transient convective heat transfer in a helical coiled tube with pulsatile fully developed turbulent flow. *International Journal of Heat and Mass Transfer*, Vol. 41:2867-2875.

Guo, L., Feng, Z., and X. Chen. 2001a. An experimental investigation of the frictional pressure drop of steam-water two-phase flow in helical coils. *International Journal of Heat and Mass Transfer*, Vol. 44:2601-2610.

Guo, L., Feng, Z., and X. Chen. 2001b. Pressure drop oscillations of steam-water two-phase flow in helically coiled tube. *International Journal of Heat and Mass Transfer*, Vol. 44:1555-1564.

Guo, L., Z. Feng, and X. Chen. 2002. Transient convective heat transfer of steam-water two-phase flow in a helical tube under pressure drop type oscillations. *International Journal of Heat and Mass Transfer*, Vol. 45:533-542.

Grindley, J. H. and A. H. Gibson. 1908. On the frictional resistance of air through a pipe. *Proc. R. Soc. London Ser. A* 80:114-39.

Grundmann, R. 1985. Friction diagram of the helically coiled tube. *Chemical Engineering Process*, Vol. 19:113-115.

Hameed, M. S. and M. S. Muhammed. 2003. Mass transfer into liquid falling tubes in straight and helically coiled tubes. *International Journal of Heat and Mass Transfer*, Vol. 46:1715-1724.

Haraburda, S. 1995. Consider helical-coil heat exchangers. *Chemical Engineering*, Vol. 102(7):149-151.

Hart, J., J. Ellenberger, and P. J. Hamersma. 1988. Single and two-phase flow through helically coiled tubes. *Chemical Engineering Science*, Vol. 45(4):775-783.

Havas, G., A. Deak, and J. Sawinsky. 1987. Heat transfer to helical coils in agitated vessels. *The Chemical Engineering Journal*, Vol. 35:61-64.

Hawthorne, W. R. 1951. Secondary circulation in fluid flow. *Proceedings of the Royal Society of London, Series A, Mathematical and Physical Sciences*, Vol. 206(1086):374-387.

Heldman, D. R. 1989. Establishing aseptic thermal processes for low-acid foods containing particulates. *Food Technology*, Vol. 43(3):122-123, 131.

Heppell, N. J. 1985. Comparison of the residence time distributions of water and milk in an experimental UHT sterilizer. *Journal of Food Engineering*, Vol. 4:71-84.

Hon, R., J. A. C. Humphrey and F. Champagne. 1999. Transition to turbulence of the flow in a straight pipe downstream of a helical coil. *Physics of Fluids*, Vol. 11(10):2993-3002.

Horlock, J. H. 1956. Some experiments on the secondary flow in pipe bends. *Proceedings of the Royal Society of London, Series A, Mathematical and Physical Sciences*, Vol. 234(1198):335-346.

Hüttl, T. J., and R Friedrich. 2000. Influence of curvature and torsion on turbulent flow in helically coiled pipes. *International Journal of Heat and Fluid Flow*, Vol. 21(3):345-353

Hüttl, T. J., and R Friedrich. 2001. Direct numerical simulation of turbulent flows in curved and helically coiled pipes. *Computers and Fluids*, Vol. 30:591-605.

Hsu, C. F. and S. V. Patankar. 1982. Analysis of laminar non-Newtonian flow and heat transfer in curved tubes. *AIChE Journal*, Vol. 28(4):610-616.

Inagaki, Y., Koiso, H., Takumi, H., Ioka, I., and Y. Miyamoto. 1998. Thermal hydraulic study on a high-temperature gas-gas heat exchanger with helically coiled tube bundles. *Nuclear Engineering and Design*, Vol. 185:141-151.

Ito, H. 1959. Friction factors for turbulent flow in curved pipes. *Journal of Basic Engineering, Transactions of the ASME*, Vol. 81:123-134.

Jeschke, D. 1925. Heat transfer and pressure loss in coiled pipes. *Ergaenzungsheft Z. Ver. Disch. Ing.*, Vol. 68:24-28.

Janssen, L. A. M. 1976. Axial dispersion in laminar flow through coiled tubes. *Chemical Engineering Science*, Vol. 31:215-218.

Janssen, L. A. M. and C. J. Hoogendoorn. 1978. Laminar convective heat transfer in helical coiled tubes. *International Journal of Heat and Mass Transfer*, Vol. 21: 1197-1206.

Janssen, P. W. M. 1994. Measurement of residence time distribution of processing plant using a cross correlation technique. *Journal of Food Engineering*, Vol. 21:215-223.

Jayanti, S. and G. F. Hewitt. 1991. On the Paradox concerning friction factor ratio in laminar flow in coils. *Proceedings: Mathematical and Physical Sciences*, Vol. 432(1885):291-299.

Jensen, M. K. and A. E. Bergles. 1982. Critical heat flux in helical coils with a circumferential heat flux tilt toward the outside surface. *International Journal of Heat and Mass Transfer*, Vol. 25(9):1383-1395.

Jha, R. K. and M. R. Rao. 1967. Heat transfer through coiled tubes in agitated vessels. *International Journal of Heat and Mass Transfer*, Vol. 10:395-397.

Johnson, M. and R. D. Kamm. 1986. Numerical studies of steady flow dispersion at low Dean number in a gently curving tube. *Journal of Fluid Mechanics*, Vol. 172:329-345.

Jones, J. R. 1960. Flow of a non-Newtonian liquid in a curved pipe. *Quarterly Journal of Mechanics and Applied Mathematics*, Vol. 13(4):428-443.

Jones, S. W., O. M. Thomas, and H. Aref. 1989. Chaotic advection by laminar flow in a twisted pipe. *Journal of Fluid Mechanics*, Vol. 209:335-357.

Joseph, B., and R. J. Adler. 1975. Numerical treatment of laminar flow in helically coiled tubes of square cross section – Part II. Oscillating helically coiled tubes. *AIChE Journal*, Vol. 21(5):974-979.

Joseph, B., Smith, E. P., and R. J. Adler. 1975. Numerical treatment of laminar flow in helically coiled tubes of square cross section – Part I. Stationary helically coiled tubes. *AIChE Journal*, Vol. 21(5):965-974.

Kaji, M., K. Mori, S. Nakanishi, K. Hirabayashi and M. Ohishi. 1995. Dryout and wall-temperature fluctuations in helically coiled evaporating tubes. *Heat Transfer – Japanese Research*, Vol. 24(3):239-254.

Kalb, C. E. and J. D. Seader. 1972. Heat and mass transfer phenomena for viscous flow in curved circular tubes. *International Journal of Heat and Mass Transfer*, Vol. 15:801-817.

Kalb, C. E. and J. D. Seader. 1974. Fully developed viscous-flow heat transfer in curved circular tubes with uniform wall temperature. *AIChE Journal*, Vol. 20(2):340-346.

Kalb, C. E. and J. D. Seader. 1983. Entrance region heat transfer in a uniform wall-temperature helical coil with transition from turbulent to laminar flow. *International Journal of Heat and Mass Transfer*, Vol. 26(1):23-32.

Kapur, J. N., V. P. Tyagi, and R. C. Srivastava. 1964. Streamline flow through a curved annulus. *Applied Sciene Research*, Vol. 14:253-267.

Kao, H. C. 1987. Torsion effect on fully developed flow in a helical pipe. *Journal of Fluid Mechanics*, Vol. 184: 335-356.

Karahalios, G. T. 1990. Mixed convection flow in a heated curved pipe with core. *Physics of Fluids A*, Vol. 2(12):2164-2175.

Kasturi, G. and J. B. Stepanek. 1972. Two phase flow – I. Pressure drop and void fraction measurements in cocurrent gas-liquid flow in a coil. *Chemical Engineering Science*, Vol. 27:1871-1880.

Kays, W. M. and H. C. Perkins. 1973. Section 7: Forced convection, internal flow in ducts. In: *Handbook of Heat Transfer*, W. M. Rohsenow and J. P. Hartnett, eds. McGraw-Hill, New York, pp 7.1-7.193.

Kelder, J. D. H., K. J. Ptasinski, and P. J. A. M. Kerkhof. 2002. Power-law foods in continuous coiled sterilizers. *Chemical Engineering Science*, Vol. 57:4605-4615.

Kelder, J. D. H., K. J. Ptasinski, and P. J. A. M. Kerkhof. 2004. Starch gelatinization in coiled heaters. *Biotechnol. Prog.*, Vol. 20:921-929.

Klunge, T., A. Kalra, and G. Belfort. Viscosity effects on Dean vortex membrane microfiltration. *AIChE Journal*, Vol. 45(9):1913-1926.

Koutsky, J. A. and R. L. Adler. 1964. Minimization of axial dispersion by use of secondary flow in helical tubes. *The Canadian Journal of Chemical Engineering*, Vol. 42:239-245.

Kozicki, W., C. H. Chou, and C. Tiu. 1966. Non-Newtonian flow in ducts of arbitrary cross-sectional shape. *Chemical Engineering Science*, Vol. 21:665-769.

Kubair, V. and N. R. Kuloor. 1966. Heat transfer to Newtonian fluids in coiled pipes in laminar flow. *International Journal of Heat and Mass Transfer*, Vol. 9:63-75.

Kubie, J. and G. C. Gardner. 1977a. Drop sizes and drop dispersion in straight tubes and in helical coils. *Chemical Engineering Science*, Vol. 32:195-202.

Kubie, J. and G. C. Gardner. 1977b. Flow of two liquids in a helix: an analogue of high pressure helical boilers. *International Journal of Multiphase Flow*, Vol. 3:353-366.

Lee, C. S., J. J. Ou, and S. H. Chen. 1987. Quantification of mixing from the Eulerian perspective: flow through a curved tube. *Chemical Engineering Science*, Vol. 42(10):2484-2486.

Lee, J. B., H. A. Simon, and J. C. F. Chow. 1985. Buoyancy in developed laminar curved tube flows. *International Journal of Heat and Mass Transfer*, Vol. 28(2):631-640.

Lemenand, T. and H. Peerhossaini. 2002. A thermal model for prediction of the Nusselt number in a pipe with chaotic flow. *Applied Thermal Engineering*, Vol. 22:1717-1730.

Li, L. J., C. X. Lin, and M. A. Ebadian. 1998. Turbulent mixed convective heat transfer in the entrance region of a curved pipe with uniform wall-temperature. *International Journal of Heat and Mass Transfer*, Vol. 41(23):3793-3805.

Li, L. J., C. X. Lin, and M. A. Ebadian. 1999. Turbulent heat transfer to near-critical water in a heated curved pipe under the conditions of mixed convection. *International Journal of Heat and Mass Transfer*, Vol. 42(16):3147-3158.

Liao, H-J., M. A. Rao, and A. K. Datta. 2000. Role of thermo-rheological behaviour in simulation of continuous sterilization of a starch dispersion. *IChemE Transactions Part C – Food and Bioproducts Processing*, Vol. 78(C1):48-56.

Lin, C. X., and M. A. Ebadian. 1997. Developing turbulent convective heat transfer in helical pipes. *International Journal of Heat and Mass Transfer*, Vol. 40(16):3861-3873.

Lin, C. X., and M. A. Ebadian. 1999. The effects of inlet turbulence on the development of fluid flow and heat transfer in a helically coiled pipe. *International Journal of Heat and Mass Transfer*, Vol. 42(4):739-751.

Lin, C. X., P. Zhang, and M. A. Ebadian. 1997. Laminar forced convection in the entrance region of helical pipes. *International Journal of Heat and Mass Transfer*, Vol. 40(14):3293-3304.

Liu, S., A. Afacan, H. A. Nasr-El-Din, and J. H. Masliyah. 1994. An experimental study of the pressure drop in helical pipes. *Proc. R. Soc. London Ser. A*, Vol. 444(1921):307-316.

Liu, S., and J. H. Masliyah. 1993. Axially invariant laminar flow in helical pipes with a finite pitch. *Journal of Fluid Mechanics*, Vol. 251:315-353.

Liu, S., and J. H. Masliyah. 1994. Developing convective heat transfer in helical pipes with finite pitch. *International Journal of Heat and Fluid Flow*, Vol. 15(1):66-74.

Liu, Y. and C. A. Zuritz. 1995. Mathematical modeling of particulate two-phase flow in a helical coil. *Journal of Food Engineering*, Vol. 18:321-341.

Lyne, W. H. 1970. Unsteady viscous flow in a curved pipe. *Journal of Fluid mechanics*, Vol. 45(1):13-31.

Masliyah, J. H. 1980. On laminar flow in curved semicircular ducts. *Journal of Fluid Mechanics*, Vol. 99(3):469-479.

McConalogue, D. J. and R. S. Srivastava. 1968. Motion of a fluid in a curved tube. *Proceedings of the Royal Society of London, Series A, Mathematical and Physical Sciences*, Vol. 307(1488):37-53.

Mihail, R. and S. Straja. 1981. The behaviour of the helically coiled tube as a polymerization reactor. *Chemical Engineering Science*, Vol. 36:1296-1266.

Mokrani, A., C. Castelain and H. Peerhossaini. 1997. The effects of chaotic advection on heat transfer. *International Journal of Heat and Mass Transfer*, Vol. 40(13):3089-3104.

Mori, Y. and W. Nakayama. 1965. Study on forced convective heat transfer in curved pipes (1st report, laminar region). *International Journal of Heat and Mass Transfer*, Vol. 8:67-82.

Mori, Y. and W. Nakayama. 1967a. Study on forced convective heat transfer in curved pipes (2nd report, turbulent region). *International Journal of Heat and Mass Transfer*, Vol. 10:37-59.

Mori, Y. and W. Nakayama. 1967b. Study on forced convective heat transfer in curved pipes (3rd report, theoretical analysis under the condition of uniform wall temperature and practical formulae). *International Journal of Heat and Mass Transfer*, Vol. 10:681-695.

Nandakumar, K. and J. H. Masliyah. 1982. Bifurcation in steady laminar flow through curved tubes. *Journal of Fluid Mechanics*, Vol. 119:475-490.

Nauman, E. B. 1977. The residence time distribution for laminar flow in helically coiled tubes. *Chemical Engineering Science*, Vol. 32:287-293.

Nunge, R. J., T.-S. Lin and W. N. Gill. 1972. Laminar dispersion in curved tubes and channels. *Journal of Fluid Mechanics*, Vol. 51(2):363-383.

Nunge, R. J. and T.-S. Lin. 1973. Laminar flow in strongly curved tubes. *AIChE Journal*, Vol. 19(6):1280-1281.

Owhadi, A., K. J. Bell, and B. Crain. 1968. Forced convection boiling inside helically-coiled tubes. *International Journal of Heat and Mass Transfer*, Vol. 11:1779-1793.

Ozisik, M. N., and H. C. Topakoglu. 1968. Heat transfer for laminar flow in a curved pipe. *Journal of Heat Transfer*, Vol. 90:313-318.

Padmanabhan, N. 1987. Entry flow in heated curved pipes. *International Journal of Heat and Mass Transfer*, Vol. 30(7):1453-1463.

Palazoglu, T. K. and K. P. Sandeep. 2002. Effect of holding tube configuration on the residence time distribution of multiple particles in helical tube flow. *Journal of Food Process Engineering*, Vol. 25:337-350.

Park, H., Moore, J. A., Trass, O., and M. Ojha. 1999. Laser photochromic velocimetry estimation of the vorticity and pressure field – two-dimensional flow in a curved vessel. *Experiments in Fluids*, Vol. 26:55-62.

Patanker, S. V. 1980. *Numerical Heat Transfer and Fluid Flow*. Taylor & Francis, Levitown, PA, 197 pp.

Patankar, S. V., Pratap, V. S., and D. B. Spalding. 1974. Prediction of laminar flow and heat transfer in helically coiled pipes. *Journal of Fluid Mechanics*, Vol. 62(3):539-551.

Patankar, S. V., Pratap, V. S., and D. B. Spalding. 1975. Prediction of turbulent flow in curved pipes. *Journal of Fluid Mechanics*, Vol. 67(3):583-595.

Patil, R. K., Shende, B. W., and P. K. Ghosh. 1982. Designing a helical-coil heat exchanger. *Chemical Engineering*, Vol. 92(24):85-88.

Petrakis, M. A., and G. T. Karahalios. 1996. Technical note: steady flow in a curved pipe with a coaxial core. *International Journal for Numerical Methods in Fluids*, Vol. 22(12):1231-1237.

Petrakis, M. A., and G. T. Karahalios. 1997. Exponential decaying flow in a gently curved annular pipe. *International Journal of Non-Linear Mechanics*, Vol. 32(5):823-835.

Petrakis, M. A., and G. T. Karahalios. 1999. Fluid flow behaviour in a curved annular conduit. *International Journal of Non-Linear Mechanics*, Vol. 34(1):13-35.

Prabhanjan, D. G. 2000. *Influence of Coil Characteristics on Heat Transfer to Newtonian Fluids*. Ph. D. Thesis, McGill University, Montreal. 169 p.

Prabhanjan, D. G., G. S. V. Raghavan, and T. J. Rennie. 2002. Comparison of heat transfer rates between a straight tube heat exchanger and a helically coiled heat exchanger. *International Communications in Heat and Mass Transfer*, Vol. 29(2):185-191.

Prabhanjan, D. G., T. J. Rennie, and G. S. V. Raghavan. 2004. Natural convection heat transfer from helical coiled tubes. *International Journal of Thermal Sciences*, Vol. 43(4):359-365.

Prasad, B. V. S. S. S., D. H. Das, A. K. Prabhakar. Pressure drop, heat transfer and performance of a helically coiled tubular exchanger. *Heat Recovery Systems & CHP*, Vol. 9(3):249-256.

Rabadi, N. J., J. C. F. Chow, and H. A. Simon. 1982. Heat transfer in curved tubes with pulsating flow. *International Journal of Heat and Mass Transfer*, Vol. 25(2):195-203.

Rabin, Y. and E. Korin. 1996. Thermal analysis of a helical heat exchanger for ground thermal energy storage in arid zones. *International Journal of Heat and Mass Transfer*, Vol. 39(5):1051-1065.

Rajasekharan, S., V. G. Kubair, and N. R. Kuloor. 1966. Secondary flow of non-Newtonian fluids in helical coils. *Indian Journal of Technology*, Vol. 4:33-35.

Rajasekharan, S., V. G. Kubair, and N. R. Kuloor. 1970. Heat transfer to non-Newtonian fluids in coiled pipes in laminar flow. *International Journal of Heat and Mass Transfer*, Vol. 13:1583-1594.

Ramaswamy, H. S., K. A. Abdelrahim, B. K. Simpson, and J. P. Smith. 1995. Residence time distribution (RTD) in aseptic processing of particulate foods: a review. *Food Research International*, Vol. 28(3):291-310.

Rangacharyulu, K. and G. S. Davies. 1984. Pressure drop and holdup studies of air-liquid flow in helical coils. *The Chemical Engineering Journal*, Vol. 29:41-46.

Rao, B. K. 1994. Turbulent heat transfer to power-law fluids in helical passages. *International Journal of Heat and Fluid Flow,* Vol. 15(2):142-148.

Rennie, T. J., and G. S. V. Raghavan. 2000. Outside heat transfer from a helically coiled heat exchanger. *Presented at the 2000 ASAE Annual International Meeting, Paper 00-6137*, ASAE, 2950 Niles Rd., St. Joseph, MI 49085-9659 USA. 13 pp.

Rindt, C. C. M., J. J. M. Sillekens and A. A. van Steenhoven. 1999. The influence of the wall temperature on the development of heat transfer and secondary flow in a coiled heat exchanger. *International Communications in Heat and Mass Transfer*, Vol. 26(2):187-198.

Robertson, A. M. and S. J. Muller. Flow of Oldroyd-B fluids in curved pipes of circular and annular cross-section. *International Journal of Non-Linear Mechanics*, Vol. 31(1):1-20.

Rogers, G. F. C. and Y. R. Mayhew. 1964. Heat transfer and pressure loss in helically coiled tubes with turbulent flow. *International Journal of Heat and Mass Transfer*, Vol. 7:1207-1216.

Rose, J. W. 2004. Heat-transfer coefficients, Wilson plot and accuracy of thermal measurements. *Experimental Thermal and Fluid Science*, Vol. 28:77-86.

Ruthven, D. M. 1971. The residence time distribution for ideal laminar flow in a helical tube. *Chemical Engineering Science*, Vol. 26(7):1113-1121.

Sahoo, P. K., Md. I. A. Ansari, and A. K. Datta. 2002. Computer-aided design and performance of an indirect type helical tube ultra-high temperature (UHT) milk sterilizer. *Journal of Food Engineering*, Vol. 51:13-19.

Sahoo, P. K., Md. I. A. Ansari, and A. K. Datta. 2003. A computer based iterative solution for accurate estimation of heat transfer coefficients in a helical tube heat exchanger. *Journal of Food Engineering*, Vol. 58:211-214.

Salengke, S. and S. K. Sastry. 1994. Residence time distribution of cylindrical particles in a curved section of a holding tube: the effect of particle size and flow rate. *Journal of Food Process Engineering*, Vol. 18:363-381.

Salengke, S. and S. K. Sastry. 1996. Residence time distribution of cylindrical particles in a curved section of a holding tube: the effect of particle concentration and bend radius of curvature. *Journal of Food Engineering*, Vol. 27:159-176.

Sancho, M. F. and M. A. Rao. 1992. Residence time distribution in a holding tube. *Journal of Food Engineering*, Vol. 15:1-19.

Sandeep, K. P. and T. K. Palazoglu. 1999. Secondary flow in coiled tubes. Presented at the *1999 ASAE Annual International Meeting*. Paper No. 996148. ASAE, 2950 Niles Rd., St. Joseph, MI 49085-9659 USA.

Sandeep, K. P., C. A. Zuritz, and V. M. Puri. 1997. Residence time distribution of particles during two-phase non-Newtonian flow in conventional as compared with helical holding tubes. *Journal of Food Science*, Vol. 62(4):647-652.

Sarin, V. B. 1997. The steady laminar flow of an elastico-viscous liquid in a curved pipe of varying elliptic cross section. *Mathematical and Computer Modelling*, Vol. 26(3):109-121.

Sawyers, D. R., M. Sen, and H.-C. Chang. 1996. Effect of chaotic interfacial stretching on bimolecular chemical reaction in helical-coil reactors. *The Chemical Engineering Journal*, Vol. 64(1):129-139.

Saxena, A. K. and K. D. P. Nigam. 1979. On RTD for laminar flow in helical coils. *Chemical Engineering Science*, Vol. 34:425-426.

Saxena, A. K. and K. D. P. Nigam. 1984. Coiled configuration for flow inversion and its effect on residence time distribution. *AIChE Journal*, Vol. 30(3):363-368.

Seban, R. A. and E. F. McLaughlin. 1963. Heat transfer in tube coils with laminar and turbulent flow. *International Journal of Heat and Mass Transfer*, Vol. 6:387-395.

Sedahmed, G. H., L. W. Shemilt, and F. Wong. 1985. Natural convection mass transfer characteristics of rings and helical coils in relation to their use in electrochemical reactor design. *Chemical Engineering Science*, Vol. 40(7):1109-1114.

Shah, R. K. 1990. Assessment of modified Wilson plot techniques used for obtaining heat exchanger design data, in: *Heat Transfer 1990. Proceedings of the 9th International Heat Transfer Conference*, Vol. 5:51-56.

Shah, R. K. and S. D. Joshi. 1987. Chapter 5: Convective heat transfer in curved ducts. In: *Handbook of Single-Phase Convective Heat Transfer*, S. Kakac, R. K. Shah, and W. Aung, eds., Wiley-Interscience, NY, pp 5.1-5.46.

Shetty, V. D. and K. Vasudeva. 1977. Effect of Schmidt number on laminar dispersion in helical coils. *Chemical Engineering Science*, Vol. 32:782-783.

Shimizu, A., S. Hasegawa, and R. Echigo. 1984. Convective heat transfer of a gaseous solid suspension flow in a curved tube. *International Communications in Heat and Mass Transfer*, Vol. 11:537-544.

Sieder, E. N. and G. E. Tate. 1936. Heat transfer and pressure drops of liquid in tubes. *Ind. Eng. Chem.*, Vol. 28:1429-1435.

Sillekens, J. J. M., C. C. M. Rindt and A. A. Van Steenhoven. 1998. Developing mixed convection in a coiled heat exchanger. *International Journal of Heat and Mass Transfer*, Vol. 41(1):61-72.

Silva, R. J., R. M. Valle, and M. Ziviani. 1999. Numerical hydrodynamic and thermal analysis of laminar flow in curved elliptic and rectangular channels. *International Journal of Thermal Sciences*, Vol. 38:585-594.

Simpson, S. G. and M. C. Williams. 1974. An analysis of high temperature/short time sterilization during laminar flow. *Journal of Food Science*, Vol. 39:1047-1054.

Singh, M. P. 1974. Entry flow in a curved pipe. *Journal of Fluid mechanics*, Vol. 65(3):517-539.

Singh, R. P. and D. R. Heldman. 1993. *Introduction to Food Engineering, second edition*. Academic Press, Inc., San Diego, CA, 499 pp.

Smith, F. T. 1976. Steady motion within a curved pipe. *Proc. R. Soc. London Ser. A* 347:345-370.

Soeberg, K. 1988. Viscous flow in curved tubes – I. Velocity profiles. *Chemical Engineering Science*, Vol. 43(4):855-862.

Son, S. M. and R. K. Singh. 2002. Turbulence modeling and verification for aseptically processed soybean milk under turbulent flow conditions. *Journal of Food Engineering*, Vol. 52:177-184.

Sreenivasan, K. R. and P. J. Strykowski. 1983. Stabilization effects in flow through helically coiled pipes. *Experiments in Fluids*, Vol. 1:31-36.

Stepanek, J. B. and G. Kasturi. 1972. Two phase flow – II. Parameters for void fraction and pressure drop correlations. *Chemical Engineering Science*, Vol. 27:1881-1891.

Styrikovich, M. A., V. S. Polonsky, and V. V. Reshetov. 1984. Experimental investigation of the critical heat flux and post-dryout temperature regime of helical coils. *International Journal of Heat and Mass Transfer*, Vol. 27(8):1245-1250.

Taherian, H. and P. L. Allen. 1997. Natural convection from vertical helical coils in a cylindrical enclosure. *Proceedings of the ASME Heat Transfer Division, HTD*-Vol. 353:135-142.

Taherian, H. and P. L. Allen. 1998. Experimental study of natural convection shell-and-coil heat exchangers. *ASME Proceedings of the 7th AIAA/ASME Joint Thermophysics and Heat Transfer Conference, HTD*-Vol. 357-2.

Takahashi, M. and Y. Momozaki. 2000. Pressure drop and heat transfer of a mercury single-phase and an air-mercury two-phase flow in a helical tube under a strong magnetic field. *Fusion Engineering and Design*, Vol. 51-52:869-877.

Tarbell, J. M. and M. R. Samuels. 1973. Momentum and heat transfer in helical coils. *The Chemical Engineering Journal*, Vol. 5:117-127.

Taylor, G. I. 1929. The criteria for turbulence in curved pipes. *Proceedings of the Royal Society of London, Series A*, Vol. 124:243-249.

Thomas, R. H. and K. Walters. 1963. On the flow of an elastico-viscous liquid in a curved pipe under a pressure gradient. *Journal of Fluid Mechanics*, Vol. 16:228-242.

Thomas, R. H. and K. Walters. 1965. On the flow of an elastico-viscous liquid in a curved pipe of elliptical cross-section under a pressure gradient. *Journal of Fluid Mechanics*, Vol. 21(1):173-182.

Thomson, D. L., Y. Bayazitoglu, and A. J. Meade. 2001. Series solution of low Dean and Germano number flows in helical rectangular ducts. *International Journal of Thermal Sciences*, Vol. 40:937-948.

Topakoglu, H. C. 1967. Steady laminar flows of an incompressible viscous fluid in curved pipes. *Journal of Mathematics and Mechanics*, Vol. 16(12):1321-1337.

Trivedi, R. N. and K. Vasudeva. 1974. RTD for diffusion free laminar flow in helical coils. *Chemical Engineering Science,* Vol. 29:2291-2295.

Trivedi, R. N. and K. Vasudeva. 1975. Axial dispersion in laminar flow in helical coils. *Chemical Engineering Science,* Vol. 30:317-325.

Truesdell, L. C., and R. J. Adler. 1970. Numerical treatment of fully developed laminar flow in helically coiled tubes. *AIChE Journal*, Vol. 16(6):1010-1015.

Tuttle, E. R. 1990. Laminar flow in twisted pipes. *Journal of Fluid Mechanics*, Vol. 219:545-570.

Unal, H. C., M. L. G. van Gasselt, and P. m. van't Verlaat. 1981. Dryout and two-phase flow pressure drop in sodium heated helically coiled steam generator tubes at elevated pressures. *International Journal of Heat and Mass Transfer*, Vol. 24:285-298.

van Andel, E., H. Kramers, and A. de Voogd. 1964. The residence time distribution of laminar flow in curved tubes. *Chemical Engineering Science*, Vol. 19(1):77-79.

Van Dyke, M. 1978. Extended Stokes series: laminar flow through a loosely coiled pipe. *Journal of Fluid Mechanics*, Vol. 86:129-145.

Verma, P. D. S. and P. Ram. On the low-Reynolds number magnetic fluid flow in a helical pipe. *International Journal of Engineering Science*, Vol. 31(2):229-239.

Wang, C. Y. 1981. On the low-Reynolds-number flow in a helical pipe. *Journal of Fluid Mechanics*, Vol. 108:185-194.

Wang, J. W. and J. R. G. Andrews. 1995. Numerical Simulation of Flow in Helical Ducts. *AIChE Journal*, Vol. 41(5):1071-1080.

Watanabe, O., K. Nakajima and H. Fujita. 1993. Characteristics of liquid-film thickness of air-water annular two-phase flow in helically coiled tubes. *Heat Transfer – Japanese Research*, Vol. 22(5):447-461.

Webster, D. R., and J. A. C. Humphrey. 1993. Experimental observations of flow instability in a helical coil. *Transactions of the ASME, Journal of Fluids Engineering*, Vol. 115(3):436-443.

Webster, D. R., and J. A. C. Humphrey. 1997. Traveling wave instability in helical coil flow. *Physics of Fluids*, Vol. 9(2):407-418.

Whalley, P. B. 1980. Air-water two-phase flow in a helically coiled tube. *International Journal of Multiphase Flow*, Vol. 6:345-356.

White, C. M. 1929. Streamline flow through curved pipes. *Proceedings of the Royal Society of London, Series A*, Vol. 123(792):645-663.

White, F. M. 1984. *Heat Transfer*. Addison-Wesley Publishing Company, Inc., 588 pp.

Williams, G. S., Hubbell, C. W., and G. H. Fenkell. 1902. Experiments at Detroit, Mich., on the effect of curvature upon the flow of water in pipes, *Trans. ASCE* 47:1-196.

Xie, D. G. 2001. Torsion effect on secondary flow in a helical pipe. *International Journal of Heat and Mass Transfer,* Vol. 11(2):114-119.

Xin, R. C., A. Awwad, Z. F. Dong and M. A. Ebadian. 1996. An investigation and comparative study of the pressure drop in air-water two-phase flow in vertical helicoidal pipes. *International Journal of Heat and Mass Transfer*, Vol. 39(4):735-743.

Xin, R. C., A. Awwad, Z. F. Dong and M. A. Ebadian. 1997. An experimental study of the single-phase and two-phase flow pressure drop in annular helicoidal pipes. *International Journal of Heat and Fluid Flow*, Vol. 18:482-488.

Xin, R. C., and M. A. Ebadian. 1996. Natural convection heat transfer from helicoidal pipes. *Journal of Thermophysics and Heat Transfer*, Vol. 10, No. 2:297-302.

Xin, R. C., and M. A. Ebadian. 1997. The effects of Prandtl numbers on local and average convective heat transfer characteristic in helical pipes. *Journal of Heat Transfer*, Vol. 119:467-473.

Yamamoto, K., T. Akita, H. Ikeuchi and Y, Kita. 1995. Experimental study of the flow in a helical circular tube. *Fluid Dynamics Research,* Vol. 16:237-249.

Yamamoto, K., S. Yanase and R, Jiang. 1998. Stability of the flow in a helical tube. *Fluid Dynamics Research*, Vol. 22:153-170.

Yang,, R., S. F. Chang, and W. Wu. 2000. Flow and heat transfer in a curved pipe with periodically varying curvature. *International Communications in heat and Mass Transfer,* Vol. 27(1):133-143.

Yang, G., F. Dong, and M. A. Ebadian. 1995. Laminar forced convection in a helicoidal pipe with finite pitch. *International Journal of Heat and Mass Transfer*, Vol. 38(5):853-862.

Yang, G., and M. A. Ebadian. 1996. Turbulent forced convection in a helicoidal pipe with substantial pitch. *International Journal of Heat and Mass Transfer*, Vol. 39(10):2015-2022.

Yao, L.-S., and S. A. Berger. 1978. Flow in heated curved pipes. *Journal of Fluid Mechanics*, Vol. 88(2):339-354.

Yi, J., Z. H. Liu, J. Wang. 2003. Heat transfer characteristics of the evaporator section using small helical coiled pipe in a looped heat pipe. *Applied Thermal Engineering*, Vol. 23:89-99.

Yu, B, J. T. Han, H. J. Kang, C. X. Lin, A. Awwad, and M. A. Ebadian. 2003. Condensation heat transfer of R-134a flow inside helical pipes at different orientations. *International Communications in Heat and Mass Transfer*, Vol. 30(6):745-754.

Zabielski, L. and A. J. Mestel. 1998a. Steady flow in a helically symmetrical pipe. *Journal of Fluid Mechanics*, Vol. 370:297-320.

Zabielski, L. and A. J. Mestel. 1998b. Unsteady blood flow in a helically symmetrical pipe. *Journal of Fluid Mechanics*, Vol. 370:321-345.

Zalosh, R. G. and W. G. Nelson. 1973. Pulsating flow in a curved tube. *Journal of Fluid Mechanics*, Vol. 59(4):693-705.

Zapryanov, Z., Christov, C. and E. Toshev. 1980. Fully developed laminar flow and heat transfer in curved tubes. *International Journal of Heat and Mass Transfer*, Vol. 23:873-880.

Zhao, L., L. Guo, B. Bai, Y. Hou, and X. Zhang. 2003. Convective boiling heat transfer and two-phase flow characteristics inside a small horizontal helically coiled tubing once-through steam generator. *International Journal of Heat and Mass Transfer*, Vol. 46:4779-4788.

Zheng, B., C. X. Lin, and M. A. Ebadian. 2000. Combined laminar forced convection and thermal radiation in a helical pipe. *International Journal of Heat and Mass Transfer*, Vol. 43:1067-1078.

APPENDIX A

This appendix gives a brief overview of the computational fluid dynamics software PHOENICS 3.3 that was used in this work along with some explanation of its use to model the double-pipe helical heat exchanger.

A.1 Governing Equations

The physical phenomena of fluid flow and heat transfer with constant density, ρ, and viscosity, μ, can be described in Cartesian Coordinates (x, y, z) by the following:

Continuity Equation:

$$\rho\frac{\partial u}{\partial x}+\rho\frac{\partial v}{\partial y}+\rho\frac{\partial w}{\partial z}=0 \qquad \text{(A.1)}$$

Navier-Stokes Equations (Momentum Equations):

$$\rho\frac{\partial u}{\partial t}+\rho u\frac{\partial u}{\partial x}+\rho v\frac{\partial u}{\partial y}+\rho w\frac{\partial u}{\partial z}=\mu\left(\frac{\partial^2 u}{\partial x^2}+\frac{\partial^2 u}{\partial y^2}+\frac{\partial^2 u}{\partial z^2}\right)-\frac{\partial P}{\partial x} \qquad \text{(A.2)}$$

$$\rho\frac{\partial v}{\partial t}+\rho u\frac{\partial v}{\partial x}+\rho v\frac{\partial v}{\partial y}+\rho w\frac{\partial v}{\partial z}=\mu\left(\frac{\partial^2 v}{\partial x^2}+\frac{\partial^2 v}{\partial y^2}+\frac{\partial^2 v}{\partial z^2}\right)-\frac{\partial P}{\partial y} \qquad \text{(A.3)}$$

$$\rho\frac{\partial w}{\partial t}+\rho u\frac{\partial w}{\partial x}+\rho v\frac{\partial w}{\partial y}+\rho w\frac{\partial w}{\partial z}=\mu\left(\frac{\partial^2 w}{\partial x^2}+\frac{\partial^2 w}{\partial y^2}+\frac{\partial^2 w}{\partial z^2}\right)-\frac{\partial P}{\partial z} \qquad \text{(A.4)}$$

Energy Equation:

$$\rho\frac{\partial T}{\partial t}+\rho u\frac{\partial T}{\partial x}+\rho v\frac{\partial T}{\partial y}+\rho w\frac{\partial T}{\partial z}=\frac{k}{c_p}\left(\frac{\partial^2 T}{\partial x^2}+\frac{\partial^2 T}{\partial y^2}+\frac{\partial^2 T}{\partial z^2}\right) \qquad \text{(A.5)}$$

P, T, u, v, and w represent the pressure, temperature, and velocities in the x, y, and z directions, respectively. The thermal properties such as thermal conductivity and specific heat are represented by the symbols, k, and c_p, respectively.

A.2 Discretization of the Governing Equations

In computational fluid dynamics (CFD) software, such as PHOENICS 3.3, the above equations are solved simultaneously using a numerical procedure. Once the domain (for which these equations are to be solved within) is determined, the domain is divided into numerous cells and the partial differential equations are then applied to each cell. Therefore, within each cell that makes up the domain, the above partial differential equations are first discretized (expressed in algebraic terms) and then applied to the cell. Discretization of the equations is often based on approximating the differential equations by truncated Taylor series expansions or by other similar methods. Let us consider a simple heat conduction problem in 2-dimensions (Figure A.1). The domain is divided into cells (control volumes) and the energy equation is applied to each control volume (the area inside the dashed lines of Figure A.1).

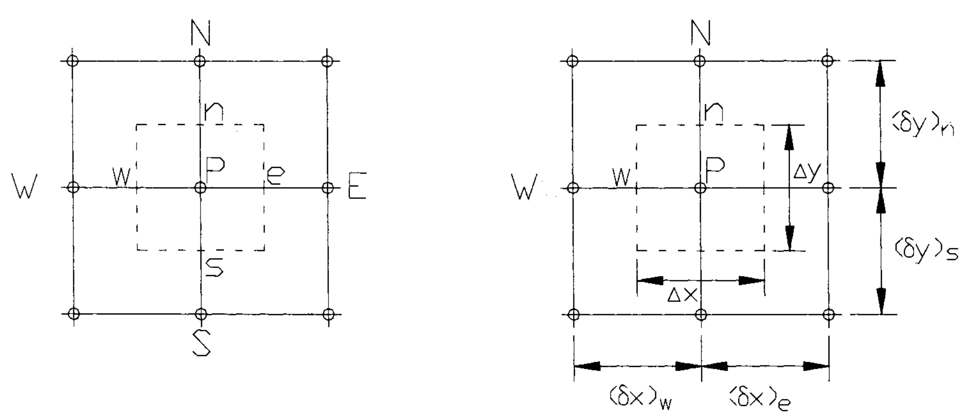

Figure A.1: Control volume for 2-dimensional conduction

The governing differential equation for unsteady state conductive heat transfer without heat generation is:

$$\rho \frac{\partial T}{\partial t} = \frac{k}{c_p}\left(\frac{\partial^2 T}{\partial x^2} + \frac{\partial^2 T}{\partial y^2}\right) \tag{A.6}$$

This equation can be discretized to the following algebraic expressions:

$$a_P T_P = a_E T_E + a_W T_W + a_N T_N + a_S T_S + a_P^0 T_P^0 \tag{A.7}$$

where:

$$a_E = k_e \frac{\Delta y}{(\delta x)_e} \tag{A.8}$$

$$a_W = k_w \frac{\Delta y}{(\delta x)_w} \tag{A.9}$$

$$a_N = k_n \frac{\Delta x}{(\delta y)_n} \tag{A.10}$$

$$a_S = k_s \frac{\Delta x}{(\delta y)_s} \tag{A.11}$$

$$a_P^0 = (\rho c_p)\frac{\Delta x \Delta y}{\Delta t} \tag{A.12}$$

$$a_P = a_E + a_W + a_N + a_S + a_P^0 \tag{A.13}$$

Thus, an algebraic expression for the temperature of every cell can be formulated in the form of Equation A.7, which is simply a function of all the surrounding temperatures and the properties of the environment (thermal conductivity and specific heat). The temperature distribution may now be determined by solving the set of algebraic equations, given the appropriate boundary conditions.

This is a simplified version of the calculation procedure that does not consider fluid flow. The approach to systems with fluid movement become more difficult to solve, but the same basic approach is used. A thorough description of all the intricacies for solving the fully coupled heat and mass transfer equations using numerical methods is beyond the scope of this appendix. The main goal here is to show the interested reader some of the basics.

A.3 Model Development in PHOENICS 3.3

The coils were created in AutoCAD 14 and imported into PHOENICS as stereolithography files. Figure A.2 shows the full domain of the heat exchanger after the coils were imported into PHOENICS.

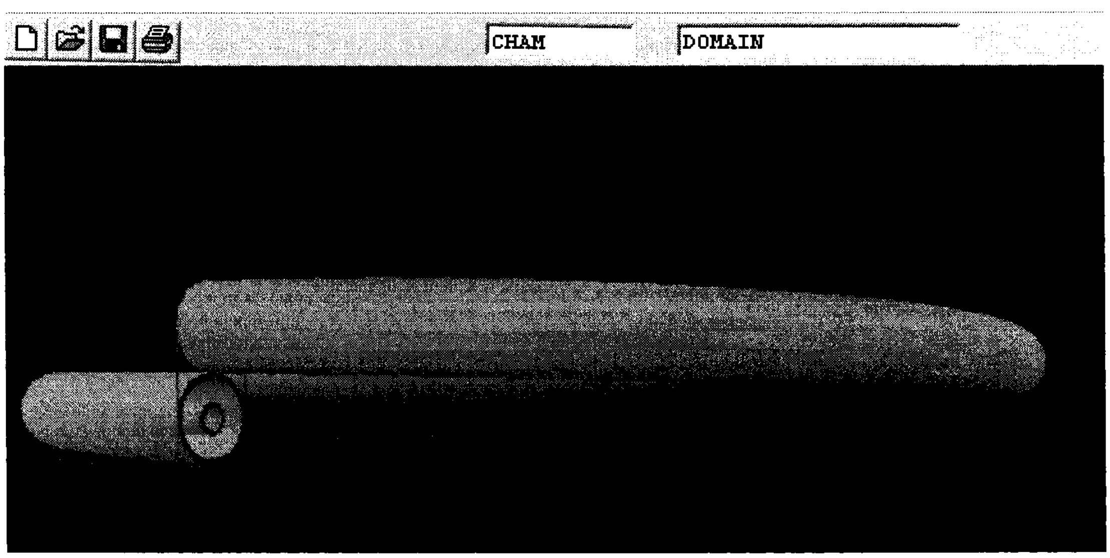

Figure A.2: Double-pipe helical heat exchanger in PHOENICS

The domain was divided into a mesh of 30 x 40 x 80 in the x-, y-, and z-directions, respectively, where the x-direction is the main axial direction and the y-direction is the radial direction. Several different mesh sizes were tried, with this configuration giving the fastest convergence without compromising the solution accuracy. Figure A.3 shows the inlet area of the heat exchanger with the y-z grid.

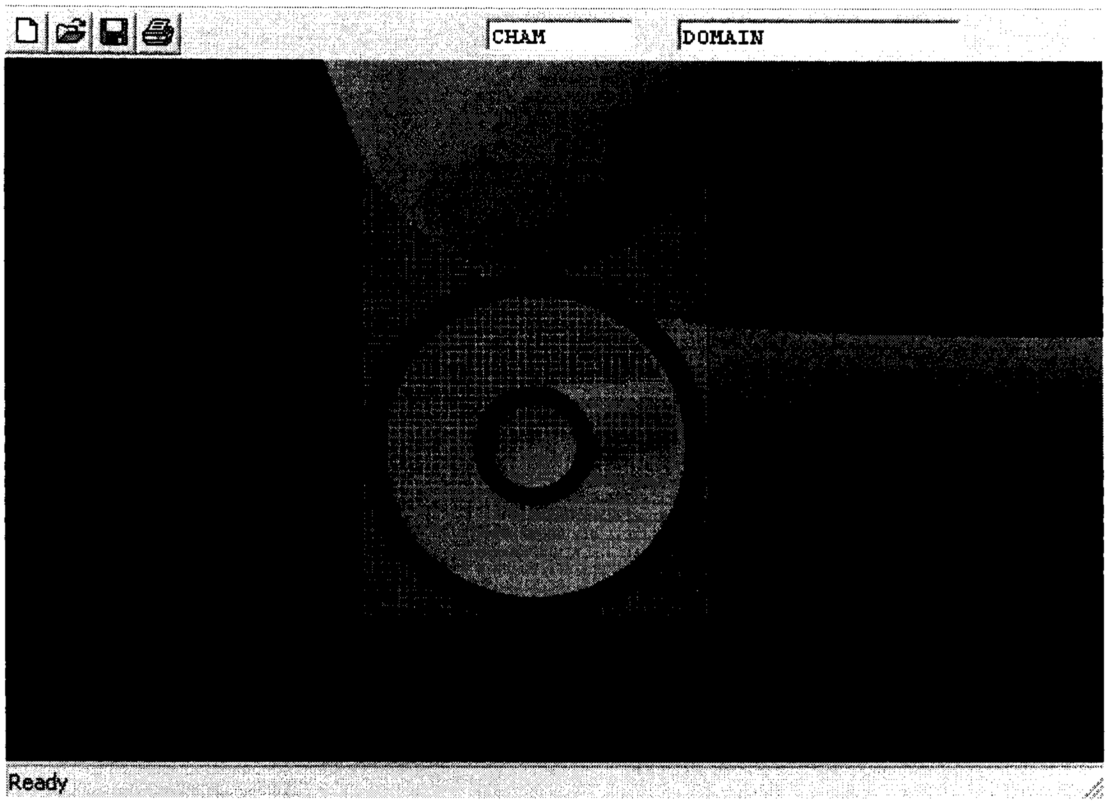

Figure A.3: Inlet with meshing

Inlet objects were placed at $x = 0$ and outlet objects at $x = 2\pi$. There were separate objects for the inner tube and the annulus. The inlet object allowed the inlet velocity to be set and the type of fluid. Fluid properties were stored in a separate file that PHOENICS refers to. This file has a set of standard fluids, though other fluids could be added. The fluids could also be modified during the model setup, such as making properties temperature dependent. The outlet object was set with a pressure at the outlet of zero. For the counterflow simulations, the inlet and outlet objects of the annulus were switched.

The model used an elliptical solution method, and employed the SIMPLEST algorithm, which is a derivative of the SIMPLE algorithm described in Patankar (1980). Relaxation factors were used for all variables; these were determined by trial and error. The outputs of the simulations were saved to file. Values for the pressure, three velocities, temperature, and material property (149 in the case of stainless steel and 0 in the case of the fluid) were saved for every node of the domain. This resulted in 96 000 values for each variable. The data was then analyzed in a spreadsheet. The results of the simulations could also be viewed graphically in PHOENICS using the sub-program VR Viewer. Typical velocity vectors and velocity counters are shown in Figure A.4.

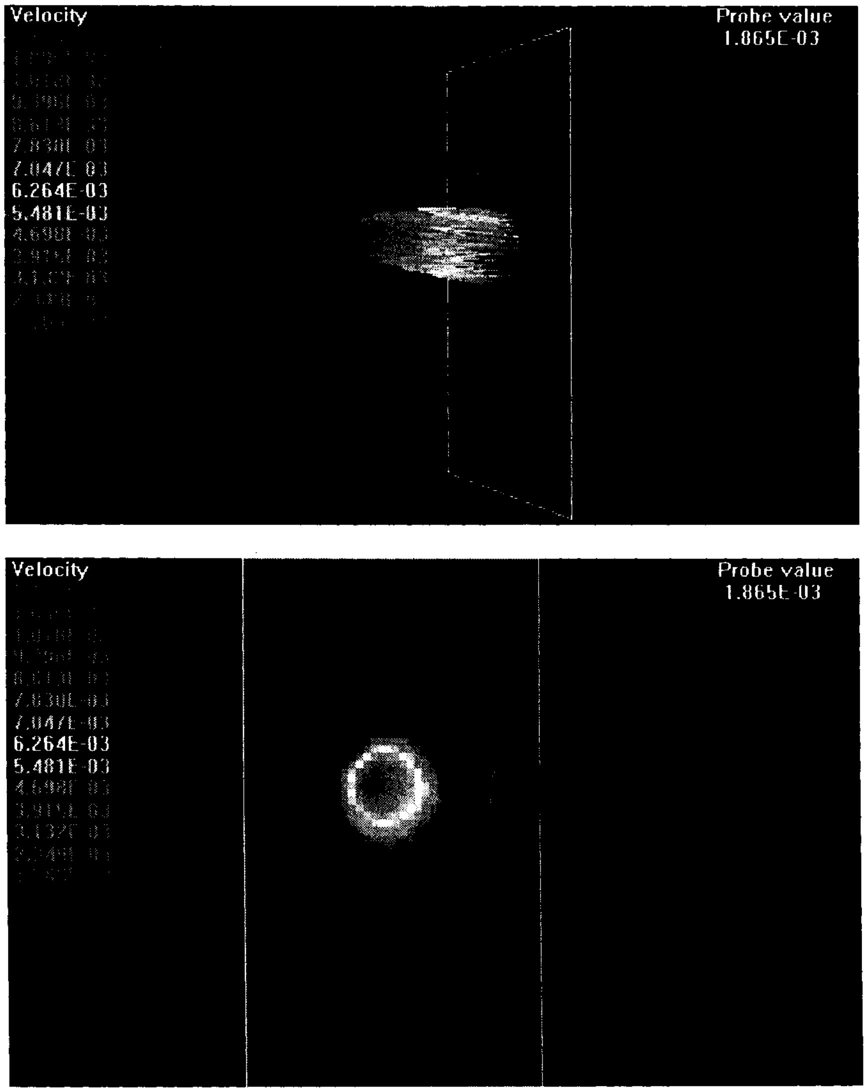

Figure A.4: Typical velocity vectors (top) and velocity contours (bottom)

A.4 References

Patanker, S. V. 1980. *Numerical Heat Transfer and Fluid Flow.* Taylor & Francis, Levitown, PA, 197 pp.